Establishment of a 3D cell culture perfused system to investigate mechanisms of blood vessel lumen morphogenesis: the role of cilia and cytoskeletal regulators in flow sensing

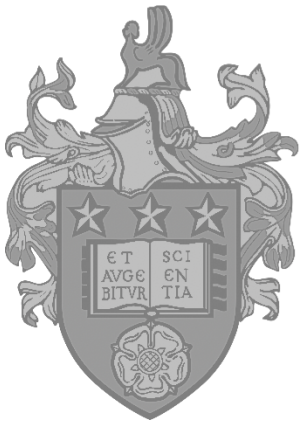

Safoura Zahed Mohajerani

Submitted in accordance with the requirements for the degree of Doctor of Philosophy (PhD)

The University of Leeds

Leeds Institute of Medical Research

October 2022

The candidate confirms that the work submitted is her own and that appropriate credit has been given where reference has been made to the work of others.

I dedicate this piece to my husband and to my son, Reza and Aiden.

Without their encouragement, this accomplishment wasn't possible.

Acknowledgements

First and foremost, I am grateful to British Heart Foundation for the funding opportunity to undertake my study.

I would like to express my sincere gratitude to both of my supervisors, Dr Georgia Mavria and Professor Colin A. Johnson for their unwavering support and belief in me. Georgia, you have been a great supervisor, friend, and mentor. I am deeply grateful for your assistance at every stage of this research project. You have encouraged me to strive for better, as a person and as a researcher, thanks for believing in me. Colin, thanks for your invaluable supervision, continuous support, and patience during my PhD study. I appreciate the way you always motivate me during my PhD. Thanks to both of you, your immense knowledge and plentiful experience have encouraged me in all the time of my academic research. I am indebted to both of you for your advice, support and the insight you gave me in to new techniques, they have undoubtedly catalysed my growth as a researcher over the course of this doctorate.

I would like to express gratitude to Dr Chiara Galloni for her support, Chiara thanks for being the best mentor, post-doc, and friend. I would like to thank my collaborator Dr Matthew Bourn, I cannot thank you enough for your patience, and assistance with the microfluidic device. I would like to thank Dr Gary Shaw, Dr Leander Stewart, Dr Clair Smith, Dr Katarzyna Szymanska, Dr Basudha Basu, Dr Alice Lake and Rowan Taylor for their support and help during my PhD project.

I would like to thank my friends, Dr Helen Carrasco Hope, Laura Heskin and Dr Anastasia Widyadari for a cherished time spent together in the lab, and in social settings. I am grateful you are in my life and for our beautiful friendship.

On a personal level, I am deeply grateful for the support of my family; I would like to offer my special thanks to my husband, Reza Asghari and to my son, Aiden Asghari, I am indebted to your constant support, your patience and grace. Reza, without your tremendous understanding and encouragement in the past few years, this thesis would have never seen the light of day. You never fail to support

me even on the toughest days. It is an honour to have you by my side and no words can fully express my gratitude. I would like to extend my sincere appreciation to both of my parents, Ozra and Ali, and my brother Hooman; without your encouragement and belief in me in the first step, my enthusiasm for science would have not been realised and I wouldn't be in the position I am today.

To everyone I have crossed paths with, has mentored me, and worked with me over the past four years, I sincerely thank you, your contribution does not go unnoticed.

Safoura Zahed Mohajerani, October 2022

Abstract

Cardiovascular function relies on stable and continuous formation of the blood vessel network by endothelial cells (ECs) to sustain blood flow and tissue viability. Although much is known regarding the molecules that control the initial stages of blood vessel growth, current understanding of the mechanisms by which the blood vessel lumen develops and expands to allow and sustain blood flow remain poorly elucidated. Endothelial primary cilia, microtubule-based organelles that protrude from the plasma membrane into the vessel lumen, mediate mechanotransduction of blood flow. Therefore, this thesis assesses the effects of genetic ablation of cilia, and cytoskeletal regulators DOCK4 and ROCK involved in ciliogenesis, on flow sensing and lumen formation under conditions of fluid flow.

A promising approach for understanding the mechanism behind development of a functional circulatory system is the use of perfused endothelial tubes in three-dimensional (3D) organotypic co-cultures of endothelial cells and fibroblasts. The system which was established in this study allowed manipulation of molecules associated with flow sensing under conditions of fluid flow. Molecular mechanisms of vascular lumen formation and lumen expansion were investigated using this system.

This study concludes that primary cilia are necessary for vascular tube formation in the co-culture model as their ablation inhibited lumen formation and expansion, and ROCK inhibition leading to disruption of proper cilium assembly inhibits vascular lumen formation. Furthermore, knockdown of GEF DOCK4 under conditions of FGF stimulation, increases angiogenesis in co-culture through higher EC proliferation accompanied by decreased cilia incidence. Finally, during this study a serotonin receptor HTR6-CFP2 fusion protein was cloned into a lentiviral vector and the protein was successfully expressed in ECs for assessment of ciliary dynamics in live cells.

Table of Contents

Acknowledgements……iv
Abstract……vi
Table of Contents……vii
List of Figures……xiv
List of Tables……xvii
List of Abbreviations……xviii
Chapter 1 Introduction 1
1.1 The circulatory system 2
1.1.1 Blood vessels and the endothelium 3
1.1.2 The peripheral vascular system 4
1.1.2.1 Arteries and arterioles 4
1.1.2.2 Venules and veins 5
1.1.2.3 Capillaries 5
1.1.3 Collateral arteries 7
1.1.4 Mural cells 7
1.2 Development of blood vessels 8
1.2.1 Expansion of vascular network 8
1.2.2 Maturation of vascular network 9
1.2.3 Angiogenesis growth factors FGF and VEGF 10
1.3 Pathological angiogenesis 11
1.3.1 Tumour angiogenesis 12
1.3.2 Retinopathy 13
1.3.3 Tissue ischemia 14
1.4 Mechanisms of blood vessel growth 14
1.4.1 Vasculogenesis 14
1.4.2 Angiogenesis 15
1.4.2.1 Sprouting angiogenesis 15

1.4.2.2 Intussusceptive angiogenesis 17
1.5 Lumen formation 18
1.5.1 Mechanisms of lumen formation 18
1.5.2 ECs acquisition of apical polarity 20
1.5.3 The role of adherens junctions in lumen formation 20
1.5.4 Lumen expansion and the role of fluid flow 21
1.6 Co-culture angiogenesis assay 22
1.7 Microfluidic device 22
1.7.1 Construction and use of microfluidic devices 22
1.7.2 Components of microfluidic devices 25
1.7.3 Coculture angiogenesis system in microfluidic devices 26
1.8 Primary cilia 27
1.8.1 Primary cilia structure 28
1.8.2 Primary cilia assembly and disassembly 30
1.8.3 Vascular endothelial cilia 32
1.8.4 Ciliary proteins 33
1.8.4.1 IFT88 33
1.8.4.2 RPGRIP1L 35
1.8.4.3 Serotonin receptor HTR6 35
1.8.5 Endothelial cilia and their role in sensing blood flow 36
1.8.6 Cilia and the actin cytoskeleton 37
1.8.6.1 Actin cytoskeleton and regulation of ciliogenesis 39
1.8.6.2 Regulation of cilia by ROCK 40
1.8.6.3 ROCK and lumen formation 41
1.9 Cytoskeletal regulators 41
1.9.1 Rho GTPases and the actin cytoskeleton 42
1.9.2 Guanine nucleotide exchange factors (GEFs) 44

1.9.2.1 DOCK4 45
1.9.2.2 The role of DOCK4 in vascular development and angiogenesis 46
1.10 Preliminary work leading to this thesis 48
1.10.1 Cilia and ROCK 48
1.10.2 Stimulation of angiogenesis in co-culture by bFGF 48
1.11 Aims 51
Chapter 2 Materials and methods 52
2.1 Cell culture 53
2.1.1 Cell culture conditions 53
2.1.2 Plate coating 53
2.1.3 Cell lines 53
2.1.4 Freezing and thawing cells 54
2.1.5 Standard solutions 55
2.1.6 Bacterial cell culture 57
2.2 Cell culture techniques 57
2.2.1 Production of lentiviral vectors in 293T cells 57
2.2.2 HUVEC lentiviral transduction 57
2.2.2.1 IFT88 and RPGRIP1L lentiviral transduction 58
2.2.2.1.1 Doxycycline induction 58
2.2.2.2 Generation of serotonin receptor HTR6-CFP2 lentivirus for cilia monitoring 58
2.2.2.2.1 Lentiviral vector preparation 58
2.2.2.2.2 HiFi assembly cloning 59
2.2.2.2.3 Sequencing 60
2.2.2.2.4 Agarose gel electrophoresis 61
2.2.3 FACS sorting 61
2.2.4 HUVEC-HDF co-culture angiogenesis assay 61

2.2.5 In-vitro ciliogenesis assay 62
2.3 Imaging techniques and immunostaining 62
2.3.1 Co-culture fixation and immunofluorescence (IF) staining 62
2.3.2 Cilia fixation and staining 63
2.3.3 Immunohistochemistry staining (IHC) 64
2.3.4 Confocal imaging 65
2.3.4.1 HUVEC-HDF co-culture confocal imaging 65
2.3.4.2 Cilia imaging 65
2.3.5 Imaging using an EVOS microscope 66
2.4 Image analysis 66
2.5 Microfluidic devices 66
2.5.1 Single chamber microfluidic device fabrication 68
2.5.2 Microfluidic organotypic co-culture 68
2.6 Western blotting analysis (Biochemical techniques) 70
2.6.1 Protein quantification by BCA protein assay 70
2.6.2 SDS-PAGE 70
2.6.3 Western blotting and detection 70
2.6.4 Stripping and reprobing 71
2.7 Statistical analysis 72
Chapter 3 Development of endothelial fibroblast co-culture in microfluidic devices and marking of cilia 73
3.1 Introduction 74
3.2 Optimisation of the organotypic co-culture assay to model angiogenesis *in vitro* 75
3.3 Visualisation of HUVEC in the organotypic co-culture 77
3.4 Marking HUVEC with red fluorescent protein 78
3.5 Employing VE-cadherin-RFP to mark HUVEC with red fluorescent protein 80

3.6 Analysis of tubule and lumen formation in the organotypic co-culture assay…. 82

3.7 Growth factors bFGF and VEGFA stimulate angiogenesis 84

3.8 Single-chamber microfluidic device selected for this project 86

3.9 Single-chamber microfluidic device design 87

3.10 Microfluidic device fabrication 89

3.11 Troubleshooting the loading of cell-fibrin mixture into the chamber of the microfluidic device..... 90

3.12 Tubule formation in the microfluidic device 92

3.13 Anastomosis of the tubules inside a chamber with side channels..... 93

3.14 Angiogenic sprouting and lumen formation modelled by HUVEC in fibrin gels in the microfluidic device 94

3.15 Confirmation of tubule perfusion in the microfluidic device..... 96

3.16 Fluid flow establishes tube hierarchy in the microfluidic device..... 97

3.17 Quantification of tubule and lumen formation in the microfluidic device…. 99

3.18 Circulation and extravasation of cancer cells from endothelial lumens…. 101

3.19 Interaction of injected HUVEC-RFP with pre-established HUVEC-EGFP endothelial tubules 103

3.20 Injected HUVEC-RFP follow the paths formed by pre-established HUVEC-EGFP tubules 105

3.21 Interaction of HUVEC-RFP with pre-established HUVEC-EGFP tubules in the microfluidic device 106

3.22 Assessing live primary cilia dynamics during lumen expansion under conditions of fluid flow 109

3.23 HiFi DNA assembly cloning of the serotonin receptor HTR6-CFP2 fusion into the pWPXL lentiviral vector 110

3.24 Discussion 111

Chapter 4 Effects of primary cilia ablation and ROCK inhibition on blood vessel lumen formation 114
4.1 Introduction 115
4.2 Primary cilia in endothelial cells 116
4.3 Ciliary protein IFT88 knockdown using pTRIPZ system 118
4.4 Ciliary protein RPGRIP1L knockdown using the pTRIPZ system 120
4.5 IFT88 knockdown inhibits tubule formation 121
4.6 RPGRIP1L knockdown inhibits tubule formation 123
4.7 IFT88 knockdown inhibits lumen formation under conditions of fluid flow…. 124
4.8 RPGRIP1L knockdown inhibits lumen formation under conditions of fluid flow…. 126
4.9 IFT88 knockdown inhibits lumen expansion under conditions of fluid flow…. 127
4.10 Localization of HTR6-CFP2 in primary cilia 129
4.11 Characterization of primary cilia in hTERT-RPE1 transduced with HTR6-CFP2 130
4.12 Serotonin receptor HTR6-CFP2 localizes to a longer compartment in primary cilia compared to ARL13B 131
4.13 Serotonin receptor HTR6-CFP2 localizes to primary cilia in HUVEC 132
4.14 ROCK inhibition disrupts lumen formation under conditions of fluid flow…. 133
4.15 Discussion 137
Chapter 5 Role of DOCK4 on tubule and lumen formation under conditions of FGF stimulation 139
5.1 Introduction 140
5.2 Generating endothelial cells with stable DOCK4 knockdown 141
5.3 DOCK4 suppresses FGF driven angiogenesis in the organotypic co-culture assay 142

5.4 DOCK4 influences tubule establishment under FGF and VEGF conditions 144

5.5 DOCK4 does not regulate lateral adhesions under conditions of FGF stimulation 146

5.6 Influence of HUVEC with DOCK4 knockdown on control HUVEC 149

5.7 DOCK4 suppresses EC proliferation under FGF stimulation conditions… 151

5.8 DOCK4 stimulates cilia incidence and suppresses tubule formation under FGF conditions 153

5.9 Effect of DOCK4 knockdown on tubule and lumen formation under conditions of flow 155

5.10 Discussion 157

Chapter 6 Discussion 159

6.1 Introduction 160

6.2 Forming a closed circulatory system of perfused endothelial tubes in the microfluidic device 161

6.3 Role of cilia and ROCK in lumen formation and expansion 164

6.4 DOCK4 suppresses angiogenesis downstream of FGF signalling ... 169

6.5 Concluding remarks 172

List of references……174

List of figures

Figure 1.1 The human circulatory system. 6
Figure 1.2 Sprouting angiogenesis and blood vessel lumen formation. 17
Figure 1.3 The structure and compartment of the primary cilium. 30
Figure 1.4 Primary cilia assembly and disassembly in endothelial cells. 32
Figure 1.5 Four groups of the DOCK family proteins and the domain structure of DOCK4. 46
Figure 1.6 The role of VEGFA and bFGF in tubule formation in the organotypic angiogenesis assay. 50
Figure 2.1 Microfluidic devices for the growth of organotypic co-cultures. 67
Figure 3.1 Organotypic co-culture angiogenesis assay in the absence of fluid flow. 76
Figure 3.2 Modification of HUVEC prior to co-culturing with HDF. 77
Figure 3.3 Comparison of transduction efficiency of lentiviruses harbouring red fluorescent proteins. 79
Figure 3.4 Transduction efficiency of the VE-cadherin-RFP lentivirus. 81
Figure 3.5 Analysis of tubule and lumen formation in the organotypic co-culture assay in the absence of fluid flow. 83
Figure 3.6 Stimulation of organotypic co-cultures with angiogenic growth factors. 85
Figure 3.7 Growth of organotypic co-cultures in the microfluidic devices. 87
Figure 3.8 Detailed design and flow rate in the single-chamber microfluidic device. 88
Figure 3.9 Fabrication of microfluidic devices for introducing fluid flow in organotypic co-cultures. 89
Figure 3.10 Troubleshooting cell-fibrin mixture loading into the chamber of microfluidic device. 91
Figure 3.11 Tubule formation in the microfluidic device under conditions of fluid flow. 92
Figure 3.12 Injection of HUVEC-EGFP for anastomosis of tubules with the microfluidic side channels. 93
Figure 3.13 Lumen formation under conditions of fluid flow in the microfluidic device. 95

Figure 3.14 Flow of fluorescent dextran into the endothelial tubes in the microfluidic device. 96
Figure 3.15 Hierarchy of tubes forming in the microfluidic device under conditions of fluid flow. 98
Figure 3.16 Quantification of tubule and lumen formation in the microfluidic device. 100
Figure 3.17 Visualisation of breast cancer cells and extravasation in the microfluidic device. 102
Figure 3.18 Interaction of HUVEC-RFP injected for anastomosis with pre-established EGFP tubules in the microfluidic device. 104
Figure 3.19 Injected HUVEC-RFPs follow the pre-established HUVEC-EGFP tubules in the microfluidic device. 105
Figure 3.20 Modes of interaction of HUVEC-RFP with pre-established HUVEC-EGFP tubules. 108
Figure 3.21 Schematic of the strategy for insertion of serotonin receptor HTR6 cDNA fused to PS-CFP2 into the pWPXL lentiviral expression vector. 109
Figure 3.22 Strategy for HiFi DNA assembly cloning of serotonin receptor HTR6-CFP2 into the pWPXL lentiviral vector in order to mark cilia (HiFi DNA assembly cloning). 110
Figure 4.1 Primary cilia in a HUVEC monolayer and organotypic co-culture tubules. 117
Figure 4.2 Knockdown of IFT88 using inducible shRNA. 119
Figure 4.3 Knockdown of RPGRIP1L using inducible shRNA. 120
Figure 4.4 Knockdown of ciliary protein IFT88 inhibited tubule formation in organotypic co-culture. 122
Figure 4.5 Knockdown of ciliary protein RPGRIP1L inhibits tubule formation in co-culture. 124
Figure 4.6 IFT88 knockdown inhibits lumen formation in tubules under conditions of flow. 125
Figure 4.7 RPGRIP1L knockdown inhibits lumen formation in tubules under conditions of flow. 126
Figure 4.8 Knockdown of IFT88 inhibited lumen expansion under conditions of flow. 128

Figure 4.9 Transient transfection of hTERT-RPE1 with HTR6-CFP2 lentiviral vector..... 129
Figure 4.10 Visualization of primary cilia in hTERT-RPE1 transduced with HTR6-CFP2. 130
Figure 4.11 Comparison of ciliary length determined by HTR6-CFP2 stable expression and ARL13B staining in hTERT-RPE1. 131
Figure 4.12 Visualization of primary cilia in HUVEC transduced with serotonin receptor HTR6-CFP2..... 132
Figure 4.13 Effect of early ROCK inhibition on lumen formation under conditions of flow. 134
Figure 4.14 Effect of late ROCK inhibition on lumen formation under conditions of flow. 135
Figure 4.15 Effect of ROCK inhibition on lumen formation under conditions of flow (very late treatment). 136
Figure 5.1 DOCK4 knockdown in HUVEC. 141
Figure 5.2 Effect of DOCK4 knockdown on tubule formation in the presence of FGF or VEGF. 143
Figure 5.3 Effect of DOCK4 knockdown on tube and lumen formation..... 146
Figure 5.4 The effect of DOCK4 knockdown on lateral adhesion. 148
Figure 5.5 Tubules with DOCK4 knockdown do not influence newly forming HUVEC-RFP (control) tubules. 151
Figure 5.6 DOCK4 knockdown stimulates endothelial cells proliferation in tubules under FGF conditions. 152
Figure 5.7 Effect of DOCK4 knockdown on cilia. 154
Figure 5.8 Effect of DOCK4 knockdown on tubule formation and lumenised length under condition of flow..... 156

List of tables

Table 2.1 List of commonly used standard solutions used throughout this study. 56
Table 2.2 List of primary antibodies used for immunofluorescence. 63
Table 2.3 List of secondary antibodies used for immunofluorescence. 64
Table 2.4 List of antibodies used for immunoblot assays. 72
Table 3.1 Readouts of tubule morphology in organotypic co-cultures. 84

List of Abbreviations

ARL13B	ADP-Ribosylation Factor-like Protein 13B
bFGF	basic fibroblast growth factor
bp	base pair
BPI	Branch point index
CD31	Cluster of differentiation 31 (PECAM-1)
CDC42	Cell division control protein 42 homolog
CTS	Ciliary targeting sequence
DAPI	4′,6-diamidino-2-phenylindole
DHR1	DOCK homology region1
DHR2	DOCK homology region2
DMEM	Dulbecco's Modified Eagle Medium
DMSO	Dimethyl sulfoxide
DNA	Deoxyribonucleic acid
DOCK	Dedicator of Cytokinesis
DOCK4	Dedicator of Cytokinesis 4
Dock4het	Dock4 heterozygous knockout mice
ds-Red	Discosoma Red fluorescent protein
DTT	Dithiothreitol
EC	Endothelial cell
ECM	Extracellular matrix
EGF	Endothelial growth factor
EGFR	Epidermal growth factor receptor
ELMO	Engulfment and cell motility
eNOS	Endothelial nitric oxide synthase
FACS sorting	Fluorescence activated cell
F-actin	Filamentous actin
FBS	Fetal Bovine Serum
FCS	Foetal Calf Serum
FGF	Fibroblast growth factor
FGFR	Fibroblast growth factor receptor
FITC	Fluorescein isothiocyanate

g	gravitational acceleration
G-actin	Globular actin
GAP	GTPase activating proteins
GAPDH	Glycerinaldehyde-3-Phosphate-Dehydrogenase
GDI	Guanine dissociation inhibitors
GDP	Guanine diphosphate
GEF	Guanine nucleotide exchange factors
GF	Growth factor
EGFP	Enhanced Green Fluorescent Protein
GTP	Guanine triphosphate
HCMEC	Human Cerebral Microvascular Endothelial Cells
HDF	Human Dermal Fibroblast
HEK 293T	Human Embryonic Kidney Cells 293T
HH	Hedgehog pathway
HRP	Horseradish peroxidase
hTERT-RPE1	hTERT-immortalized retinal pigment epithelial cells
HTR6	5-hydroxytryptamine receptor 6
HUEC	Human umbilical vein endothelial cells
IF	Immunofluorescence
IFT	Intraflagellar transport
IHC	Immunohistochemistry
IP	Immunoprecipitation
KO	Knockout
L1CAM	L1 cell adhesion molecule
LB	Lysogeny broth
LIMR	Leeds Institute of Medical Research
LVEM	Large Vessel Endothelial Medium
MAPK	P42/44 mitogen-activated protein kinases
mCherry	monomer Cherry
NOTCH	Notch homolog
PBS	Phosphate Buffered Saline solution
PCMC	periciliary membrane compartment

PECAM	Platelet endothelial cell adhesion molecule 1
PFA	Paraformaldehyde
PH	Pleckstrin Homology
PI3K	Phosphatidylinositol-3-kinase
PS-CFP2	Photoswitchable Cyan fluorescent protein
RAC	Ras-related C3 botulinum toxin substrate
RFP	Red fluorescent protein
Rho	Ras homolog
RhoA	Rho GTPases member A
RNA	Ribonucleic acid
ROCK	Rho associated coiled-coil protein kinase
RPGRIP1L	Retinitis Pigmentosa GTPase Regulator 1 Interacting Protein 1 Like
Rpm	revolutions per minute
RT	Room Temperature
SDS-PAGE	Sodium Dodecyl Sulfate Polyacrylamide Gel Electrophoresis
SGEF	Src homology 3 domain-containing Guanine
SH3	Src-Binding
shRNA	short hairpin Ribonucleic Acid
siRNA	small interfering Ribonucleic Acid
SMC	Smooth muscle cell
TBS	Tris-Buffered Saline
TBST	Tris buffered saline + Tween
TNF-α	Tumour necrosis factor alpha
VE-cadherin	Vascular endothelial cadherin
VEGF	Vascular endothelial growth factor
VEGFA	Vascular endothelial growth factor A
VEGFR	Vascular endothelial growth factor receptor
VSMC	Vascular smooth muscle cells
WT	Wild type

Chapter 1

Introduction

1.1 The circulatory system

Healthy tissue homeostasis requires efficient and simultaneous blood transportation, gas exchange and efficient waste product removal via the circulatory system. The circulatory network consists of: heart, the blood vessels and the lymphatic vessels. The circulatory system performs a fundamental role in tissue homeostasis through delivery of oxygen and nutrients and waste removal to and from all cells and tissues in the entire body. It also plays roles in transporting immune cells, inflammatory cytokines, signalling molecules and growth factors (GFs) to distinct sites (R. H. Adams & Alitalo, 2007).

The blood circulatory system (cardiovascular system) is an enclosed system composed of the heart and blood vessels. Heart is central of the circulatory system pumping blood into the network of blood vessels. This muscular pump is made up of four chambers: the left and right atriums, and the left and right ventricles. These chambers are separated with one-way valves to keep the blood flow unidirectional. The heart pumps blood all over the body through the heartbeat which is contraction and relaxation of the heart muscles (Carmeliet, 2000).

Blood vessels form a closed circulatory system all over the body and are lined by a specialized layer of endothelial cells (ECs). The complex network of blood vessels is composed of arteries, veins and capillaries, each with unique structure and function. Arteries transfer oxygenated and nutrient-rich blood away from the heart to tissues in the body, whilst veins return deoxygenated and low-nutrient blood back to the heart. Capillaries are networks of small blood vessels that bridge arteries and veins, and function in delivering blood deeper into cells and tissues.

The function of blood vascular system is complemented by the lymphatic system which regulates tissue fluid balance, immunological functions and facilitates interstitial protein transport (Pepper & Skobe, 2003). The lymphatic vasculature comprises a unidirectional network of blunt-ended capillaries (terminal lymphatics) that drain lymph (fluid that leaks from blood vessels) and carry it into

the tissues. Lymph empties back into the venous circulation via lymphatic-venous junctions after being filtered through the lymph nodes. Lymphatic vessels are lined by lymphatic endothelial cells (Alitalo et al., 2005).

1.1.1 Blood vessels and the endothelium

The vascular network shows hierarchy (Branching morphogenesis) and is made up of two independent networks which work together to establish blood flow throughout the body, the systemic and the pulmonary systems. Through the systemic system the main artery (aorta) branches from the heart into arteries which lead to smaller vessels termed arterioles and then to a network of small capillary vessels known as the capillary network, where the blood releases oxygen and nutrients to tissues and cells. In return blood collects waste products and carbon dioxide through the capillary system which then travel through the veins to the heart. Later the pulmonary circulation which is responsible for providing fresh oxygen and removing carbon dioxide from the blood takes over, and transfers low-oxygen blood into the pulmonary artery. This then branches into arteries and capillaries which exchange carbon dioxide for oxygen.

The ECs line the whole cardiovascular system from the heart to the arteries, veins and small capillaries (Rajendran et al., 2013). A cohort of ECs dynamically assemble into a vascular network. Individual ECs perform coordinates migration, cell-cell and cell-extracellular matrix (ECM) adhesion, proliferation, degradation of ECM and sprouting of the vascular network. Blood vessels may specialize to acquire functional characteristics dependent on their location. Nonetheless, human blood vessels maintain the same histological organization of an endothelial single layer, with a luminal-abluminal polarity. The layer of ECs arranges into a tube connected to vascular basement membrane, and a layer of mural cells including smooth muscle and pericytes on the abluminal side (Lammert & Axnick, 2012). Following blood flow establishment, ECs acquire planar cell polarity which is a pathway of signalling cascade to coordinate the morphogenic movements (Lizama & Zovein, 2013). The endothelium forms a

tubular vascular structure vital in maintaining a non-thrombogenic blood-tissue interface that regulates blood flow, vascular tone, thrombosis, thrombolysis and platelet adherence. In the same time vasculature functions as secretory, synthetic, metabolic and immunologic entity (Cines et al., 1998) and (Verhamme & Hoylaerts, 2006).

Endothelial cells form a dynamic barrier that is covered by smooth muscle cells (SMCs) and ECM dominantly comprised of collagen and elastin in larger vessels. The endothelium is a selective permeable barrier between tissue and circulation blood and control vasodilation and blood vessel generation (Herbert & Stainier, 2011).

1.1.2 The peripheral vascular system

All the blood vessels outside the heart are known as peripheral vascular system (PVS) which includes the aorta, arterioles, capillaries, venules and veins. The structure and function of each vessel is modified according to the organ it supplies (Tucker et al., 2022). Aside from capillaries, all blood vessels comprise three layers: tunica adventitia, tunica media and tunica intima. The tunica adventitia is the outermost layer of the abluminal side of blood vessels and is a supportive layer that primarily consists of extracellular matrix, fibroblasts and progenitor cells; tunica media is the middle layer comprising an elastic and muscular tissue that consists of smooth muscle cells which regulates the internal diameter of the blood vessels; the innermost layer is the tunica intima comprises ECs which line the blood vessel lumen (Mazurek et al., 2017). Capillaries are lined by one cell layer, the tunica intima (Mazurek et al., 2017) (Figure 1.1).

1.1.2.1 Arteries and arterioles

Arteries has a crucial role in nourishing tissues and organs through blood delivery. There are two types of arteries; Arteries as they are closer to the heart,

known as elastic arteries, have a thicker layer of elastic tissue that enable them to alter the diameter and increase in size, and less smooth muscle; Arteries branching into the smaller vessels in organs, known as muscular arteries, have less elastic tissue and more smooth muscle cells (Tucker et al., 2022). Arterioles regulate blood flow in the vascular system because they are major source of resistance (Delong & Sharma, 2022).

1.1.2.2 Venules and veins

Venules have very thin walls and they transfer blood from capillaries to the veins. Veins retain related structure to arteries with the same three layers, but have thinner walls and less elasticity. Unlike arterial pressure, the venous pressure is low. The veins hold a large volume of the blood in circulation, at any time point around three-fourths of the blood volume is contained in the venous system. In order to guide blood circulation back to heart there are one-way valves in the vessels located deep inside body and called deep veins (Tucker et al., 2022).

1.1.2.3 Capillaries

Capillaries are patterned by endothelial cells surrounded by pericytes and a layer of basement membrane in abluminal side. Capillaries arise from the arterioles and converge into venules (Murrant et al., 2017). Capillaries comprise the main site of gas and nutrient exchange between blood and tissues because of their thin wall structure and large surface area to volume ratio (E. Kang & Shin, 2016).

Arterioles and venules have more coverage of mural cells compared to veins. Arteriole and venule wall are formed by ECs covered by internal elastic lamina, smooth muscle actin and basement membrane and on top by external elastic lamina in abluminal side. Elastic laminae and SMCs regulate vessel tone and as a result modulate vessel diameter and blood flow. Arterioles and venules are covered by mural cells more than capillaries (Jain, 2003).

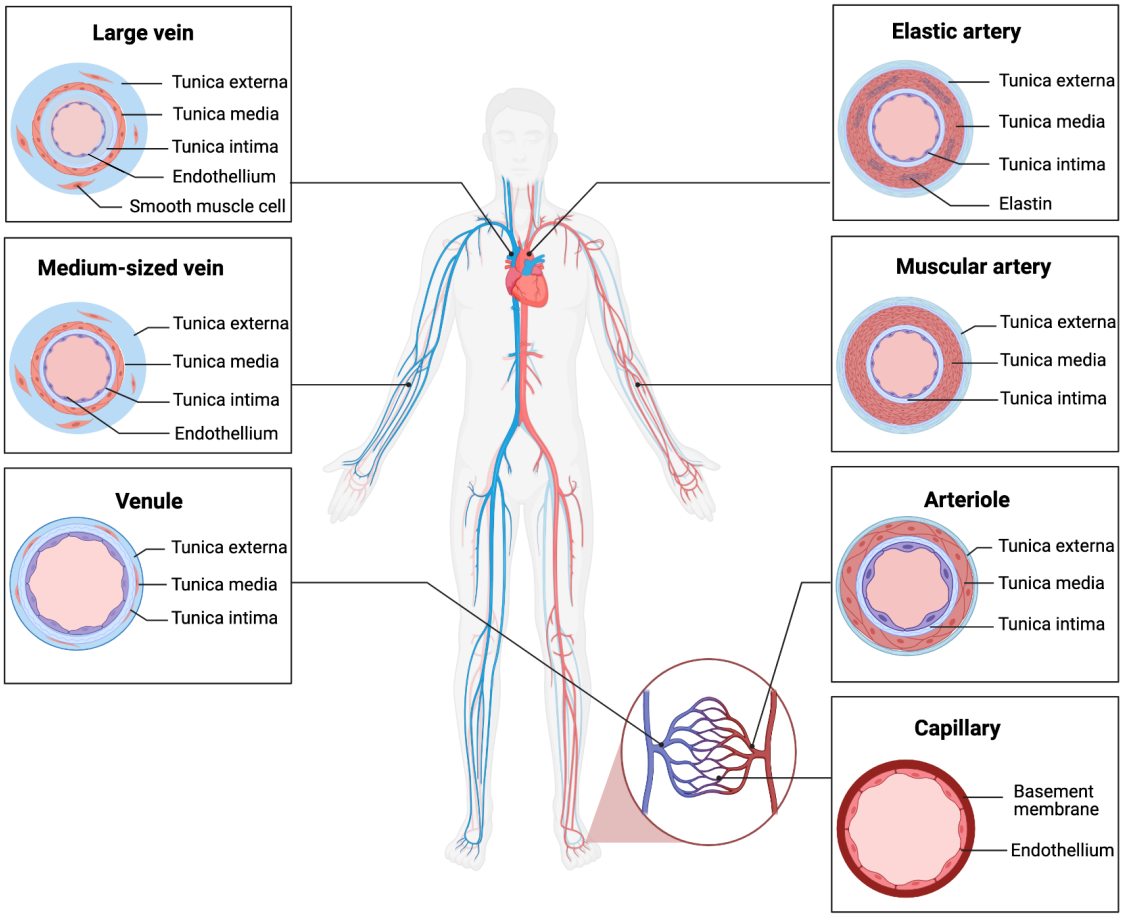

Figure 1.1 The human circulatory system.

Diagram of the circulatory system in human: arteries, arterioles, veins, venules and capillaries. Arteries have three structural layers: The tunica externa, tunica media, and tunica intima. The tunica externa is the outer layer of arteries and consists of connective tissue, collagen, and elastic fibres. The tunica media, the middle layer includes smooth muscle cells and elastic fibres. The tunica intima is the inner most layer of the arteries and is comprised of endothelial cells. There are three types of arteries: elastic arteries, muscular arteries, and arterioles. Veins also have three distinct layers; the tunica externa, tunica media, and the tunica intima. The tunica media of veins contain an irregular covering of vascular smooth-muscle cells and pericytes. Capillaries are small vessels formed by a single layer of flattened ECs with no muscular layer. Created with BioRender.com.

1.1.3 Collateral arteries

In order to overcome hypoperfusion of certain areas in the adult body, there are two crucial mechanisms of circulation growth. One is angiogenesis, or growth of new capillaries under hypoxic conditions described in section 7.2; and the second is arteriogenesis or remodelling of pre-existing collateral arterioles towards functional arteries.

Collateral arteries created by anastomosis of non-functional but active collateral arterioles with functional arterioles, so it bypasses the site of obstruction and maintains viability of the tissue that is threatened by ischaemia (de Groot et al., 2009). Once blood flow to the collateral artery anastomoses has been initiated, sheer stress of the blood flow drives arteriogenesis of the dormant micro vessel to develop into a full-grown conductance artery. The number and patterning of pre-existing collateral arteries prior to an occlusion markedly influence the adequacy of the diversion of blood flow to the affected tissue (Ramo et al., 2016).

1.1.4 Mural cells

Mural cells in the vasculature refer to both the SMC and pericytes (Lin et al., 2021). For maturation of nascent vasculature, recruitment of mural cells is necessary and depends on the location and function of blood vessels.

Mural cells stabilize nascent vessels by inhibiting proliferation and migration of endothelial cells, and by increasing production of extracellular matrix (Carmeliet, 2000). Mural cells that are responsible for contraction and dilation of blood vessels, provide scaffold to vascular structures. Mural cells have direct contact with ECs to co-regulate vascular function by paracrine signalling (Gerhardt et al., 2003) (Vanlandewijck et al., 2018). They are essential for control of blood pressure, regulation of blood distribution and the structural integrity and support to the vascular wall (Zhuge et al., 2020). Vascular SMCs (VSMCs) are located in the tunica media of the arteries and arterioles wall and are responsible for

contraction and relaxation, whilst pericytes which are their equivalent are located around venules and capillaries (Attwell et al., 2016).

VSMCs dysfunction can causes cardiovascular diseases such as atherosclerosis (Tabas et al., 2015) and pericyte dysfunction plays a crucial role in neurodegenerative diseases such as Alzheimer's and Parkinson's diseases (Sweeney et al., 2018).

1.2 Development of blood vessels

Blood vessels development occurs through the process of angiogenesis, vasculogenesis and arteriogenesis. As mentioned earlier angiogenesis refers to sprouting of blood vessels followed by stabilization of sprouts by mural cells, whilst arteriogenesis refers to collateral growth of pre-existing vessels to form a bridge between arterial networks (Carmeliet, 2003). During vasculogenesis, mesodermal cells differentiate to endothelial cell precursors known as angioblasts (Risau, 1997) which develop into the mesodermal compartment and generate endothelial cells in the blood islands (Palis & Yoder, 2001). Endothelial precursors differentiate to ECs and coalesce into cord-like structures (Risau & Flamme, 1995) (Coultas et al., 2005). Vasculogenesis and early vessel formation occurs in the absence of blood flow and it can be guided by genetics, environmental and mechanical inputs (E. A. Jones et al., 2006). Early blood vessels remodel and expand via the process of angiogenesis.

1.2.1 Expansion of vascular network

Angiogenesis initially happens after vasculogenesis and formation of early primitive vascular structure. During this highly dynamic process, ECs of vessels undergo various cellular processes including sprouting, migration, proliferation and polarization in response to external stimuli (Carmeliet & Jain, 2011). Angiogenic vessels sprout, and shape the whole circulatory system into a

functional organ that reaches all tissues in the body, and vessels specialise according to their location in different tissues (Kwei et al., 2004). During development of the coronary plexuses arterial and venous blood vessels become segregated through expression of specific molecular markers. Pre-arterial endothelial cells express ephrinB2 and neuropilin 1 (NRP1) (R. H. Adams & Alitalo, 2007). Whilst venous endothelial cells express EphB4 (erythropoietin-producing human hepatocellular receptor 4) (Borasch et al., 2020).

1.2.2 Maturation of vascular network

Blood vessel maturation defines as stepwise transition of actively growing vasculature to a quiescent, completely formed and functional network (Torres-Vazquez et al., 2003). Maturation of the nascent vasculature requires: suppression of endothelial proliferation and sprouting, stabilization of existing vascular tubes, protection against growth factor (VEGF) withdrawal, cellular differentiation processes like formation of valves, fenestrations or tight-junction barriers, and mural cell recruitment into the vessel wall and generation of extracellular matrix (Jain, 2003). During embryonic development, the nascent vascular network is formed by vasculogenesis and angiogenesis. The least understood step in maturation of vessels is organ-specific specialization of blood vessel network structure (Ruoslahti, 2002). Capillaries organ-specific specialization includes arterio-venous determination, formation of heterotypic and homotypic junctions, and EC differentiation to form organ-specific capillary structures (Jain, 2003). New vessel growth, maturation and maintenance are highly complex and coordinated processes that need the sequential activation of an array of receptors by various ligands (Yancopoulos et al., 2000) (Ferrara & Alitalo, 1999).

1.2.3 Angiogenesis growth factors FGF and VEGF

EC specific growth factors and their receptors are classified into vascular endothelial growth factor (VEGF) and angiopoietin (Ang) families (Korpelainen & Alitalo, 1998). Other growth factors like bFGF mostly secreted by fibroblast and bound to extracellular matrix are important angiogenic factors (Ferrara & Davis-Smyth, 1997). bFGF and VEGFA are necessary for vasculogenesis/angiogenesis and arteriogenesis during embryonic (Tomanek et al., 2008) and postnatal development (Tomanek et al., 2001).

VEGF known as vascular permeability factor (VPN) is a growth factor produced by many cells. VEGF comprises five members: VEGF- A, B, C, D and placenta growth factor (PGF). All members of the VEGF family bind to tyrosine kinase receptors (the VEGFRs) on the cell surface to stimulate cellular responses. VEGFA specifically acts on vascular ECs and binds to VEGFR1 and VEGFR2. VEGFR2 regulate almost all of the known endothelial cellular responses to VEGF. VEGFR1 responsibility is not well understood but it's thought it modulates VEGFR2 signalling.

VEGFA is expressed by fibroblasts, macrophages, monocytes and lymphocytes and acts as mitogen of ECs. Hypoxia, activated oncogenes and cytokines are stimulants of VEGF expression (Krock et al., 2011). The HIF-1 releasing commences transcription of VEGF in hypoxia. Moreover, VEGF has a vital role in pathological angiogenesis by inducing anti-apoptotic proteins expression in ECs contributing to tumour growth (Haase & Kamm, 2017).

Expression of VEGFR2 is the earliest marker of angioblasts. VEGFR2 knockout mice die in utero between E8.5 and 9.5 because of lack of EC differentiation, blood island formation and vasculogenesis (Shalaby et al., 1995). Deficiency in VEGFA which is the ligand for VEGFR2 caused abnormal blood vessel development and embryonic death (Carmeliet et al., 1996).

In human there are 23 members of FGF family proteins including FGF-1-23. FGF2 also known as basic fibroblast growth factor bFGF is a signalling protein

encoded by the FGF2 gene and bind to fibroblast growth factor receptor (FGFR) proteins.

For the growth of the endothelial plexuses during vasculogenesis, the interplay among VEGFs expressed in the myocardium which bind to receptors specific to the endothelium (VEGFR) is essential. bFGF are essential where VEGF initially regulates tubulogenesis and bFGF regulates the proliferation of ECs (Pennisi & Mikawa, 2005) (Tomanek et al., 2001) (Tomanek et al., 2010). VEGF is a secreted angiogenic mitogen (Leung et al., 1989). During angiogenesis, endothelial tip cells are stimulated and directed by an extracellular gradient of VEGFA and bFGF (Ruhrberg et al., 2002) (Beckers et al., 2010) (Wojciak-Stothard & Ridley, 2002). VEGFR2 control most of the EC responses to VEGFA including induction of tip cell filopodia and EC migration, proliferation, survival and vascular permeability (Olsson et al., 2006). VEGF and bFGF are sequestered in the extracellular matrix (Jain, 2003) and working together for developmental angiogenesis, FGF effect on blood vessels are VEGF dependent, whilst VEGF-induced tubulogenesis required FGF signalling (Tomanek et al., 2010). Angiogenic growth factors operate in perfect harmony in a complementary and coordinated manner to form functional blood vessels (Gale & Yancopoulos, 1999).

1.3 Pathological angiogenesis

Angiogenesis plays a crucial role during development whilst in the adult deficiency in its regulation can cause a variety of pathological conditions including ischemic and inflammatory diseases. Furthermore, vascular abnormalities can contribute to the pathology of several diseases including primary and metastatic tumour growth, diabetic retinopathy, macular degeneration, tissue ischemia and cardiovascular diseases (Gupta & Qin, 2003).

When physiological stress or pathological conditions disturb the cells and disrupt homeostasis, the organ reacts primarily by inflammation. When this protective

reaction is chronic, pathologies increase (Taniguchi & Karin, 2018). Blood vessels when permeable allow crossing of inflammatory mediators and immune cells to the site of stress or injury (Aguilar-Cazares et al., 2019). Overall, cross talk amongst components of the tissue microenvironment including vascular ECs, parenchymal cells, stromal cells and extracellular matrix are necessary for organ to function (Hinshaw & Shevde, 2019). ECs control the microenvironment in an organ-specific manner as well as providing barrier function (Augustin & Koh, 2017). Angiogenesis and inflammation play a cooperative role together in many inflammatory diseases, and hypoxia play a role as a common stimulus for both (Costa et al., 2007). During inflammation, proliferating tissue is full of inflammatory cells, growth factors, macrophages and other immune cells that under hypoxic conditions release various angiogenic factors (Jackson et al., 1997). In turn, angiogenesis assists the inflammatory site by providing the oxygen, nutrients and enormous surface area for the production expression and trafficking of essential cytokines, adhesion molecules and other inflammatory mediators (Costa et al., 2007).

1.3.1 Tumour angiogenesis

Pro- and anti-angiogenic factors regulate vascular homeostasis, the vasculature remains quiescent and ECs are non-proliferative as long as these factors are in balance. Initiation of angiogenic switch and rapid growth of malignant cells occurs in tumours when pro-angiogenic signalling is dominating (Hanahan & Folkman, 1996) and new blood vessels are forming. The angiogenic switch can be initiated by additional genetic changes in tumour cells, or by tumour-associated inflammation and recruitment of immune cells, or expression of pro-angiogenic factors by other components of the tumour microenvironment such as stromal fibroblasts (Lugano et al., 2020).

Malignant cells need oxygen and nutrients to proliferate and survive, in order to access the blood circulation, they reside close to blood vessels to access the blood circulation system. Therefore, tumour progression is accompanied by

ingrowth of blood vessels (Folkman, 1971). Tumours can be vascularised by inducing new vascular formation or co-option of the pre-existing vessels (Kuczynski et al., 2019) or by inducing new vascular formation.

Tumour growth, maintenance and metastasis are highly dependent on the process of angiogenesis which is initially starts from the capillaries. Blood vessel formation in tumours can be induced by different cellular processes including Sprouting or intussusceptive angiogenesis, vasculogenesis (formation of blood vessels from endothelial progenitor cells (EPCs)), following recruitment differentiation to ECs, vasculogenic mimicry (formation of vascular-like structures by tumour cells), and trans-differentiation of cancer stem cells (differentiation of cancer cells to cancer stem cells and then to ECs) (Lugano et al., 2020). EPCs contribute to postnatal vasculogenesis can be differentiated from hematopoietic stem cells, myeloid cells, circulating mature endothelial cells or other progenitor cells (Chopra et al., 2018) and differentiate into mature ECs and incorporate into sites of active neovascularization (Reale et al., 2016).

1.3.2 Retinopathy

Two vascular networks supply blood to the retina; the retinal vasculature supports the inner retina and the choroidal vasculature supplies the retinal pigment epithelium and photoreceptors (Campochiaro, 2015). Retinopathy occurs as a consequence of pathological alteration in the ocular vasculatures. In the adult abnormal growth of chroidal vessels causes wet Age-related macular degeneration with Choroidal neovascularization and in preterm neonates abnormal growth of retinal vasculature causes Retinopathy of prematurity (Dai et al., 2021).

1.3.3 Tissue ischemia

Tissue ischemia is a restriction in blood supply to a tissue which as result becomes unable to meet metabolic demands (Sidawy, 2019). Tissue ischemia causes neovascularization and the formation of new vessels is through the process of angiogenesis in response to a hypoxic environment, arteriogenesis by progression and expansion of existing collateral smooth muscle-type vessels, or vasculogenesis from progenitor cells or stem cells (Silvestre et al., 2008). Atherosclerosis can obstruct an arterial lumen or cause a rupture and cause hypoxia (low levels of oxygen) or ischemia (restricted or reduced blood and as a result oxygen) of the tissue (Jaipersad et al., 2014). Atherosclerosis happens by development of calcium, fibrin, cellular waste products and lipid rich plaques inside the layers of the arterial wall followed by monocyte infiltration and the lipid core formation (Glass & Witztum, 2001).

1.4 Mechanisms of blood vessel growth

1.4.1 Vasculogenesis

Vasculogenesis is the process of *de novo* blood vessel formation induced by differentiation of EPCs into ECs in embryonic development and *de novo* formation of a primitive vascular network (Risau et al., 1988) or after birth during capillary formation post ischemia (Asahara et al., 1997) or in tumours (Bussolati et al., 2011). In the embryo blood islands form by the cluster of progenitor cells. Endothelial progenitor cells (EPCs) are circulating cells that express cell surface markers same as those expresses by vascular ECs and they can participate in formation of new blood vessels. EPCs are mostly originate from bone marrow (M. C. Yoder, 2012).

1.4.2 Angiogenesis

Angiogenesis is formation of new vessels branch from pre-exciting vessels which causes vascular development through sprouting angiogenesis (Eilken & Adams, 2010), and intussusceptive angiogenesis (V. Djonov et al., 2000).

1.4.2.1 Sprouting angiogenesis

Angiogenesis is the formation of blood vessels from pre-existing vasculature. In the adulthood, vasculature is almost quiescent with little vessel growth or remodelling. However, angiogenesis is necessary in response to injury, pregnancy, menstrual cycle, reduced oxygen or hypoxic conditions, inflammation, tumour growth, tissue healing and placental vascularization (Carmeliet, 2005) (Potente et al., 2011) (Melincovici et al., 2018). During angiogenesis, ECs secreted matrix metalloproteinases (MMPs) which are zinc-dependent proteolytic enzymes that degrading extracellular matrix, enabling new vessel sprouts to grow through the action of growth factors, promoters and inhibitors of angiogenesis, various signalling molecules and adhesion proteins (Tonini et al., 2003). ECs in response to pro-angiogenic stimuli, specialize into various subtypes and perform specific functions (Gerhardt et al., 2003). Formation of sprouts comprises multiple steps including tip cell selection, sprout extension and lumen formation.

During tip cell formation the existing vasculature wall is disassembled by enzymatic degradation of the ECM structure and basal lamina (Kubis & Levy, 2003). A cell among ECs in a vessel becomes a tip cell and guides the migration of the vascular branch by responding to angiogenic cues and blocking follower ECs by a lateral inhibition process (Lugano et al., 2020). Stalk cells are located behind the tip cells and proliferate to extend the vascular branch. A stalk cells can be induced to become a new tip-cell and take the position of an old tip cell (Phng & Gerhardt, 2009). The tip cell extends through the chemotactic path followed by trailing stalk cells and at the end the luminal space of the sprout connects with the lumen of the parent vessel (Lugano et al., 2020). Endothelial

tip cells and stalk cells are distinguished by their position, dynamic filopodia formation and migratory behaviour that determine the direction of new sprout growth (Blanco & Gerhardt, 2013).

The arrangement of endothelial cells in tip and stalk cells are the main operator of sprouting angiogenesis and regulated by cross-talk between the VEGF and Delta-like 4 (DLL4)-Notch (DLL4/Notch) pathways (Jakobsson et al., 2009). DLL4/Notch signalling is responsible for the selection of tip- and stalk-cells; Tip cells are subject to higher levels of Notch signalling compared to stalk cells because of higher level of DLL4 (Hellstrom et al., 2007). The level of VEGFRs in ECs is influenced by Notch signalling (Williams et al., 2006). In response to VEGF, production of DLL4 ligand and blockage of Notch signalling happen in tip cells, followed by enhance in sprouting, branching, migratory capacity and filopodia formation in tip cells (Jakobsson et al., 2010). DLL4 secretion by tip cells activate Notch signalling in the neighbouring ECs and suppressing their transformation to tip cell (Hellstrom et al., 2007). After the vasculature has fully expanded, EC proliferation and migration are prevented by anti-angiogenic factors (Benson & Southgate, 2021). At this point the vessel is remodelled, the basal lamina reconstitutes and the vessel wall re-assembles, followed by re-stabilisation and maturation by pericytes or smooth muscle cells (Kubis & Levy, 2003) (Figure 1.2).

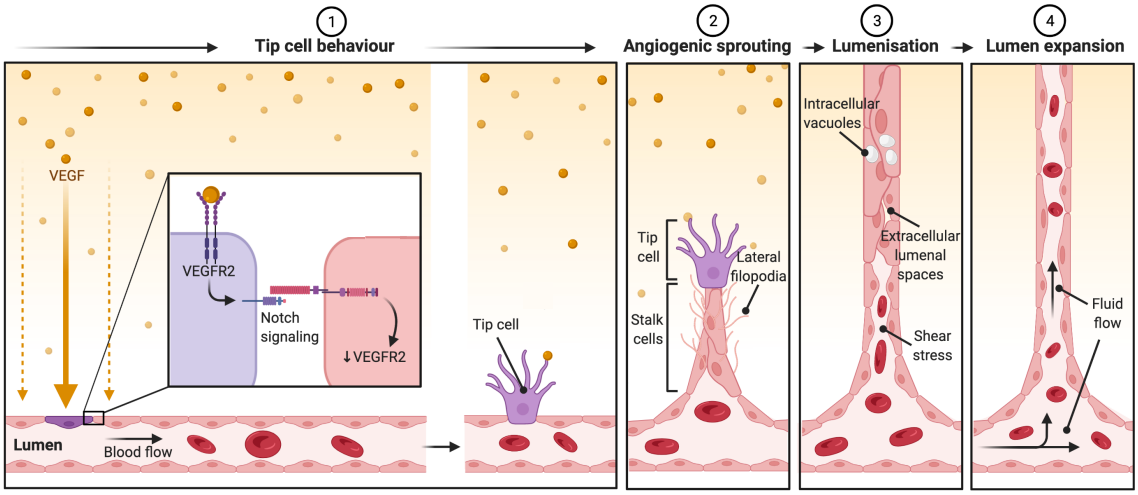

Figure 1.2 Sprouting angiogenesis and blood vessel lumen formation. **A.** VEGF binds and activate VEGFR1 and VEGFR2 in vascular ECs. VEGFR2 control almost all of the known cellular responses to VEGF. VEGFR1 responsibility is not well understood but it is thought it modulates VEGFR2 signalling. **B.** VEGF selects tip cell in order to start sprout extension, EC migration and proliferation. Stalk cells are located behind the tip cells and proliferate to extend the vascular branch. **C.** Lumen forms by shear stress and by connection of intracellular vacuoles together or to extracellular luminal spaces. **D.** Fluid flow and shear stress complete lumen formation and lumen expansion. I made this figure because it is the best understood process of lumen formation and lumen expansion. Created with BioRender.com.

1.4.2.2 Intussusceptive angiogenesis

Intussusceptive angiogenesis (IA) or nonsprouting angiogenesis is a dynamic intravascular process that forms new blood vessels by the division of a single vessel into two lumens (Konerding et al., 2010) (Mentzer & Konerding, 2014). The first step in intussusceptive angiogenesis is the generation of trans-vascular tissue pillars which are cylindrical microstructure that generate the blood vessel lumen and microcirculation (Burri et al., 2004) (Mentzer & Konerding, 2014). The advantage of the IA is that vasculature is formed more rapidly, and the formed

capillaries are less leaky (Ribatti & Djonov, 2012). Caduff et al. (1986) study on the developing rat lung demonstrated that throughout the rapid alveolarization and capillary growth, microcirculation was extending without capillary sprouts, but with the small holes in the alveolar microvasculature that generated multiple new blood vessels. Pillar extension occurs by remodelling, duplication of an existing vessel, and pruning of a redundant vessel (Mentzer & Konerding, 2014). In the chicken chorioallantoic membrane local blood flow acceleration and high blood pressure results in intussusceptive pillar formation (V. G. Djonov et al., 2002) (V. Djonov et al., 2003) (Kurz et al., 2003). Initiating of the pillar formation has been influenced by changes in fluid flow (Burri et al., 2004), and pillar extension depends on intravascular fluid flow (Mentzer & Konerding, 2014). In most of the studies intravascular pillars have been identified in capillaries and small vessels, for instance in the developing chick chorioallantoic membrane (Makanya et al., 2009); in a number of tumours (Ribatti & Djonov, 2012); murine chemically-induced colitis (Konerding et al., 2010); and the physiologic angiogenesis in skeletal muscle (Egginton et al., 2001).

1.5 Lumen formation

Lumen formation is the process of transformation of cords into perfusable vascular tubes. Lumen morphogenesis requires, cell-cell contact, establishment of polarity, dynamic contact of the cells with underlying ECM, and actin cytoskeleton rearrangement to expand the luminal side (Parsons et al., 2010).

1.5.1 Mechanisms of lumen formation

Lumen formation happens in a heterogeneous manner through various mechanisms (Charpentier & Conlon, 2014). Two cellular mechanisms have been described, intracellular lumen formation and extracellular lumen formation.

Intracellular lumen formation is hollowing by a vacuolation mechanism (cell hollowing). Individual ECs generate vacuole-like structures via membrane internalization and the vacuoles fuse and form a hollow tube with no ECM (vacuole coalescence), later when vacuolated cells form a network unicellular tube is made without cell-lumen boundary. Then the luminal side of opening extends further by invagination of the membrane (apical membrane invagination) to the point of contact between cells resulting in one continuous lumen. Therefore, each cell makes up a unicellular tube which has an intracellular lumen (Davis & Bayless, 2003).

Blood vessel lumens may form extracellularly between ECs joined by adherence junctions (cord hollowing). The lumen forms by movement of junction from the centre to the periphery and formation of the luminal compartment between ECs originally joined by lateral adhesions. Before separation of ECs, cell polarization takes place through localization of a number of molecules to the apical surface where the lumen will be generated including the positively charged glycoprotein podocalyxin. Electrostatic repulsion due to the positive charge then opens up the lumen (Strilic et al., 2009). Extracellular lumens can arise in zebrafish ISV as well as mouse DA by cord hollowing (Blum et al., 2008).

New vessels can be also formed by extracellular mechanism during anastomosis or fusion of two perfused blood vessels to combine luminal compartments. For example, formation of zebrafish dorsal longitudinal anastomosing vessel (DLAV) through anastomosis of arteries (Herwig et al., 2011) and palatocerebral artery (PLA) in the cranial vasculature (Lenard et al., 2013). In both the DLAV and PLA, apical membrane invagination and blood vessel lumen generation is dependent on blood flow force, whilst junctional rearrangement and polarity still takes place in the absence of flow (Herwig et al., 2011).

In the majority of blood vessels cord hollowing is the common mechanism of blood vessels lumen formation (Reviewed by Lammert and Axnick (2012)). The predominant cellular mechanism of lumen formation appears be the extracellular mechanism like the dorsal aorta formation. Whereas small-caliber vessels such as ISVs and capillaries may using a combination of cell and cord hollowing

(Charpentier & Conlon, 2014). These processes of *de novo* lumen formation are independently of blood flow.

1.5.2 ECs acquisition of apical polarity

ECs first step to form lumen is to have specialized distinction between the inside and outside of the tube, and they establish polarity to have apical/luminal polarity inside the tube and basal/abluminal outside the vessel surface (Lizama & Zovein, 2013). This apicobasal polarity can be seen in other tubular organs including the kidney and intestine (Rodriguez-Fraticelli et al., 2011).

Markers localize preferentially to either the basal or apical side of ECs-lined the tube. CD34, podocalyxin-like proteins 1 and 2 (PODXL/PODXL2), and the Ezrin-Radixin-Moesin (ERM) protein Moesin are localize at the apical membrane (Nielsen & McNagny, 2008) (Strilic et al., 2009) (Lampugnani et al., 2010) (Y. Wang et al., 2010). The partition-defective (Par) polarity complex (Par3/Par6/atypical protein kinase C [aPKC]) also has effect on apical polarity in EC and epithelial cells, and the Par complex disruption results in failed lumen formation (Joberty et al., 2000) (Zovein et al., 2010). Deficiency of Par3 and Par6 in ECs caused failed in intracellular lumen formation, and chemical inhibition of PKC in DA of mouse prevents lumen formation (Koh et al., 2008) (Strilic et al., 2009). On the basal surface of the blood vessel, ECs contact different cargos of the ECM that has effect on vessels to be quiescent and stable or activated to sprout (Hynes, 2007). Basement membrane markers are fibronectin, collagen IV, laminin and integrins (Kucera et al., 2009) (Strilic, Kucera, et al., 2010).

1.5.3 The role of adherens junctions in lumen formation

In extracellular lumen formation first step towards polarity is coalescence of ECs into cords and then adherence of ECs together via adherens junctions. Vascular endothelial (VE)-cadherin (also known as Cdh5) is a special marker of EC

junctions (Lampugnani, 2012) and plays a vital role in vascular morphogenesis. Depletion of VE-cadherin in mice caused early embryonic lethality because of fail in establishment of yolk sac vasculature, disorganised embryonic blood vessels and minimal or absent of lumens (Carmeliet et al., 1999) (Gory-Faure et al., 1999). Blood vessels network with lumen fails to form in VE-cadherin depleted zebrafish embryos (Montero-Balaguer et al., 2009) (Abraham et al., 2015). Aberrant lumen morphogenesis caused by deficiency of VE-cadherin in animals is due to deficiency in cell-polarity establishment. Strilic et al. (2009) showed that in VE-cadherin null mouse DA lumen did not generate as a result of absence of apical markers including CD34, PODXL, and Moesin in the cell-cell contact (Strilic et al., 2009) and confirmed in zebrafish (Y. Wang et al., 2010). HUVEC in the absence of VE-cadherin have aberrant localization of PODXL and collagen IV as well as absent of Par complex member with small differences between apical and basal membrane with demolished lumen (Lampugnani et al., 2010).

1.5.4 Lumen expansion and the role of fluid flow

Following lumen formation, how blood vessel lumens are maintained and constantly adapt to metabolic needs of tissues and organs remains poorly understood. Blood flow plays an important role in the remodelling of vessels network (Q. Chen et al., 2012) (Kochhan et al., 2013) and lumen formation in new vascular connections (Herwig et al., 2011) (Lenard et al., 2013). Gebala et al. (2016) shows in zebrafish that lumen expansion requires haemodynamic-force-driven and myosin-II-dependent cellular mechanism of spherical deformations of the ECs apical membrane that known as inverse membrane blebbing. In the inverse blebbing lumen formation occur before anastomosis of blood vessels (Gebala et al., 2016) that is following the importance of haemodynamic forces in zebrafish vasculature development (Herbert & Stainier, 2011) (Lenard et al., 2013). Therefore, haemodynamic and blood fluid pressure are key contributors of lumenization in the developing vasculature network (Reichman-Fried & Raz, 2016). It has been proposed that cilia act to sense fluid flow (Reviewed by Praetorius (2015)). Haemodynamic forces also regulate blood vessel patterning,

maintain vascular identity by affecting vessel fusion and control blood vessel pruning and guides sprouts (le Noble et al., 2008).

1.6 Co-culture angiogenesis assay

In vitro angiogenesis assays attempt to mimic *in vivo* angiogenesis. Co-culture angiogenesis assay of endothelial cells and fibroblasts results in the formation of 3D tubules. Importantly, the endothelial-fibroblast organotypic co-culture assay recapitulates several crucial events of angiogenesis including assembly, ECs proliferation, sprouting and tube and lumen formation (Wayne W. Wu, 2016). Tubule formation and lumenogenesis are tracked by labelling ECs prior to their co-culture with fibroblasts with fluorescent markers, such as enhanced green fluorescent protein (EGFP) through retroviral or lentiviral transduction (Hetheridge et al., 2011). Negatively charged podocalyxin (PODXL) at the apical surface of ECs is the catalyst of lumen initiation (Strilic, Eglinger, et al., 2010) that can be used as a marker for lumen formation.

1.7 Microfluidic device

1.7.1 Construction and use of microfluidic devices

Microfluidic devices are biomimetic microsystems that resemble minimum functional units of living tissues and organs that imitate their vital structures and integrated functionalities, and also create chemical microenvironments. Microfluidic devices have been used widely in so many different areas such as the biomedical field, cell biology research, protein crystallization, drug screening, glucose tests, chemical microreactors, microprocessor cooling, electrochemistry and micro fuel cells.

Microfluidic devices are a good way to do research compare to *in vivo* and other *in vitro* technologies. Microfluidic devices are popular *in vitro* models due to their

capability to recapitulating *in vivo* microenvironments compared with other *in vitro* models. In contrast to the *in vitro* research on a culture plates or dishes, cells can be exposed to flow and shear stress in microfluidic devices (Zervantonakis et al., 2012) (Bhatia & Ingber, 2014) (Booth et al., 2014). Shear stress is triggered by circulation of liquids or gases inside the channels and chambers of microfluidic devices

Microfluidic devices are valuable compared to *in vivo* approaches. *In vivo* models can be technically challenging as well as expensive and controversial (Kilkenny et al., 2010) (Huh et al., 2012); for example visualisation of neovasculature growth in animals can be limited unless advanced techniques such as multiphoton microscopy are employed with cost and impact on animal welfare (Haase & Kamm, 2017). For drug testing microfluidic devices are prime because of being a time- and cost-saving alternative to *in vivo* models. It is approximated that in animal models, only 20% of successful drug candidates passed clinical trials (Perrin, 2014) due to differences among human and animal pathophysiologies and limitation in methodologies of *in vivo* research (Hackam, 2007) (Shanks, Greek, and Greek 2009) (van der Worp et al., 2010). In the field of angiogenesis, microfluidic -based assays allow visualisation of most angiogenic steps including degradation of the surrounding matrix, invasion, proliferation, morphogenic reorganisation and blood vessel stabilization (Song & Munn, 2011) (Vickerman & Kamm, 2012). Despite aforementioned benefits of using microfluidic devices, those remain *in vitro* approaches that do not fully recapitulate complex *in vivo* systems. This is likely to be improved by the culture of organoids in the microfluidic devices for which size limitation may prove a considerable challenge. Nonetheless, microfluidic devices were remaining a key step between cell culture and animal experimentation.

Culturing cells using 2D surfaces, such as culture flasks or well plates, has long been the conventional methods by which cells are grown and used for experiments. However, in recent years it has become apparent that results observed when testing new potential therapeutics on 2D cultures, do not necessarily reflect the observed results *in vivo*. This is because of the failing of 2D cultures to effectively reproduce the physiological environment of *in vivo* cells,

resulting in cultures lacking the appropriate cell-cell connections, multicellular compositions and surrounding extracellular matrix of 3D environments. The most notable effects of these failings are the differences in cell viability, metabolism and differentiation observed in 2D monolayers. Increased cell-cell connections in 3D cultures allow cells to remain viable in sub-optimal conditions, whereas 2D monolayers are considerably more sensitive to changes in environmental conditions. Both increased and decreased sensitivity has been observed to various drugs, highlighting the need for models like microfluidic device which produce results that reflect the *in vivo* effects of drug treatments (Tung et al., 2011) (Vinci et al., 2012) (Reynolds et al., 2017). Microfluidic devices supply a 3D controllable microenvironment with the opportunity to modulate mechanical properties (L. J. Chen & Kaji, 2017).

Combination of use of microfluidic devices and cell biology techniques rise the opportunity of precise control of dynamic fluid flow and shear stress and mimic cell culture microenvironments that demonstrate cells with appropriate organ-specific chemical gradients and dynamical mechanical cues. In this way cells can be induced to have normal phenotype expression, and ECM molecules can induce same level of organ-specific differentiation to ECM cell culture (El-Ali et al., 2006) (Whitesides, 2006). The technology of microfluidic devices recapitulates the structural tissue pattern and functional complexity of body organs, exposing cells to relevant microarchitecture and microenvironmental signals. Therefore, microfluidic technology allow research in various biological processes which are not possible with 2D or 3D cell culture systems and animal models (Huh et al., 2011) (van der Meer & van den Berg, 2012).

Microfluidic devices are suitable for modelling biological barriers under more physiologically realistic conditions (Bhatia & Ingber, 2014) (Esch et al., 2015) (van der Helm et al., 2016) (Wilmer et al., 2016) because microchannel fluid flow models the blood flow and body fluids. Biological barriers create homeostasis for physiological processes and protect the body from outside agents (Yu et al., 2018). These barriers are epithelium in the intestinal and respiratory systems and vasculature endothelium. As biological barriers impede drug delivery (Alonso,

2004), microfluidic devices modelling them can be used to improve and test treatment effectiveness in drug delivery.

Microfluidic devices have so far been used to model a variety of tissues and processes like pancreatic islets isolated from mice (Sankar et al., 2011), liver culture and hepatic transport system (Allen et al., 2005) (Domansky et al., 2010) (Goral et al., 2010), organ formation and function (Derda et al., 2009), chemotaxis of cancer cells (Torisawa et al., 2010), in the embryo regulation of mesenchymal condensation that drives odontogenic differentiation during development (Mammoto et al., 2011). Furthermore, microfluidic devices have been used in studies of fluid shear stress in the kidney (Jang & Suh, 2010); effect of shear stress and rearrangement of the actin cytoskeleton and trafficking of water transport protein (Jang et al., 2011); polymerase chain reaction (Ahrberg et al., 2016); blood plasma separation (Mielczarek et al., 2016); lung-on-a-chip models (Huh et al., 2010); gut-on-a-chip models (H. J. Kim et al., 2012); drug development (Theberge et al., 2015); vascular sprouting and effect of physiological fluid forces (Song & Munn, 2011). Microfluidic devices have been useful for disease models that resemble pathological physical microenvironments, like manipulation of cells that provide ventilator-induced lung injury (Douville et al., 2011) and induction of electrical stimulation to neonatal rat ventricular cardiomyocytes (Grosberg et al., 2011).

1.7.2 Components of microfluidic devices

A microfluidic device is a bundle of micro-channels and micro-chambers molded into a material composed of a polymer such as PolyDimethylSiloxane (PDMS), silicon, ceramics, glass or metal, and connected to the outside by inputs and outputs pierced through the microfluidic device. Fluid flow within the microfluidic device is regulated by an external active system such as a pressure controller, syringe pump or peristaltic pump, or passive way like hydrostatic pressure through simple holes, tubing, or syringe adapters.

The most common polymer used for molding microfluidic devices is PDMS which is a transparent, deformable, biocompatible and inexpensive elastomer, easy to bond onto coverslips or glass.

First step in fabrication of a microfluidic device is to design microfluidic channels using a dedicated software such as AUTOCAD, Illustrator or LEDIT. This is followed by transferring onto a photomask, which can be a chrome coated glass plate or plastic film. Then photolithography is used to transfer microchannel patterns from the photomask onto a mold. Therefore, visible micro-channels are sculpted on the mold and can be carved in the future material of microfluidic device (Park & Shuler, 2003) (Madou, 2011).

1.7.3 Coculture angiogenesis system in microfluidic devices

The development of vascularised microfluidic cultures manifested a crucial step forwards in the production of a physiologically complete vascular system. Blood vessels play a critical role in providing the surrounding tissues with oxygen and nutrients, and blood flow throughout them provides the appropriate biomechanical queues in the form of shear stress and interstitial flow. Microfluidic technology is a valuable platform to study angiogenesis (Song & Munn, 2011) (Song et al., 2012) (Bischel et al., 2013), endothelium migration (Vickerman et al., 2008) (S. Kim et al., 2013), and microvasculature formation. Vascular networks in microfluidic devices are generated by two mechanisms: through endothelial lined patterned channels, or by ECs self-assembling into networks. Both of these systems have their own benefits. Combining vascularization methods and microfluidic advances is a promising approach towards engineering of functional tissues. Microfluidic devices supply networks of micron-scale channels that are same size and architecture to *in vivo* microvessels (Akbari et al., 2017).

Vascularised organs-on-chip have been used in a number of studies (Hasan et al., 2014) (Akbari et al., 2017) (Kuzmic et al., 2019) to investigate vascular

biology. Different microfluidic devices were used to study different aspects of angiogenesis for example, Das et al. (2010) device model is useful to understand fundamental processes of angiogenesis. (Di Costanzo et al., 2016) developed a model to study EC migration and Serini et al. (2003) made an adhesion-type model (Gamba et al., 2003). Kuzmic et al. (2019) developed a microfluidic cell culture system to study cell migration and angiogenic sprouting.

1.8 Primary cilia

Primary cilia are microtubule-based structures that protrude from the apical surface of cells (Malicki & Johnson, 2017) and are approximately 1-5μm in length (Louvi & Grove, 2011). Primary cilia are found on a large number of cells in the mammalian body, including endothelial, epithelial, stem, muscle cells, and neurons (Wheatley, 1982). Primary cilia respond to inputs from the extracellular environment, serving diverse roles in chemo-, mechano- and photo -sensation, transduction and, in turn, regulating developmental signalling, cell polarity and cell proliferation (Ross et al., 2005) (Smith et al., 2020). Examples of stimuli include mechanical stimuli such as shear stress from fluid flow in epithelial cells of the kidney (Schwartz et al., 1997); and examples of chemical stimuli including ligand proteins of developmental pathways such as Sonic Hedgehog (Shh) pathway (Huangfu et al., 2003), neurotransmitters such as dopamine (Atkinson et al., 2015), and other extracellular signals such as growth factors, odorants, hormones and developing morphogens (Collin et al., 1989) (Singla & Reiter, 2006).

Defects in assembly and function of primary cilia result in a wide range of inherited developmental disorders termed ciliopathies. The clinical features of these conditions include polycystic kidney disease (PKD), obesity-associated diseases, retinal degeneration, severe neurodevelopmental abnormalities and skeletal dysplasia (Tobin & Beales, 2009) (Waters & Beales, 2011). Ciliopathies are caused by mutations that disrupt the organization or function of the main ciliary compartments such as the transition zone, basal body, the ciliary trafficking

process termed Intraflagellar transport (IFT), or transcriptional programmes that mediate ciliogenesis. A separate group of motile ciliopathies is caused by mutations that disrupt the structure, organization or expression of ciliary dynein subunits in motile cilia, or in the accessory proteins that mediate correct chaperoning and folding of the dynein subunits (Reiter & Leroux, 2017). Motile ciliopathies will not be discussed further (Reviewed by Wallmeier et al. (2020)).

1.8.1 Primary cilia structure

The primary cilium is composed of the basal body, the axoneme, the ciliary matrix and the ciliary membrane. The basal body is localized at the base of the cilium. It is derived from the mother centriole of the pre-existing centrioles when it migrates to the surface of the cell and docks onto the actin-rich cell cortex. The formation of basal body prompts the local reorganization of the actin-bound layer from cortex to the plasma membrane (Francis et al., 2011). Basal body position and orientation guide the alignment of the forming cilium. Primary cilia have ability to release microvesicles known as ectosomes that can be used for exchanging genetic material and protein inside cells (Salinas et al., 2017). The basal body associates with membrane vesicles en route to the cortex and forming the ciliary vesicles, and the subsequent fusion of the ciliary vesicles to the plasma membrane is probably to establish the ciliary membrane compartment. Finally, the basal body nucleates outgrowth of axonemal microtubules that protrude below an extension of membrane, generating cilium (Ishikawa & Marshall, 2011).

The axoneme is enclosed by the ciliary membrane which is continuous with the plasma membrane (Satir & Christensen, 2007). The ciliary axoneme is constructed by nine pairs of doublet microtubules (9+0). Axonemal microtubules have a doublet structure consist of one complete microtubule (the A tubule) connected to an incomplete second microtubule (the B tubule) including fewer protofilaments. The tubulin of the outer doublets has various post-translational modifications composed of acetylation, glutamylation and glycylation (Gaertig & Wloga, 2008) that appear to modulate axonemal stability, ciliary assembly and

motility (Thazhath et al., 2004) (Pathak et al., 2007) (Kubo et al., 2010). IFT trains which moves along microtubules carry ciliary building blocks during the time of assembly and disassembly of the cilium. There is preferential use of the A- and B- tubules of microtubule doublets for retrograde and anterograde IFT respectively which prevents head-on collisions of the IFT trains. Retrograde IFT trains move along A-microtubules, and anterograde trains travel along B-microtubules (Stepanek & Pigino, 2016). Axoneme of primary cilia lack the central pair of microtubules and the axonemal dyneins (molecular motors) which are key elements in ciliary motility of motile cilia.

The “ciliary gate” consisting of two sub-regions of the transition zone (TZ) and transition fibers (TFs) (Garcia-Gonzalo & Reiter, 2012) (Goncalves & Pelletier, 2017). Cilium is a compartment that is separate from the cell body: the ciliary membrane is not continuous with the plasma membrane, and this allows ciliary components for example for signalling to be sequestrated inside the organelle. The transition zone is located at the distal region of the basal body, where the outer doublets begin to form, and at the proximal end of the axoneme, serving as a barrier to regulate intracellular trafficking to and from the ciliary compartment (Garcia-Gonzalo & Reiter, 2012). The TZ connect the axonemal microtubule (MT) to the ciliary membrane. The TZ mediates docking of the mother centriole to the Golgi-derived membrane, and is the original attachment point of cilia to the membrane by a structure known as the ciliary necklace (Gilula & Satir, 1972). This is thought to be a barrier between the ciliary membrane and the general cell membrane. The TZ is distal to the TFs and has Y-shaped linkers (Ishikawa & Marshall, 2011). TFs, also termed distal appendages, attach the mother centriole to the plasma membrane by the centrosomal proteins such as CEP164 and ODF2. IFT complexes are thought to assemble at the TFs (Satir & Christensen, 2007). The ciliary pocket, an invagination of the plasma membrane at the root of cilium (H. Kang et al., 2012), is thought to regulate ciliary endocytic activity and vascular trafficking and may have a role as an interface with the actin cytoskeleton (Ishikawa & Marshall, 2011) (Figure 1.3).

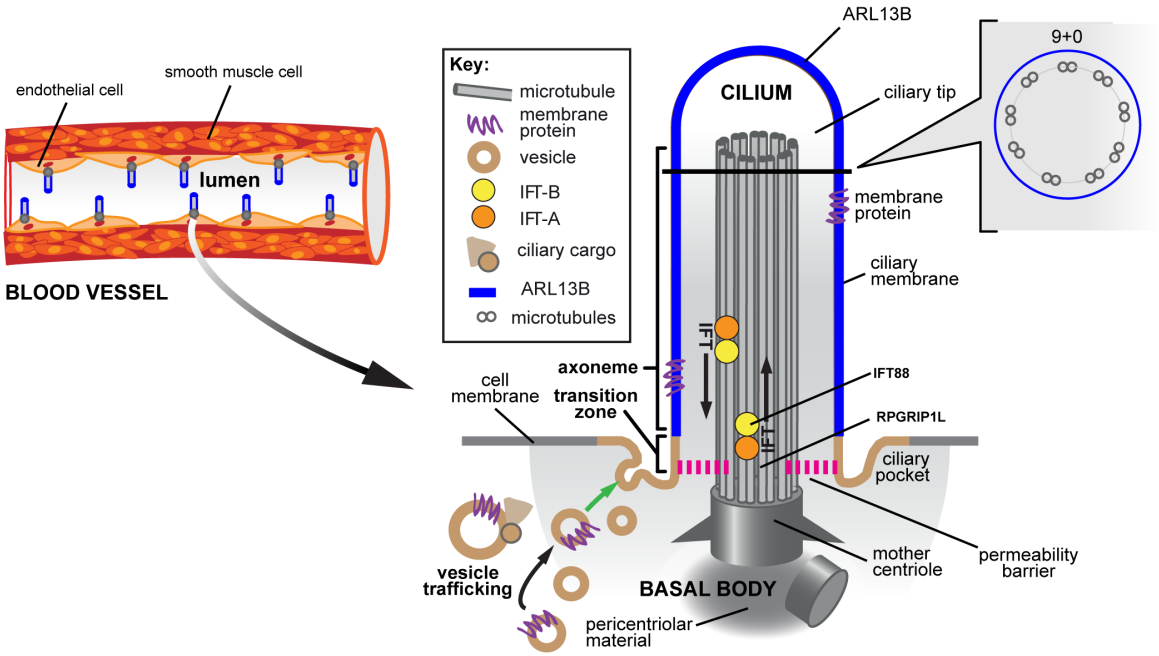

Figure 1.3 The structure and compartment of the primary cilium.

The primary cilium protrudes from the cell surface of ECs into the blood vessel lumen. The primary cilium consists of the basal body (grey at the bottom), the axoneme, the ciliary matrix and the ciliary membrane (cyan). The primary cilium forms when the mother centriole docks at the apical membrane to generate the basal body and then cilia anchor from the basal body at the region called the periciliary membrane compartment (PCMC). Ciliary doublet microtubules (grey cylinders) nucleate at the basal body and grow throughout the TZ to form the ciliary axoneme with a 9+0 microtubule arrangement. Shipping of cargo (indicated by arrows) up and down the axoneme is carried out by IFT protein complexes (orange and yellow) by using microtubule-based motor proteins. The actin cytoskeleton regulates ciliogenesis over effects on vesicle trafficking (tan symbols and arrow at the lower left). Adapted from Smith et al. (2020).

1.8.2 Primary cilia assembly and disassembly

The balance of assembly and disassembly regulates the steady-state ciliary length, with the inherent length-dependence of IFT (Ishikawa & Marshall, 2011). Cilia assemble and disassemble in synchrony with the cell cycle. The assembly of the cilium requires the coordination of motor-driven IFT, membrane trafficking

and selective import of cilium-specific proteins via the “ciliary gate” barrier at the ciliary transition zone. Primary cilia assemble during cell growth arrest, and ciliogenesis occurs when the cells begin to be confluent and reach stationary phase. Therefore, cells reassemble primary cilia during G1 or G0 phases and maintain the cilia when cells growth arrest (G0) or become post-mitotic when the centrosome is not required for mitotic functions (Mirvis et al., 2018). Loss of repressors of ciliogenesis CP110 and CEP97 causes formation of primary cilia at this stage (Tsang et al., 2008). Cilium assembly by IFT commence whilst the centrosome is located at Golgi apparatus close to the nucleus, followed by cilia elongation after docking of the nascent cilium at the cell surface, then microtubule pairs are assembled to form the axoneme (Wheatley, 1969) (Archer & Wheatley, 1971) (Fonte et al., 1971). Cargo is transferred by IFT which is essential for growth and maintenance of cilia (Rosenbaum & Witman, 2002). During ciliary growth the axoneme is assembled by addition of new axonemal subunits to its distal tip (Piperno et al., 1996) (Rosenbaum & Witman, 2002). The timing of cilia regrowth is regulated by cell cycle stage and centriole age, older centrioles are faster in forming cilia than the younger centrioles (Anderson & Stearns, 2009).

Ciliary disassembly is needed in order to detach the centriole from the plasma membrane, duplicated and then segregated during cell division (Sanchez & Dynlacht, 2016) (Goto et al., 2017). Primary cilia disassemble for cell division, subsequently leading to the consequence formation of the mitotic spindle. Deciliogenesis and repositioning of the centrioles to the cell interior are required because the centrioles that specify the spindle poles form part of the ciliary base. Despite cell division, there is sometimes partial resorption in G1, but the reason is unclear. After completing ciliary growth, the cilium stays highly dynamic. In dividing cells, the cilium is disassembled just before entering mitosis in S/G2 and the centrioles are inherited by the daughter cells that act as a template for the generation of new cilia in new cells (Ishikawa & Marshall, 2011) (Figure 1.4). It is unknown if cilia disassemble from the tip down, or if they resorb from the base. Ciliary resorption or disassembly before cell division appears to be mediated by two mechanisms that are not mutually exclusive: cleavage of the cilium away from the centriole mediated by the katanin family of microtubule-severing enzymes (Parker et al., 2010), or cilia resorption from the ciliary tip (Pan & Snell,

2005) (Piao et al., 2009). Two proteins have been discovered to regulate ciliary disassembly including the basal body-associated protein Pitchfork (Kinzel et al., 2010) and the scaffolding protein human enhancer of filamentation 1 (HEF1) (Pugacheva et al., 2007).

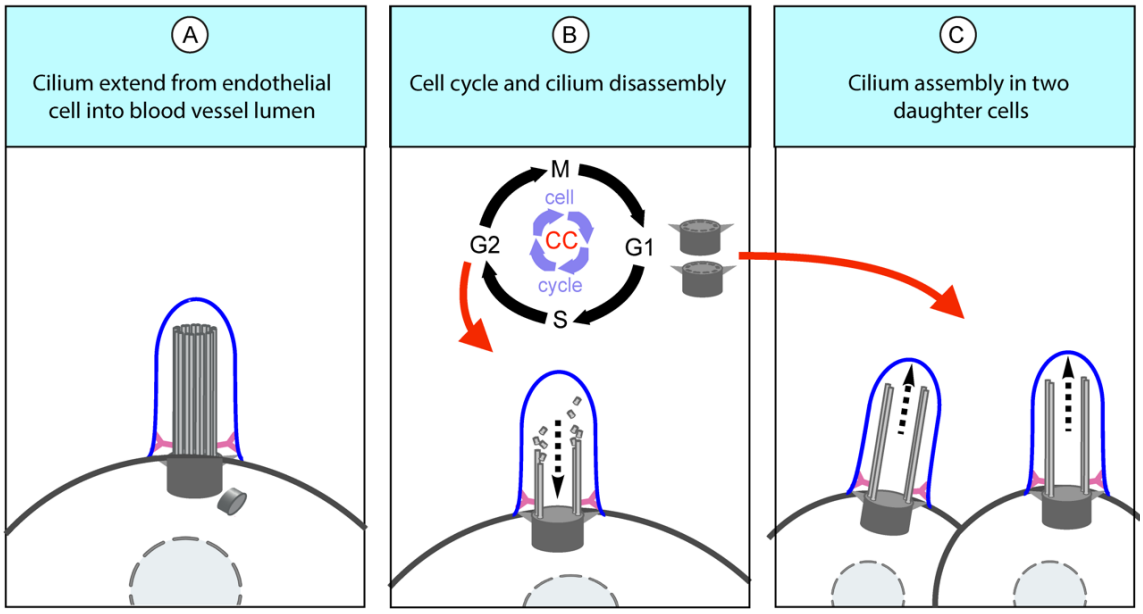

Figure 1.4 Primary cilia assembly and disassembly in endothelial cells. Primary cilia assemble and disassemble in synchrony with the cell cycle in order to form mitotic spindle. **A.** The primary cilium extends from the cell surface of EC. **B.** During cell division, the primary cilium is disassembled during S/G2. **C.** Cells reassemble primary cilia in two daughter cells during G1 phase and maintain the cilia when cells growth arrest (G0).

1.8.3 Vascular endothelial cilia

The primary cilia are ubiquitous in mammals vascular endothelial cells (Satir & Christensen, 2008) (Yu et al., 2016) (Y. Yang et al., 2019) (Ran et al., 2020). Primary cilia extend into the blood vessel lumen from the surface of vascular endothelial cells and play an important role as a sensor, and transmit extracellular signals into the cell (R. Pala et al., 2017). Vascular endothelial cilia regulate blood

vessel function via sensing of blood flow, calcium (Ca^{2+}) and nitric oxide (NO) signalling (Nauli et al., 2008) (T. J. Jones et al., 2012). Following regulation of Ca^{2+} diffusion by cilia, endothelial nitric oxide synthase (eNOS) is activated and triggers upregulation of NO which in turn dilates vessels and prevents blood vessels rupture due to excessive blood flow. Jin et al. (2014) shows that fluid shear stress opens Ca^{2+} channels on cilia which is mediated by polycystin 2 (PC2). Therefore, the regulation of Ca^{2+} signalling by cilia could be in response to the blood flow and shear stress. Several vascular diseases are proposed to be associated with defects in endothelial primary cilia such as atherosclerosis, hypertension, and aneurysms (Reviewed by Mohieldin et al. (2016) and Luu et al. (2018)), but the causal molecular mechanisms of disease remain unclear.

1.8.4 Ciliary proteins

1.8.4.1 IFT88

Intraflagellar transport (IFT) is a two-way transport system located between ciliary membrane and axonemal microtubules (S. C. Goetz & Anderson, 2010). IFT transports IFT-particle protein complexes and ciliary building blocks including subcomplexes A, B and cargo proteins (Yamamoto & Mizushima, 2021), bidirectional from the cytoplasm to the ciliary tip and back to the cytoplasm along the axoneme (Pedersen & Rosenbaum, 2008) in order to balance proteins in cilia (Lechtreck et al., 2013). IFT transport along axonemal in the anterograde (base-to-top) and retrograde (tip-to-base) directions by motor proteins of kinesin 2 and cytoplasmic dynein 2 respectively (Satir et al., 2010). IFT is necessary for cilium assembly and maintenance by transporting ciliary precursors such as tubulin in the anterograde direction. Functional IFT is necessary for the constant renewal of ciliary membrane proteins and signal transduction.

Intraflagellar transport (IFT) 88 (IFT88) is an important compartment of IFT complex B (Tian et al., 2017) and is the main transport system in cilia (S. C. Goetz & Anderson, 2010). IFT88 is necessary for the assembly and maintenance of

primary cilia (Pazour et al., 2002). Deletion of IFT88 leads to loss of cilia (Wann et al., 2012) or sever defect in ciliogenesis (Pazour et al., 2000) (Haycraft et al., 2001) (Huangfu et al., 2003). Furthermore, IFT88 has cilia-independent functions in non-ciliated cells as well as ciliated cells for example, IFT88 is required for cleavage furrow ingression, spindle orientation and organization, extra centrosome clustering in dividing cells (Reviewed by Peralta et al. (2020)) and regulating G1-S transition progression during the cell cycle (Robert et al., 2007). Furthermore, IFT88 has been recognized as a tumour suppressor gene in breast carcinoma (Degnim et al., 2015), hepatocellular carcinoma (Bonura et al., 1999), and basal cell carcinoma (Wong et al., 2009). Moreover, in papillary thyroid cancers (PTCs) mutation of the IFT88 gene was observed. However, the mechanism of effect of IFT88 as a tumour suppressor remain unknown and needs to be investigated.

The loss of IFT causes abnormal cilia (Rosenbaum & Witman, 2002). Conditional IFT88 knockout mice showed severe acute kidney injury compare to the wild type (S. Wang et al., 2021). In the *in vivo* study by Singh et al. (2020) on EC-specific IFT88-knockout mice, IFT88 -silencing of ECs caused significant reduction in expression of endothelial markers including CD31, Tie-2 and VE-cadherin and also mesenchymal cells-like alterations in ECs particularly towards pulmonary fibrosis. Mice with IFT88 mutation shows defects in neural tube patterning, polydactyly and left-right axis determination defects (Tian et al., 2017). Study on C. reinhardtii showed that as flagellar length increase, IFT train size decrease, whereas frequency of IFT remains independent of flagellar length (Engel et al., 2009), but how IFT train size is regulated is unknown. IFT protein mutation in zebrafish brain increased the probability of intracranial haemorrhage compared with the control group (Kallakuri et al., 2015). Mutation in Tg737 of Chlamydomonas IFT88 trigger cells with no cilia or shorter cilia (Pazour et al., 2000). Mice with Tg737 mutations develop polycystic kidney disease (PKD) (Moyer et al., 1994). Tian et al. (2017) found a novel mutation in IFT88 through whole exome sequencing of three members of a family who affected with isolated cleft lip and palate. Moreover, whole genome sequencing (WGS) of a Caucasian family identified IFT88 mutations and the mutant IFT88 resulted in the abnormal

ciliary structures formation in individuals with non-syndromic recessive retinal degeneration. However, role of IFT88 in human disease has yet to be elucidated.

1.8.4.2 RPGRIP1L

Retinitis Pigmentosa GTPase Regulator 1 Interacting Protein 1 Like (RPGRIP1L) encodes the RPGRIP1L protein that localizes to the transition zone of primary cilia (Wiegering et al., 2018). RPGRIP1L has a crucial role in TZ assembly, it establishes a ciliary zone of exclusion (CIZE) at the TZ which control signalling proteins to ciliary subdomains distally from the TZ (Jensen et al., 2015).

Mutation in RPGRIP1L causes ciliopathies with a broad range of clinical phenotypes in many organ systems such as eye, brain, lung, heart, kidneys, liver, limb and skin (Reviewed by Wiegering et al. (2018)). RPGRIP1L mutations caused Meckel syndrome (MKS), Joubert syndrome (JBTS), Cerebellar Vermis Aplasia Oligophrenia Congenital Ataxia Coloboma Hepatic Fibrosis (COACH), Nephronophtisis (NPHP), Bardet-Biedl syndrome (BBS), Retinitis Pigmentosa (RP) and Leber's Congenital Amaurosis (LCA) (Arts et al., 2007) (Delous et al., 2007) (Wolf et al., 2007) (Brancati et al., 2008) (Khanna et al., 2009) (Doherty et al., 2010) (Chaki et al., 2011) (Fahim et al., 2011) (Otto et al., 2011) (Alazami et al., 2012) (Halbritter et al., 2012) (Szymanska et al., 2012) (Summers et al., 2017).

1.8.4.3 Serotonin receptor HTR6

The 5-hydroxytryptamine receptor 6 (HTR6) is a subtype of the 5-hydroxytryptamine (5HT; also known as serotonin) receptor class and belongs to the G-protein-coupled receptor (GPCR) family (P.Reynolds, 2010). It is the only 5HT receptor that localises to primary cilia (Brailov et al., 2000) (Berbari et al., 2007). HTR6 receptors have a ciliary targeting sequence (CTS) that several studies have shown is necessary and sufficient for HTR6 receptor trafficking into

primary cilia (Berbari et al., 2008) (Nachury et al., 2010) (Nagata et al., 2013). However, another study by Brodsky et al. (2017) showed that CTS is not responsible for HTR6 receptor trafficking to cilia.

Changes in ciliary length has been reported by heterologously-expressed HTR6 receptors (Guadiana et al., 2013) (Duhr et al., 2014). In my study, overexpression of HTR6 caused observation of longer cilia when compared with the length of cilia determined by ARL13B and glutamylated tubulin (GT335) antibodies in hTERT RPE-1 cells. My finding agreed with the other studies that showed longer cilia with HTR6 overexpression such as: a study by Hu et al. (2017) that showed ciliary length increased by overexpression of HTR6 in wild-type mouse hippocampal neurons, whereas knockdown of HTR6 by siRNA caused in shorter cilia formation. Ciliary length was decreased by blocking HTR6 receptor activity (Brodsky et al., 2017). In cultured neurons, ciliary length was reduced by using selective HTR6 antagonists derived from wild-type mice (Brodsky et al., 2017). The reason explained by Brodsky et al. (2017) mentioned that it could be because overexpression of HTR6 resulted in localization of HTR6 outside of the cilia and had no effect on cilia morphology.

1.8.5 Endothelial cilia and their role in sensing blood flow

ECs receptors sense the flow and transmit mechanical signals to recipient molecules via mechanosensitive signalling pathways which results in phenotypic and functional alterations. Primary cilia are thought to sense and transduce extracellular fluid shear into biochemical signalling changes inside vascular ECs. Indirect evidence to support these functions is provided by the observation that each EC possesses a single primary cilium on its apical surface that contain ciliary proteins such as polycystin-1 and IFT88 (Nauli et al., 2008). The presence of endothelial primary cilia has also been observed in HUVEC (Iomini et al., 2004), endocardium of the developing chicken (Van der Heiden et al., 2006) and aortic endothelia of the embryonic E15.5 mouse (Nauli et al., 2008). Haemodynamic forces affect the functional properties of vascular endothelium

(Chistiakov et al., 2017) and transform to the chemical signalling pathways by using the mechanotransduction effect of cilium.

What is known regarding the sensing of external mechanical forces such as fluid shear stress by vascular endothelial cells is limited. However, it is known that shear stress can activate several biochemical and mechanochemical pathways in ECs (Nauli et al., 2008). The ciliary mechanosensory function depends on IFT88 and the mechanosensing polycystin-1 protein, encoded by the PKD1 gene (Nauli et al., 2008). Polycystin-1 is a mechanosensitive ion channel (Nauli et al., 2003) (Xu et al., 2007) localized to primary cilia (Nauli et al., 2008) that can mediate the sensitivity of kidney epithelial cells to fluid shear stress (Nauli & Zhou, 2004) (B. K. Yoder et al., 2002). Mutations in either PKD1 or IFT88 both result in ciliary-related polycystic kidney disease (PKD) ("Polycystic kidney disease: the complete structure of the PKD1 gene and its protein. The International Polycystic Kidney Disease Consortium," 1995). With alterations in fluid shear stress, ECs show an increase in release of cytosolic calcium following by nitric oxide (NO) release which is essential for regulation of vascular contractility (Boo & Jo, 2003). Abnormalities in NO release, associate with endothelial dysfunction and hypertension (Thuillez & Richard, 2005). Nauli et al. (2008) has shown that both polycystin-1 for cilia function and polaris for cilia structure and maintenance are essential for transduction of the mechanical signals of fluid shear into the calcium signalling changes and NO synthesis by ECs in response to fluid shear stress. In summary, polycystin-1 and IFT88 mediate fluid shear stress-dependent alterations in calcium and NO through a specific pathway.

1.8.6 Cilia and the actin cytoskeleton

Studies showed four specific cellular processes that regulate cilia formation and maintenance including structural influences of the actin cytoskeleton, cell cycle, cellular proteostasis and signalling pathways. The actin cytoskeleton regulates ciliogenesis via impacts on both actin cytoskeleton remodelling expressed by

acto-myosin contractions, as well as vesicle trafficking which transfer membrane proteins to the cilia (Harvey F. Lodish 2016).

Actin is a ubiquitous intracellular cytoskeletal protein in eukaryotic cells (Smith et al., 2020). Actin filaments are the main component of the actin cytoskeleton which are polar linear polymers of the cytoplasmic protein actin (Svitkina, 2018). The actin cytoskeleton is formed by microfilaments that are made by filamentous (F) polymers of globular G-actin subunits (Harvey F. Lodish 2016). Actin filament dynamics such as the actin filament nucleation, elongation, and disassembly are controlled by regulatory proteins (Pollard, 2016). Inside the cell, actin has both forms of monomer (globular, G-actin) and a polymer (filamentous, F-actin) (278). Both polymerization and depolymerization require actin binding proteins. Actin binds and hydrolyses ATP to ADP upon microfilament assembly. Profilin can catalyze ADP to ATP and changes the monomers to the more polymerizable ATP-bound form. Cilia actin polymerization can be forbidden and therefore excises primary cilia tips in the process known as cilia decapitation (Phua et al., 2017). Although current understanding regarding proteins involved in actin depolymerization are limited, members of the yeast actin depolymerization factor (ADF)/cofilin family can increase dissociation of monomers from microfilaments. Actin polymerization requires nucleating factors like spire or formins, or the actin-related protein complex (ARP 2/3) (Goley & Welch, 2006) (Dominguez, 2009). Actin filaments are assembled by actin-binding proteins into networks and remodel constantly according to the cell needs (Svitkina, 2018).

The actin cytoskeleton generates forces for multiple cell-motility events such as pulling, pushing and resistance forces. Cell movement occurs by repeating cycles of cell protrusion an attachment of the front cell, followed by disconnection and retraction of the rear cells (Svitkina, 2018). During cell migration, actin filament bundles assemble either as axial stress fibers or radially at the leading edge (Dawe et al., 2007) (Valente et al., 2010). F-actin is a major component of the cytoskeleton and maintain shape and polarity of cells and assist in migration. F-actin exists in cells in part as a microfilament networks are attached to the cell membrane by different cross-linking proteins and makes up the cortical actin

layer (Smith et al., 2020). F-actin branching is crucial in the cellular protrusions formation such as cilia, microvilli and lamellipodia (Khaitlina, 2014).

Because cilia have microtubule-based structure, the traditional view is that cilia do not contain actin. However, the ciliary membrane needs actin cytoskeleton to maintain structure (Smith et al., 2020) and a few studies have observed labelling of the actin cytoskeleton within the cilium (Chaitin & Burnside, 1989) (S. Lee et al., 2018). Other studies reported association of F-actin in ciliary decapping (Phua et al., 2017) and microvesicles/ectosome excision (Nager et al., 2017). Recently, actin in cilia were detected at molecular resolution by Kiesel et al. (2020) which discovered bundles of actin cytoskeleton close to the ciliary membrane and F-actin-like structures that intertwined with axoneme microtubules. Furthermore, there is a pool of F-actin at the ciliary base within the ciliary pocket (Molla-Herman et al., 2010) that is important in disassembly of cilia. F-actin polymerization is the earliest known step in disassembly of cilia (A. Li et al., 2011). Although the exact mechanism for delivery of ciliary membrane proteins is poorly understood and needs more investigation, ciliary-specific vesicles with cargo inside are trafficked along the actin cytoskeleton (Cao et al., 2012) (J. Kim et al., 2015) and move by involvement of myosin motors (DePina & Langford, 1999).

1.8.6.1 Actin cytoskeleton and regulation of ciliogenesis

Actin cytoskeleton remodelling modulates ciliogenesis initiation and cilia length (Smith et al., 2020). Two main regulators of ciliogenesis and cilia length, and also a regulator of actin filament stabilization, are gelsolin (GSN) and actin-related protein 3 (ACTR3). GSN is a positive regulator and severs actin filaments. ACTR3 is a negative regulator and inhibits branching (J. Kim et al., 2010). Destabilized F-actin enhances vesicle trafficking, whilst stabilized F-actin makes a physical barrier to ciliary vesicle trafficking in the base of the cilium or centrosome throughout ciliogenesis (J. Kim et al., 2010).

The actin cytoskeleton has various roles at different stages of the ciliary life cycle including regulation of vesicle accumulation and fusion in order to form the ciliary vesicle, and basal body migration and docking by focal adhesion complex (Antoniades et al., 2014). These two mechanical forces can regulate ciliary length during ciliogenesis and disassembly, but the mechanism is poorly understood (Mirvis et al., 2018). Stress fibers are formed by F-actin microfilament bundles, non-muscle myosin-based motor proteins and actin cross-linking proteins such as alpha-actinin and they play an important role in adhesion, migration, morphogenesis and mechanotransduction (Tojkander et al., 2012). Stress fibre formation increases by mutations in ciliopathy genes and as a result impairs ciliogenesis (Dawe et al., 2007) (Valente et al., 2010). By contrast, ciliogenesis is stimulated by inhibition of actin polymerization (Bershteyn et al., 2010) (J. Kim et al., 2010) (Sharma et al., 2011). Therefore, these results suggest that ciliogenesis increases by depolymerization or depletion of actin cytoskeleton, whereas cilia formation is decreased by polymerization of the actin, the formation of stress fibers and F-actin branching (Avasthi & Marshall, 2012) (Malicki & Johnson, 2017). Notably, ciliogenesis was induced in hTERT RPE-1 cells after treatment with different actin polymerization inhibitors such as cytochalasin D which destabilizes actin (J. Kim et al., 2010) (Nagai & Mizuno, 2017), and latrunculin B (Nagai & Mizuno, 2017) which binds the actin-monomers and prevents polymerization (Morton et al., 2000). Furthermore, ciliary length was increased by cytochalasin D that induces actin depolymerization (J. Kim et al., 2015).

1.8.6.2 Regulation of cilia by ROCK

Rho-associated coiled-coil forming protein serine/threonine kinase (ROCKI1/2) commonly known as ROCK are downstream effectors of the Ras homolog gene family, member A (RhoA). ROCK plays a crucial role in many different cellular processes, the regulation of the actin cytoskeleton being one of the best characterised (Deng et al., 2019). Cytoskeletal regulators are discussed in more detail in section (1.8.6.1). Increase in ROCK activity increases stress fibre formation and F-actin stabilization in almost all cell types (Smith et al., 2020).

RhoA is the regulator of ROCK, a crucial regulator of actin remodelling and the generation of stress fibres (Ridley & Hall, 1992) (Ridley, 2006). Increased actin polymerization resulted in shorter cilia (Streets et al., 2020) because apical actin filaments are required to stabilize cilia generation by inducing centrosome migration, axoneme growth and basal body docking (Pan et al., 2007). In the study by Rangel et al. (2019) pan-specific ROCK inhibition by Y-27632 increased ciliary length in different cell lines and disrupted the apical cytoskeleton.

1.8.6.3 ROCK and lumen formation

ROCK has been implicated in the control of blood vessel lumen formation (Barry et al., 2016). It was suggested that lumens respond differently to changes in RhoA activity at different stages of their development with RhoA-ROCK signalling being dispensable at early stages, whereas at later stages chemical inhibition of ROCK increased vessel diameter (Barry et al., 2016).

The study by M. Kim et al. (2015) on MDCK cysts showed that ROCK inhibition downstream of RhoA resulted in the formation of multiple lumens because inhibition of this pathway blocked cell movement which is required for consolidating multiple lumens into one lumen. The same effect happened by inhibition of myosin II which is downstream of ROCK, suggesting that myosin II is involved in lumen consolidation in tubules.

1.9 Cytoskeletal regulators

In most biological processes, cell movement is a crucial phenomenon in embryonic morphogenesis, angiogenesis and tissue repair, regeneration and immune surveillance amongst other processes (McMahon & Gallop, 2005) (Hussey et al., 2006). Actin cytoskeleton dynamics act as a vital part in most of these processes, regulating the cellular structures formation including filopodia,

lamellipodia, stress fibers and focal adhesions that are regulated by Rho GTPases (Bailly & Condeelis, 2002).

1.9.1 Rho GTPases and the actin cytoskeleton

The actin cytoskeleton and related cellular processes are controlled by the activity of Rho-GTPases (Hall, 1998). Actin cytoskeleton dynamics and as a result cell movements and biological processes require dynamic transition of the actin between its monomeric (G-actin) and filamentous (F-actin) forms. Actin is a family of multi-functional proteins that produce microfilaments in the cytoskeleton and underlie the plasma membrane. Actin monomers bond the barbed (or+) growing end of the actin filament in the ATP-bound state and leave the actin filament from the pointed (or-) end in the ADP state, giving rise to the process known as actin filament threadmilling (Smith et al., 2020). The transition between F- and G-actin is mediated by a large number of F- and G-actin binding proteins (ABPs) which are responsible for actin filament nucleation, capping, severing, elongation and crosslinking and actin monomer sequestration (Pollard & Borisy, 2003).

Rho GTPases act as molecular switches, switching between their active guanosine-5′-triphosphate (GTP)-bound and inactive guanosine diphosphate (GDP)-bound states (Hall & Nobes, 2000). The best-studied Rho GTPases are Ras homolog family member A (RhoA) which is regulator of ROCK, ras-related C3 botulinum toxin substrate 1 (RAC1) and cell division cycle 42 (CDC42) (Bryan & D'Amore, 2007). Variety in the spatiotemporal activation of Rho GTPases is important because Rho GTPases control the stimulation of actomyosin contraction effector proteins via Diaphanous-related formins (Dia), formation of actin fibers via Rho associated kinase (ROCK) and stimulate polymerisation of branched actin in membrane protrusions through Arp2/3 (Ridley, 2006) (Machacek et al., 2009). Rho GTPase activity is regulated by the opposing actions of guanine nucleotide exchange factors (GEFs), GTPase-activating proteins (GAPs), and guanine nucleotide dissociation inhibitors (GDIs). GEF

activate GTPases by stimulating the exchange of GDP to GTP. The Rho GEF family consist of about 80 members and they divided into typical (Dbl) and atypical (DOCK) categories (Cook et al., 2014) (Gadea & Blangy, 2014). In opposite the GAP family composed of approximately 60 members, inactivate GTPases by promoting the conversion of the active GTP form to the GDP form (Cherfils & Zeghouf, 2013) (van Buul et al., 2014). GDIs stabilise GDP-bound small GTPases, thereby maintaining the GTPases in the inactive form (Cherfils & Zeghouf, 2013).

RAC1 regulate lamellipodia formation and stimulate migration, angiogenic sprouting, adhesion and the permeability responses to VEGF in ECs (Tan et al., 2008) (Kesavan et al., 2009) (Barry et al., 2015) (Caron et al., 2016). CDC42/RAC1-regulated lamellipodia and filopodia formation is driven by WASP-related WAVE regulatory complex, that stimulates direct activation of formin family proteins through actin filament nucleation and later extension of actin filaments (Mehidi et al., 2019). Wiskott-Aldrich syndrome proteins (WASPs) signal upregulates the actin-related protein 2/3 (ARP2/3) complex in order to form branched actin filament networks (Sinha & Yang, 2008). Actin elongates by activation of vasodilator-stimulated phosphoprotein (VASP) and formin family members (J. Li et al., 2017). The serine/threonine-protein kinase (PAK) family activate when bound to either RAC1 or CDC42, and contribute towards polymerization of actin in both filopodia and lamellipodia formation (Szczepanowska, 2009). LIM kinase (LIMK) which is PAKs downstream effector, promote actin polymerisation and bundling (Szczepanowska, 2009).

Dynamic actin cytoskeletal rearrangement and assembly, formation the basis of cell-to-cell adhesion and migration are regulated by GEF-mediated activation of Rho GTPases (Kesavan et al., 2009) (Barry et al., 2015). CDC42 is a regulator of actin-based morphogenesis and cell polarity (Lavina et al., 2018), directional filopodia formation, cell adhesion, migration and invasion (Kesavan et al., 2009) (Barry et al., 2015). CDC42 activation induces actin polymerisation to form filopodia at the cell membrane (Fischer et al., 2019). CDC42 can stimulate the activation of the IRSp53 adapter protein that connect actin to the membrane and stimulate clustering of the uncapping protein (Krugmann et al., 2001) (Vaggi et

al., 2011). Filopodia generation is a dynamic process and requires constant assembly and disassembly of the actin filaments. Disassembly of actin at the filopodium tip is gelsolin- or cofilin-mediated, but it could be driven by the actin depolymerization and retraction imposed by non-muscle myosin II (Benson & Southgate, 2021).

1.9.2 Guanine nucleotide exchange factors (GEFs)

Two families of guanine nucleotide exchange factor (GEF) exist for Rho GTPases: the classical Dbl-related exchange factors and DOCK family. They both catalyse the same conversion of Rho-GDP to Rho-GTP but through unrelated mechanism (Gadea & Blangy, 2014).

Rho GEF activity and membrane localisation of Dbl GEFs rely on the PH (scale of acidity or basicity of liquid solutions) and Dbl homology (DH) domains, but DOCK (Dedicator of cytokinesis) proteins do not contain those domains and they are unrelated to Dbl GEFs (Cote et al., 2005) (Miyamoto et al., 2007), DOCK proteins comprise conserved functional DHR-1 and DHR-2 domains. DHR-1 regulates the DOCK protein localization to the plasma membrane via interaction with a lipid known as phosphatidylinositol (3,4,5)-trisphosphate (PIP3) (Kobialka & Graupera, 2019). The DHR-2 domain binds to the small Rho GTPase to catalyse GDP-GTP exchange and thus causing actin polymerisation and in turn filopodia and lamellipodia formation via activation of the downstream effectors (Cote et al., 2005) (J. Yang et al., 2009). The SH3 domain in DOCK-A and -B subfamilies, is required for activation of DOCK GEF activity (Sevajol et al., 2012) (Toret et al., 2014). C-terminal proline-rich region of DOCK proteins binds to phosphatidic acid (PA) as well as SH3-containing adaptor proteins, such as CRK which required for DOCK-mediated Rho GTPase activity (Sanematsu et al., 2010) (Chang et al., 2020) (Figure 1.5).

The DOCK proteins function as regulators of RAC1 and CDC42. The DOCK family comprises 11 proteins and subdivided into four groups (A, B, C, D)

according to their GTPase specificity and functional domains. Members of every subfamily distribute similar protein structure and functional domains. DOCK4 along with DOCK3 are in group B and are specific for RAC1 activation (Fukui et al., 2001) (Hamel, 2010).

1.9.2.1 DOCK4

Dedicator of cytokinesis 4 (DOCK4) is a membrane-associated cytoplasmic protein that associate in actin cytoskeleton regulation (Yajnik et al., 2003) (Kawada et al., 2009) (Gadea & Blangy, 2014). DOCK4 is a member of Rho GEFs and is a GEF for RAC1. The protein comprises an N-terminal Src homology 3 (SH3) domain, two DOCK homology regions (DHR-1 and DHR-2), an armadillo repeat motif and a C-terminal proline-rich domain (Fukui et al., 2001) (Hamel, 2010) (Figure 1.5).

DOCK4 regulates the activity of RAC1 (Yan et al., 2006) (van Buul et al., 2014) (Hernandez-Garcia et al., 2015). RAC1 activation require binding of DHR-2 domain (Kawada et al., 2009). SH3 domain in DOCK4 can negatively regulate RAC1 activity (Kawada et al., 2009). In 2006, (Hiramoto et al.) showed that when the DHR-2 domain of DOCK4 is mutated in HEK293T cells, the activation of Rac1 by DOCK4 is suspended, suggesting that RAC activation happens via the DHR-2 domain. Moreover, in the same study, they implicated the small GTPase RhoG and its effector ELMO (Engulfment and cell motility) in the regulation of DOCK4 and cell migration through RAC1 activation. In 2008, (Upadhyay et al.) contributed to the new understanding of DOCK4's role in Wnt/beta-catenin signalling pathway via RAC1 activation important in cell proliferation and migration, and also tumorigenesis using HEK293T and NIH3T3 cells, both of which have an intact Wnt pathway.

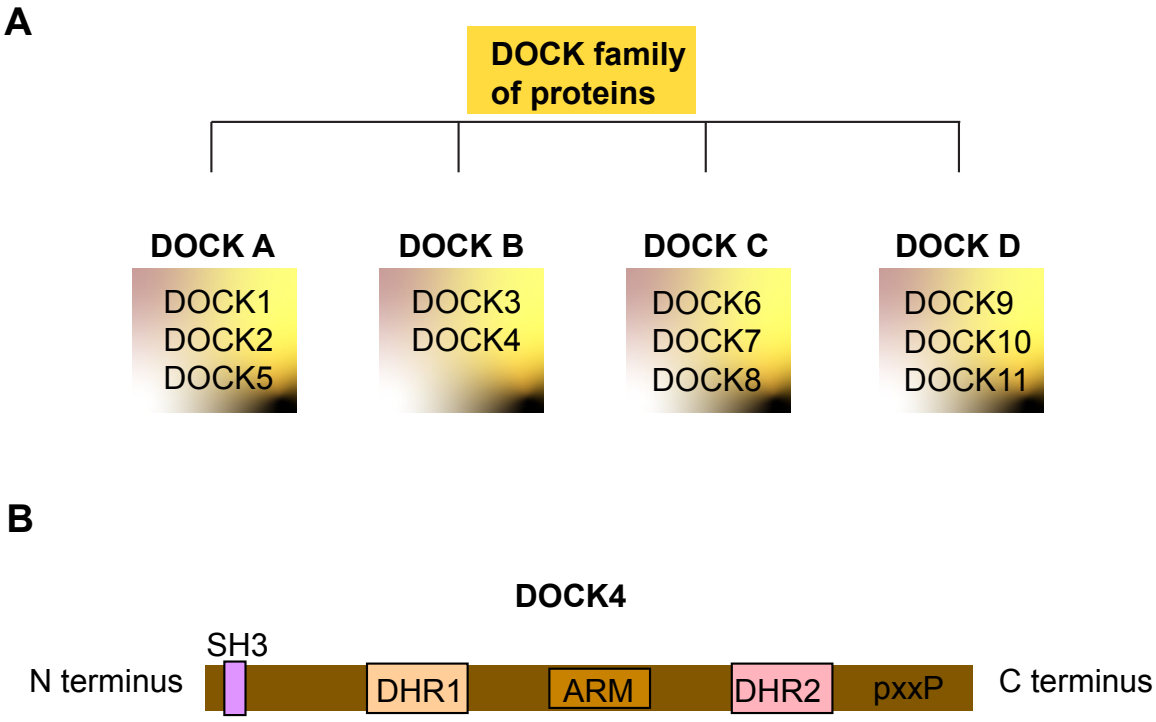

Figure 1.5 Four groups of the DOCK family proteins and the domain structure of DOCK4.

A. The DOCK protein family has 11 members and divided into four groups on the basis of primary-sequence conservation. DOCK-A includes DOCK-1, -2, and -5. DOCK- B includes DOCK-3 and -4. DOCK-C includes DOCK-6, -7 and -8. DOCK-D includes Dock-9, -10 and -11. **B.** DOCK4 is comprised of the DHR1 and DHR2 domains, both which are conserved in all mammalian DOCK family proteins. On the N-terminus, DOCK4 contains an SH3 domain, and on the C-terminus, a proline rich (PxxP) domain. Adapted from L. Shi (2013).

1.9.2.2 The role of DOCK4 in vascular development and angiogenesis

The generation of a functional vasculature demands important cellular mechanisms such as cell proliferation, migration and adhesion which are all closely linked to the activity of small Rho GTPases. Activity of small Rho GTPases is regulated in part by the dedicator of cytokinesis (DOCK) protein family (Benson & Southgate, 2021), with association of several angiogenic

signalling pathways such as chemokine receptor type 4 (CXCR4), VEGF and phosphatidylinositol 3-kinase (PI3K), in the regulation of specific DOCK proteins. There are growing evidences in the important role of DOCK proteins in the complex mechanisms of blood vessel formation in development and disease. To date, 7 out of 11 DOCK proteins have been implicated with the regulation of blood vessel formation (Benson & Southgate, 2021). Initially H. Kang et al. (2012) showed that DOCK4 expressed in vascular smooth muscle cells (VSMCs). DOCK4 is expressed in so many tissues including human umbilical vein endothelial cells (HUVEC) (van Buul et al., 2014). DOCK4 downregulation using small interfering RNA (siRNA), reduced vSMC motility and contraction (H. Kang et al., 2012). Multiple DOCK proteins function within the blood vessel system (Benson & Southgate, 2021). 64% (7/11) of DOCK proteins are regulators of vascular processes (Benson & Southgate, 2021).

DOCK4 contribute towards cell migration (Ueda et al., 2008) (Kawada et al., 2009) (Abraham et al., 2015). This has been shown in fibroblast cells by Kawada et al. (2009) where RAC1 is activated by DOCK4 at the cell membrane. Furthermore, cell migration was significantly increased by over-expression of wild type DOCK4 (Kawada et al., 2009). In the study by Abraham et al. (2015) in organotypic co-culture of HUVEC with fibroblasts, knockdown with DOCK4-specific siRNA resulted in a significant decrease in the number of vessel branches, suggesting that DOCK4 stimulate vessel sprouting. The remaining tubules had less diameter and with fewer lateral cell-cell junctions, implicating crucial role of DOCK4 in tubule development, filopodia formation and endothelial cell adhesion (Abraham et al., 2015). *In vivo* study by Yajnik et al. (2003) in normal mouse, siRNA-mediated DOCK4 depletion demonstrated significant suppression of adherens junctions. Whilst the study on mouse elicited early embryonic lethality with homozygous DOCK4 knockdown, however heterozygous DOCK4 +/- mouse showed angiogenesis-associated defects such as reduction in the blood vessel lumen size in the brain parenchyma of E13.5 embryo (Abraham et al., 2015). The decrease in lumen size showed in these studies were not associated with pericyte coverage of the vessel, suggesting involvement of another mechanism like cell contractility or motility (H. Kang et al., 2012) (Abraham et al., 2015). All together the results show an important role for

DOCK4 in EC protrusive activity, organization of lateral contacts, tubule remodelling and lumen formation. DOCK4 also implicated in a mechanism for atherogenesis, in neovascularisation, and the generation of arterial fatty deposits (Stewart et al., 2018) (L. Huang et al., 2019). DOCK4 has been observed as an interacting partner of scavenger receptor class B type 1 (SR-B1) which is a receptor that bind to LDL and mediate delivery of LDL into the arteries in developing atherosclerosis (L. Huang et al., 2019). Moreover, RAC1 GEF DOCK4 through interaction with CDC42 GEF DOCK9 regulates formation of EC filopodial protrusions which is essential for the lateral organization ECs, dynamic remodelling of tubules and lumen morphogenesis (Abraham et al., 2015).

1.10 Preliminary work leading to this thesis

1.10.1 Cilia and ROCK

Primary cilia are microtubule-based organelles. Cilia are recognised as a mediator for mechanosensation of blood flow and growth factor signalling (J. G. Goetz et al., 2014) (Spasic & Jacobs, 2017). Previous work in the lab had shown that ROCK inhibition by Y-27632 (10μM and 50μM) increases ciliary length in hTERT RPE-1 cells (Grant, G., PhD Thesis). Furthermore, the Johnson group by siRNA screens showed that ROCK2 is a vital regulator of cilium formation and function (Lake et al., 2020). Therefore, the effect of cilia and ROCK on lumen formation and lumen expansion has to be elucidated.

1.10.2 Stimulation of angiogenesis in co-culture by bFGF

Previous work in the laboratory by (Stewart, L., PhD Thesis) showed that although VEGF and FGF both act as angiogenic factors in the co-culture angiogenesis assay, stimulation with these two growth factors results in tubules with different characteristics. Although both FGF and VEGF promote tubule growth has indicated by a similar increase in total tubule length, there was

significantly higher increase in average tubule length with FGF compared to VEGF stimulation. Furthermore, the longest tubule length within a microscopic field area was higher under conditions of bFGF stimulation compared to VEGF stimulation. VEGF but not FGF significantly increased the formation of branches (Figure 1.6). Previous study in the Mavria group showed that DOCK4 is a key regulator of sprouting and lumen formation (Abraham et al., 2015). Although studies showed that DOCK4 regulate sprouting downstream of VEGF signalling, it's role downstream of FGF signalling has to be investigated.

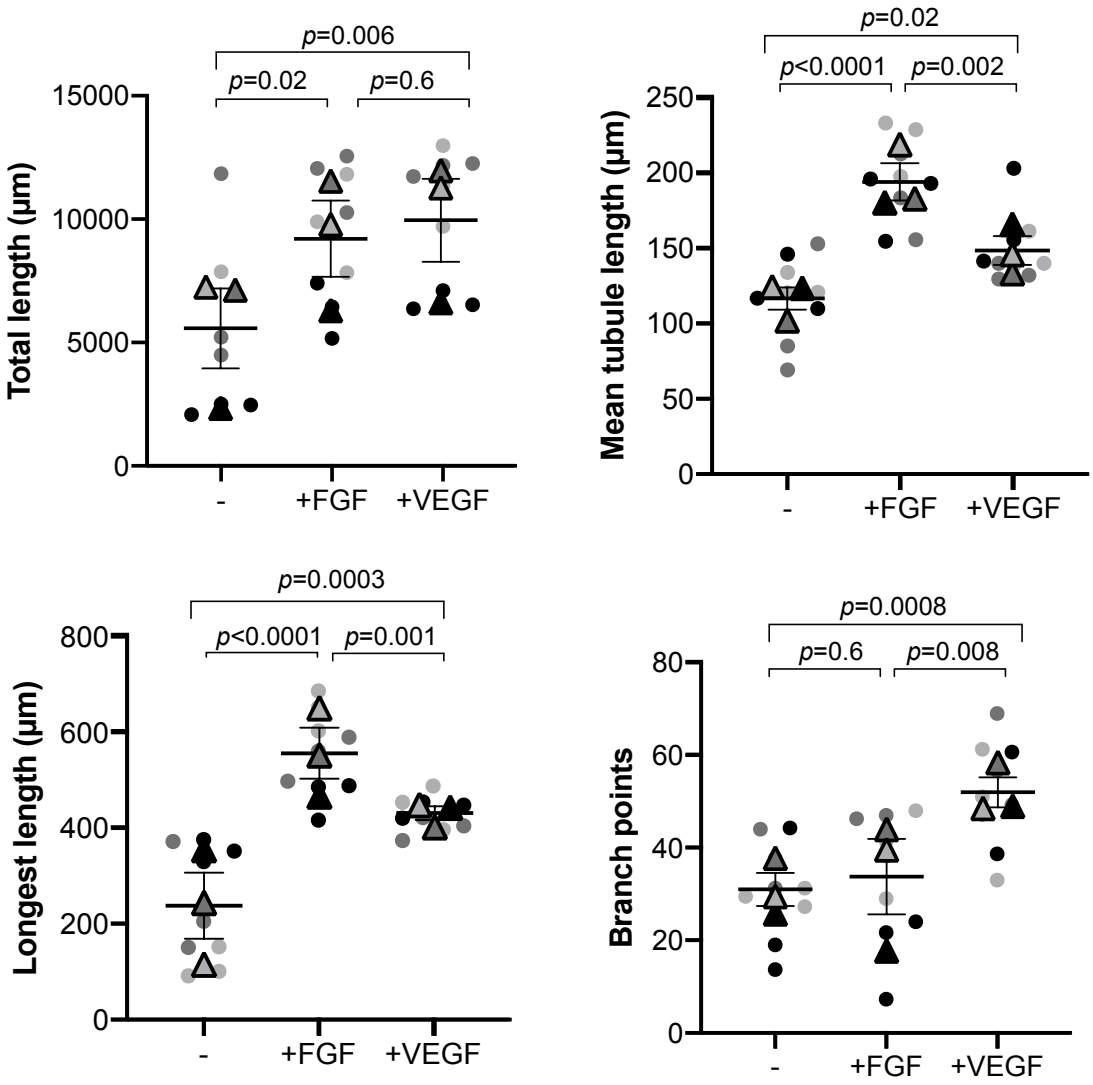

Figure 1.6 The role of VEGFA and bFGF in tubule formation in the organotypic angiogenesis assay.

In order to assess the effect of growth factors FGF and VEGF on tubule formation in the organotypic co-culture assay, co-cultures were treated with either of the growth factors FGF or VEGF or both of the growth factors. HUVEC were used to set up organotypic co-culture assays with HDF cells. VEGFA (25 ng/ml) or bFGF (10 ng/ml) treatments, separately or in combination, were applied to the media on days two, four and six following seeding of HUVEC onto confluent HDF to stimulate angiogenesis. Dot plots show quantifications of total tubule length (µm), mean tubule length (µm), longest length (µm) and branch points. N=9 organotypic co-cultures from three independent experiments (indicated by different grey dots on the dot plot). Statistical test for pair-wise comparison is Student t-test. Stewart, L., PhD Thesis.

1.11 Aims

The overarching aim of the project has been to establish a 3D cell culture perfused system and investigate mechanisms of blood vessel lumen morphogenesis, specifically the role of cilia and cytoskeletal regulators in sensing of fluid flow. Furthermore, to investigate whether DOCK4 is required for angiogenesis downstream of FGF signalling. The objectives were as follows:

1) Establish a 3D culture system of perfused endothelial tubes, and observe the process of blood vessel lumen formation under conditions of fluid flow.

2) Assess the effects of primary cilia ablation and inhibition of cytoskeletal regulator ROCK on blood vessel lumen formation and expansion.

3) Investigate the role of Rac1 GEF DOCK4 on tubule and lumen formation under conditions of FGF stimulation.

Chapter 2
Materials and methods

2.1 Cell culture

2.1.1 Cell culture conditions

Cells were maintained in humidified incubator at 37°C supplied with 5% carbon dioxide (CO_2) and 95% air.

2.1.2 Plate coating

Poly-L-lysine coating for HEK 293T expansion after thawing from frozen done as follow: T75 tissue culture flask was coated with filter sterilized 40% poly-L-lysine diluted in PBS. 4ml was added to the flask and left for 10mins at room temperature to cover the plate before being rinsed one time with sterile PBS. Plate was used immediately or sorted in PBS at 4°C for up to a week.

2.1.3 Cell lines

Angio-tested Human Dermal Fibroblast (HDF)-tested to perform in the angiogenesis co-culture assay from Cellworks (Buckingham, UK). HDF purchased at passage 6 were cultured in Dulbecco's Modified Eagle's Medium (DMEM) (Cat#: D5671) supplemented with 10% (v/v) heat-inactivated foetal calf serum (FCS) supplied from Sigma-Aldrich, UK, plus 100ug/ml penicillin/streptomycin and 100mg/ml L-Glutamine (Sigma-Aldrich). HDFs were thawed in the water bath at 37°C and cultured in tissue culture T75 flask in 15ml media. HDFs were split 1:5 when they reached almost 80% confluency. HDF cells were used up to passage 11 for co-culture assays.

Angiogenesis tested Human Umbilical Vein Endothelial Cells (HUVEC)-tested to perform in the angiogenesis co-culture assay purchased from Cellworks were grown in Human Large Vessel Endothelial Cell Growth Medium (LVE) supplemented with supplied growth supplements and antibiotics (Cellworks), or

Endothelial Cell Growth Medium-2 (Lonza). HUVEC were purchased at passage 1 and used up to passage 4. HUVEC being thawed into T75 flask with 15ml medium as per supplier instructions. After approximately 2 days, when cells reached 80% confluency, they were harvested. Cells were washed once with PBS and then coated with 1ml of trypsin EDTA 1% (Sigma Aldrich). When 90% of cells had detached, 10 ml pre-warmed media were used to resuspend cells and transfer them for freezing, culture or splitting. Cells were counted manually using a haemocytometer. For splitting purpose detached cells were resuspended in 10ml media and split into T75 flasks at 1:4 ratio. Cells were grown to 80% confluency prior to splitting with media refreshed every 48 hours.

hTERT-RPE1 (hTERT-immortalized retinal pigment epithelial cells) from ATCC were cultured in DMEM/F-12 10% FBS. hTERT-RPE1 were grown to confluency before being split at a ratio of 1:5 once a week.

HEK-293T (Human embryonic kidney cells) were cultured in DMEM 10% FBS, 100mg/ml L-glutamine, 100µg/ml penicillin and 100µg/ml streptomycin. Cells were brought into culture in 40% poly-L-lysine coated T75 flasks. Cells were harvested at 90% confluency and split at a ratio of 1:6.

All cells were cultured in humidified atmosphere with 5% CO_2 tissue culture incubators at 37°C.

2.1.4 Freezing and thawing cells

All cell stocks were stored at -196°C in vapour stage liquid nitrogen Dewar. Cells were transferred on dry ice and defrosted quickly in a 37°C water bath prior to be added to warm media.

To generate frozen cell stocks for long term storage, when cells were sub-confluent and actively proliferating, they were washed once in PBS and trypsinised. When completely detached, cells were re-suspended in media and

transferred to a falcon tube. Cells were spun down at 22°C, HDF at 290 g for 5mins and HUVEC at 163 g, 6mins. Once a pellet was deposited on the bottom of the tube, the supernatant was aspirated, and the pelleted cells re-suspended in pre-chilled freezing medium (FM) containing 90%FBS and 10% dimethyl sulfoxide (DMSO). Between 0.5 and $1x10^6$ cells were resuspended in 1ml FM into 1.5ml cryogenic vials, stored at -80°C overnight prior to long term storage in liquid nitrogen and were transferred to liquid nitrogen (LN2) after 24 hours.

Frozen cells were recovered by thawing a frozen aliquot in a 37°C water bath and transferring cells to an appropriate flask required for culturing. After thawing, cells resuspended in fresh medium before cultured in a T75 or T150 flask.

2.1.5 Standard solutions

List of commonly used solutions used throughout this thesis are shown in Table 2.1. Solutions were either purchased or prepared in the lab according to experimental requirements.

Standard solution	Company	Recipe
DMEM (Dulbecco's modified Eagles medium	Sigma-Aldrich	
Freezing medium		90% FBS with 10% DMSO (Invitrogen)
LB (Luria broth)	Sigma-Aldrich	20g LB powder in 1L distilled water. Autoclaved
LVE (Large vessel endothelial cell medium)	Cellworks	

Trypsin EDTA (ethylenediaminetetraacetic acid)	Sigma-Aldrich	
TE (Tris EDTA) buffer		1ml of 1MTris-HCL (pH 8.0) and 0.2ml EDTA (0.5 M) up to 100ml with distilled water
TBS (Tris buffer saline, pH8)		50mM Tris, 150mM NACL
TBST (Tris buffer saline Tween)		TBS with 0.1% Tween 20 (Sigma-Aldrich)
PBS (phosphate buffered saline)	Sigma-Aldrich	500ml disH20 + 2 PBS tablets (P4117, Sigma) + 1 PBS tablet (BR0014G, OXOID). Autoclaved
Transfer buffer		25mM Tris, 190mM glycine, 20% methanol
Running buffer	Invitrogen	10X solution dilutes with distilled water to 1X
4% PFA (Paraformaldehyde)	Sigma-Aldrich	20 g Paraformaldehyde in 500 ml dH_2O heated at 55°C, 50 ml 10X PBS. pH adjusted to ~7.5
HUVEC optimized medium (Angiogenesis growth medium)	Cellworks	

Table 2.1 List of commonly used standard solutions used throughout this study.

2.1.6 Bacterial cell culture

All shRNAs clone for lentiviral knockdown were stored at -80°C. All shRNA clones were cultured at 37°C in LB broth medium plus 100µg/ml ampicillin. In summary, bacterial stock was partly defrosted and bacterial culture from glycerol stock was streaked on LB agar plates containing ampicillin. Then a 10µl inoculum of the bacterial colony was added to 100ml of LB plus 100µg/ml ampicillin at 37°C and shaken overnight. Cultures were pelleted to obtain plasmid extraction using a Midiprep Kit (Qiagen) according to the manufacturer's protocol.

2.2 Cell culture techniques

2.2.1 Production of lentiviral vectors in 293T cells

Virus production done according to Tornolab protocols. After coating the plate with 40% poly-L-lysine $2.5x10^6$ HEK 293T cells were plated in a 10cm plate and grown for 3 days to get confluency of 70%. Calcium-phosphate precipitate was prepared (1ml/10cm plate) (transfer vector 20µg, packaging plasmid 15µg, Envelope plasmid 6µg) vectors were added to 0.5ml of dH_2O and 50µg 2.5M $CaCl_2$ before the stage of adding 0.5ml 2xHBS drop by drop to the solution whilst it is under vortex agitation. The precipitate was left for 20 mins at RT then added dropwise to the plate. The plate was mixed by tilting plate from side to side. The media was discarded and replaced with fresh warm medium. After 7 hours media was collected and replaced with fresh media as before. Collected media was filtered through a 0.45µm filter and stored at 4°C before moving to -80°C for long term storage. The collecting of media was repeated after 24 hours.

2.2.2 HUVEC lentiviral transduction

In a T75 tissue culture dish, $5x10^5$ HUVEC were seeded for the purpose of transduction. 2ml virus was added to 2ml LVE media with 8µg/µl polybrene and

replaced the cells media. After 16 hours combination of virus plus media was removed and replaced by fresh media. For instance, lentivirus harbouring EGFP was used to infect HUVEC followed by sorting to generate HUVEC-EGFP.

2.2.2.1 IFT88 and RPGRIP1L lentiviral transduction

This was performed using IFT88 shRNA, RPGRIP1L shRNA and Nontargeting shRNA lentivirus stocks already available in the laboratory. HUVEC were plated in T75 flasks and grown until they gained almost 70% confluency. Afterwards they were infected by pTRIPZ shRNAs including IFT88-1, RPGRIP1L and Nontargeting. Viruses were diluted in LVE medium containing 8µg/µl polybrene and incubated with cells for almost 16 hours.

2.2.2.1.1 Doxycycline induction

Doxycycline induction (2µg/µl) was done on day 9 on the transduced HUVEC with IFT88 shRNA, RPGRIP1L shRNA and Nontargeting shRNA. The media were subsequently replenished with addition of doxycycline on days 10,12 and 13 of the co-culture assay. Tubules and tube formation were visualised by IHC using an EVOS microscope and the knockdown was confirmed by western blotting.

2.2.2.2 Generation of serotonin receptor HTR6-CFP2 lentivirus for cilia monitoring

2.2.2.2.1 Lentiviral vector preparation

Lentiviral vector pWPXL gifted from Heiko Wurdak was used for the cloning of mouse serotonin receptor 5-hydroxytryptamine receptor 6 (HTR6) and cyan-to-green photoswitchable fluorescent protein PS-CFP2 genes. Bacterial cultures harbouring the lentiviral vector from glycerol stock were streaked on LB agar

plates containing ampicillin. Then inoculation was carried out either by adding a bacterial colony or 10µl glycerol stock into 100ml of LB with 100µg/ml ampicillin in a flask followed by shaking in an incubator at 37°C overnight. Cultures were pelleted for plasmid extraction using a Midiprep Kit (Qiagen) according to the manufacturer's protocol.

To generate the lentiviral vector harbouring HTR6 and PS-CFP2, a restriction digestion was first carried out to remove EGFP from the pWPXL vector using BamHI and EcoRI restriction enzymes and NEBuffer 2.1. Incubation carried out at 37°C for 1 hour followed by heat inactivation of the enzymes at 65°C for 20mins. Then the products plus 6xloading dye were run on 2% agarose gel containing Midori Green. Following electrophoresis, the digest products were visualised by fluorescent Midori Green and the linearized pWPXL was cut from the gel. Subsequently, the Gel Extraction Kit (QIAquick) was used to elute the DNA.

2.2.2.2.2 HiFi assembly cloning

Both HTR6 and PS-CFP2 genes were obtained from Addgene. In order to amplify pWPXL-HTR6-CFP2 and HTR6-CFP2-pWPXL fragments, asymmetrical cleavage made to create overhangs by Q5 Taq polymerase PCR reaction, using Forward primer1,
5'AGGTTTAAACTACGGGATCCAGGCCTAAGCTTACGCGTCCTAGCGCTAC
CGGTCGCCACCATGGTTCCAGAGCCCGG3'
and reverse primer2,
3'GCTCGGCGCCCTTGCTCACGTTCATGGGGGAACCAAGTG5'
to obtain HTR6 with overhangs. Also forward primer3,
5'CACTTGGTTCCCCCATGAAC GTGAGCAAGGGCGCCGAGC3'
and reverse primer4,
3'TATGACTAGTCCCGGGAATTCTTACTTGTACAGCTCATCCATG5'
to obtain HTR6-CFP2-pWPXL fragments.

PCR products were separated by gel electrophoresis, the fragments were cut from the gel using a scalpel and the DNA was extracted using QIAquick Gel Extraction Kit. The HiFi Cloning Kit (New England Biolabs) was used to sub-clone DNA fragments into pWPXL lentiviral vector, including two positive controls (pUC19 plasmid and NEBuilder positive control provided by manufacturing) and negative control (only inserts without vector). Transformation of plasmid DNA into E. coli carried out by using the heat shock method by 30 minutes incubation on ice, followed by heat shock at 42°C for 30 seconds, and incubation on ice for 2 minutes. Then the cells shake for 1 hour on shaking incubator (250rpm) with SOC media (provided by manufacturing). The cells were spun at 13000rpm for 1 minute and resuspended in 70µl SOC media. Transformed cells were spread on pre-warmed ampicillin LB plates and incubated overnight. Transformations from single colonies on agar plates were grown on Lb overnight in a shaking incubator. The QIAprep Spin Miniprep Kit was utilised to elute DNA. To verify that clones contain correct plasmids, restriction enzyme digests were set up, followed by separating the DNA fragments by agarose gel electrophoresis.

2.2.2.2.3 Sequencing

Sequencing reactions were carried out by preparing a master mix for five designed primers:
forward primer1, 5'GCAACAGACATACAAACTAAAGAATTA3',
reverse primer2, 3'CATAGCGTAAAAGGAGCAACA5',
forward primer3, 5'ATCCTGATCGAGCTGAATGG3',
forward primer4, 5'GCTACCTGCTCATCCTCTCG3',
forward primer5, 5'ACAGTAGGCGTCTGACCACC3'
which were run on a thermal cycle. This was followed by precipitation and sequencing using a DNA sequencer (Applied BioSystems).

2.2.2.2.4 Agarose gel electrophoresis

Agarose gel electrophoresis was used to separate DNA fragments. Agarose gel was prepared by adding 4g agarose to 200 ml of 1X TBE (Tris/Borate/EDTA) buffer, which was then microwaved for 3-4 minutes followed by adding 8 µl Midori Green (0.004%) to the mixture. The mixture was loaded into the casting tray with combs to set the wells. After 20 min, the gel cast was ready and transferred into the tank. For every 5µl of sample 1µl gel loading buffer was added with a total of 25 µl being loaded onto the wells in the gel. A 2000 bp DNA Ladder was added into the first well of the row as a marker. The gel was run for 45 minutes at 120V. The image of the DNA fragments was captured using the BIO-RAD Molecular Imager Gel Documentation System.

2.2.3 FACS sorting

HUVEC transduced with a lentivirus were trypsinised, and collected for fluorescent activated cell sorting, HUVEC were centrifuged (163 g), resuspended in PBS twice at maximum concentration $5x10^6$ cells/ml and transferred to sterile polystyrene FACS tubes. The LIMM Cell Sorting Facility sorted the cells based on pre-determined gates based on the level of EGFP expression. Sorted HUVEC were placed back in culture for 48 hours or used directly for experimentation.

2.2.4 HUVEC-HDF co-culture angiogenesis assay

$2x10^4$ HDF at passage 6-11 were plated into glass-bottom 24-well plates (*In Vitro* Scientific) and cultured for six days to form a confluent layer without changing medium. 8500 HUVEC-EGFP cells seeded onto a confluent layer of HDFs and grown in 50:50 DMEM:LVE medium for 7 days before being changed to optimized medium (Angiogenesis Growth Medium Package) to aid in lumen formation. Media was refreshed every 48 hours. Angiogenesis was induced by using growth factors. Unless otherwise stated, only Vascular Endothelial Growth Factor A

(VEGFA) (25 ng/ml; Sigma-Aldrich) and basic Fibroblast Growth Factor (bFGF) (10 ng/ml; Peprotech) was used in this study on days two, four and six of seeding HUVEC on HDF. Cells were either fixed and stained on day seven in ice cold 70% ethanol for 20 minutes by immunohistochemistry (IHC) to assess tubule formation and sprouting, or on day fourteen by 4%PFA for immunofluorescence (IF) to assess lumen formation.

2.2.5 In-vitro ciliogenesis assay

Cells to be studied in the ciliogenesis assays were grown on 35mm glass bottom plate (ibidi, Germany) for imaging. hTERT-RPE1 were grown to 70% confluency in DMEM/F-12 10% FBS and HUVEC grown in LVE plus supplements and antibiotics. Cells were then serum starved for 18 hours for hTERT-RPE1 in DMEM/F-12 0.2% FBS and HUVEC in LVE plus antibiotics without supplements.

2.3 Imaging techniques and immunostaining

2.3.1 Co-culture fixation and immunofluorescence (IF) staining

Co-cultures were fixed in 4% paraformaldehyde for 20 minutes at room temperature on day 14 of co-culture for visualisation of lumens. Cultures were then washed three times with PBS and permeabilised with 0.1% TX100/PBS for 20 minutes at RT before being blocked in 0.5% BSAPBS for 20 minutes at RT. Primary antibodies were diluted with blocking solution and added to the cells and left in an fridge overnight at 4°C. Used primary antibodies are listed in Table 2.2. The following day, cells were washed three times with PBS and secondary antibodies diluted with blocking solution were applied and incubated for 1 hour at 37°C. DAPI (4',6-diamidino-2-phenylindole) 1µg/ml for nucleic acid staining was added same as secondary antibodies (Table 2.3).

2.3.2 Cilia fixation and staining

For the purpose of visualizing cilia, cells were serum starved for 18 hours (hTERT-RPE1 in DMEM/F-12 0.2% FBS; HUVEC in LVE plus antibiotics without supplements). 20 minutes before fixing the cells with 4%PFA, media was replaced by PBS and the cells left on ice for 20 minutes. Then cells were fixed in 4% paraformaldehyde for 20 minutes. they were washed three times with PBS and permeabilised with 0.1% TX100/PBS for 20 minutes and blocked in 2% BSAPBS for 20 minutes. Primary antibodies were diluted with o.5% BSAPBS and added to the cells and left in fridge overnight at 4°C. The following day, cells were washed three times with PBS and secondary antibodies were applied and incubated for 1 hour at 37°C.

Antibody	Target	Type	Host/ Isotype	Supplier	Dilution
Podocalyxin Af-1658	Apical side of ECs during cell polarization	Polyclonal	Goat IgG	R+D systems	1:100
VE-cadherin Sc-9989	Cell-cell contacts of ECs	Monoclonal	Mouse IgG	Santa Cruz	1:100
CD31 ab28364	Endothelial cells	Polyclonal	Rabbit IgG	Abcam	1:100
ARL13B 17711-1-AP	Axoneme of cilia	Polyclonal	Rabbit IgG	Proteintech	1:250
GT335 AG-20B-0020-C100	Polyglutamylated tubulins	Monoclonal	Mouse IgG	Adipogen	1:500

Table 2.2 List of primary antibodies used for immunofluorescence.

Antibody	Target species	Type	Isotype	Supplier	Dilution
Alexa Fluor 488	Mouse	Polyclonal	IgG	Invitrogen	1:1000
Alexa Fluor 488	Rabbit	Polyclonal	IgG	Invitrogen	1:1000
Alexa Fluor 594	Mouse	Polyclonal	IgG	Invitrogen	1:1000
Alexa Fluor 594	Rabbit	Polyclonal	IgG	Invitrogen	1:1000
Alexa Fluor 633	Rabbit	Polyclonal	IgG	Invitrogen	1:1000
Alexa Fluor 647	Rabbit	Polyclonal	IgG	Invitrogen	1:1000
DAPI (Localization: Nucleus, Nucleic Acids)	N/A	N/A	N/A	Sigma-Aldrich	1:2000
TOTO3 (Localization: Nucleus, Nucleic Acids)	N/A	N/A	N/A	Fisher Scientific	1:2000

Table 2.3 List of secondary antibodies used for immunofluorescence.

2.3.3 Immunohistochemistry staining (IHC)

In order to visualise tubule formation, cells were immunostained for CD31 (PECAM-1). Co-cultures were immunostained according to binding of an alkaline phosphatase-coupled anti-CD31 antibody linked to an insoluble chromogenic substrate that stained tubules with a dark purple colour. Cells were washed with Phosphate-Buffered Saline (PBS) (made by dissolving 2XPBS tablets (Sigma-Aldrich) with 1XPBS (DulbeccoA, OXID) in 500ml H_2O followed by autoclave). An ice-cold fixative (70% ethanol) was incubated with cells at room temperature (RT) for 30 minutes. Cells were washed three times with PBS and primary antibody mouse anti-human CD31(1:400 in 1%BSAPBS) was added to the cells and incubated for 60 minutes at 37°C. Goat anti-mouse IgG AP conjugate diluted 1:500 in 1%BSAPBS was then added and incubated for 60 minutes at 37°C.

Finally, cells were washed three times with dH_2O. Two insoluble chromogenic substrate tablets were dissolved in 20ml dH_2O, filtered substrate using disposable syringe and 0.2µm filter disc. Substrate added to each well and incubated at RT until tubules developed a dark purple colour. Wells washed with dH_2O for three times.

2.3.4 Confocal imaging

All confocal imaging was done on a Nikon A1R confocal microscope controlled by NIS-Elements software. For imaging of immunofluorescence-stained samples at high resolution and quality, an advanced fully automated Nikon A1R confocal microscope was used equipped with a hybrid confocal scan head incorporating a resonant scanner for high-speed imaging, and galvo scan for high-resolution image acquisition. The NIS-Elements C Advanced Software Platform (Nikon Instruments) was used to control microscope functions.

2.3.4.1 HUVEC-HDF co-culture confocal imaging

Co-culture imaging was carried out using 12 confocal images from three wells (N=3 organotypic co-cultures) using a 40X oil immersion CFI S. Fluor objective lens and galvo scan head for the purpose of quantification.

2.3.4.2 Cilia imaging

Ciliated cells in a monolayer or in co-culture were imaged using 40X and 100X oil immersion lenses and a galvo scan head of confocal microscope.

2.3.5 Imaging using an EVOS microscope

Fully integrated digital inverted EVOS microscope was used to visualise tubule formation in co-cultures and microfluidic devices. In the plate 12 Images of tubules from 3 wells (N=3 organotypic co-cultures) were taken using 4X and 20X objective lenses at EVOS microscope for quantification.

2.4 Image analysis

Quantification carried out manually as explained in Table 3.1. In order to calculate the branch point index, the number of branches divided by total tubule length.

2.5 Microfluidic devices

In order to introduce flow in the organotypic fibroblast-endothelial cell co-cultures microfluidic devices were used. This project initially utilised two different microfluidic device designs one with a single chamber designed by Dr Matthew Bourn (Sally Peyman lab, Faculty of Mathematics and Physical Sciences, University of Leeds) (Figure 2.1 A) and the other one has three-chamber designed by Dr Graeme Whyte (Biophysics and Bioengineering, Institute of Biological Chemistry, Herriot Watt University) (Figure 2.1 B). Both devices contain four reservoirs (Figure 2.1 C). The microfluidic devices consist of a set of micro-channels and micro-chambers moulded into polydimethylsiloxane (PDMS) fabricated by photolithographic method. Micro-chambers and micro-channels are connected to external cell loading and gel loading ports and reservoirs that are punched through the chip. The difference between the two devices is the number of chambers and presence of gel loading ports. The single chamber device (Figure 2.1 A) has no separate gel loading port, whereas the three-chamber device (Figure 2.1 B) has four gel loading ports. Four external reservoirs were used to introduce fluid flow inside the channels by means of controlling hydrostatic pressure through manipulating the height of media inside the

reservoirs. This allows control of flow and the resultant shear stress (Figure 2.1 C).

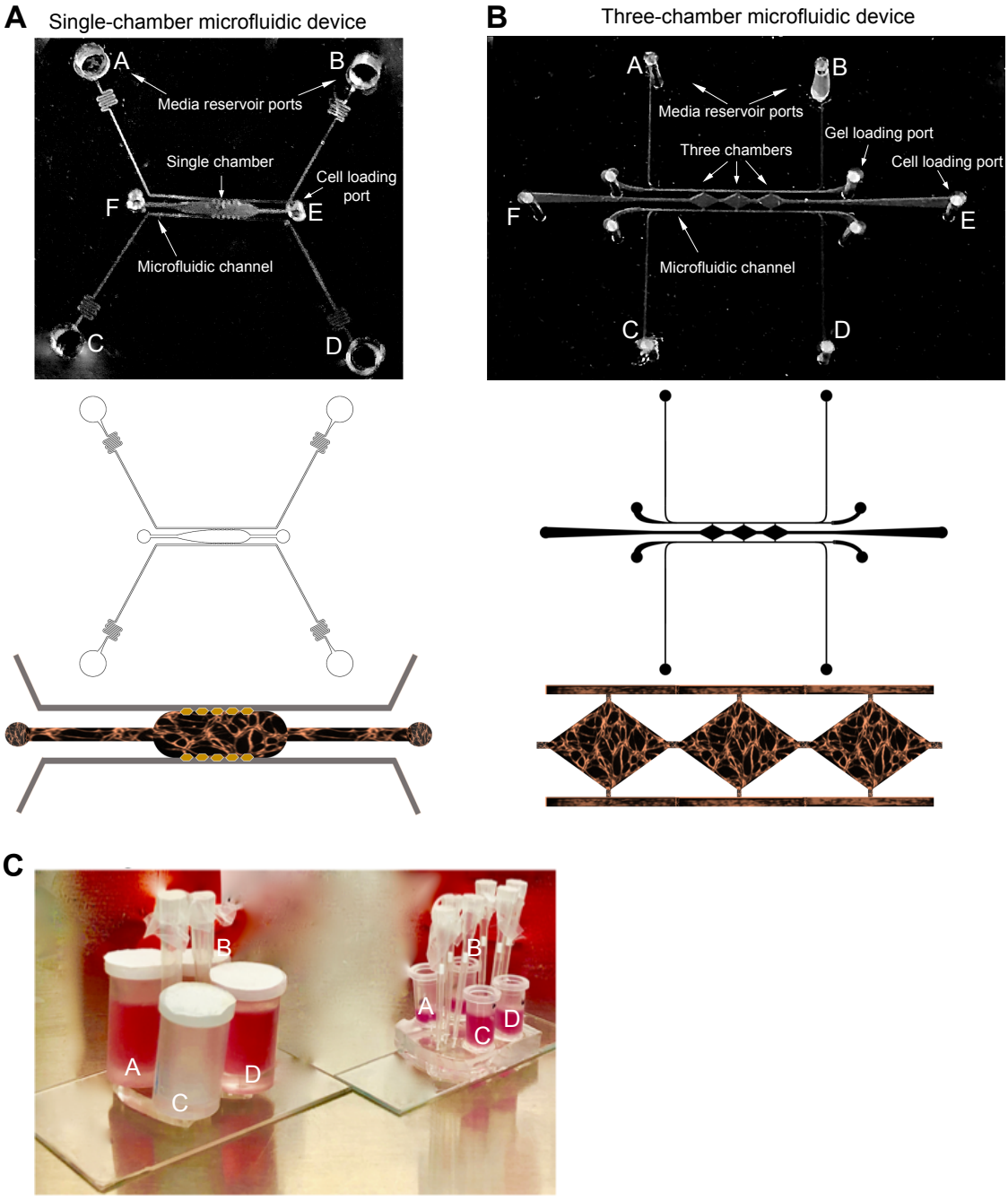

Figure 2.1 Microfluidic devices for the growth of organotypic co-cultures. Two microfluidic devices were designed both of which were sealed circulatory systems based on the original configuration by Moya and co-workers (Moya et al., 2013). The differences between the two devices were the number of

chambers, circulation system inside the device and gel loading ports. **A.** The single-chamber microfluidic device has one chamber connected to the two side channels by six openings created by 5 pillars, four media reservoir ports and two cell loading ports. Flow is introduced into the single chamber via the pillars. **B.** The three-chamber device has three chambers and flow is introduced through individual openings on either side of each chamber, in the absence of pillars. **C.** The four reservoirs in each microfluidic device, single-chamber (left-hand side) and three-chamber (right-hand side), are filled with defined heights of media in order to establish hydrostatic pressure thus circulating fluid inside the microfluidic devices.

2.5.1 Single chamber microfluidic device fabrication

The devices were fabricated from Polydimethylsiloxane (PDMS) on coverslips. An inverted master mould that made from a SU8 layer on a silicon wafer was used to form PDMS microfluidic structures.

PDMS (Sylgard 184, Dowsil) was mixed in a 10:1 base (Silicone Elastomer base) and curing agent (Silicone Elastomer curing agent) ratio. The mixture was centrifuged at 3220 g for one minute. The solution was then poured onto the wafer and desiccated for 40 min to allow air bubbles to rise to the top of the container. PDMS was poured to produce 1 mm thick devices and then cured by placing in an oven at 80°C for 1 hour. The devices were then cut following by punching reservoirs and loading port holes. Oxygen plasma was used to bond the surfaces and bond the device to the coverslip.

2.5.2 Microfluidic organotypic co-culture

Following fabrication, Fabricated devices and reservoirs were then sterilised in an autoclave at 120°C for 40 min. Reservoir lids made from attaching 0.22µm PTFE filters (Cole-Parmer) onto the top of Delrin (Par-group) rings sterilised with

ethanol for one minute prior to experimental use. Fibrinogen (100MG, Sigma-Aldrich) was prepared by dissolving 100 mg of power into 10ml of warm buffer containing 0.9 % NaCl. The solution was gently agitated until a cloudy solution was formed. The solution was then separated into 100 µL aliquots and frozen at -20°C. Thrombin powder (100UN, Sigma-Aldrich) was dissolved in 2 ml of buffer containing 0.1 % bovine serum albumin (BSA) to give a 50U/ml solution. The solution then aliquoted into 20µl and frozen at -20°C. Single aliquots of both fibrinogen and thrombin were defrosted prior to experimental use.

Both HUVEC and HDF cells were detached from their culture flasks and the cells numbers determined. In order to seed $6x10^4$ HUVEC and $6x10^4$ HDF cells in fibrin in the device, cells were counted, spun to pellet and resuspended together in 8µl fibrinogen. The fibrinogen-cell mixture was then split into 8µl aliquots in separate 1.5ml centrifuge tubes. Thrombin was diluted with PBS 1:1 to give a final concentration of 50U/ml. Thrombin polymerises fibrinogen to fibrin within 10 seconds of mixing and, once polymerised, the mixture is no longer possible to manipulate. Therefore 0.6µl of diluted thrombin was rapidly mixed with the 8µl fibrinogen-cell suspension. The mixture was pipetted into the microfluidic chamber via the cell loading port (port E). Devices were then placed on a hotplate at 37°C for 20 minutes to allow the thrombin to polymerise the fibrinogen into fibrin. Four reservoirs were attached (Figure 2.1 C), and filled with 2.5 ml media in two reservoirs (A and D) and no media in the other two reservoirs (B and C) to obtain fluid flow by hydrostatic pressure. The microfluidic device was then placed in an incubator. Flow direction was reversed daily, and media changes were performed every 24 hours. 50:50 DMEM:LVE medium plus VEGFA (25 ng/ml) and bFGF (10 ng/ml) were added to reservoirs before being replaced by angiogenesis media on day 11. On day six $3.0x10^4$ endothelial cells combined with 30µl LVE medium were injected into side channels and continued with LVE medium with VEGFA (25 ng/ml) and bFGF (10 ng/ml) in order to achieve anastomosis of the cells in side channels with the tubules formed inside the chamber.

2.6 Western blotting analysis (Biochemical techniques)

2.6.1 Protein quantification by BCA protein assay

After preparing total cellular lysates, proteins were quantified by the BCA (bicinchoninic acid) method (Smith et al., 1985). This method combines the biuret reaction with the violet-coloured complex formation of copper ions by bicinchoninic acid. A standard curve of BCA ranging from 25µg -2mg of protein was prepared and used to quantify samples. Protein standards and unknown samples were distributed in triplicate into a flat bottom 96-well plate. BCA reagent was added to each well and allowed to react for 30 minutes at 37°C. Following by protein concentration measurement on a spectrophotometer at 562nm wavelength and was calculated on Microsoft Excel.

2.6.2 SDS-PAGE

To identify proteins of interest, after protein quantification samples were analysed using Sodium Dodecyl Sulphate Polyacrylamide Gel Electrophoresis (SDS-PAGE). Quantified proteins were resuspended in 4X loading buffer (NuPAGE, Invitrogen) plus 50mM DTT, then heated at 70°C for 10minutes. Samples of protein (25 µl) were loaded into lanes, separated on 3-8% precast Tris-Acetate gels (Invitrogen). Electrophoresis was performed at 100V for 2-3 hours in 20X Tris-Acetate SDS Running Buffer (NuPAGE). 5µl of protein standard ladder (Dual colour marker, Proteintech, 10-180kDa) was loaded to compare proteins' size.

2.6.3 Western blotting and detection

After completion of SDS-PAGE electrophoresis the gels were transferred to 50ml of transfer buffer for equilibration. Gels were then transferred to polyvinylidene difluoride (PVDF) membranes (pre-activated in 100% methanol for 10 seconds) and sandwiched between 4 sheets of Whatman paper and 2 sponges. The

sandwich was then placed in a transfer tank prefilled with 1X transfer buffer. Transfer was done at 1A at 4°C overnight.

Enhanced chemiluminescence (ECL) method was used to visualise membrane. Membrane was first blocked in 5% milk powder in TBST for 1 hour at room temperature. The PVDF membranes were incubated with primary antibody 1:1000 in TBST 5% BSA at 4°C overnight. After three 10 minutes washes in TBST at room temperature, secondary antibody (horseradish peroxidase enzyme conjugated) was added 1:5000 in TBST 5% BSA for 45 minutes at room temperature. Primary and secondary antibodies are listed in Table 2.4. All secondary antibodies are anti-IgG1. Membrane was then washed three 10 minutes in TBST before adding ECL solution (Amersham ECL solutions A and B, 1:1 ratio) for 1 minute at room temperature. Membranes were exposed on X-ray film (Amersham Hyperfilm). Band intensities analysed using Image J software.

2.6.4 Stripping and reprobing

PVDF membrane was stripped and reprobed for a loading control GAPDH. To strip membrane, it was washed in ultrapure water for 10 minutes at room temperature, then 0.5M sodium hydroxide for 10 minutes and finally ultrapure water for 10 minutes. Membrane was then re-blocked in 5% milk powder and probed with primary antibody.

Primary antibody	Molecular weight	Type	Host/ Isotype	Supplier	Dilution/ concentration
DOCK4 A302-263A	190 kDa	Polyclonal	Rabbit/ IgG	Bethyl	1:1000
IFT88 13967-1-AP	94 kDa	Polyclonal	Rabbit/ IgG	Proteintech	1:1000
RPGRIP1L 55160-1-AP	151 kDa	Polyclonal	Rabbit/ IgG	Proteintech	1:1000
GAPDH Ab9485	36 kDa	Polyclonal	Rabbit/ IgG	Abcam	1:1000
Secondary antibody	**Target species**	**Host species**	**Isotype**	**Supplier**	**Dilution/ concentration**
HRP	Rabbit	Goat	IgG	Abcam	1:5000

Table 2.4 List of antibodies used for immunoblot assays.

2.7 Statistical analysis

Data were analysed using GraphPad Prism Version 8.4.3 (GraphPad Software Inc., California, USA). Data has normal distribution and equal co-variance. Statistical analysis and determination of P-values was carried out using Student t-test. For student t-test, a P-value of equal or less than 0.05 was considered as statistically significant. All data figures were produced using Adobe Illustrator, Version 25.4.8 (Adobe, California, USA). Unless otherwise stated, all error bars in the graphs represent S.E.M for 3 or more biological replicates.

Chapter 3
Development of endothelial fibroblast co-culture in microfluidic devices and marking of cilia

3.1 Introduction

Blood vessels form *de novo* through the process of vasculogenesis, or expand from pre-existing blood vessels through the process of angiogenesis (Eilken & Adams, 2010). Irrespective of the mechanism of vessel growth, vessel lumens form through the process of lumenogenesis (Carmeliet, 2000). Angiogenesis involves the process of growth, migration and differentiation of endothelial cells which are covering the side of blood vessels. This process is regulated by chemical signals including vascular endothelial growth factor A (VEGFA) and basic fibroblast growth factor (bFGF). These bind to their receptors on endothelial cells and promote growth and survival of new blood vessels. In response to VEGF, endothelial tip cells, which are the leading cells at the tips of a vascular sprout, extend through the proliferation of trailing stalk cells. Equally, angiogenesis inhibitors are chemical signals that inhibit blood vessel formation. The balance between the inhibition and stimulation of angiogenesis is critical for the formation and maintenance of blood vessels.

The initial stages of lumenogenesis take place through complex cellular mechanisms, including the rearrangement of lateral cellular junctions. This allows organisation of endothelial cells into 3D tubular structures and can take place in the absence of flow (Y. Wang et al., 2010). Recent studies *in vivo* using zebrafish show that haemodynamic forces expand a provisional vessel lumen through deformations of the endothelial apical membrane, resulting in actomyosin recruitment and contraction (Gebala et al., 2016). Lumen expansion, and stabilization by perivascular cells that allows perfusion of the circulatory network, is intimately linked to the onset of fluid flow (Herwig et al., 2011) (Lenard et al., 2013).

To mimic the cardiovascular transport system *in vitro* and to allow easy genetic or pharmacological manipulation of developing tubes, this study employs microfluidic devices to establish a 3D co-culture system of perfused endothelial tubes that allow easy manipulation of the processes involved in flow sensing, and the development and regulation of blood vessel lumens. The microfluidic devices host organotypic endothelial-fibroblast co-cultures seeded in a 3D fibrin matrix

inside the chamber where blood vessel networks initially form via vasculogenesis and later expand through angiogenesis. This system of perfused endothelial tubes is based on the endothelial-fibroblast coculture system used extensively in Mavria's lab (Abraham et al., 2015). Organotypic co-culture in microfluidic devices make a closed circulatory system comprising a network of naturally-developing endothelial tubes capable of transporting fluid that allow genetic manipulation of ECs prior to coculture. The subsequent monitoring of lumen formation, flow sensing and lumen expansion under fluid flow can provide valuable insights into the mechanotransduction of flow and its influence on lumen development. Specifically, for this project, the microfluidic device was employed to investigate the role of ciliary proteins and cytoskeletal regulators ROCK and DOCK4 in flow sensing and the development of vessel lumens under conditions of flow.

3.2 Optimisation of the organotypic co-culture assay to model angiogenesis *in vitro*

In order to establish 3D system of perfused endothelial tubes, an *in vitro* organotypic co-culture model was used that recapitulates the stage specific to tubule formation. Primary human umbilical vein endothelial cells (HUVEC) were cultured with human dermal fibroblast cells (HDF) to set up an organotypic co-culture assay. The HDF generate a natural 3D environment containing matrix and growth factors (Greenberg et al., 2008) to which exogenous angiogenic growth factors may be added (Mavria et al., 2006). Nascent endothelial tubes were allowed to form after addition of VEGFA (25 ng/ml) or bFGF (10 ng/ml) to the media on days two, four and six following seeding of HUVEC onto confluent HDF to stimulate angiogenesis. Following adding growth factors to the cluster of HUVEC, they remodel dynamically and sprout for approximately 7 days before they form lumens on day 14. At day 7, tubule formation can be assessed by immunohistochemistry (IHC), CD31 staining and bright field microscopy or live cell imaging. To promote tubule establishment and lumen formation, on day 9 the culture media are switched to Optimised media (TCS Cellworks) that contain a

lower concentration of growth factors. In order to form lumen, stalk cells must establish lateral cell-cell adhesion and proliferate by down-regulating their response to angiogenic growth factors (Blanco & Gerhardt, 2013). Lumen formation was then assessed by immunofluorescence staining using a Nikon A1R confocal microscopy on day 14 (Figure 3.1). At the start of the project, the number of HUVEC and HDF in co-cultures were varied and the optimal tubule formation was observed with 8,500 HUVEC and $2x10^4$ HDF. Subsequent experiments used these cell numbers.

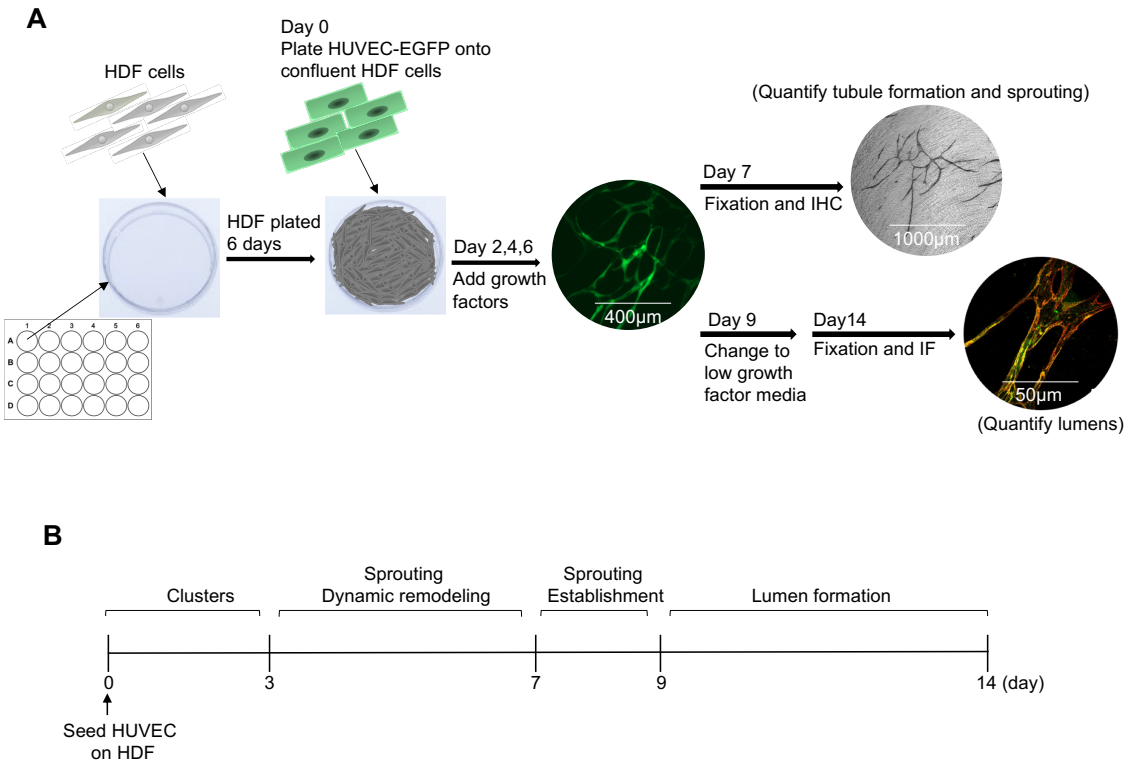

Figure 3.1 Organotypic co-culture angiogenesis assay in the absence of fluid flow.

A. Schematic depicts set-up of the co-culture of HUVEC with HDF and tubule development over 14 days. **B.** Distinct steps of tubule development and lumen formation observed in the organotypic co-culture assay in the absence of fluid flow. Adapted from Abraham et al. (2015).

3.3 Visualisation of HUVEC in the organotypic co-culture

To visualize HUVEC in the organotypic co-culture and track tubule and lumen formation, actin cytoskeleton in HUVEC marked with LifeAct-EGFP, LifeAct-RFP or junctions marked using VE-cadherin-RFP by means of lentiviral transduction. Infection of HUVEC was performed using lentiviruses, followed by changing media after 16 hours and FACS sorting 48 hours after infection (Figure 3.2).

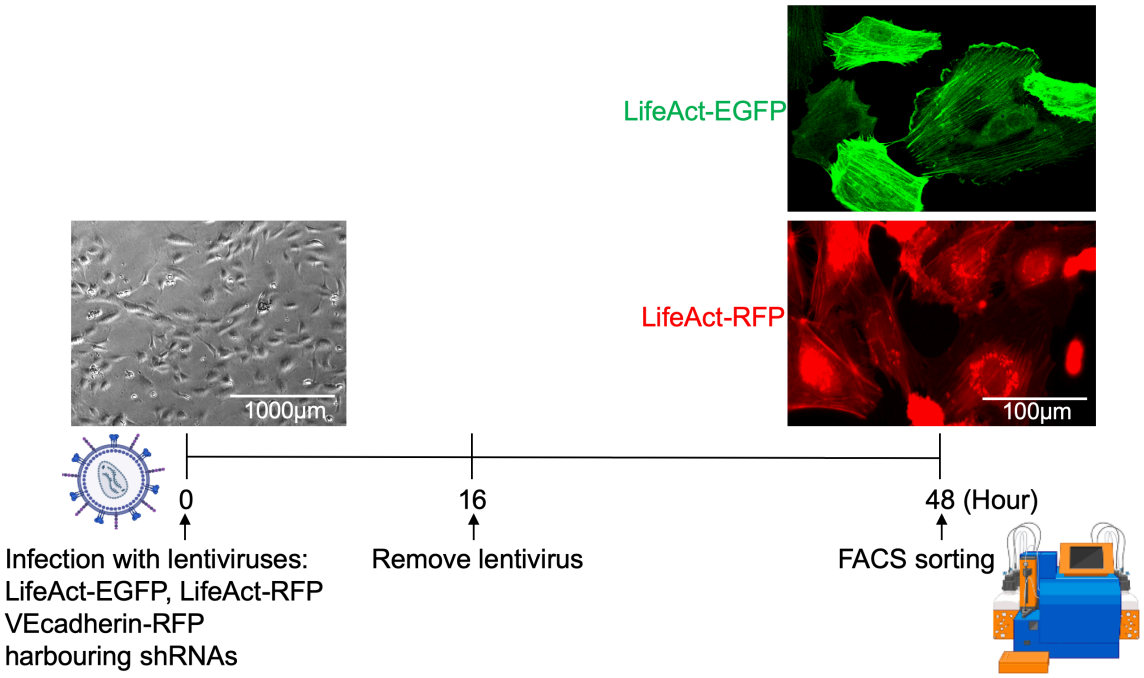

Figure 3.2 Modification of HUVEC prior to co-culturing with HDF.
The schematic depicts infection of HUVEC with lentiviruses harbouring LifeAct-EGFP or LifeAct-RFP marking the actin cytoskeleton, and VEcadherin-RFP marking endothelial cells and junctions followed by FACS sorting.

3.4 Marking HUVEC with red fluorescent protein

In order to compare and select the best lentiviruses harbouring red fluorescent protein, transduction efficiency of four different shRNAs was assessed. Ds-Red, LifeAct-RFP, mCherry and VE-cadherin shRNAs were used at dilutions of 1:2 or 1:5 of virus supernatant with LVE medium to mark HUVEC. With a dilution of 1:2, VE-cadherin demonstrated higher (more than 30 Relative Fluorescent Units (RFU)) fluorescence intensity (average fluorescence intensity corrected for background) in the same order as mCherry at 1:5 dilution (Figure 3.3). Better cell survival was observed with VE-cadherin expression, so this red fluorescent fusion protein was selected to be tested on HUVEC at dilutions of 1:2, 1:5, 1:10 and 1:20 (Figure 3.4).

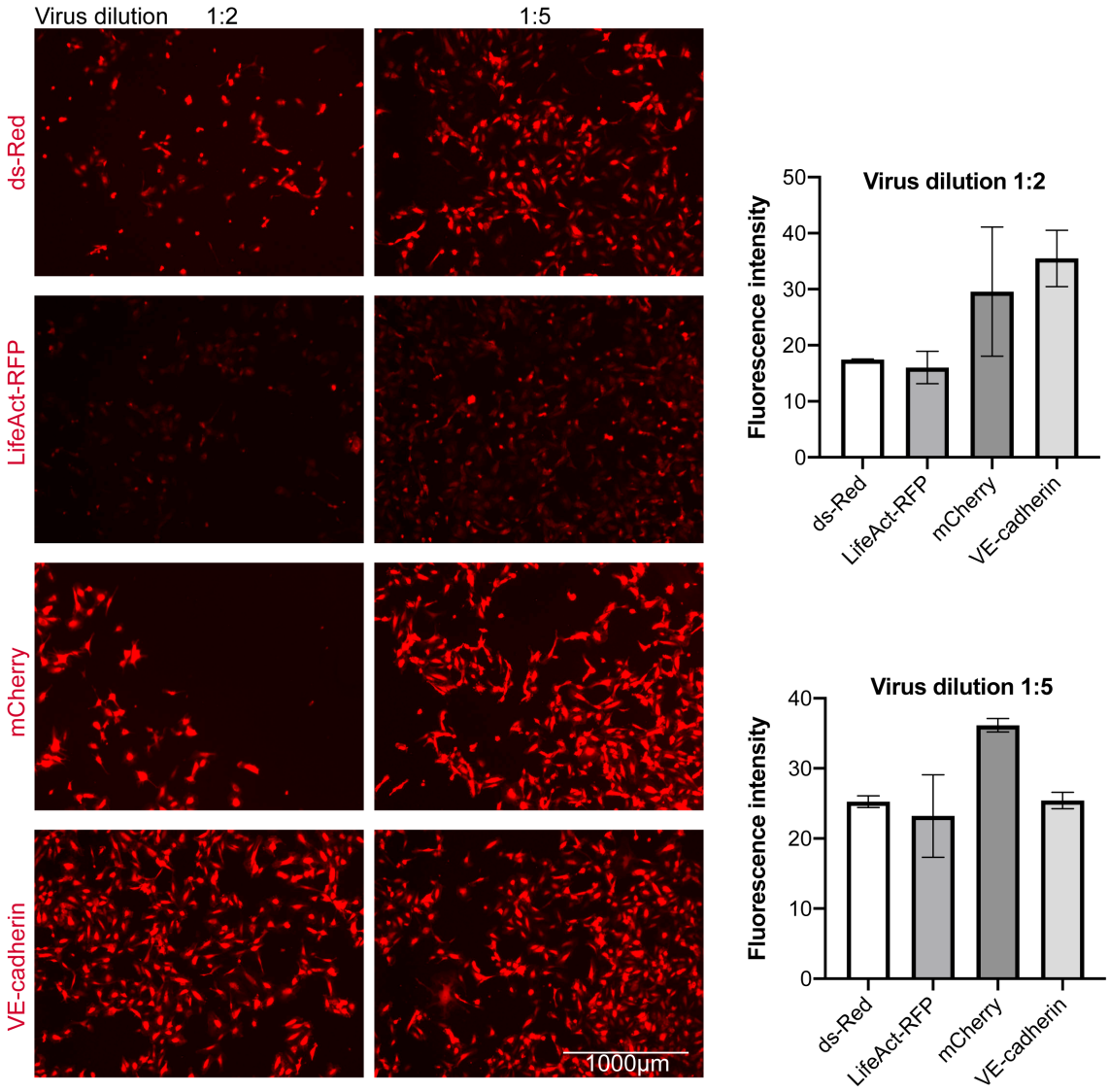

Figure 3.3 Comparison of transduction efficiency of lentiviruses harbouring red fluorescent proteins.

Epifluorescence images show HUVEC infected with lentiviruses harbouring ds-Red, LifeAct-RFP, mCherry or VE-cadherin-RFP at dilutions of 1:2 or 1:5 of virus supernatant with LVE medium. Images were taken using an EVOS microscope, 4X magnification. Scale bar, 1000µm. Bar graphs show quantification of fluorescence intensity (RFU) following infection with virus supernatants at the indicated dilutions. The data are from two images per condition from n=1 biological replicate (indicated by different grey bars on the bar plot). Error bars show the range of fluorescence intensity.

3.5 Employing VE-cadherin-RFP to mark HUVEC with red fluorescent protein

Vascular endothelial cadherin (VE-cadherin) is highly expressed in endothelial cells and is a component of the endothelial adherens junctions. Lentiviruses harbouring VE-cadherin-RFP were used at dilutions of 1:2, 1:5, 1:10 and 1:20 of virus supernatant with LVE medium and polybrene (8μg/μl) for 16 hours. The media was then replaced and cells were FACS sorted after 48 hours. Transduction efficiency as assessed by fluorescence intensity was higher with 1:2 dilution. At this concentration all cells appeared uniformly marked whilst viability was not affected. Hence this dilution was used for subsequent experiments (Figure 3.4).

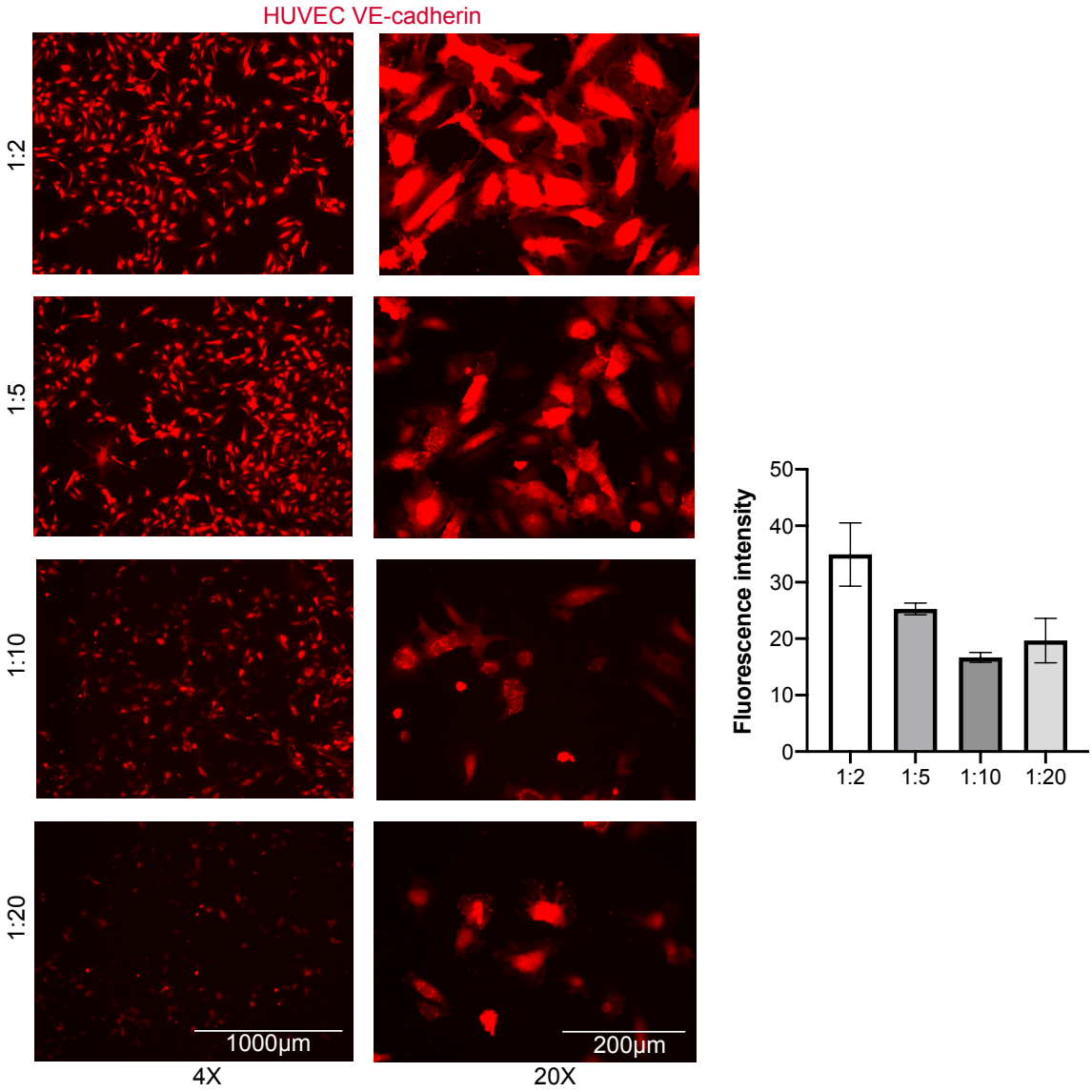

Figure 3.4 Transduction efficiency of the VE-cadherin-RFP lentivirus.
Epifluorescence images show HUVEC infected with VE-cadherin-RFP lentivirus supernatant at dilutions of 1:2, 1:5, 1:10 and 1:20. Images were taken using an EVOS microscope, 4X and 20X magnification. Scale bars, 1000µm and 200µm. Bar graph shows quantification of fluorescence intensity following infection with VE-cadherin-RFP lentivirus supernatant at the indicated dilutions. The data are from two images at 4X magnification per condition from n=1 biological replicate (indicated by different grey bars on the bar plot). Error bars show the range of fluorescence intensity.

3.6 Analysis of tubule and lumen formation in the organotypic co-culture assay

In the organotypic angiogenesis assay tubule branches form when endothelial tip cells followed by stalk cells lead and guide blood vessel sprouts out from the existing blood vessel. Stalk endothelial cells behind the leading tip cells establish lateral cell-cell adhesions and form the lumen, whilst endothelial cells take on an elongated shape and align next to each other in elaborate branched networks. Quantification of tubule formation is possible by measuring several morphological elements that include the length of a tubule (defined as the distance between two branch points, or a branch point and the tubule tip cell, or two ends of a tubule with no branches). Also, by measuring branch points which are sprout connection points to pre-formed tubules or tubes (Figure 3.5 A). Moreover, the formation of apical membrane and lumen formation can be observed on day 14, and can be quantified by the expression levels of the apical marker podocalyxin that localises at the apical surface of a developing lumen (Figure 3.5 B) (Table 3.1).

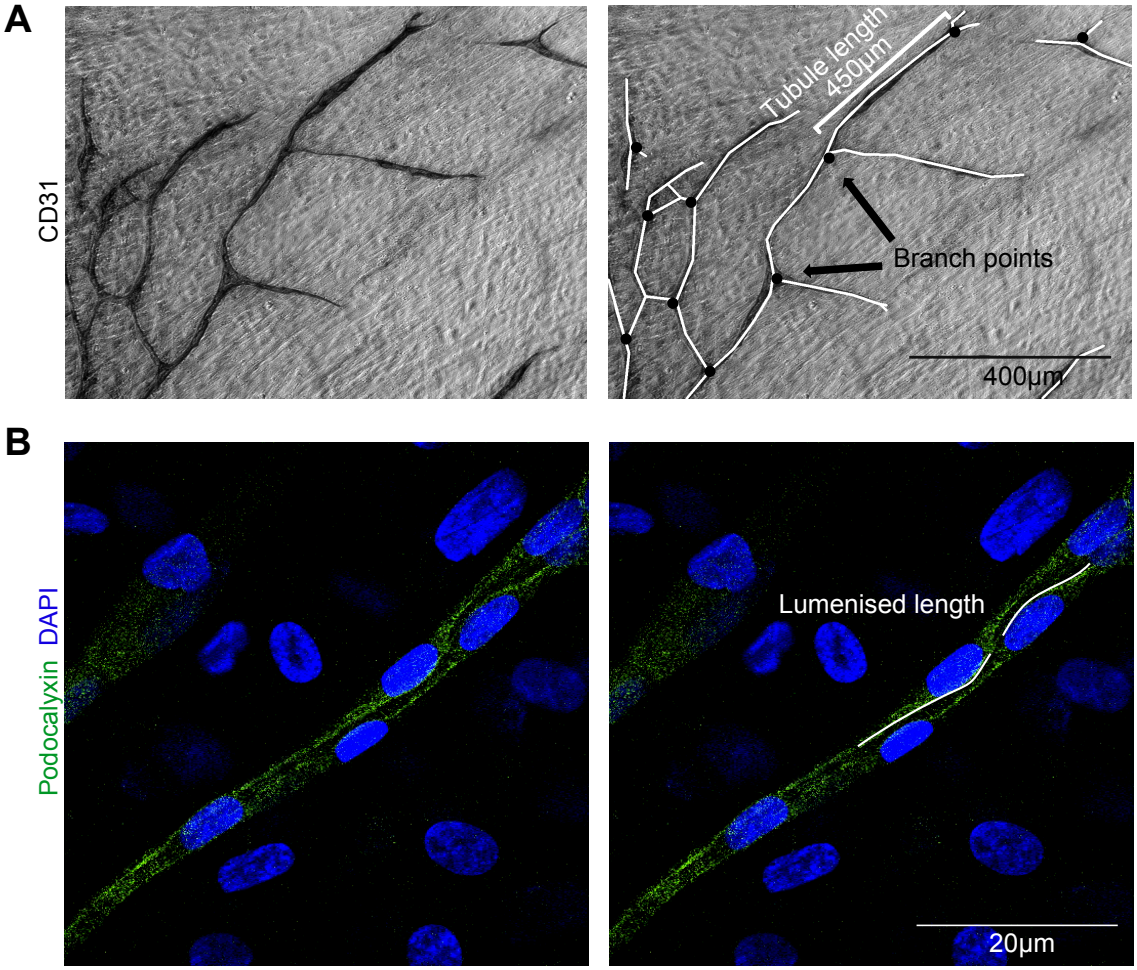

Figure 3.5 Analysis of tubule and lumen formation in the organotypic co-culture assay in the absence of fluid flow.

A. Image depicts tubule formation 7 days after seeding HUVEC onto confluent HDF detected by immunohistochemistry (IHC). On the right-hand side the tubules (white line) and branch points (black dot) are marked on the image for quantification of tubule length and branch points by ImageJ as described in Materials and Methods. Image taken using an EVOS microscope, 10X magnification. Scale bar, 400µm. **B.** Image depicts tubule formation 14 days after seeding HUVEC onto confluent HDF detected by immunofluorescence (IF). On the right-hand side the apical localisation of podocalyxin is marked (white line) for quantification of lumen formation by ImageJ. Image taken using a Nikon A1R confocal microscope, 40X magnification. Scale bar, 20µm.

Readout	Definition
Tubule length	Distance between two branch points, branch point and the tubule end, or two ends of a tubule with no branches
Total tubule length	Sum of lengths of all tubules in a microscopic field (Figure 3.5 A, white lines)
Branch points	Position of sprouts, or mid length anastomoses (Figure 3.5 A, black dots)
Branch point index	Number of branches divided by total tubule length
Lumenised length	Length with open lumen and/ or apical localisation of podocalyxin (Figure 3.5 B, white lines)

Table 3.1 Readouts of tubule morphology in organotypic co-cultures.
Table shows definition of readouts used for the purpose of quantification of angiogenesis in organotypic co-cultures of HUVEC and HDF.

3.7 Growth factors bFGF and VEGFA stimulate angiogenesis

In order to assess the effect of growth factors FGF and VEGF on tubule formation in the organotypic co-culture assay, co-cultures were treated with either of the growth factor or combination. HUVEC stably expressing EGFP, and were used to set up organotypic co-cultures with HDF cells in LVE media. VEGFA (25 ng/ml) or bFGF (10 ng/ml) treatments, separately or in combination, were applied to the media on days two, four and six following seeding of HUVEC onto confluent HDF, in order to stimulate angiogenesis. Untreated wells served as a control. To promote tubule establishment and lumen formation media were changed to low growth factor medium (Optimised) on day 9 and lumen formation was assessed on day 14 by immunofluorescence staining for podocalyxin. The analyses indicated that total length and branch points were stimulated significantly by adding both or either of growth factors compared to no growth factor conditions. There was no difference in total tubule length when either of growth factors added to the co-culture were compared to addition of both growth factors. However, branch points were more stimulated by addition of both growth factors compare

to VEGF only. Interestingly, I noticed that VEGF promoted cell elongation and increased the distance between nuclei, whilst in the presence of FGF there appeared to be more nuclei that were not elongated (Figure 3.6).

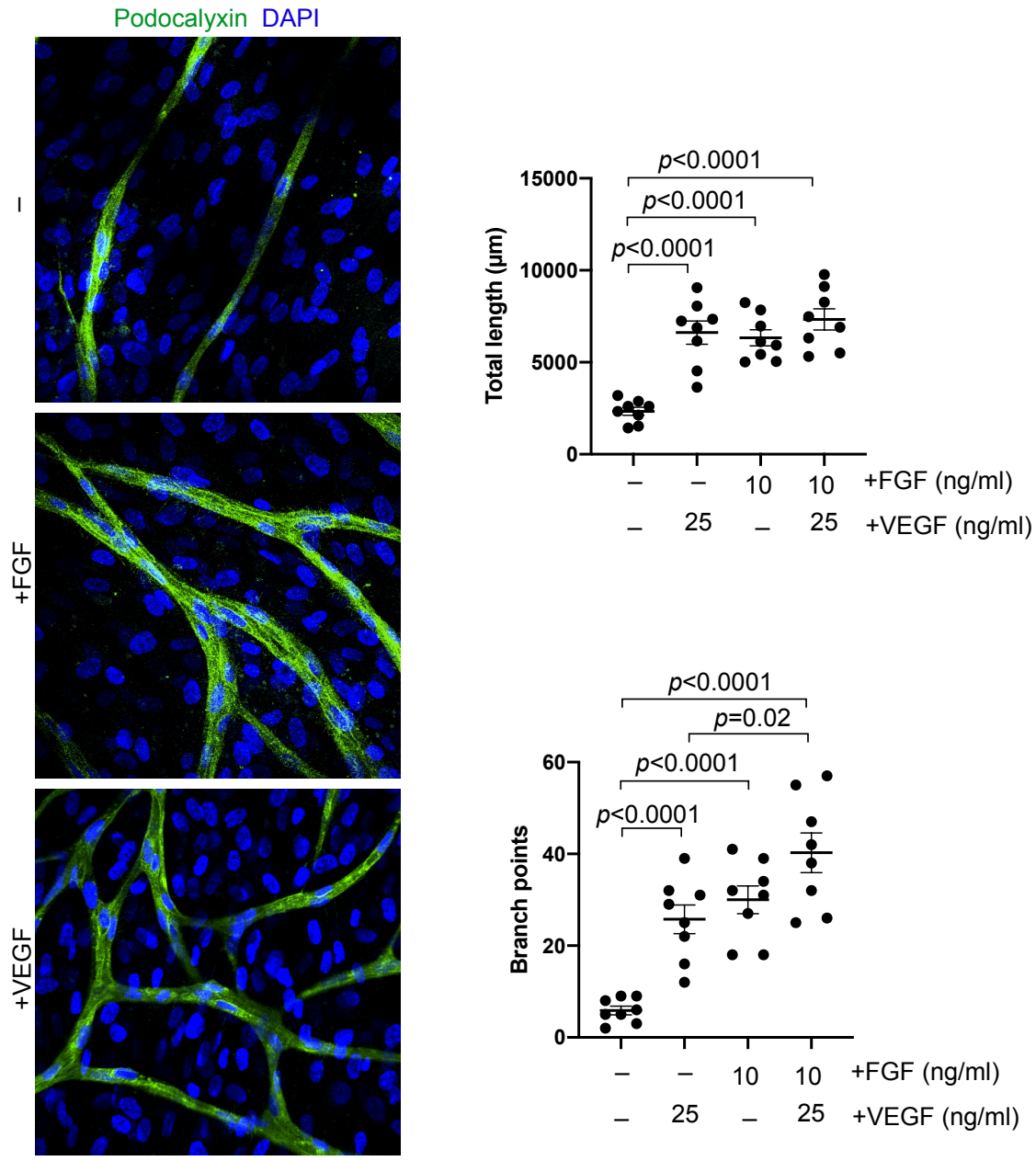

Figure 3.6 Stimulation of organotypic co-cultures with angiogenic growth factors.

Immunofluorescence images show tubule formation in organotypic co-cultures with no added growth factors, or in the presence of bFGF or VEGFA at 14 days after seeding HUVEC onto confluent HDF. Growth factors were applied on days

two, four and six after seeding. Images were taken using a Nikon A1R confocal microscope, 40X magnification. Scale bar, 50μm. Dot plots show quantifications of total length (μm) and branch points in organotypic co-cultures stimulated with the indicated growth factors. N=3 organotypic co-cultures from one experiment (the data are from eight images indicated by black dots on the dot plot). Statistical test for unpair-wise comparison is Student t-test.

3.8 Single-chamber microfluidic device selected for this project

To mimic the vascular transport system *in vitro* and to allow easy genetic or pharmacological manipulation of developing tubes, a system of organotypic tubules in microfluidic devices was set up (Moya et al., 2013). In order to choose the most efficient microfluidic device for the purpose of this study, HUVEC-EGFP and HDF mixed with fibrin were loaded through the cell loading ports of the single chamber and three-chamber microfluidic devices. The microfluidic devices then hosted developing tubules in 3D fibrin matrix inside the chambers. Optimisation steps were performed in order to seed the optimum number of cells and fibrin mixture in the chambers. After loading cells in the single-chamber microfluidic device, organotypic coculture with the ideal number of cells were formed successfully inside the chamber (Figure 3.7 A). However, cells did not survive after loading into the three-chamber microfluidic devices potentially due to issue with the distribution of cells inside the microchambers or due to lack of enough pressure of circulating media. (Figure 3.7 B). Therefore, the single-chamber microfluidic device design was used for all subsequent experiments in this study. This system was established in order to investigate the effects of ciliogenesis suppression and cytoskeletal regulators on tubule and lumen formation, flow sensing and lumen expansion under conditions of fluid flow.

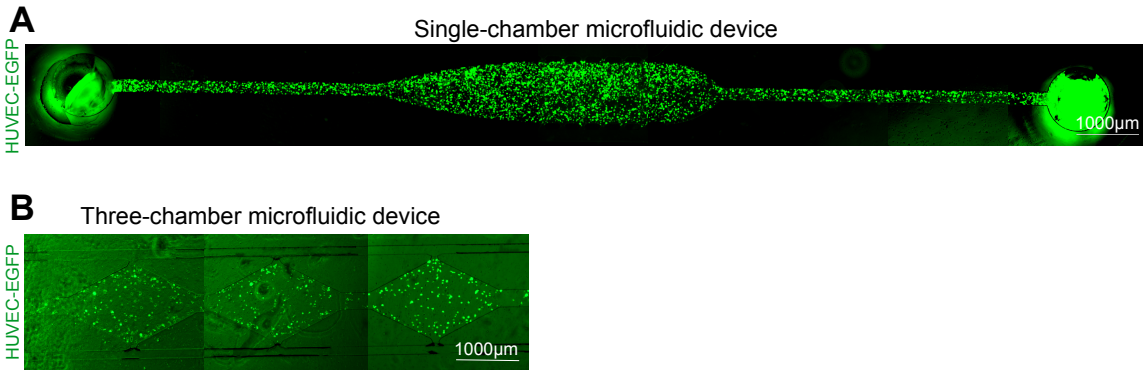

Figure 3.7 Growth of organotypic co-cultures in the microfluidic devices. HUVEC-EGFP ($6x10^4$) and HDF ($6x10^4$) were mixed with fibrin and injected into the cell loading port E of single-chamber and three-chamber microfluidic devices. **A.** Epifluorescence image shows appearance of enough cells in co-culture in the single-chamber device on the day of cell loading (Day 0). **B.** Epifluorescence image shows appearance of the cells in co-culture in the three-chamber device on the day of cell loading (day 0). The single chamber microfluidic device was chosen for further experiments. Images taken using an EVOS microscope, 4X magnification. Scale bar, 1000µm.

3.9 Single-chamber microfluidic device design

A single-chamber microfluidic device that was employed for this project had one chamber connected to the four reservoir ports (A-B and C-D) by the two side channels through six openings created by 5 pillars. Flow was introduced into the single chamber via the pillars. Fluid circulated through the 10.6mm channel from one reservoir to the other reservoir in the same side, channel width is 100µm. This device design has two cell loading ports (E and F), and the cell-fibrin mixture was injected into port E on day 0 to be seeded in a single chamber with the width of 1000µm (Figure 3.8 A).

The average flow rate in this device is 50-60µl/h which depends also on the dynamic viscosity of the culture media. This rate decreased over a time period of 24 hours, due to decreasing height differences between the fluid levels in the two

reservoirs of each side (A-B and C-D). Therefore, fluid inside the reservoirs must be replaced every 24 hours (Figure 3.8 B).

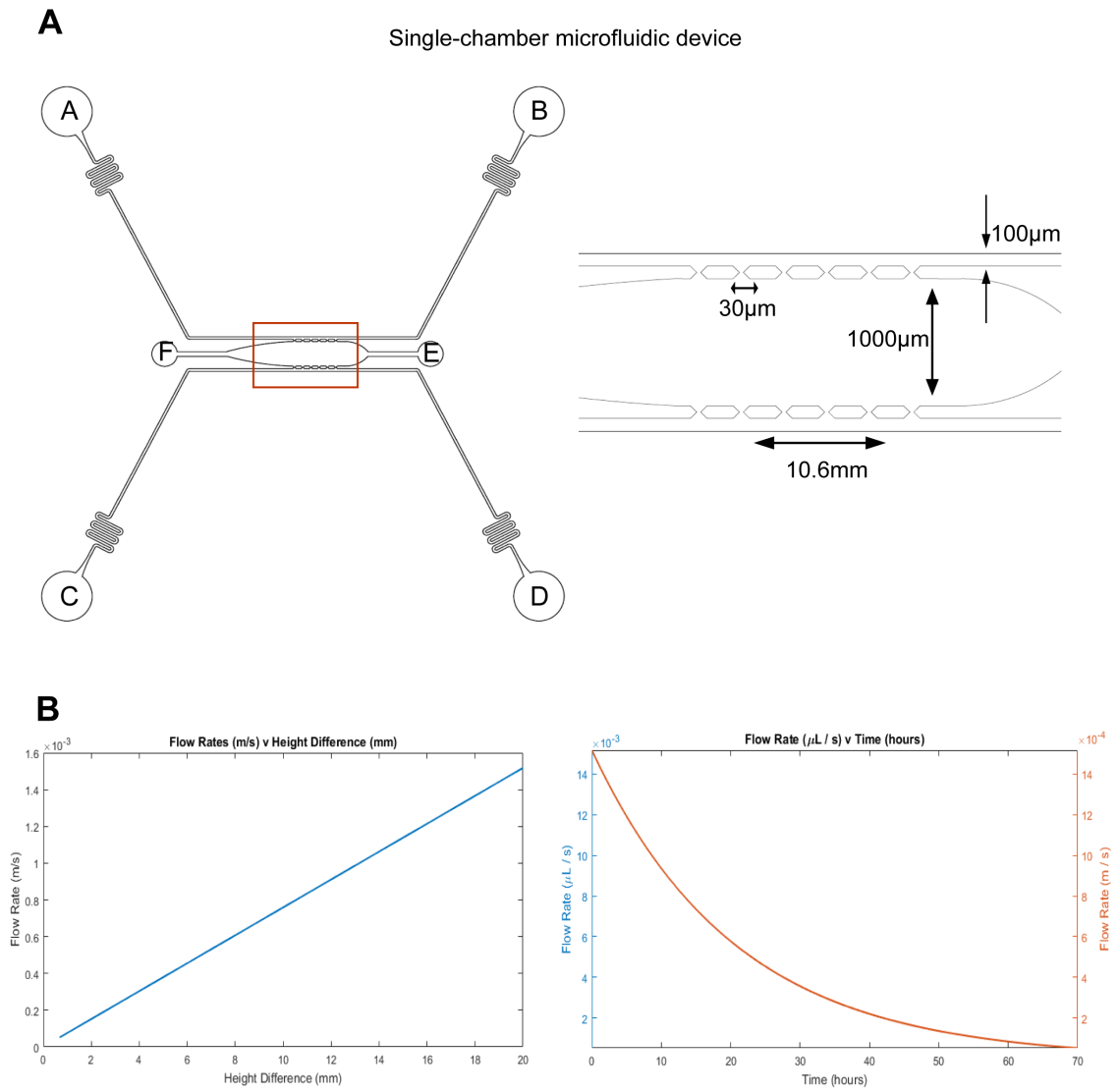

Figure 3.8 Detailed design and flow rate in the single-chamber microfluidic device.

A. Detailed design of single-chamber microfluidic device with chamber dimensions. A single-chamber microfluidic device has one chamber connected to the four reservoir ports (A-B and C-D) by the two side channels through six openings created by 5 pillars. The cell-fibrin mixture was injected through cell loading port E into a chamber. On the right-hand side, the dimensions specified are as follows: the chamber width (1000μm), side channel width (100μm),

distance between pillars (30μm) and length of side channel (10.6mm). **B.** Graphs show the variation of flow rate with height difference (mm) and time (hour) between reservoirs A-B and C-D. Flow rate inside the channels are 50-60μl/h. Adapted from (Bourn, M., PhD Thesis).

3.10 Microfluidic device fabrication

To fabricate single-chamber microfluidic devices, PDMS was mixed in a 10:1 base (Silicone Elastomer base) and curing agent (Silicone Elastomer curing agent) ratio. The mixture was centrifuged at 3220 x *g* for one minute. The solution was poured onto a silicon wafer and desiccated for 40 min to allow air bubbles to rise to the top of the container. PDMS was cured by placing in an oven at 80°C for 1 hour. The devices were then cut and the reservoirs and loading port holes were punched. Oxygen plasma was used to bond the surface of the device to the coverslip (Figure 3.9).

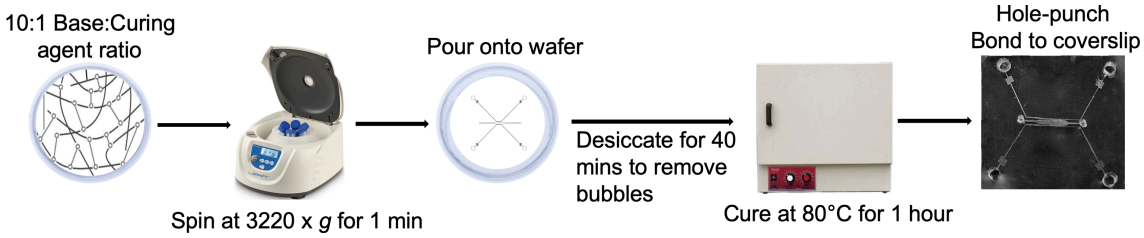

Figure 3.9 Fabrication of microfluidic devices for introducing fluid flow in organotypic co-cultures.

Schematic view of microfluidic device fabrication with 10:1 base to curing agent ratio. After pouring PDMS onto a prefabricated wafer and desiccated for 40 minutes to remove any bubbles, devices were cured at 80°C for 1 hour. Devices were cut, hole-punched to create space for the reservoirs, and the PDMS was bonded to coverslips using oxygen plasma.

3.11 Troubleshooting the loading of cell-fibrin mixture into the chamber of the microfluidic device

Fibrin is a three-dimensional extracellular matrix microenvironment that aids sprouting angiogenesis. The first step of loading HUVEC-EGFP and HDF into the chamber was to combine cells with fibrinogen, followed by mixing with thrombin immediately prior to injection. Air bubbles can be introduced into the cell-fibrin mixture during mixing or loading into the camber, and can be trapped inside the fibrin. The problem with air bubbles were overcome by increasing the amount of the prepared mixture compared to the amount required for injection (Figure 3.10 A). The polymerisation of the cell-fibrinogen mixture occurred quickly after addition of thrombin to the fibrinogen, even before fully occupying the microchamber in the device. This was overcome by determining the optimal time for loading, and by increasing the speed of loading the mixture into the chamber before a fibrin clot formed. This precaution prevented the fibrin from polymerising and solidifying before the desired time (Figure 3.10 B). However, this optimal loading of cell-fibrin mixture into the chamber was not possible because rapid injection of the mixture could burst the fibrin-air interface at the chamber-channel pore. Fibrin could then leak into the side channels and cause blockage of the fluid flow circulation around the microfluidic device (Figure 3.10 C). Burst pressure breakage was overcome by increasing the speed of combining fibrinogen with thrombin before injection, followed by slow loading into the devices.

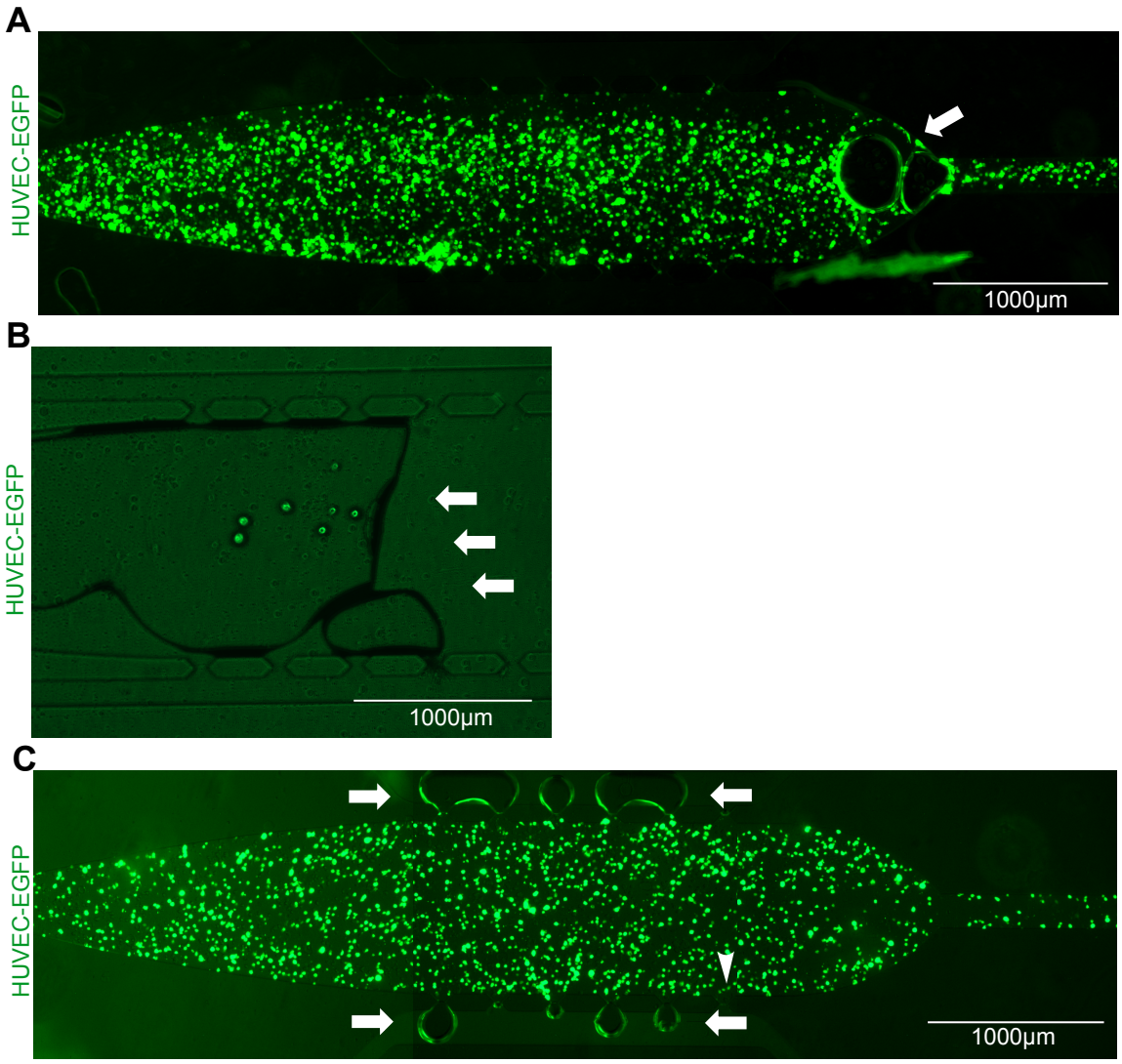

Figure 3.10 Troubleshooting cell-fibrin mixture loading into the chamber of microfluidic device.

A. Epifluorescence image shows air bubbles introduced into the microfluidic device following loading of HUVEC-EGFP with HDF in fibrin into the chamber on day 0. Arrow points to the area with bubbles. This was overcome by increasing the amount of prepared mixture compare to the amount required for injection. **B.** Polymerisation of the cell-fibrin mixture prior to occupying the microchamber uniformly due to a delay in loading. Arrows point to the areas where the mixture set. This was overcome by determining the optimal time of loading which was 10 seconds. **C.** Burst pressure optimization and example of fibrin-air interface maintenance and bursting. Arrow head marks an area of normal fibrin-air interface at the chamber-channel pore. Arrows point to areas of bursting of the fibrin-cell mixture into the microchannel, and blockage of the microchannel due

to the high pressure loading of the mixture into the chamber. This was overcome by maintaining an optimal pressure and loading time of the cell-fibrin mixture through the cell loading port. Images taken using an EVOS microscope, 4X magnification. Scale bar, 1000µm.

3.12 Tubule formation in the microfluidic device

The single chamber microfluidic system is based on the organotypic endothelial-fibroblast tube formation model. In order to form tubules in the microfluidic device and under conditions of flow, HUVEC-EGFP ($6.0x10^4$) and HDF ($6.0x10^4$) cells were mixed with 8µl fibrinogen (100mg), followed by addition of 0.6µl thrombin (50U/ml) and rapid injection into the chamber through cell loading port E on day 0. LVE medium combined with DMEM 10%FBS at 50:50 ratio was optimised with VEGFA (25ng/ml) and bFGF (10ng/ml) added to two out of four reservoirs connected to the reservoir ports (A-B, C-D) and refreshed every 24 hours. Tubule formation was assessed on day 6 using an EVOS microscope (Figure 3.11).

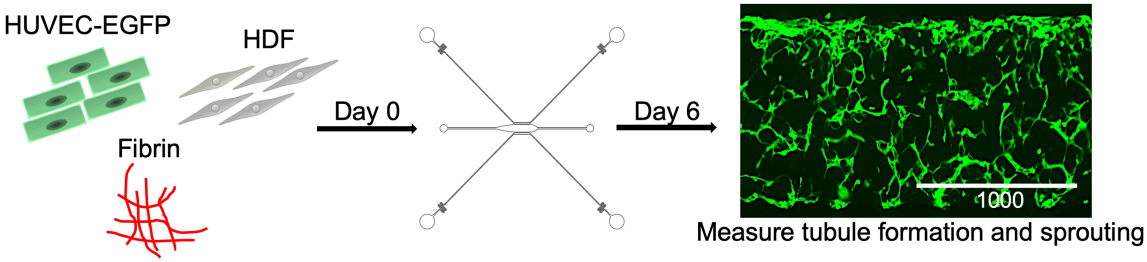

Figure 3.11 Tubule formation in the microfluidic device under conditions of fluid flow.

HUVEC-EGFP ($6.0x10^4$) and HDF ($6.0x10^4$) cells were mixed with fibrin and injected into the cell loading port of the microfluidic device. Image shows typical appearance of the co-cultures after 6 days of loading the mixture into the device. Image was taken using an EVOS microscope, 4X magnification. Scale bar, 1000µm.

3.13 Anastomosis of the tubules inside a chamber with side channels

In order to promote anastomosis and to initiate perfusion, endothelial cells were seeded into the side channels (X. Wang et al., 2016). HUVEC-EGFP cells ($3.0x10^4$) combined with 30µl LVE medium were flowed into the side channels through two out of four reservoirs, in order to cover the side channels with a layer of HUVEC-EGFP. The flow of cells stopped after 30 mins due to the balance of hydrostatic pressure between the two matched reservoirs (A-B, C-D). The device was then left without fluid flow for 3 hours to allow cells to attach to the side channels. LVE medium with added growth factors VEGFA (25ng/ml) and bFGF (10ng/ml) was circulated in the device after 3 hours and refreshed every 24 hours. Tubules forming at a later stage in the chamber connected or anastomosed to the endothelial cells in the side channels contributed to a closed circulatory system (Figure 3.12).

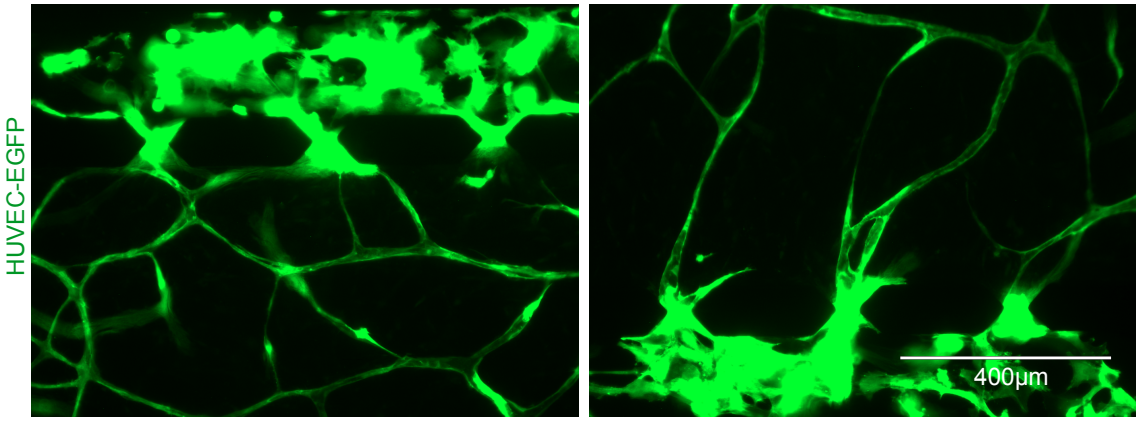

Figure 3.12 Injection of HUVEC-EGFP for anastomosis of tubules with the microfluidic side channels.

HUVEC-EGFP ($6.0x10^4$) and HDF ($6.0x10^4$) cells were mixed with fibrin, injected into the loading port of the microfluidic device and left in the chamber to form tubules. After 6 days, $3.0x10^4$ HUVEC-EGFP cells were circulated in the channels via reservoirs to promote anastomosis of tubules within the microfluidic side channels. Images show anastomosis of tubules with endothelial cells inside the channels on day 7. Images were taken using an EVOS microscope, 10X magnification. Scale bar, 400µm.

3.14 Angiogenic sprouting and lumen formation modelled by HUVEC in fibrin gels in the microfluidic device

In order to form lumens in the microfluidic device, organotypic co-cultures were grown for 14 days inside the chamber. Lumen formation was observed from day 7 (Figure 3.13 A). following anastomosis of tubules inside the chamber with endothelial cells in side channels, perfusion of tubules started alongside interstitial flow around the tubules. I anticipated that flow would drive lumen expansion in the cocultures, and would increase the percentage of lumenised tubes compared to co-cultures developing in the absence of flow. Low growth factor medium was added on day 11 for tubule establishment and lumen formation. Growing tubules for a longer period of time, tubule maturation and perfusion resulted in longer lumens observed by day 14 (Figure 3.13 B).

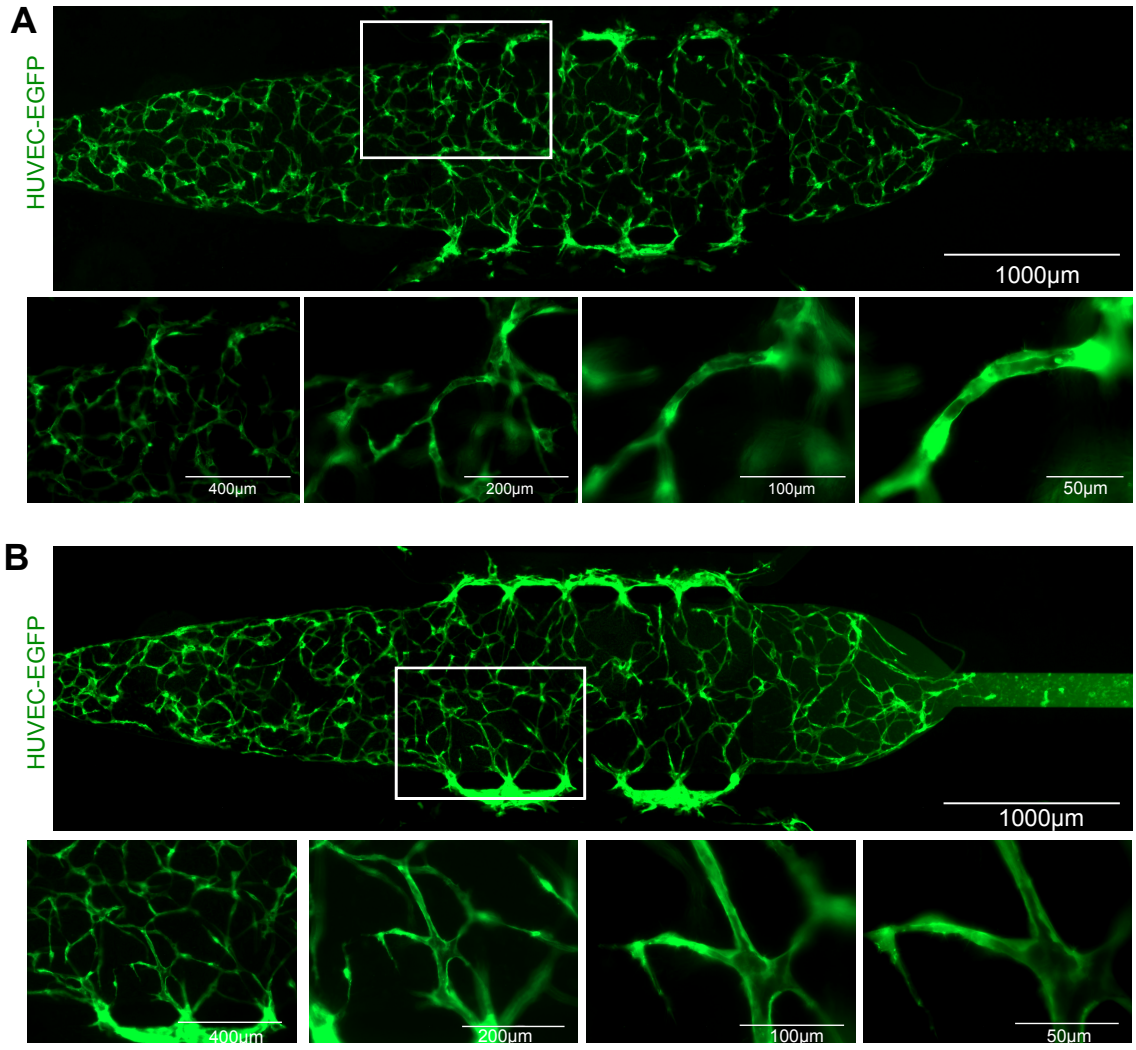

Figure 3.13 Lumen formation under conditions of fluid flow in the microfluidic device.

A. Epifluorescence images show tubule and partial lumen formation in the organotypic co-culture on day 7. Images were taken using an EVOS microscope, 4X, 10X, 20X, 40Xand 60X magnification. Scale bars, 1000, 400, 200, 100 and 50 (µm) as indicated. **B.** Epifluorescence images show tube and lumen formation in the organotypic co-culture on day 14. Images were taken using an EVOS microscope, 4X, 10X, 20X, 40X and 60X magnification. Note the formation of longer and continuous open lumens. Scale bar, 1000, 400, 200, 100, 50 (µm).

3.15 Confirmation of tubule perfusion in the microfluidic device

Tubule perfusion was visualised by delivery of fluorescent microspheres of dextran-Texas Red conjugates (70kDa) inside the channels and tubules. Following tubule maturation and lumen formation on day 14, 100µl dextran-Texas red in LVE media (1mg/ml) was added into two out of four opposing media reservoirs on either side of the microfluidic device (ports A and D), and allowed to circulate in the device. Dextran-Texas red occupied the side channels and then perfused the lumenised length of tubes. Dextran-Texas red inside the tubes extravasated into the interstitial space because of the small size of dextran beads compared to endothelial cell junctions (Figure 3.14).

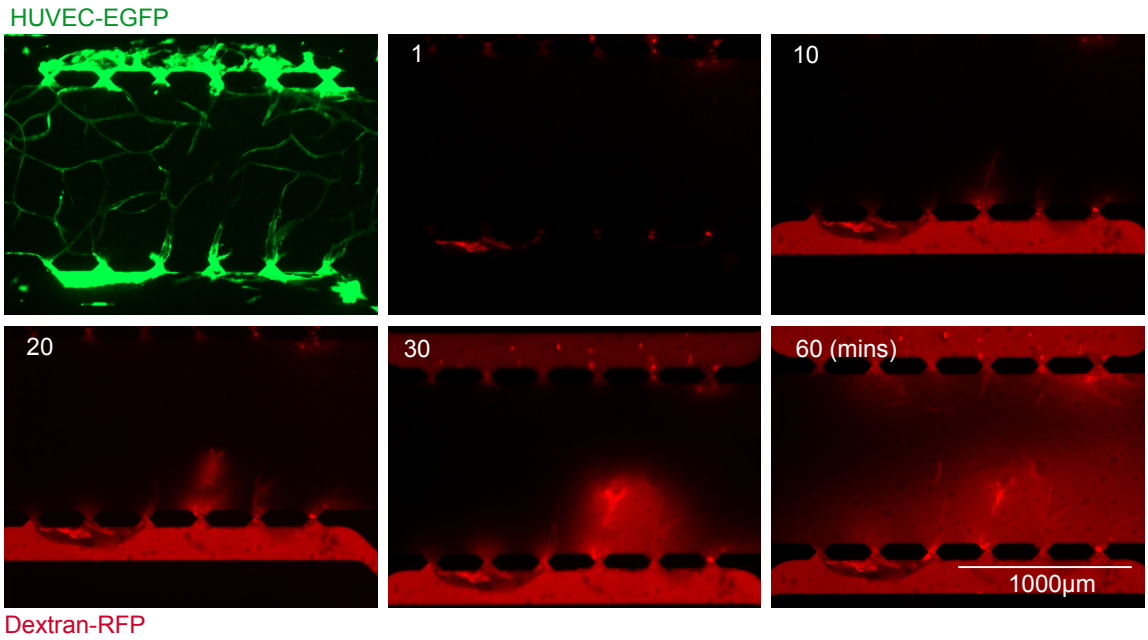

Figure 3.14 Flow of fluorescent dextran into the endothelial tubes in the microfluidic device.

Dextran-Texas Red (70kDa) was added into opposing media reservoirs on either side of the microfluidic device (ports A and D) to circulate inside the lumenised length of tubes on Day 14. Epifluorescence images show lumens of tubes perfused with fluorescent dextran after 1, 10, 20, 30 and 60 minutes. Images taken using an EVOS microscope, 4X magnification. Scale bar, 1000µm.

3.16 Fluid flow establishes tube hierarchy in the microfluidic device

Key steps of angiogenesis comprise endothelial cell proliferation, directed migration towards growth factors, endothelial cell tube formation, vessel fusion and vessel pruning. All of these steps can be observed in tubules and tubes with lumens formed in the microfluidic device. The hierarchy of the tubules resembled the patterning of arterioles, venules and capillaries. In the human body, the diameter of venules and arterioles is between 8-100μm, and capillaries 8-10μm. Lumens formed inside the microfluidic device can reach the greatest diameter of 100μm at the side of chamber where the tubes anastomose with the side channel and have higher shear stress, and resemble arteries and venules. Tubules with diameter less than 10μm are still open and perfused in the middle of the chamber, resembling capillaries. This hierarchy and the formation of long open lumens cannot be observed in the organotypic co-culture of endothelial-fibroblast cells in the absence of flow. Intussusception could also be observed within lumens formed in the microfluidic device (Figure 3.15).

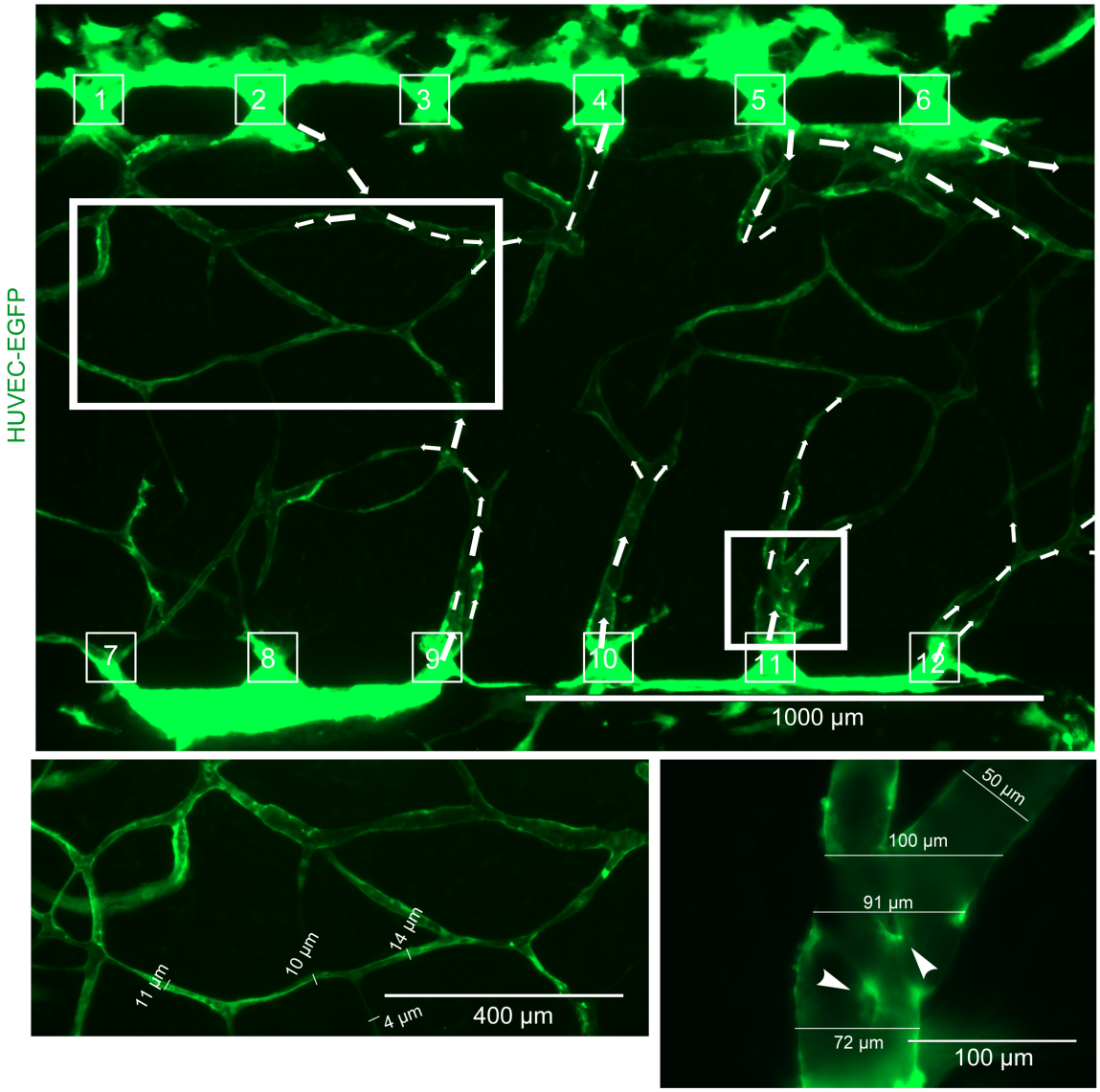

Figure 3.15 Hierarchy of tubes forming in the microfluidic device under conditions of fluid flow.

Epifluorescence images show the hierarchy of tubes formed under conditions of fluid flow in the microfluidic device on day 14. Upper panel: arrows show the direction of flow. Images taken using an EVOS microscope, 4X magnification. Scale bar, 1000µm. Lower panel: higher magnification of large and small diameter tubules shown in the upper panel. Arrowheads point to potential sites of intussusception. Images were taken using an EVOS microscope, 10X (left) and 40X (right) magnifications. Scale bars, 400µm (left) and 100µm (right).

3.17 Quantification of tubule and lumen formation in the microfluidic device

For the purpose of quantification, the microfluidic device chamber was divided into 18 equal squares. Twelve squares adjacent to the pillars at the entrance of fluid flow into the tubes were selected for quantitation. The reason for selecting theses 12 squares was due to the prominent opening of lumens at the entrance of fluid flow with higher shear stress. Therefore, tubules that are formed next to the fluid flow entrance were quantified for angiogenesis traits, and I defined each of 12 squares as a “channel square” (Figure 3.16 A). Tubule length, branch points and lumenised length were quantified in the same way as 2D co-culture assays (Table 3.1). Due to the perfusion of fluid flow inside the tubes almost 80-90% formed lumens, which I defined as lumenised lengths. Only new sprouts and tip cells that were migrating towards other endothelial cells did not have a lumen, and were defined as non-lumenised lengths (Figure 3.16 B).

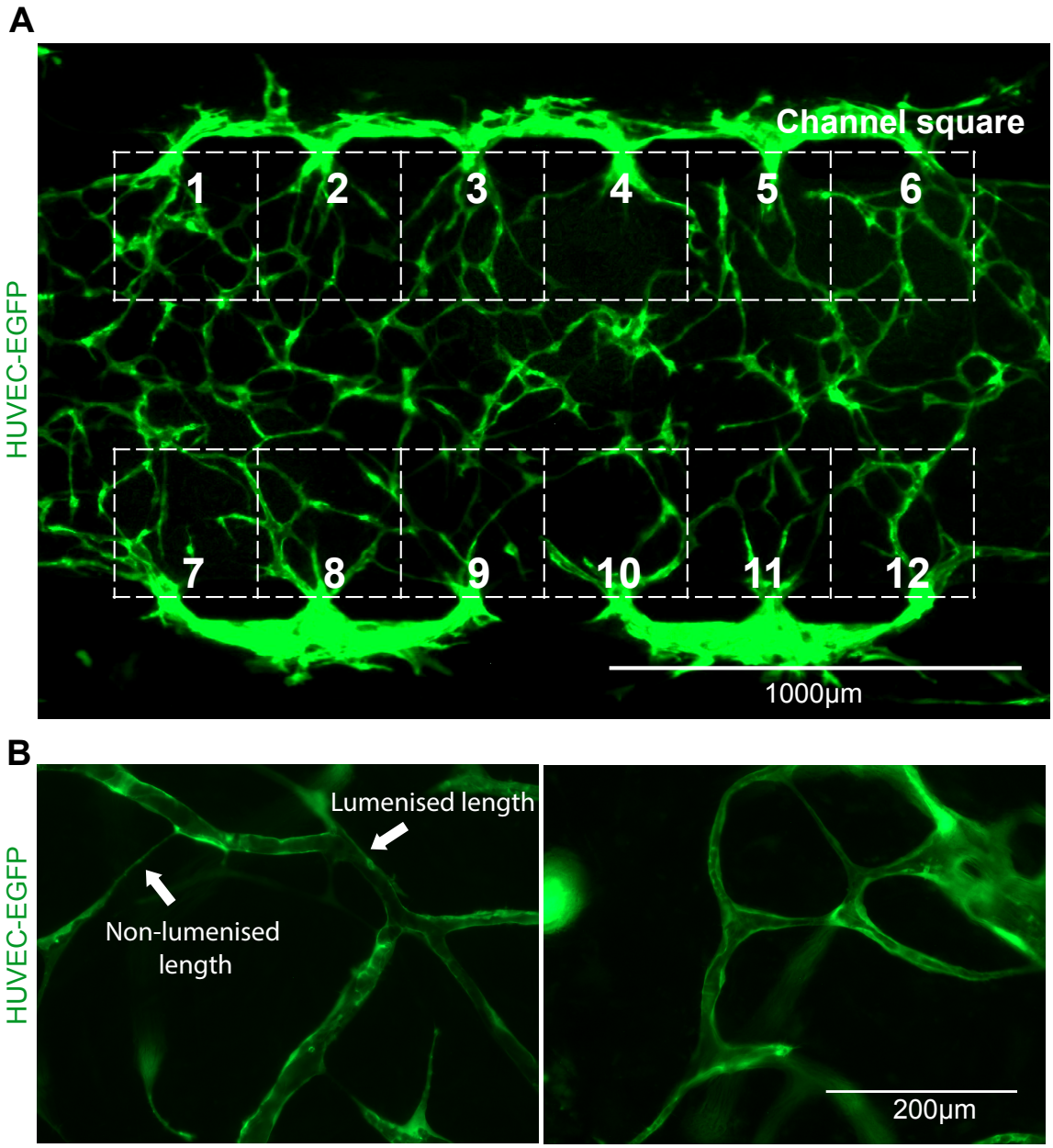

Figure 3.16 Quantification of tubule and lumen formation in the microfluidic device.

A. Epifluorescence image taken using an EVOS microscope at 4X magnification for the purpose of quantification for tubule length, lumen formation and branch points. Twelve channel squares (indicated by white frames) were selected at the spaces between pillars where anastomosis occurred between endothelial tubules and endothelial cells inside channels. Scale bar, 1000μm. **B.** Epifluorescence images taken on day 14 using an EVOS microscope at 20X magnification were used to demonstrate lumenised length and non-lumenised length parts of tubes. Scale bar, 200μm.

3.18 Circulation and extravasation of cancer cells from endothelial lumens

In order to elucidate extravasation of cancer cells from vessel lumens, the microfluidic device was used for injection of MDA-MB-231 breast cancer cells into the tubes and subsequent observation of extravasation. HUVEC-EGFP and HDF in fibrin were established in the microfluidic device and tubes were allowed to form for 14 days. MDA-MB-231 breast cancer cells labelled with CellTracker Deep Red ($8.0x10^4$) were added into the reservoirs in 100µl HCMEC (Human Cerebral Microvascular Endothelial Cell) conditional media and allowed to circulate inside the tubes of the microfluidic device for 30 mins, followed by 3 hours cell attachment in order to allow cells seed in the side channels and stop floating. Cells within the microfluidic device were visualised after 16 hours. After entering into the lumen, cancer cells either adopted a round shape and arrested within larger tubes, or elongated and extravasated from lower calibre tubes. The flow and extravasation of cancer cells was another confirmation of the presence of fluid flow inside the tubes (Figure 3.17).

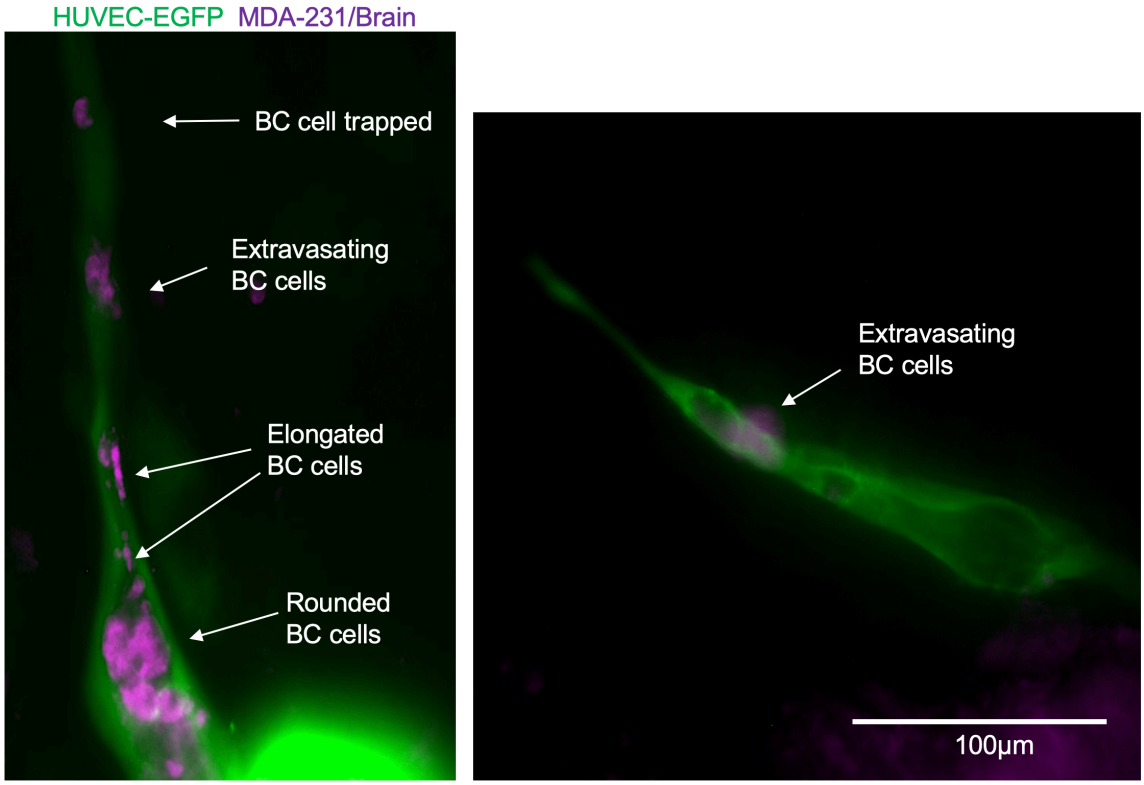

Figure 3.17 Visualisation of breast cancer cells and extravasation in the microfluidic device.

HUVEC-EGFP and HDF co-cultures were established in the microfluidic device and on day 14 MDA-MB-231 breast cancer cells marked with CellTracker™ Deep Red were injected into the medium reservoirs. The microfluidic device was visualised after 16 hours. Images show MDA-MB-231 either arresting in larger tubes or extravasating from lower calibre tubes. MDA-MB-231 cells appear elongated within the smaller diameter tubes. Images were taken using an EVOS microscope, 40X magnification. Scale bar, 100µm.

3.19 Interaction of injected HUVEC-RFP with pre-established HUVEC-EGFP endothelial tubules

In order to visualise the behaviour of HUVEC added to the chamber after tubule formation (Figure 3.12), HUVEC-RFP were added to pre-established tubules formed in the microfluidic device from co-cultures of HUVEC-EGFP with HDF under conditions of fluid flow. HUVEC-EGFP and HDF were mixed with fibrinogen, followed by addition of thrombin and rapid injection into the chamber through cell loading port E on day 0. LVE medium combined with DMEM 10% FBS at 50:50 ratio together with VEGF and FGF was added to the reservoirs and refreshed every 24 hours. HUVEC-RFP combined with 30µl LVE medium were injected into two out of four reservoirs (ports B and C) (Figure 3.8 A) on day 6 and allowed to circulate and cover the side channels. The flow of cells stopped after 30 mins due to balanced hydrostatic pressure between two reservoirs (A-B and C-D), and the device was left without fluid flow for 3 hours to allow cells to attach within the side channels. LVE medium with added growth factors VEGFA (25ng/ml) and bFGF (10ng/ml) was circulated in the device after 3 hours and refreshed every 24 hours. The media were changed to low growth factor media on day 11 for tubule establishment and lumen formation. During the development of tubules, HUVEC- RFP interacted and united with pre-established green tubules as visualised on days 7 and 14 (Figure 3.18). In this particular device, green endothelial tubules did not form a complete closed circulatory system between the two sides and there was greater retraction of HUVEC-EGFP than normal before HUVEC- RFP introduction. However, this was a useful example for observation of endothelial cell interaction and communication to form tubules. HUVEC-RFP could be observed interacting with the pre-formed EGFP tubules and crossing the chamber from one side to the other side following the fluid flow.

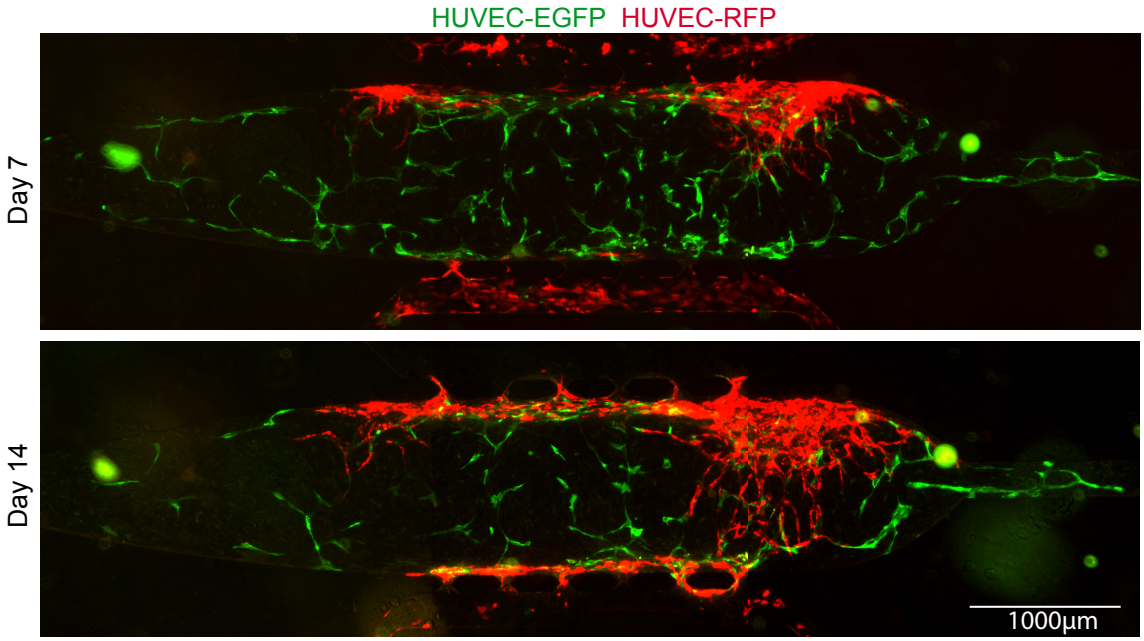

Figure 3.18 Interaction of HUVEC-RFP injected for anastomosis with pre-established EGFP tubules in the microfluidic device.

HUVEC-EGFP and HDF mixed with fibrin were loaded into the microfluidic device and after 6 days HUVEC-RFP were added into opposing media reservoirs (ports B and C) for anastomosis with HUVEC-EGFP tubules. Epifluorescence images show the interaction of HUVEC-RFP with pre-established tubules on days 7 and 14. Images were taken using an EVOS microscope, 4X magnification. Scale bar, 1000µm.

3.20 Injected HUVEC-RFP follow the paths formed by pre-established HUVEC-EGFP tubules

Observation of HUVEC-RFP interacting with pre-established HUVEC-EGFP revealed that the HUVEC-RFP followed the pre-established paths formed by the HUVEC-EGFP tubules. HUVEC-RFP circulated in the microfluidic device six days after loading HUVEC-EGFPs with HDF in fibrin inside the chamber followed by formation of tubules. HUVEC-RFP localised mostly in the areas that HUVEC-EGFP cells had formed tubules over six or 14 days of co-culture with HDF and pruning had happened (Figure 3.19).

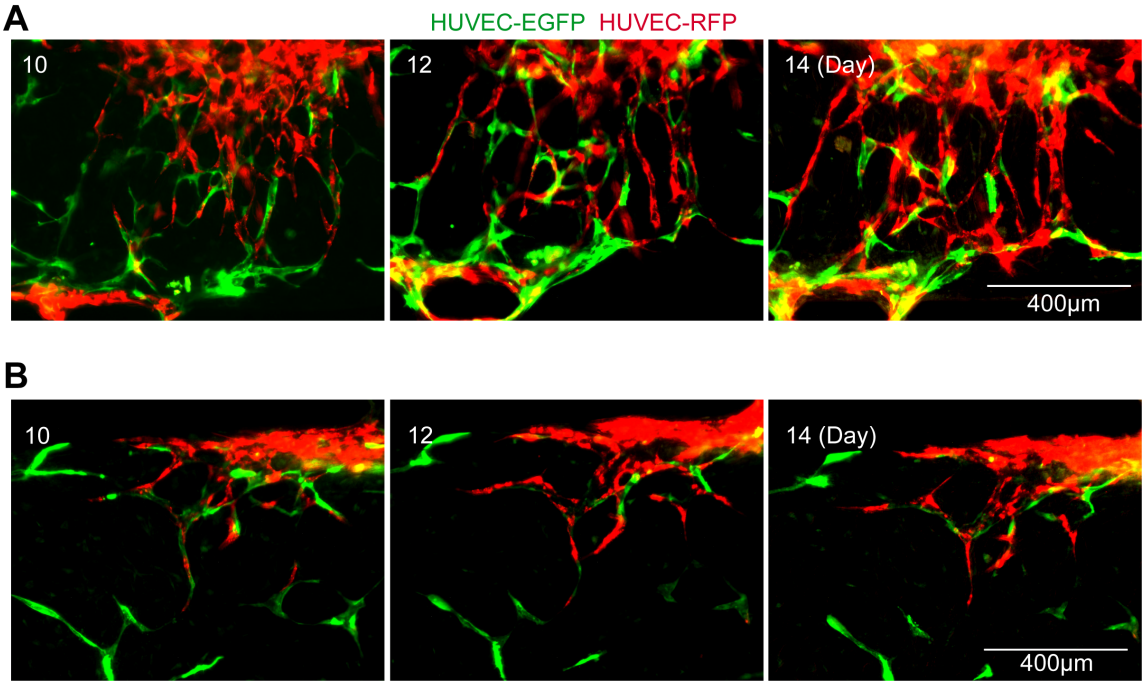

Figure 3.19 Injected HUVEC-RFPs follow the pre-established HUVEC-EGFP tubules in the microfluidic device.

A. Epifluorescence images show HUVEC-RFP tracking alongside pre-formed HUVEC-EGFP tubules in the microfluidic device on days 10, 12 and 14 after injection into a microfluidic device. Images were taken using an EVOS microscope, 10X magnification. Scale bar, 400µm. **B.** Epifluorescence images show a different area of the microfluidic device with HUVEC-RFPs tracking pre-established HUVEC-EGFP tubules. Images were taken using an EVOS microscope, 10X magnification. Scale bar, 400µm.

3.21 Interaction of HUVEC-RFP with pre-established HUVEC-EGFP tubules in the microfluidic device

In order to assess how injected HUVEC-RFP interacted with pre-established HUVEC-EGFP tubules, several regions of interest within the microfluidic device were visualised in detail. HUVEC-RFP added to the microfluidic device with pre-formed HUVEC-EGFP could either flow into HUVEC-EGFP tubes or around the tubules through interstitial flow. HUVEC-RFP appeared to interact in different ways: migration towards the HUVEC-EGFP cells to make a longer tubule; formation of a lateral adhesions with HUVEC-EGFP tubules; extension along empty sleeve; or circulation inside HUVEC-EGFP tubes and intercalation into the endothelial tube wall. Interestingly, HUVEC behaved in different ways when they contacted pre-formed HUVEC-EGFP tubules. This could be related to intercellular signals, the number of HUVEC-EGFP in tubules or the shape of tubules. HUVEC-RFP migrated and filled the gaps in between HUVEC-EGFP to form integrated, continuous tubules (Figure 3.20 A). In some areas, HUVEC-RFP slide along pre-preformed HUVEC-EGFP tubules to form lateral adhesions thus increasing tubule thickness (Figure 3.20 B). There were also sections of HUVEC-RFPs extending along empty sleeves formed by retraction of HUVEC-EGFP tubules, followed by formation of tubules by HUVEC-RFP (Figure 3.20 C). HUVEC-RFP also circulated inside HUVEC-EGFP tubes and intercalated within the HUVEC-EGFP tube wall (Figure 3.20 D).

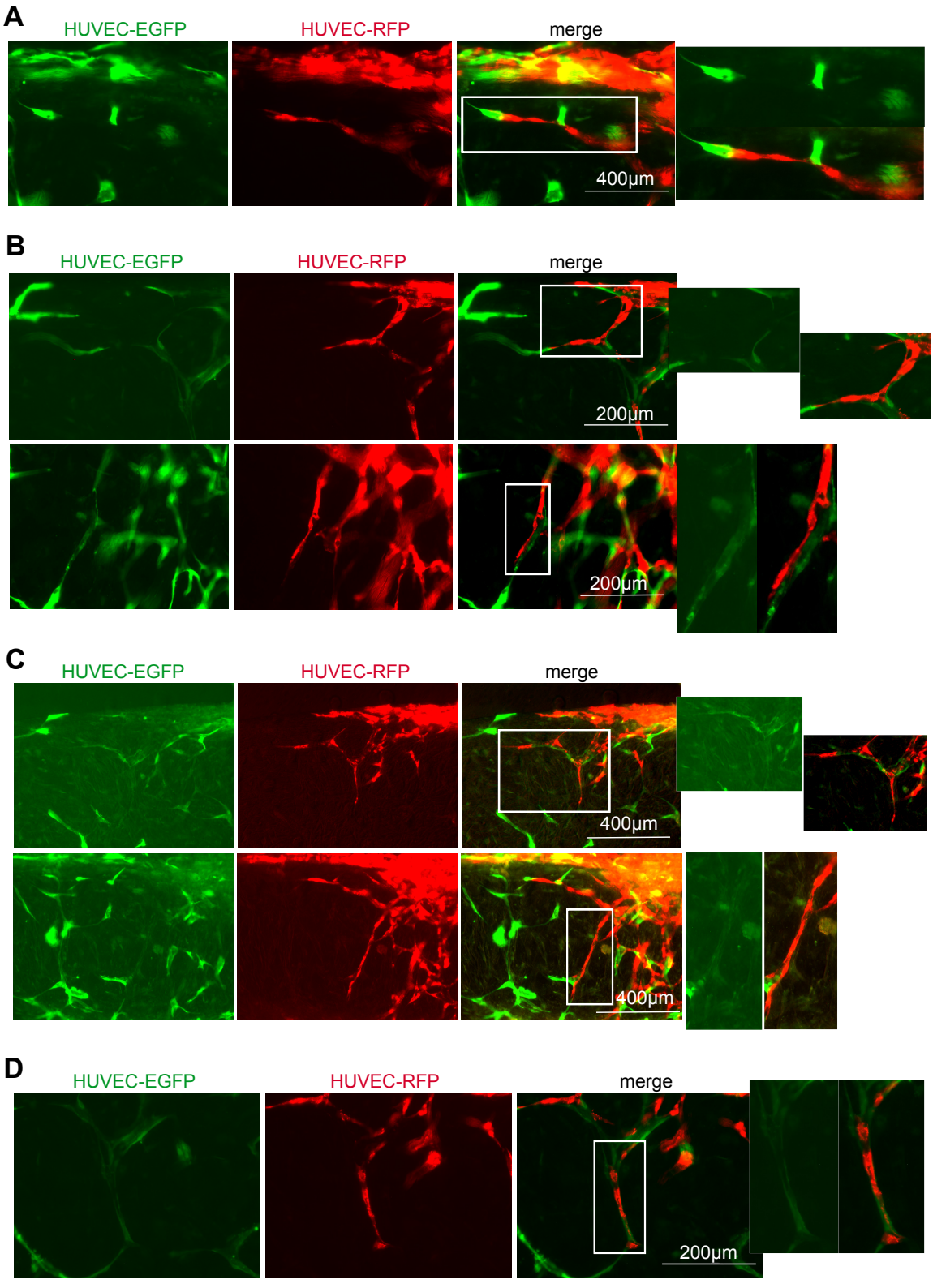
A
HUVEC-EGFP
HUVEC-RFP
merge
400μm
B
HUVEC-EGFP
HUVEC-RFP
merge
200μm
200μm
C
HUVEC-EGFP
HUVEC-RFP
merge
400μm
400μm
D
HUVEC-EGFP
HUVEC-RFP
merge
200μm

Figure 3.20 Modes of interaction of HUVEC-RFP with pre-established HUVEC-EGFP tubules.

A. HUVEC-RFP migrating towards and joining with HUVEC-EGFP to form tubules, images taken 7 days after HUVEC-RFP injection. Images were taken using an EVOS microscope, 10X magnification. Scale bar, 400μm. **B.** HUVEC-RFP forming lateral adhesions with HUVEC-EGFP tubules resulting in increased tubule thickness on Day 11. Images taken using an EVOS microscope, 20X magnification. Scale bar, 200μm. **C.** HUVEC-RFP tubules extending along empty sleeves formed by retracted HUVEC-EGFP tubules on Day 14. Images were taken using an EVOS microscope, 10X magnification. Scale bar, 400μm. **D.** HUVEC-RFP circulating inside HUVEC-EGFP tubes and intercalating within the HUVEC-EGFP tube wall on day 11. Images were taken using an EVOS microscope, 20X magnification. Scale bar, 200μm.

3.22 Assessing live primary cilia dynamics during lumen expansion under conditions of fluid flow

In order to gain insight into the effect of cilia on lumen expansion under conditions of flow in microfluidic devices, a pWPXL lentiviral expression vector was used following removal of EGFP and introduction of the serotonin receptor HTR6 receptor cDNA fused to PS-CFP2 in order to mark cilia and follow them in real time during lumen formation and expansion (Figure 3.21).

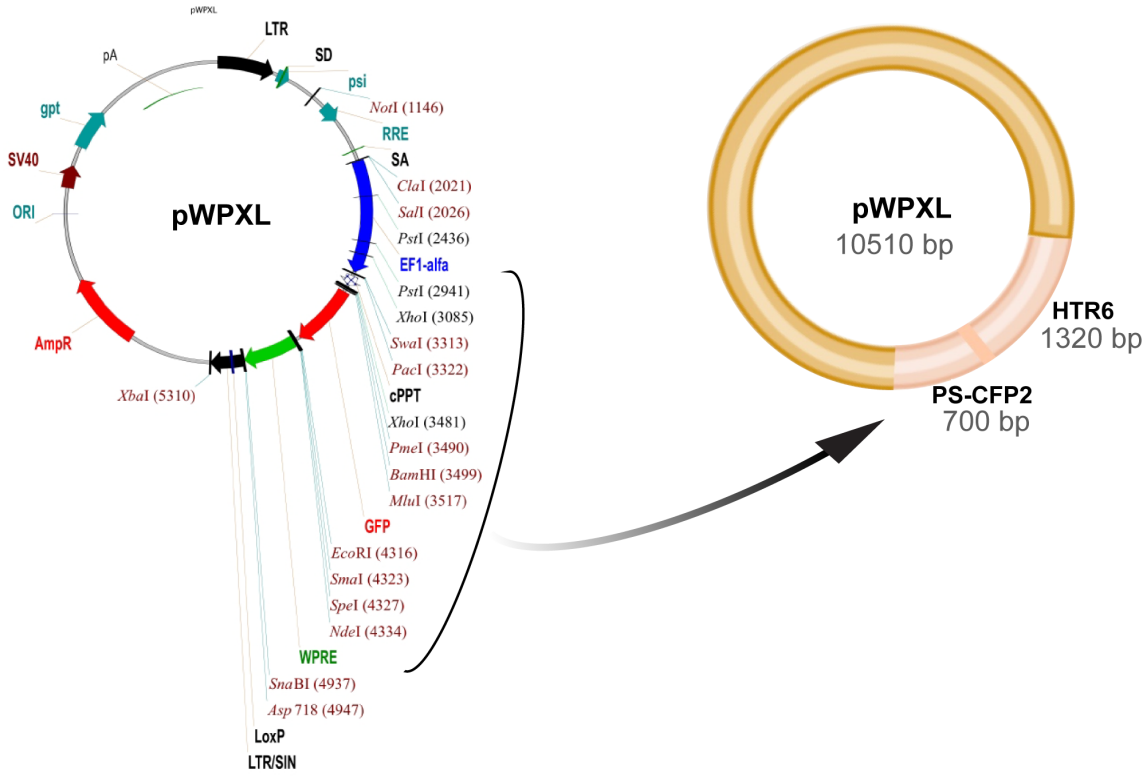

Figure 3.21 Schematic of the strategy for insertion of serotonin receptor HTR6 cDNA fused to PS-CFP2 into the pWPXL lentiviral expression vector.

Left panel: Sequence map of pWPXL. Right panel: map of pWPXL lentiviral expression construct after insertion of the serotonin receptor HTR6-CFP2 fusion.

3.23 HiFi DNA assembly cloning of the serotonin receptor HTR6-CFP2 fusion into the pWPXL lentiviral vector

To mark cilia with cyan fluorescent protein, HiFi DNA assembly cloning of serotonin receptor HTR6-CFP2 fusion into the pWPXL lentiviral vector was used. Following digestion of EGFP from the pWPXL vector, designed primers were used in PCRs to generate two fragments of comprising serotonin receptor HTR6 and PS-CFP2 sequences with overlaps for subsequent HiFi cloning. The whole plasmid vector of pWPXL with the HTR6 and PS-CFP2 amplicons was obtained by doing HiFi DNA assembly. After transformation, clear clones of transformed *E. coli* cells were achieved containing plasmids ready for sequencing. Five out of sixteen clones contained the desired DNA assembly and one of them was assessed by Sanger further sequencing. The actual sequencing results were a perfect match to the expected sequences (Figure 3.22).

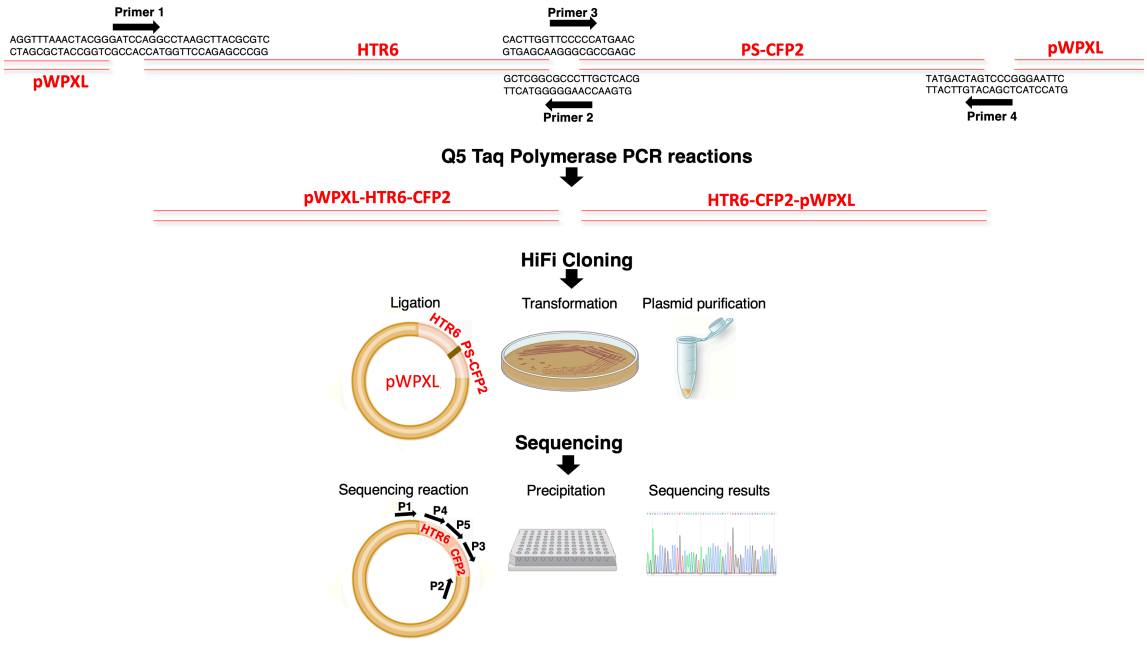

Figure 3.22 Strategy for HiFi DNA assembly cloning of serotonin receptor HTR6-CFP2 into the pWPXL lentiviral vector in order to mark cilia (HiFi DNA assembly cloning).

Overview of distinct stages of DNA fragment assembly from PCR reaction to HiFi DNA assembly cloning and sequencing.

3.24 Discussion

Vascular lumen formation is a vital step in new blood vessel formation conferring functionality for the flow of blood. Previous work in the Mavria group established an organotypic endothelial-fibroblast co-culture model that gives rise to endothelial tubes with lumens. However, as only 20-30% of tubules form lumens in the absence of fluid flow, the model was used to understand primarily molecular mechanisms of initial stages of lumen formation in the absence of flow (Abraham et al., 2015). The current work presented in this thesis established a perfused 3D model of the co-culture system that can provide valuable insights into the behaviour of endothelial cells and mechanisms of lumen expansion under conditions of fluid flow.

In this chapter, I have: (i) optimised the organotypic co-culture of HUVEC with HDF in the absence of fluid flow, and under conditions of flow inside the microfluidic device; (ii) established a circulatory system of endothelial cells in the microfluidic device under conditions of flow (X. Wang et al., 2016); (iii) identified an array of interactions between incoming HUVEC and established tubules (iii) demonstrated that cancer cells can be introduced in the tubes in the microfluidic device, thus establishing a system to investigate interaction of cancer cells with endothelial cells during the process of extravasation. The organotypic co-culture allows observation of specific stages of tubule and lumen formation for investigation and experimental manipulation. The use of microfluidic device provides the opportunity of including fluid flow in tubules in order to recapitulate *in vivo* physiological processes. The organotypic co-culture assay is an ideal method to assess the effect of ciliogenesis suppression, loss of GEFs such as DOCK4 or inhibiting the kinase ROCK on tubule morphogenesis and lumen formation under conditions of flow.

In vitro angiogenesis assays attempt to mimic the *in vivo* angiogenesis process (Nowak-Sliwinska et al., 2018). The endothelial-fibroblast organotypic co-culture assay recapitulates several crucial events of *in vivo* angiogenesis including the assembly of endothelial cells, ECs proliferation, sprouting, and tube and lumen formation when co-culturing in a plate. Furthermore, lumen expansion can be

observed and assessed in a closed circulatory system that forms in the microfluidic device under conditions of fluid flow. This 3D system of tubule formation and lumenogenesis resembles *in vivo* angiogenesis and allows tracking of ECs or genetically-encoded labelling prior to their co-culture with fibroblasts. Suitable markers introduced by lentiviral transduction include enhanced green fluorescent protein LifeAct (EGFP) or red fluorescent protein (RFP) VE-cadherin-RFP. Endothelial cells growing through multiple stages of angiogenesis and tubule formation can be labelled on day 7 using CD31 IHC staining (Figure 3.5 A). Endothelial cell rearrangement and acquirement of luminal-abluminal polarity at the site of cell-cell adhesions can be marked with podocalyxin by using IF staining (Figure 3.5 B). Therefore, by manipulating endothelial cells and adjusting cargos in the fluid flow, changes in cellular phenotypes and the morphology of tubules and lumens can be observed and assessed.

It is known that both FGF and VEGF promote proliferation (Laham et al., 1999) (Unger et al., 2000) (Elfenbein et al., 2012), but VEGF can also promote elongation and tubule morphogenesis (Rousseau et al., 2000). For microfluidic devices, the coordinated action of FGF and VEGF is necessary for optimal angiogenesis (Figure 3.6). Previous studies have shown that FGF increases the cell numbers (Tomanek et al., 2010) and VEGF turns them into the tubules (Tomanek et al., 2010). Furthermore, VEGF promotes sprouting (Abraham et al., 2015). Therefore, by measuring both total tubule length and branch points, both criteria were assessed to establish the best combination of growth factors for optimal angiogenesis, thereby establishing a system that has both stimulation of proliferation, elongation and morphogenesis.

The closed circulatory system of tubes capable of transferring fluid flow in microfluidic device, can be used for other research purposes, such as the assessment of extravasation of cancer cells or immune cells. Cancer cells can be easily observed circulating inside the endothelial tubules (Figure 3.17), allowing evaluation of their communication with endothelial cells and the process of extravasation in future studies. Furthermore, cancer cells can be co-cultured

with HUVEC and HDF cells, and the formation of new blood vessels in a process mimicking tumour angiogenesis can be observed.

Red fluorescence-labelled cells added in the microfluidic device chamber with pre-established green-labelled tubules, is a very good system to further assess the communication and interaction between incoming endothelial cells and endothelial cells in pre-established tubes (Figure 3.20). This system provides the opportunity to visualise how ECs acting when floating inside the blood vessel lumens for example in the cases of releasing EPCs that are originate from bone marrow (M. C. Yoder, 2012) into the blood vessels or after birth during capillary formation post ischemia (Asahara et al., 1997) or in tumours (Bussolati et al., 2011). The visualisation of interactions between endothelial cells, their partnership to form a tubule and their dynamics is more understandable when using different fluorescent protein labels in HUVEC.

Work presented in this chapter established a model of naturally developing tubules under conditions of fluid flow forming a closed circulatory system in a microfluidic device. The model is applicable to studies aiming to understand the processes of angiogenesis, lumenogenesis, flow sensing and pathological vasculogenesis, but also the trafficking of cancer cells and immune cells for example during the process of tumour growth and metastasis.

Chapter 4
Effects of primary cilia ablation and ROCK inhibition on blood vessel lumen formation

4.1 Introduction

Vascular endothelial cilia are microtubule-based organelles that protrude from the plasma membrane into the vessel lumen. They are thought to mediate mechanosensation of blood flow and subsequent signal transduction (J. G. Goetz et al., 2014). As mechanosensory organelles, endothelial cilia are thought to be involved in blood flow sensing (Spasic & Jacobs, 2017) and consequent alterations in vessel diameter to control blood pressure (Zaragoza et al., 2012). Although a circulatory system may form in the absence of cilia, the presence of cilia at sites of elevated flow is necessary to maintain endothelial integrity and to suppress the formation of atherosclerotic plaques (Dinsmore & Reiter, 2016). Dysfunction in endothelial cilia results in improper fluid-sensing, causing vascular disorders, such as aneurysm, hypertension and atherosclerosis (Rajasekharreddy Pala et al., 2018).

The RhoA effector Rho-associated protein kinase ROCK (ROCK1/2) is a protein kinase that mediates actin cytoskeletal remodelling and actomyosin contraction in diverse cell-types including endothelial cells (Abraham et al., 2009). ROCK has been implicated in the control of blood vessel lumen formation (Barry et al., 2016). Strikingly, Rock2 was identified in the Johnson group as the strongest positive regulator of cilia formation (Lake et al., 2020). Recent studies *in vivo* using zebrafish show that haemodynamic forces expand a provisional vessel lumen through deformations of the endothelial apical membrane, resulting in actomyosin recruitment and contraction (Gebala et al., 2016). It remains unclear how those forces are sensed and actomyosin contraction is regulated under flow, and what their precise mechanistic links are to lumen expansion.

These preliminary data suggest that there may exist functional links, potentially stage-specific, between remodelling of the actin cytoskeleton, the sensing of flow by cilia and the development of blood vessel lumens. Previous work in the Mavria group established a model of organotypic fibroblast-endothelial cell cocultures that give rise to endothelial tubes with lumens (Abraham et al., 2015). The model was used to understand the molecular mechanisms that mediate the initial stages of lumen formation in the absence of flow. My overall hypothesis is that ciliary

mechanosensing of flow regulates lumen expansion; and that cytoskeletal regulators such as ROCK act to mediate changes in the endothelial actin cytoskeleton and regulate cilia formation during lumen expansion. I assessed the impact of genetic ablation of cilia by knockdown of essential components of primary cilia comprising intraflagellar transport protein 88 (IFT88) and retinitis pigmentosa GTPase regulator interacting protein 1-like (RPGRIP1L). I hypothesized that ROCK is a cytoskeletal regulator involved in ciliogenesis, on flow sensing and lumen formation under conditions of fluid flow. I over-expressed HTR6-CFP2 (a serotonin receptor-cyan fluorescent protein fusion) to specifically mark cilia in order to track live primary cilia dynamics during lumen expansion under condition of fluid flow.

4.2 Primary cilia in endothelial cells

In order to elucidate the effect of cilia on tubule formation and lumen expansion, I first immunostained cilia in both a monolayer of endothelial cells and in organotypic co-culture of endothelial cells with HDF to determine ciliary morphology and incidence. For this purpose, a monolayer of HUVEC were seeded on a plate and cilia were marked by the ciliary protein ARL13B, and the GT335 monoclonal antibody directed against glutamylated tubulins (Figure 4.1 left panel). Furthermore, 14 days of organotypic co-culture assay was set up by seeding HUVEC onto a confluent layer of HDF cells. VEGFA (25 ng/ml) or bFGF (10 ng/ml) were applied to the media on days two, four and six to stimulate angiogenesis. I switched to low growth factor medium for tubule establishment and lumen formation on day 9. Cells were assessed on day 14 by immunofluorescence staining. Tubules were marked by the endothelial cell marker CD31 staining and ARL13B for cilia (Figure 4.1 right panel). Cilia were observed in both monolayers of endothelial cells and in organotypic co-culture tubules.

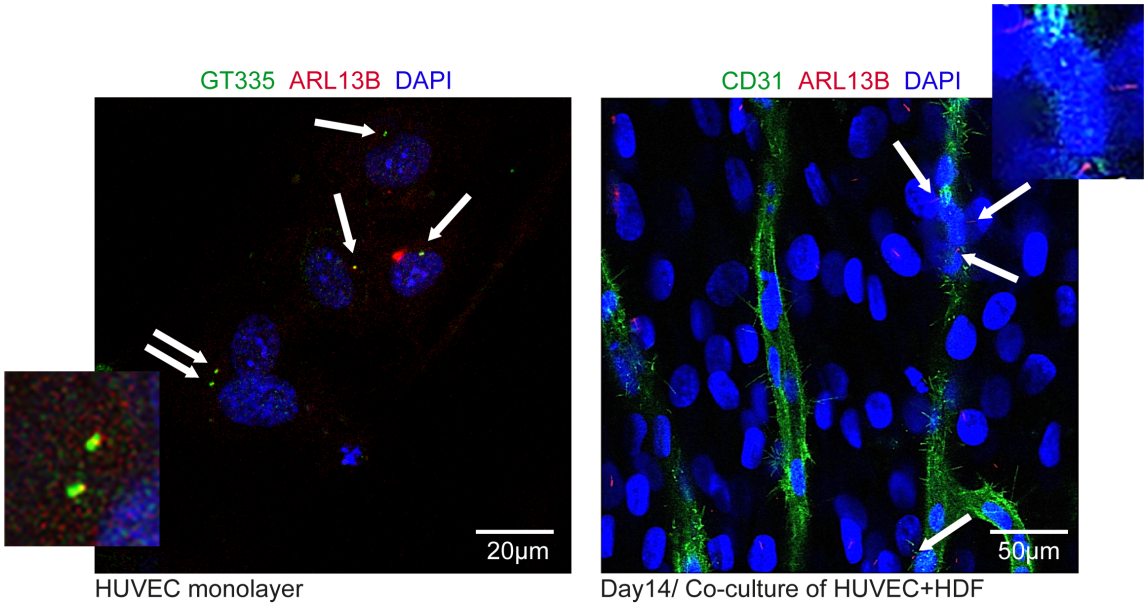

Figure 4.1 Primary cilia in a HUVEC monolayer and organotypic co-culture tubules.

Left panel: Immunofluorescence image shows primary cilia in a monolayer of HUVEC stained with the monoclonal antibody GT335 and for ARL13B as markers of cilia (white arrows). Image taken using a Nikon A1R confocal microscope, 100X magnification. Scale bar, 20µm. Green: GT335, red: ARL13B and blue: DAPI. **Right panel:** Immunofluorescence image shows primary cilia in tubules made in organotypic co-culture of HUVEC 14 days after seeding onto confluent HDF, indicated by white arrows. Image taken using a Nikon A1R confocal microscope, 40X magnification. Scale bar, 50µm. Green: CD31, red: ARL13B and blue: DAPI.

4.3 Ciliary protein IFT88 knockdown using pTRIPZ system

To suppress ciliogenesis in HUVEC, the pTRIPZ series of constructs were used to induce expression of Nontargeting shRNA or IFT88 shRNA in the presence of doxycycline. First, I generated HUVEC with Nontargeting or IFT88 knockdown by means of lentivirus transduction. Following infection with lentiviruses harbouring Nontargeting or IFT88 shRNAs alongside co-expression of TurboRFP, doxycycline was added to the monolayer of HUVEC every 24 hours and the knockdown was determined by visualisation of red fluorescent protein (Figure 4.2 A) and western blotting. Using western blot, I examined IFT88 protein ablation by measuring densitometry (average band intensity corrected for background). The results indicate greater than 50% loss of protein with the IFT88 shRNA in HUVEC after 72 hours of doxycycline induction (Figure 4.2 B), indicating successful IFT88 knockdown with a pTRIPZ lentiviral construct and doxycycline induction (Figure 4.2 C).

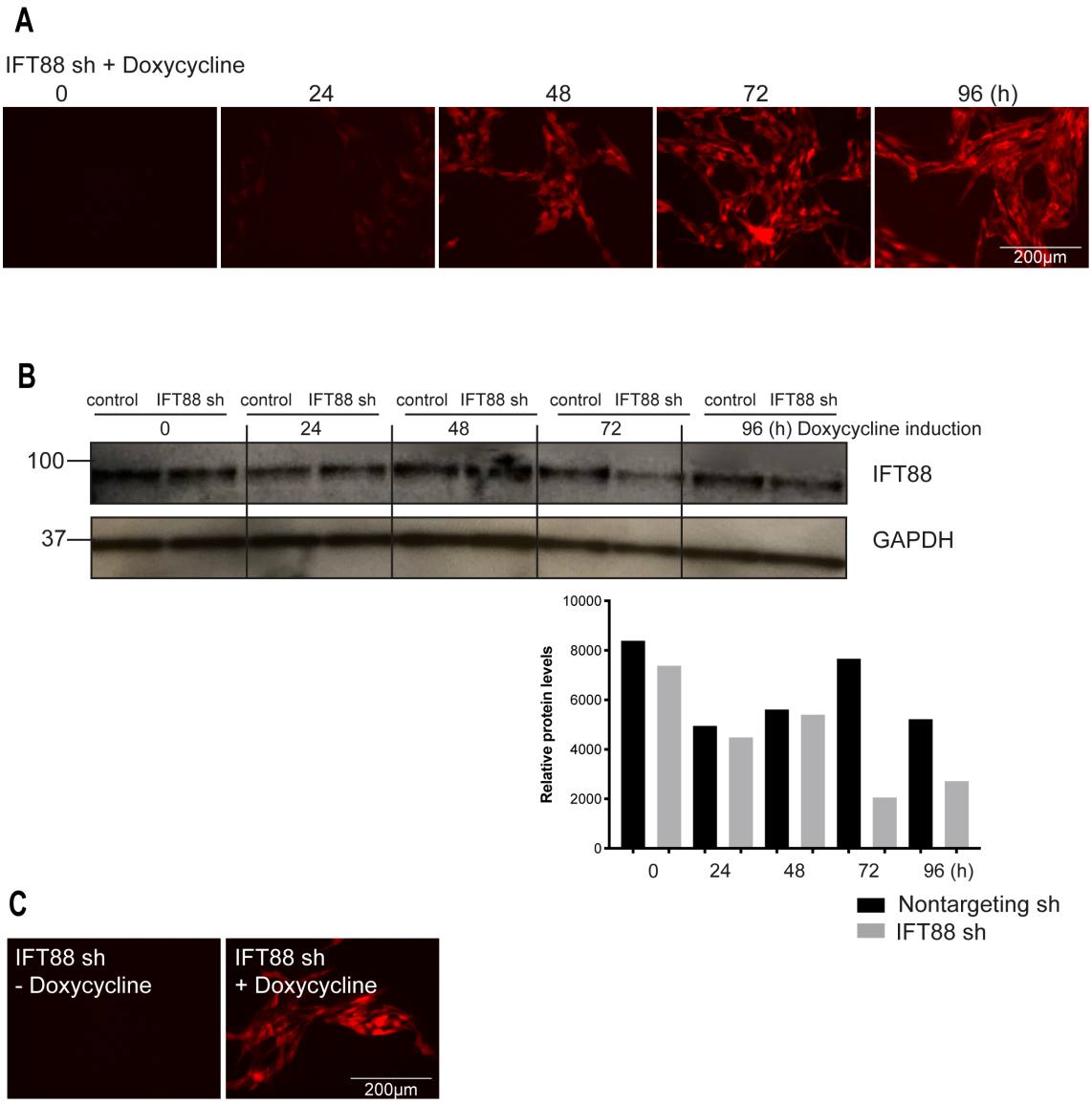

Figure 4.2 Knockdown of IFT88 using inducible shRNA.

A. Epifluorescence images show gradual increase of TurboRFP expression (red) following transduction with the pTRIPZ construct with the IFT88 shRNA after 24, 48, 72 and 96 hours. TurboRFP is co-expressed with the shRNA following doxycycline (2 µg/ml) induction. Images taken using an EVOS microscope, 20X magnification. Scale bar, 200µm. **B.** Western blot shows progressive decreases in IFT88 protein levels following transduction with the IFT88 shRNA in HUVEC but not the Nontargeting shRNA (negative control), 24, 48, 72 and 96 hours following doxycycline (2 µg/ml) induction. Bar graph shows western blot densitometry of relative protein expression 0, 24, 48, 72 and 96 hours after doxycycline induction in control HUVEC (Nontargeting shRNA; black bars), or

HUVEC with IFT88 knockdown (IFT88 sh; grey bars). The experiment was performed for one biological replicate. **C.** Fluorescence images of TurboRFP expression (red) for IFT88 knockdowns without or with doxycycline induction after 72 hours. Images taken using an EVOS microscope, 20X magnification. Scale bar, 200µm.

4.4 Ciliary protein RPGRIP1L knockdown using the pTRIPZ system

To determine if the effects on ciliogenesis following IFT88 knockdown are reproducible, I also characterized a second pTRIPZ vector. This also targeted an essential component of cilia, RPGRIP1L. HUVEC with RPGRIP1L knockdown were generated by means of lentivirus transduction. Following infection with lentiviruses harbouring RPGRIP1L shRNAs co-expressing RFP and after doxycycline induction, the level of RPGRIP1L protein was determined by western blotting (Figure 4.3).

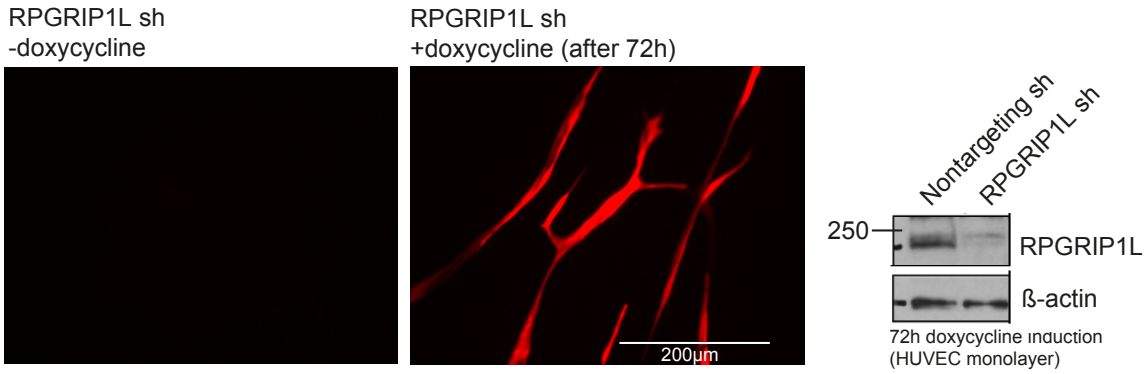

Figure 4.3 Knockdown of RPGRIP1L using inducible shRNA.
Epifluorescence images of TurboRFP expression (red) for RPGRIP1L knockdowns without or with doxycycline induction after 72 hours. Images were taken using an EVOS microscope, 20X magnification. Scale bar, 200µm. Western blot shows RPGRIP1L knockdown following transduction with RPGRIP1L shRNA in HUVEC but not the Nontargeting shRNA (negative control), 72 hours following doxycycline (2µg/ml) induction. Western blot was done by Dr Alice Lake.

4.5 IFT88 knockdown inhibits tubule formation

In this study, I set out to investigate whether cilia are required for tubule formation and lumen expansion. IFT88 is a central component of the Intraflagellar Transport (IFT) complex B, and it is critical for ciliary assembly and maintenance. Loss of IFT88 leads to the absence of cilia and causes polycystic kidney disease and disordered Hedgehog signalling, all of which are explained by abnormal ciliary function (Pazour et al., 2000). Therefore, for the purpose of cilium disassembly, IFT88 shRNA was used. HUVEC transduced with IFT88 shRNA and HUVEC with Nontargeting shRNA were used to set up organotypic co-culture assay with HDF cells to determine the effect of IFT88 knockdown on tubule formation. bFGF (10 ng/ml) was applied to the media on days two, four and six following seeding of HUVEC onto confluent HDF to stimulate angiogenesis. Media was switched to low growth factor medium on day 9 for tubule establishment and lumen formation, doxycycline induction was done between days 9-13 with treatments every 24 hours. Tubule formation was assessed on day 14 by staining for the endothelial cell marker CD31. The results show correct stimulation of angiogenesis and tubule formation in the presence of IFT88 and continued ciliogenesis. However, knockdown of IFT88 reduced tubule formation. The average total tubule length in the presence of cilia from two independent biological experiments was 13.619μm whereas with IFT88 knockdown this was significantly reduced to 4.103μm (Figure 4.4).

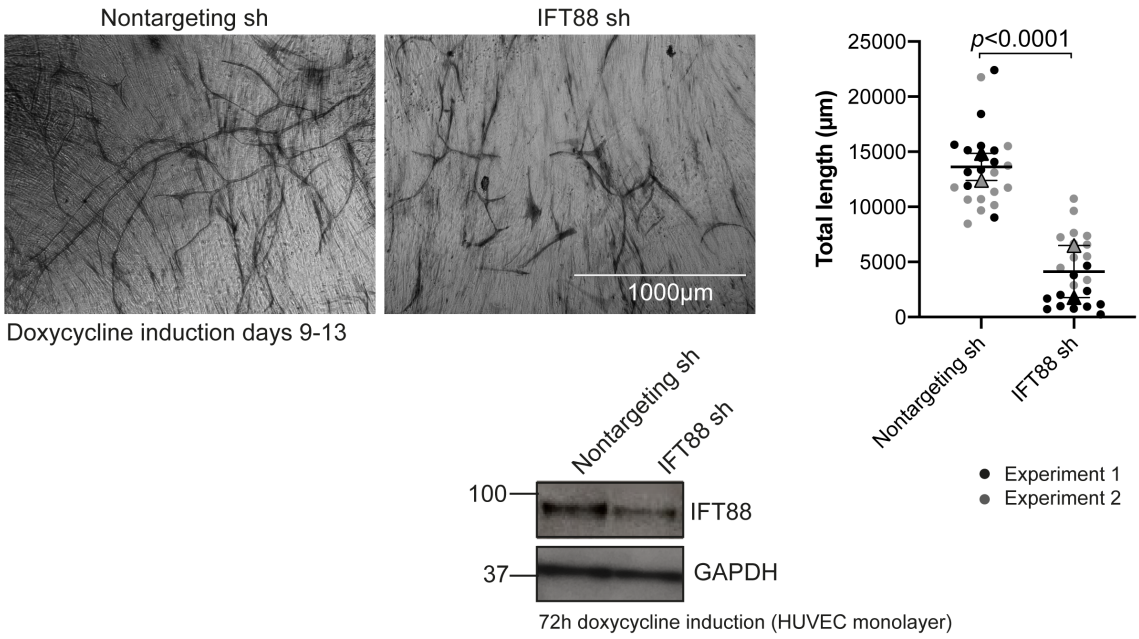

Figure 4.4 Knockdown of ciliary protein IFT88 inhibited tubule formation in organotypic co-culture.

Immunohistochemistry images show tubule formation in organotypic co-cultures of HDF with control HUVEC (Nontargeting sh), or HUVEC with IFT88 knockdown (IFT88 sh) 14 days after seeding onto confluent HDF. Doxycycline induction was done between days 9-13, with treatment every 24 hours. Images were taken using an EVOS microscope, 4X magnification. Scale bar, 1000µm. Dot plot shows individual quantifications of total length of tubules (µm) for n=6 organotypic co-cultures from two independent experiments (the data are from twenty-four images indicated by different grey dots on the dot plot). Statistical test for pair-wise comparison is Student t-test. Western blot shows IFT88 knockdown with IFT88 shRNA in HUVEC after 72 hours of doxycycline induction.

4.6 RPGRIP1L knockdown inhibits tubule formation

To confirm that suppression of ciliogenesis with the second essential component of primary cilia has same effect as IFT88 knockdown, RPGRIP1L shRNA was used to knockdown RPGRIP1L in HUVEC. RPGRIP1L is an important ciliary protein that is located in the intermediate region of a cilium between the basal body and the axoneme called the transition zone. Mutations in RPGRIP1L cause a broad spectrum of severe human diseases known as ciliopathies which are due to cilia dysfunction (Jensen et al., 2015). HUVEC transduced with RPGRIP1L shRNA and HUVEC with Nontargeting shRNA were used with HDF cells to set up organotypic co-culture assays and assess the effect of RPGRIP1L knockdown on tubule formation. bFGF (10 ng/ml) was applied to the media on days two, four and six following seeding of HUVEC onto confluent HDF to stimulate angiogenesis. Media was switched to low growth factor medium on day 9 for tubule establishment and lumen formation, doxycycline induction done between days 9-13 with treatment every 24 hours. Tubule formation was assessed on day 14 by CD31 immunostaining. The results were consistent with the IFT88 results, confirming that ciliogenesis suppression using RPGRIP1L shRNA caused a significant decrease of angiogenesis and tubule formation (Figure 4.5).

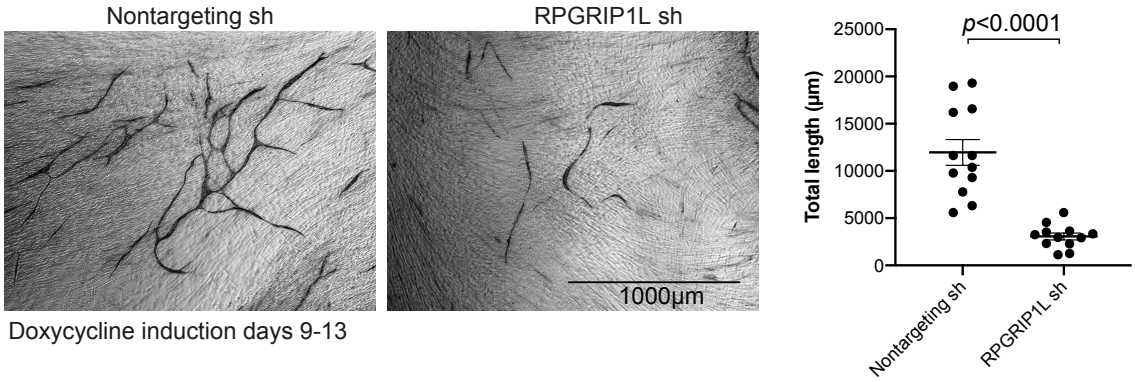

Figure 4.5 Knockdown of ciliary protein RPGRIP1L inhibits tubule formation in co-culture.

Immunohistochemistry images show tubule formation in organotypic co-cultures of HDF with control HUVEC (Nontargeting sh), or HUVEC with RPGRIP1L knockdown (RPGRIP1L sh) 14 days after seeding onto confluent HDF. Doxycycline induction done between days 9-13 every 24 hours. Images taken using an EVOS microscope, 4X magnification. Scale bar, 1000µm. Dot plot shows quantifications of total length of tubules (µm) for n=3 organotypic co-cultures from one experiment (the data are from twelve images indicated by black dots on the dot plot). Statistical test for unpair-wise comparison is Student t-test.

4.7 IFT88 knockdown inhibits lumen formation under conditions of fluid flow

Previous research has established that in the absence of flow, the developing tubules will be 20-40% lumenised (Abraham et al., 2015), in contrast to over 80% lumenised under flow conditions (Christopher Hughes, University of California-Irvine; personal communication with Georgia Mavria). To confirm this, I established organotypic co-culture under conditions of flow to investigate lumen formation without and with ciliogenesis suppression using the IFT88 shRNA to interfere with ciliogenesis. To investigate lumen formation under conditions of flow, I infected HUVEC with lentiviruses harbouring Nontargeting or IFT88 shRNAs co-expressing TurboRFP, and these were used to establish organotypic co-cultures inside the microchamber of microfluidic devices. HUVEC with

Nontargeting or IFT88 knockdown, together with HDF cells and fibrin were injected into the microchambers. The fibrin-cell mixture established a 3D system that allowed tubule and lumen formation under conditions of flow. Lumen formation was observed by TurboRFP expression in HUVEC transduced with Nontargeting or IFT88 shRNA. Doxycycline induction was performed at days 8-14 following addition of the fibrin-cell mixture, with Doxycycline treatment every 24 hours. The results indicate that cilia were necessary for lumenisation, as suppression of ciliogenesis with IFT88 knockdown under conditions of flow not only reduced tubule formation as it had been observed in the absence of flow, but also significantly reduced lumenised tubule length from 69% in the presence of cilia to 26% in the absence of cilia (Figure 4.6).

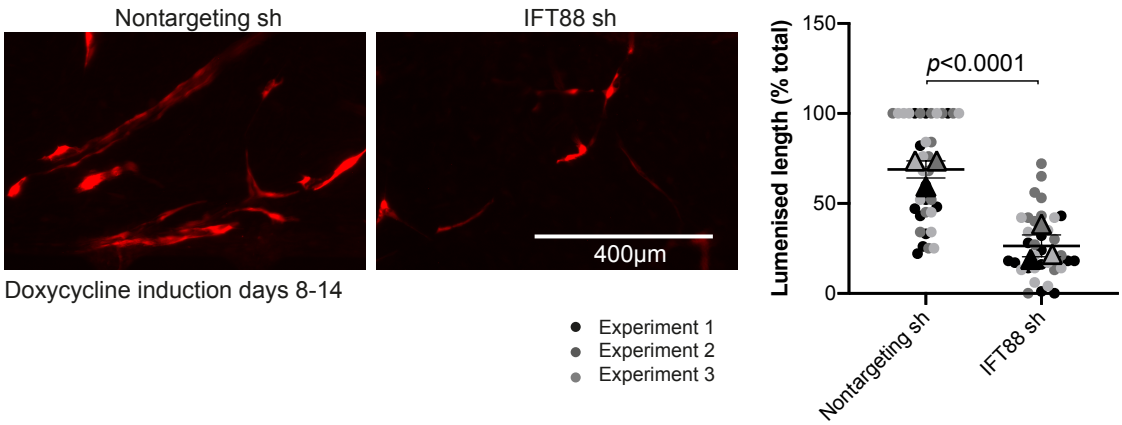

Figure 4.6 IFT88 knockdown inhibits lumen formation in tubules under conditions of flow.

Epifluorescence images show day 14 of tubule formation in organotypic co-cultures of HDF in fibrin following control TurboRFP HUVEC (Nontargeting sh), or TurboRFP HUVEC with IFT88 knockdown (IFT88 sh). Doxycycline (2 µg/ml) induction was done between days 8-14, with treatment every 24 hours. Images taken using an EVOS microscope, 10X magnification. Scale bar, 400µm. Dot plot shows quantifications of lumenised length (% total) in control HUVEC (Nontargeting sh), or HUVEC with IFT88 knockdown (IFT88 sh). The data are from thirty-six channel squares of n=3 independent experiments (indicated by different grey dots on the dot plot). Statistical test for pair-wise comparison is Student t-test.

4.8 RPGRIP1L knockdown inhibits lumen formation under conditions of fluid flow

RPGRIP1L was used to confirm the results obtained from IFT88 knockdown under conditions of flow. Consistent with the IFT88 data in Figure 4.6, ciliogenesis suppression with RPGRIP1L shRNA also decreased lumen formation. The average lumenised length (% total) with the presence of cilia from two independent experiments was 31μm, whereas RPGRIP1L knockdown significantly reduced this to 2μm (Figure 4.7).

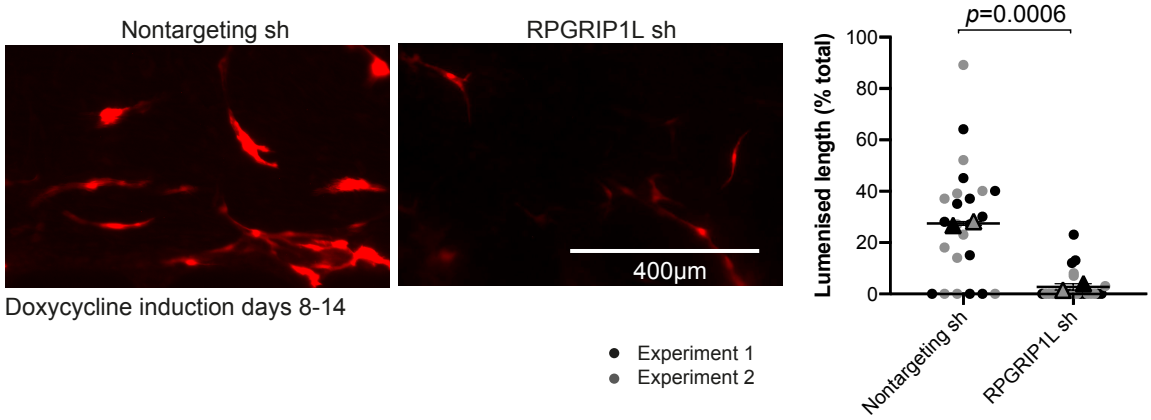

Figure 4.7 RPGRIP1L knockdown inhibits lumen formation in tubules under conditions of flow.

Epifluorescence images show day 14 of tubule formation in organotypic co-cultures of HDF in fibrin following control HUVEC (transduced with Nontargeting sh), or HUVEC following RPGRIP1L knockdown (RPGRIP1L sh). Doxycycline (2μg/ml) induction was done between days 8-14, with treatment every 24 hours. Images taken using an EVOS microscope, 10X magnification. Scale bar, 400μm. Dot plot shows quantifications of lumenised length (% total) in control HUVEC (Nontargeting sh), or HUVEC with RPGRIP1L knockdown (RPGRIP1L sh). The data are from twenty-four channel squares of n=2 independent experiments (indicated by different grey dots on the dot plot). Statistical test for pair-wise comparison is Student t-test.

4.9 IFT88 knockdown inhibits lumen expansion under conditions of fluid flow

From previous research, it is known that the initial stages of lumenogenesis take place through complex cellular mechanisms including rearrangement of lateral cellular junctions that allows organisation of endothelial cells into 3D tubular structures, and can take place in the absence of flow (Y. Wang et al., 2010). Lumen expansion and generation of perfused circulatory system is established by the onset of fluid flow (Herwig et al., 2011) (Lenard et al., 2013). Therefore, I established an organotypic co-culture of HUVEC-EGFP with Nontargeting shRNA or IFT88 shRNA with HDF and fibrin in microfluidic devices and under conditions of flow, in order to investigate if suppression of ciliogenesis affected lumen expansion. Doxycycline induction was performed at days 8-14, with treatment every 24 hours. The results indicate that although lumen expansion was similar in both control and IFT88 shRNA organotypic co-cultures before doxycycline induction and IFT88 knockdown, after doxycycline induction (commencing on day 8 and finishing on day 14), lumens expanded significantly in controls when there was ciliogenesis, in contrast to IFT88 knockdown where expansion was inhibited. These data suggest that the presence of cilia is required for correct lumen expansion (Figure 4.8).

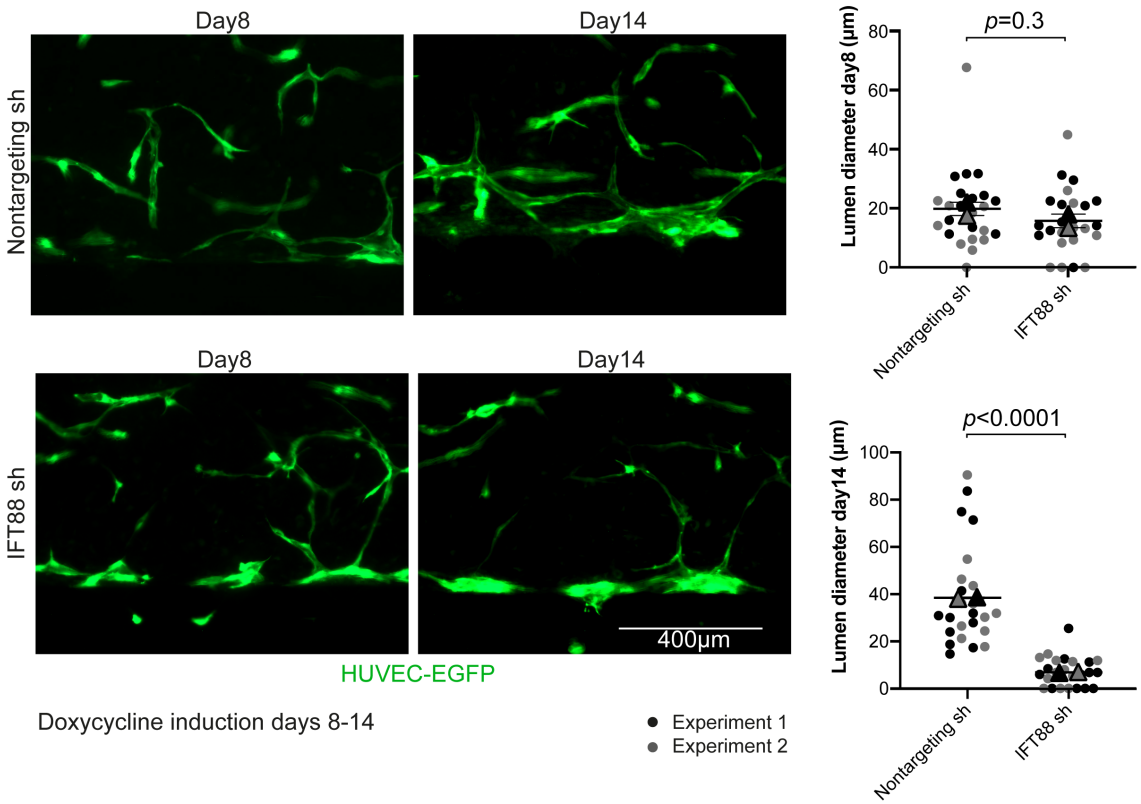

Figure 4.8 Knockdown of IFT88 inhibited lumen expansion under conditions of flow.

Epifluorescence images show day 8 and day 14 of lumen expansion in organotypic co-cultures of HDF with control HUVEC-EGFP (Nontargeting sh; green in top panels), or HUVEC-EGFP with IFT88 knockdown (IFT88 sh; green in bottom panels) in fibrin. Doxycycline induction was done between days 8-14, every 24 hours. Images were taken using an EVOS microscope, 10X magnification. Scale bar, 400µm. Dot plots show quantifications of lumen diameter (µm) on day 8 and day 14 in control HUVEC (Nontargeting sh), or HUVEC with IFT88 knockdown (IFT88 sh). The data are from twenty-four channel squares of n=2 independent experiments (indicated by different grey dots on the dot plot). Statistical test for pair-wise comparison is Student t-test.

4.10 Localization of HTR6-CFP2 in primary cilia

To determine that the blue reporter protein in HTR6-CFP2 localized specifically to primary cilia, the pWPXL-HTR6-CFP2 construct was transiently transfected into hTERT-RPE1 (hTERT-immortalized retinal pigment epithelial cells). After seeding hTERT-RPE1, transfection reagent mix (DNA and Lipofectamine 2000) was used to transfect the cells. After 72 hours cells were fixed using 4% PFA and their cilia stained for ARL13B. Imaging confirmed that HTR6-CFP2 colocalized specifically with ARL13B in primary cilia (Figure 4.9).

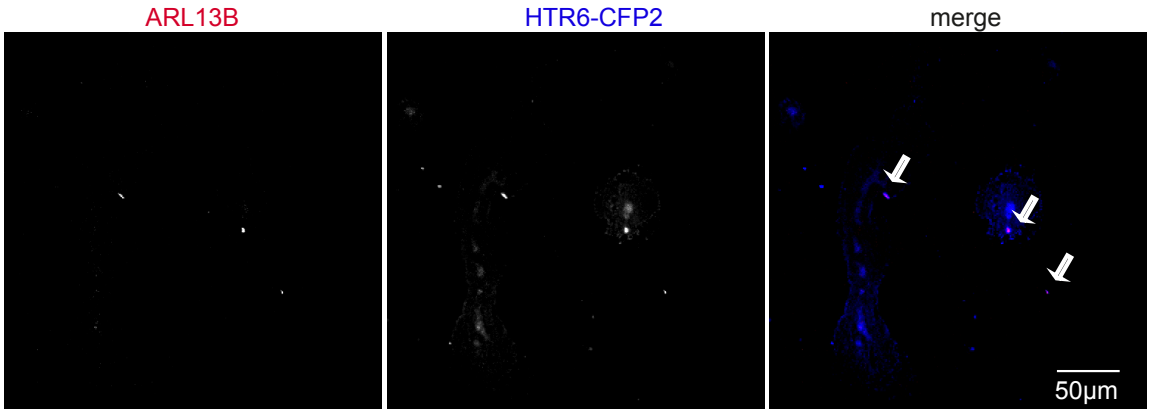

Figure 4.9 Transient transfection of hTERT-RPE1 with HTR6-CFP2 lentiviral vector.

Immunofluorescence images show transient transfection of hTERT-RPE1 with the serotonin receptor HTR6-CFP2 pWPXL lentiviral construct, showing specific localization (blue, indicated by arrowheads) to primary cilia (marked with ARL13B; red). Images taken using a Nikon A1R confocal microscope, 100X magnification. Scale bar, 50µm.

4.11 Characterization of primary cilia in hTERT-RPE1 transduced with HTR6-CFP2

First, I employed the human hTERT-RPE1 and transduced them with HTR6-CFP2. A monolayer of hTERT-RPE1 were seeded and transduced with HTR6-CFP2 lentivirus supernatant at dilutions of 1:2 of virus supernatant with DMEM/F-12 10%FBS medium. After 72 hours cells were fixed with 4% PFA and stained with the cilia markers ARL13B and GT335 to characterise cilia. The results indicate that the HTR6-CFP2 fusion protein localized to primary cilia with ciliary proteins GT335 and ARL13B (Figure 4.10). Furthermore, I observed that each ciliary protein appeared to localise to different compartments in the cilium structure. I therefore measured and compared the length of cilium that was stained by the ARL13B antibody compared to the length with HTR6-CFP2 expression in hTERT-RPE1 (Figure 4.11).

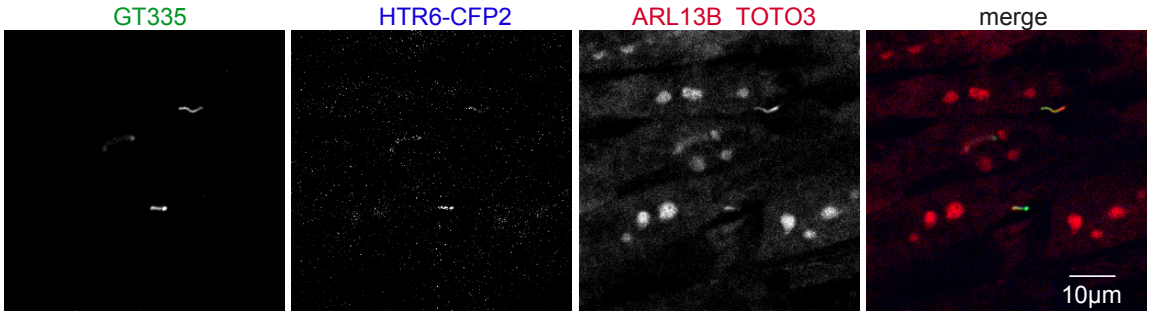

Figure 4.10 Visualization of primary cilia in hTERT-RPE1 transduced with HTR6-CFP2.

Immunofluorescence images show hTERT-RPE1 transduced with serotonin receptor HTR6-CFP2 lentiviral construct (blue) and marked for primary cilia using ARL13B (red) and poly-glutamylated tubulin (GT335; green). The counterstain for RNA (in cytoplasm and nuclei) is TOTO-3 (red). Images taken using a Nikon A1R confocal microscope, 100X magnification. Scale bar, 10μm.

4.12 Serotonin receptor HTR6-CFP2 localizes to a longer compartment in primary cilia compared to ARL13B

As discussed above ARL13B was used as a ciliary protein to measure the ciliary membrane length and to compare with the length of the ciliary membrane compartment containing HTR6-CFP2. Interestingly, whilst HTR6-CFP2 colocalised in cilia with ARL13B, it appeared to localize to a larger membrane compartment in cilia as suggested by the longer ciliary length detected by HTR6-CFP2 expression compared to ARL13B staining (Figure 4.11).

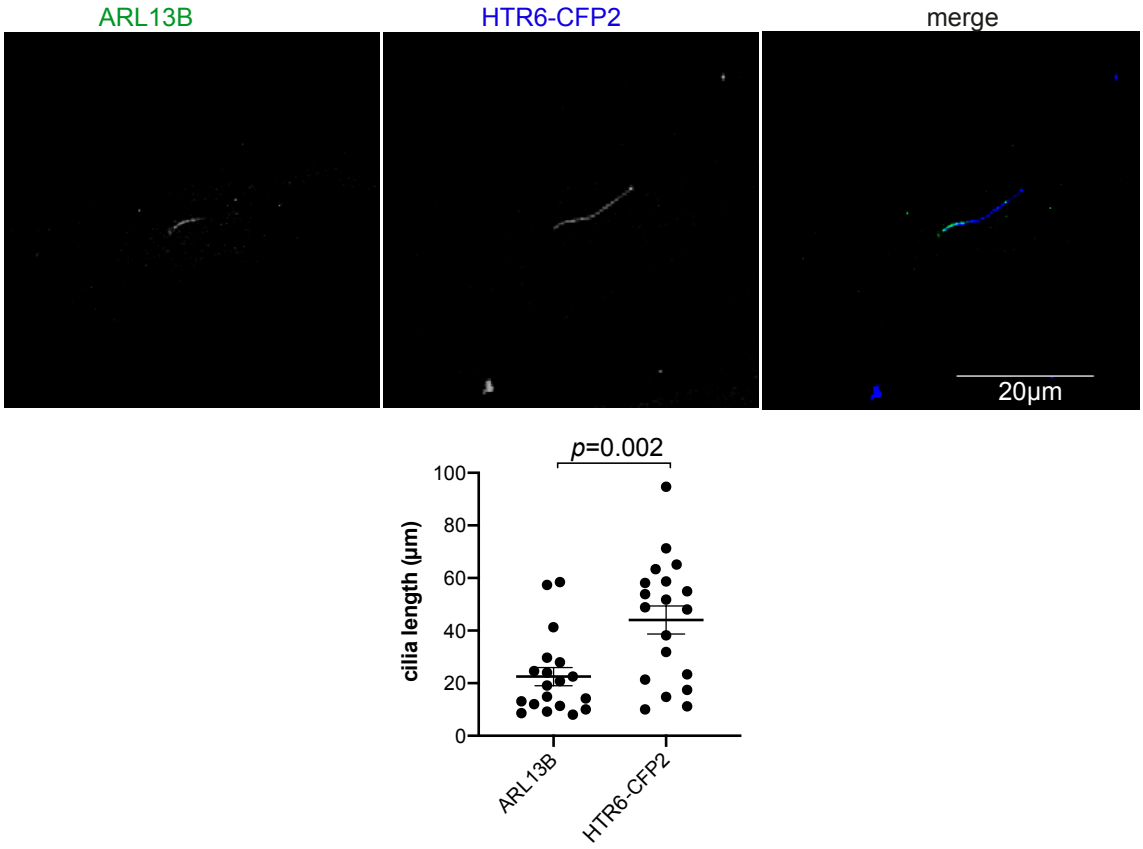

Figure 4.11 Comparison of ciliary length determined by HTR6-CFP2 stable expression and ARL13B staining in hTERT-RPE1.

Immunofluorescence images show hTERT-RPE1 transduced with serotonin receptor HTR6-CFP2 lentiviral construct (blue) and marked for primary cilia (ARL13B; green). Images taken using a Nikon A1R confocal microscope, 100X magnification. Scale bar, 20μm. Dot plot shows quantifications of cilia length (μm)

with serotonin receptor HTR6-CFP2 expression (blue) and ARL13B staining (green). The data are from nineteen primary cilia from n=2 independent experiments (indicated by black dots on the dot plot). Statistical test for unpair-wise comparison is Student t-test.

4.13 Serotonin receptor HTR6-CFP2 localizes to primary cilia in HUVEC

In order to visualize dynamic changes in primary cilia behaviour with flow and to assess the effect of cilia on lumen expansion in microfluidic devices, cilia in HUVEC were marked with HTR6-CFP2. Lentiviruses expressing the HTR6-CFP2 fusion protein were used to transduce a monolayer of HUVEC. Then, HUVEC were fixed with 4% PFA and ciliary proteins stained with antibodies. The results show colocalization of HTR6-CFP2 with GT335 and ARL13B in HUVEC. Interestingly, each protein marked specific part of a cilium (Figure 4.12).

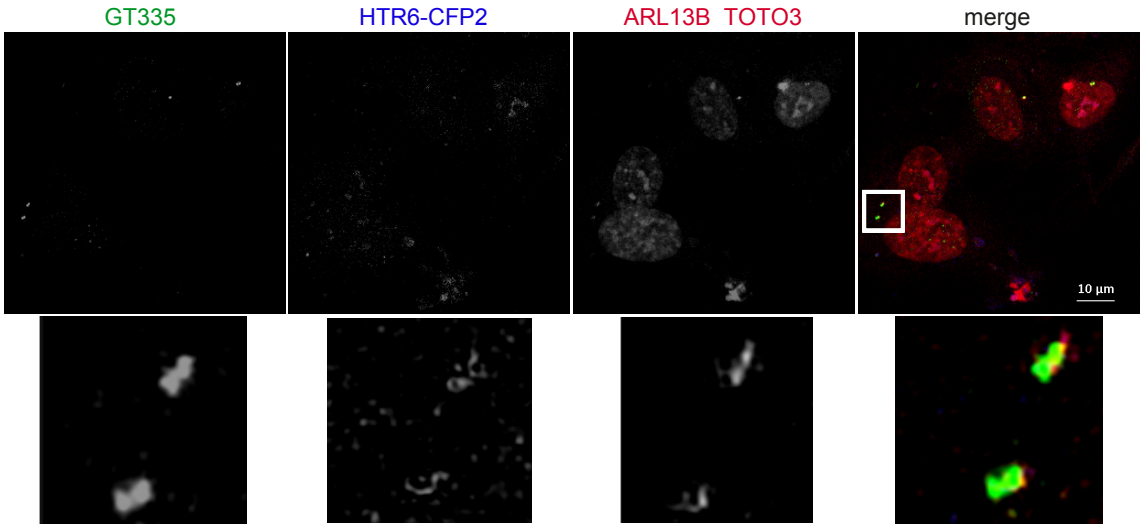

Figure 4.12 Visualization of primary cilia in HUVEC transduced with serotonin receptor HTR6-CFP2.
Immunofluorescence images show HUVEC transduced with serotonin 5HT-CFP2 lentiviral construct (blue) and marked for primary cilia using ARL13B (red) poly-glutamylated tubulin (GT335; green). Counterstain for RNA (in cytoplasm and nuclei) is TOTO-3 (red). Images taken using a Nikon A1R confocal microscope, 100X magnification. Scale bar, 10µm.

4.14 ROCK inhibition disrupts lumen formation under conditions of fluid flow

Rho-associated kinases (ROCK1 and ROCK2) are regulators of actomyosin contractility and have been implicated in the control of blood vessel lumen formation. Furthermore, previous work in the Johnson lab has found that cilia incidence and length were increased by ROCK2 siRNA-mediated knockdown and inhibition. I investigated the role of cilia in sensing fluid flow and lumen formation, then the role of cytoskeletal regulator ROCK in blood vessel lumen formation was observed. I used microfluidic devices to assess how lumen formation was affected by ROCK inhibition. HUVEC-EGFP with HDF in fibrin were added to a single chamber microfluidic device and media was changed every 24 hours. Lumen formation was assessed eight days after seeding the cells in control HUVEC or HUVEC treated with Y-27632 between days 4-8. Lumen formation was disrupted with ROCK inhibition indicating that ROCK is necessary for lumen formation and angiogenesis when there was fluid flow inside the tubules. ROCK inhibition in the organotypic co-culture significantly reduced the lumenisation and lumen formation was suppressed by lack of cytoskeletal regulator ROCK (Figure 4.13). To determine if ROCK inhibition had stage-specific effects dependent on the stage of lumen formation and maturation, ROCK inhibitor was added between days 8-12 which is the stage of lumen expansion under conditions of flow. Lumen formation was assessed twelve days after seeding the cells in microchamber for both control HUVEC or HUVEC treated with Y-27632 between days 8-12. Lumen formation was completely disrupted by ROCK inhibition at the late stage of tube formation and lumen expansion (Figure 4.14). Next, I assessed the effect of ROCK inhibition on lumen formation at very late stages, when the lumen was completely formed and expanded. Lumen formation was assessed sixteen days after seeding the cells inside the microchamber in both control HUVEC or HUVEC treated with ROCK inhibitor (Y-27632) between days 12-16. Although lumen formation was significantly inhibited by ROCK inhibition at very late stages after lumen formed, in contrast to treatment at earlier timepoints lumenised length could still be detected and the overall decrease in lumen formation was lesser with ROCK inhibition at this later timepoint. The results indicate that tubule and lumenised length decreased

following ROCK inhibition at very late stages of lumen formation (Figure 4.15). Overall, ROCK inhibition showed the highest decrease in lumenised length in late stages compare to very late stage and early stages of lumen formation respectively.

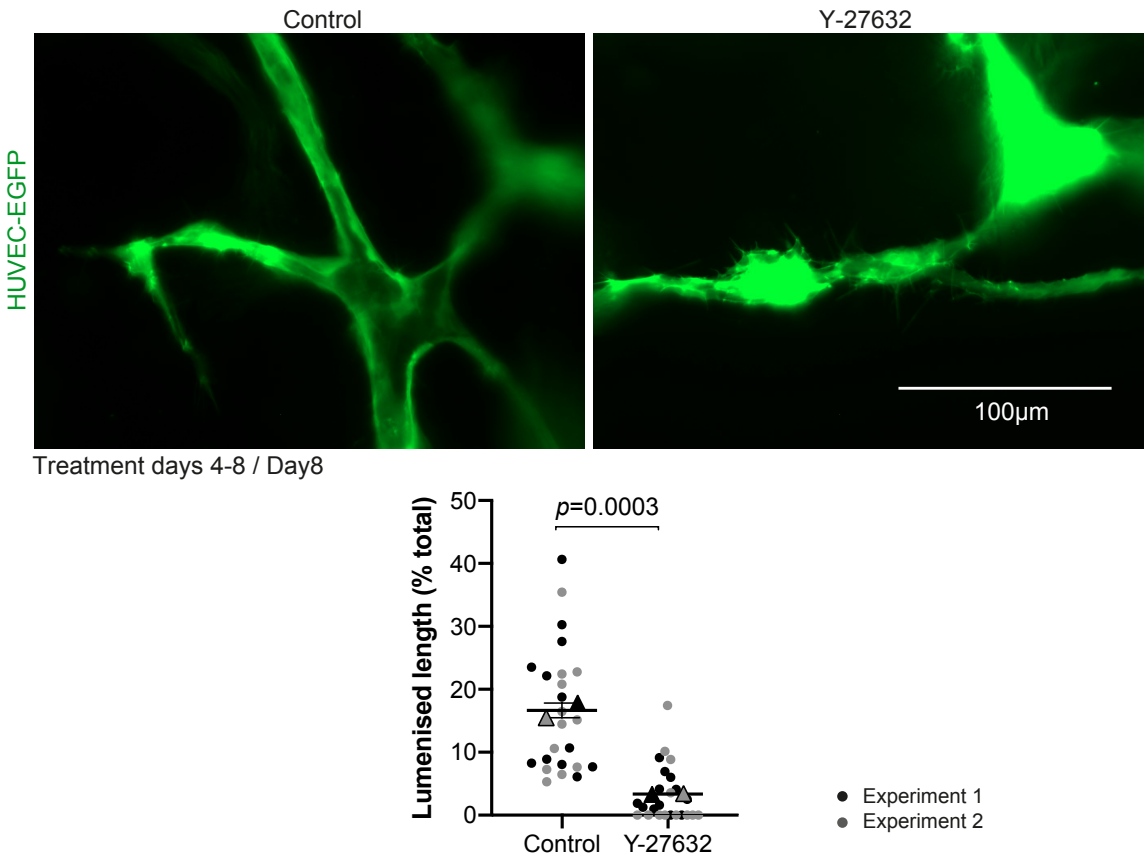

Figure 4.13 Effect of early ROCK inhibition on lumen formation under conditions of flow.

Epifluorescence images show day 8 of tubule formation in organotypic co-cultures of HDF with HUVEC-EGFP in fibrin, for control (vehicle only) and tubules following treatment with ROCK inhibitor (10µM Y-27632) between days 4-8 every 24 hours. Images taken using an EVOS microscope, 40X magnification. Scale bar, 100µm. Dot plot shows quantifications of lumenised length (% total) in control co-culture, or co-culture with ROCK inhibition. The data are from twenty-four channel squares from n=2 independent experiments (indicated by different grey dots on the dot plot). Statistical test for pair-wise comparison is Student t-test.

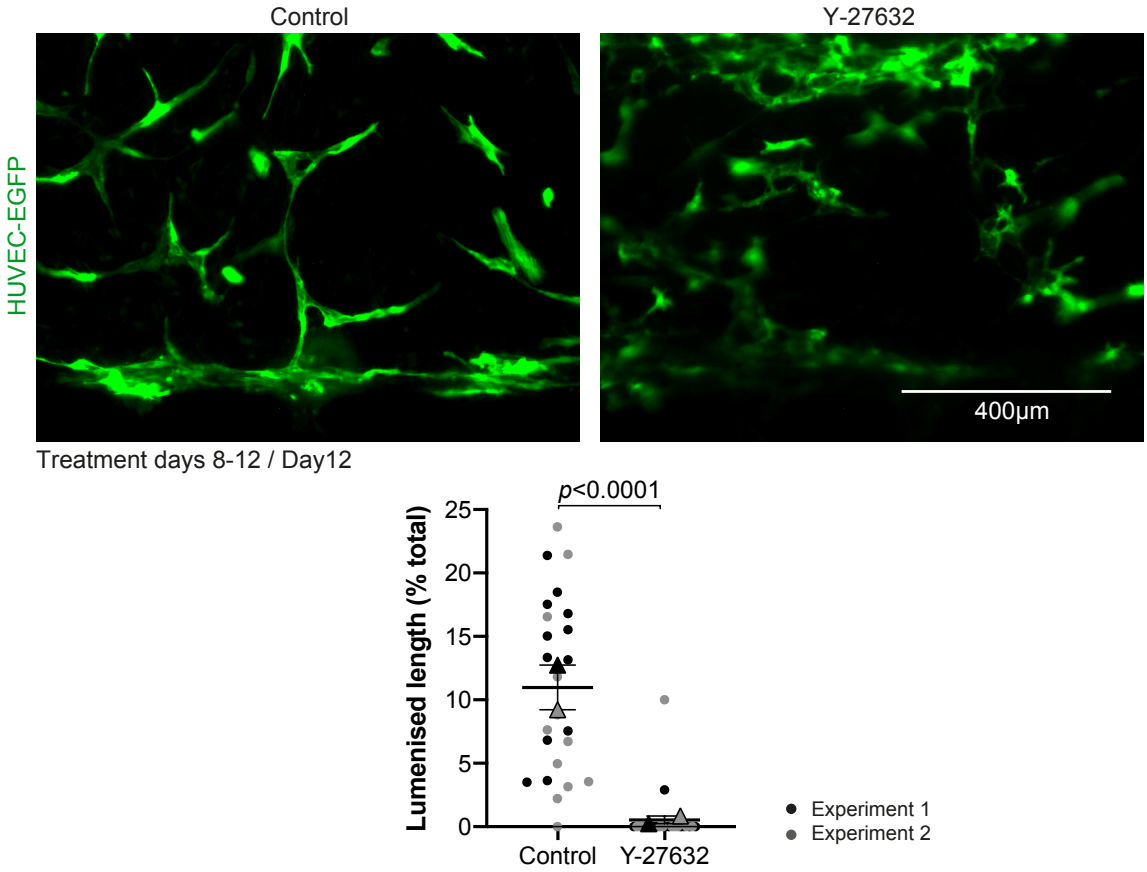

Figure 4.14 Effect of late ROCK inhibition on lumen formation under conditions of flow.

Epifluorescence images show day 12 of tubule formation in organotypic co-cultures of HUVEC-EGFP with HDF in fibrin, for control (vehicle only) and tubules with ROCK inhibitor (10µM Y-27632) between days 8-12, every 24 hours. Images taken using an EVOS microscope, 10X magnification. Scale bar, 400µm. Dot plot shows quantifications of lumenised length (% total) in control co-culture, or co-culture with added ROCK inhibitor. The data are from twenty-four channel squares from n=2 independent experiments (indicated by different grey dots on the dot plot). Statistical test for pair-wise comparison is Student t-test.

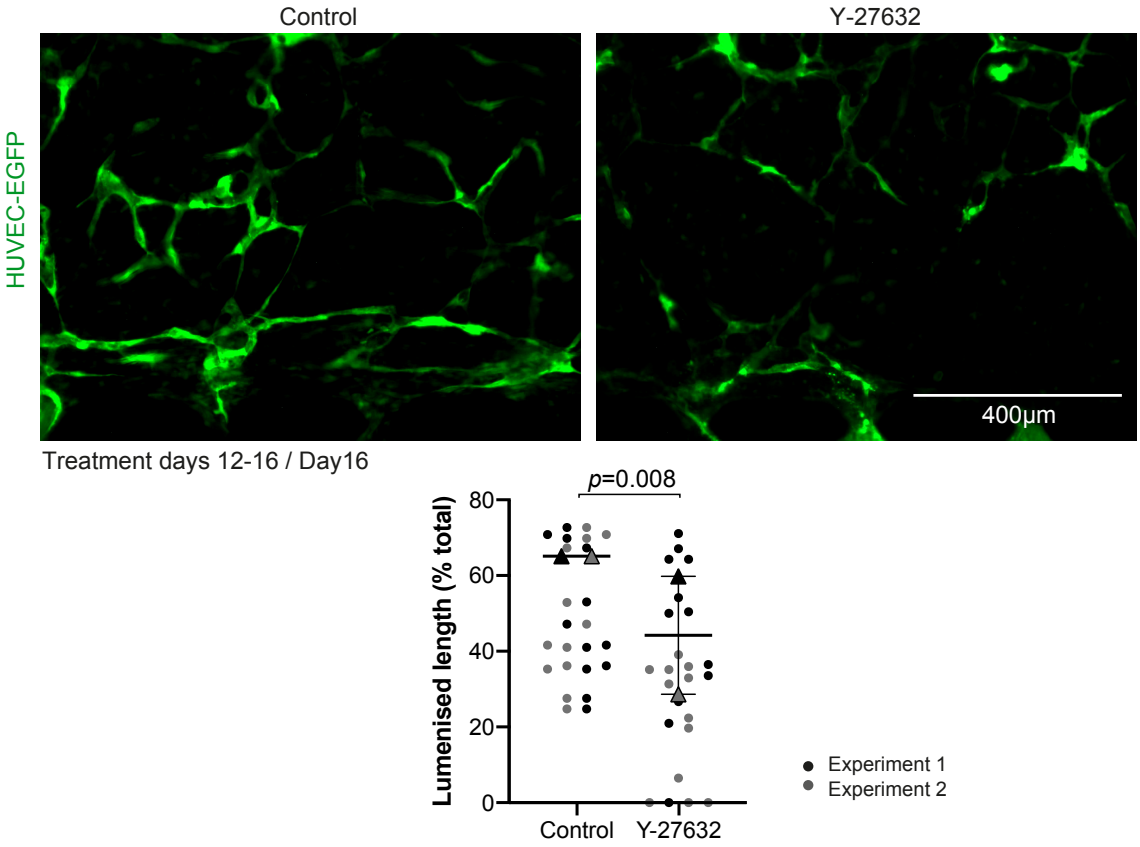

Figure 4.15 Effect of ROCK inhibition on lumen formation under conditions of flow (very late treatment).

Epifluorescence images show day 16 of tubule formation in organotypic co-cultures of HDF with HUVEC-EGFP in fibrin for control (vehicle only) and tubules with ROCK inhibitor (10µM Y-27632) between days 12-16, every 24 hours. Images taken using an EVOS microscope, 10X magnification. Scale bar, 400µm. Dot plot shows quantifications of lumenised length (% total) in control co-culture, or co-culture with added ROCK inhibitor. The data are from twenty-four channel squares from n=2 independent experiments (indicated by different grey dots on the dot plot). Statistical test for pair-wise comparison is Student t-test.

4.15 Discussion

The important role of the primary cilium in developmental processes is indicated by ciliopathies subsequent of genetic defects of cilium components. It has been shown by different studies that cilia play a role in a range of mechanosensation, chemo-sensation and signal transduction pathways. Primary cilia have been observed in areas of disturbed flow in blood vessels and their presence has been linked to atherosclerosis, but the exact role of primary cilia in the development of the vasculature is not fully understood (Van der Heiden et al., 2008).

The results of this chapter indicate that (i) primary cilia have a significant effect in blood vessel formation and vascular lumen expansion in the absence of flow and under conditions of fluid flow; (ii) the cytoskeletal regulator ROCK also known to regulate ciliary length and incidence is necessary for blood vessel lumen formation; (iii) a pWPXL lentiviral expression construct was produced by insertion of the serotonin receptor HTR6-CFP2 fusion that can be used to mark cilia and visualize live primary cilia movement.

Tubule formation in the co-culture assay and lumen expansion under conditions of flow were disrupted when cilia were ablated with knockdown of IFT88 or RPGRIP1L. This observation implies that primary cilia may trigger a pathway that regulate morphogenetic processes in the developing endothelial lumen. These findings agree with the study by J. G. Goetz et al. (2014) in zebrafish implicating endothelial cilia in sensing of flow in blood vessels and vascular remodelling. Interestingly, the study by Ernandez et al. (2017) showed that primary cilia regulate epithelial tubular lumen maturation and enlargement in renal collecting duct epithelium.

Although primary cilia are microtubule-based organelles, the actin cytoskeleton and cytoskeletal regulators appear to play a crucial role on ciliogenesis and cilia maintenance. Regulators of actin cytoskeletal dynamics have profound effects on cilia and ciliary function. It has been shown that Rho-associated kinase (ROCK1/2) signalling as an effector of actin dynamics has a significant influence on ciliogenesis. This pathway has also been suggested in many aspects of

angiogenesis and lumen formation (Reviewed by Liu et al. (2018)). It has been shown by Gary Grant that actin cytoskeleton controls the process of primary cilia lengthening and regulates cilia incidence in endothelial cells. The effect of ROCK signalling pathway on actin is well-characterized and as a Rho signalling effector, ROCK phosphorylates downstream kinases which have an effect on actin dynamics. Y-27632 is extensively used as a ROCK1 and ROCK2 inhibitor and in this chapter, I have shown that inhibition of ROCK signalling with Y-27632 results in significant suppression of the lumen formation (Figure 4.13, Figure 4.14, Figure 4.15). It is well-defined by previous studies in the lab that ROCK2 is the strongest positive regulator of cilia formation and function via effects on remodelling of actin cytoskeleton (Lake et al., 2020). Further studies using ROCK2 specific inhibitor (KD-025) can help to corroborate the findings with results obtained using Y-27632 inhibitor. The molecular basis of the dependency of primary cilia on ROCK is yet another area of enquiry for future investigation.

Furthermore, in this chapter I have shown the localization of HTR6-CFP2 in primary cilia following transduction of endothelial cells (Figure 4.12). The pWPXL lentiviral construct harbouring the serotonin receptor HTR6-CFP2 fusion protein gives an opportunity to assess live primary cilia dynamics during lumen formation and lumen expansion in endothelial cells. This construct can be used in different projects in the future to track cilia incidence, length and movement under different conditions.

Chapter 5
Role of DOCK4 on tubule and lumen formation under conditions of FGF stimulation

5.1 Introduction

During development, blood vessels are formed by endothelial cells and formed highly structured network. *De novo* formation of blood vessels from endothelial progenitor cells is called vasculogenesis and this is what forms the primitive plexus. Angiogenesis takes place to expand this pre-existing primitive network and form the hierarchical network of blood vessels. Angiogenesis occurs both through proximal elongation and lateral branching led by 'tip' endothelial cells and followed by 'stalk' cells migrating collectively (Zeng et al., 2021), and is regulated by pro- and anti-angiogenic molecules. Tip cells contain abundant actin-rich filopodial protrusions that sense the surrounding microenvironment and guide the growing sprout in response to directional cues.

During angiogenesis, sprouting and migration of endothelial cells are highly dependent on dynamic changes of the endothelial cell actin cytoskeleton controlled by the Rho family of small GTPases. Similarly, the process of lumenogenesis requires cytoskeletal rearrangements and the activity of Rho proteins and their regulators. Positive regulators or GEFs activate Rho proteins by catalysing the exchange of GDP for GTP. Abraham et al. (2015) showed that the process of lumen formation requires lateral endothelial cell-cell contacts followed by cytoskeletal rearrangements that displace the junctional molecules and establish luminal-abluminal polarity in the endothelial cells forming a hollow tube which allows the flow of blood. The Rac1 GEF DOCK4 is a regulator of both filopodia formation and sprouting, and lumen formation (Abraham et al., 2015). Whilst the studies show that DOCK4 operates downstream of VEGF signalling to control filopodia formation and sprouting, it's potential role downstream of FGF signalling has not been investigated. Moreover, in this chapter the role of DOCK4 as a potential regulator of endothelial cilia was assessed.

In this chapter, first HUVEC with stable DOCK4 knockdown or control Nontargeting were generated using a previously established shRNAs (Abraham et al., 2015). Then I explored the relationship between DOCK4 FGF driven angiogenesis, lumen formation and lumen expansion in the organotypic co-

culture angiogenesis assay in the absence or presence of fluid flow, and also effect of DOCK4 on cilia abundance and ciliary length.

5.2 Generating endothelial cells with stable DOCK4 knockdown

In order to investigate the role of DOCK4 downstream of FGF signalling, HUVEC with DOCK4 knockdown were generated by means of lentiviral transduction. Following infection with lentiviruses harbouring Nontargeting or DOCK4 shRNAs alongside co-expression of enhanced green fluorescent protein (EGFP) (Abraham et al., 2015), HUVEC were FACS sorted and the knockdown was determined by western blotting. There was over 90% knockdown of DOCK4 with DOCK4 shRNA in HUVEC (Figure 5.1).

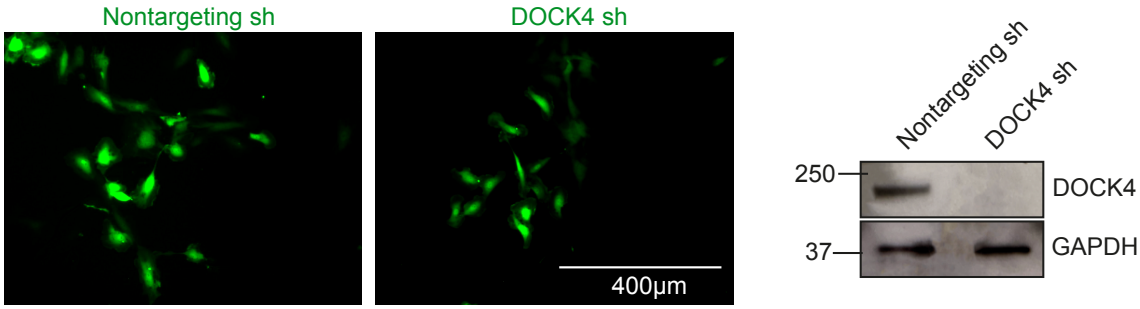

Figure 5.1 DOCK4 knockdown in HUVEC.
Florescence images show EGFP expression (green) in HUVEC with DOCK4 shRNA and control Nontargeting shRNA lentiviruses. Images taken using an EVOS microscope, 10X magnification. Scale bar, 400µm. Western blot shows DOCK4 knockdown following transduction with DOCK4 shRNA in HUVEC.

5.3 DOCK4 suppresses FGF driven angiogenesis in the organotypic co-culture assay

In this study I set out to investigate whether DOCK4 is required for FGF driven angiogenesis. HUVEC transduced with DOCK4 shRNA and HUVEC with Nontargeting shRNA were used to set up organotypic co-cultures with HDF to determine the effect of DOCK4 knockdown on tubule formation under conditions of FGF stimulation in comparison to VEGF stimulation. bFGF (10 ng/ml) or VEGF (25 ng/ml) were applied to the media on days two, four and six following seeding of HUVEC onto confluent HDF to stimulate angiogenesis, and the effects of DOCK4 knockdown on tubule formation were assessed on day 7 after seeding. Untreated organotypic cocultures were also set up as controls with changes of media lacking growth factors being the same as those with FGF or VEGF. Tubule formation was visualised by CD31 staining. Figure 5.2 shows that the average total tubule length of 2851μm under VEGF conditions in control was reduced to 1554μm with DOCK4 knockdown, although the decrease was not statistically significant. The average total tubule length of 1772μm under conditions of FGF stimulation was increased to 2228μm with DOCK4 knockdown, representing an average increase of 25.7% from 3 independent experiments. The basal tubule formation varied amongst the different experiments because of the different batches of cells used, however the stimulation of tubule formation by DOCK4 knockdown was statistically significant as assessed by using a two tailed paired t-test. Hence, DOCK4 knockdown stimulates FGF driven angiogenesis. The branch point index was not affected by DOCK4 knockdown under conditions of FGF stimulation. The branchpoint index was reduced under conditions of VEGF stimulation as shown previously by Abraham et al. (2015).

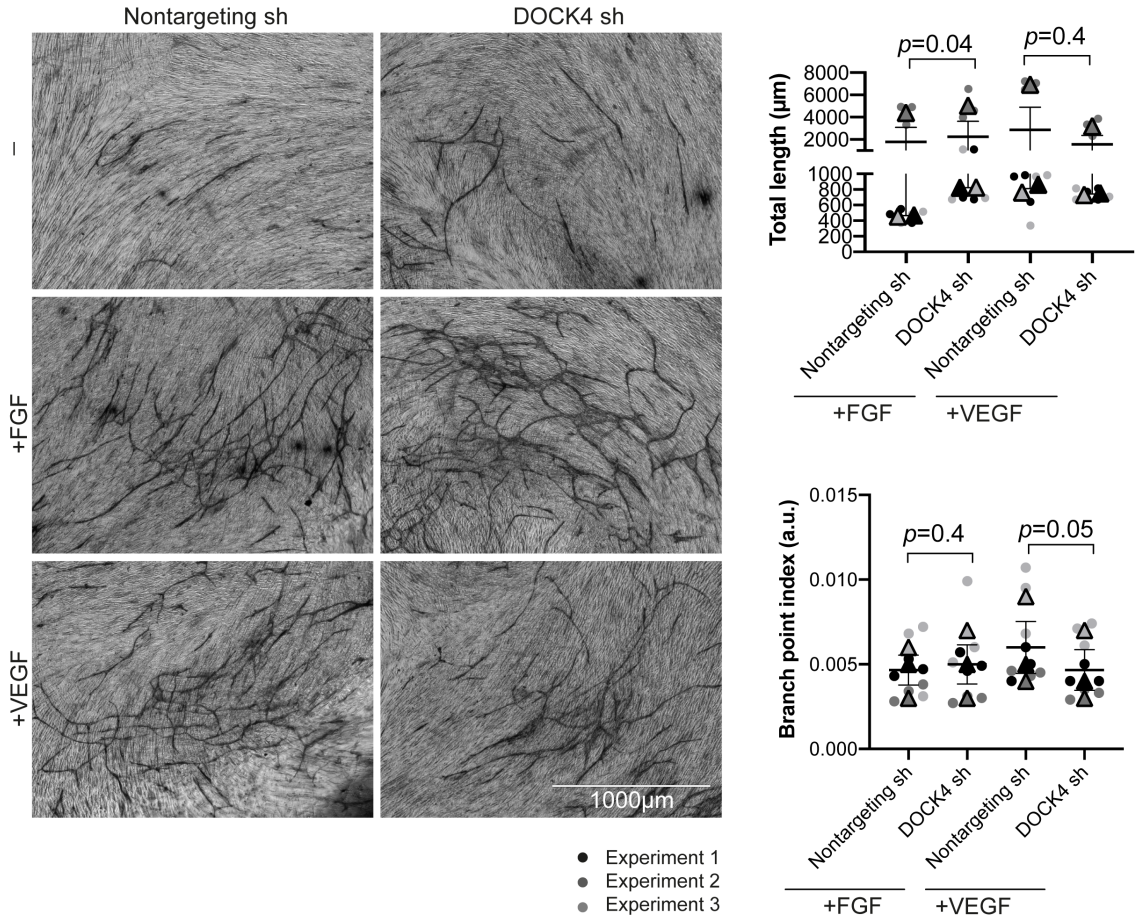

Figure 5.2 Effect of DOCK4 knockdown on tubule formation in the presence of FGF or VEGF.

Immunohistochemistry images show tubule formation in organotypic co-cultures of HDF with control HUVEC (Nontargeting sh), or HUVEC with DOCK4 knockdown (DOCK4 sh) with no added growth factors, or in the presence of bFGF (10ng/ml), or VEGFA (25ng/ml) 7 days after seeding onto confluent HDF. Growth factors were applied days two, four and six after seeding. Images taken using an EVOS microscope, 4X magnification. Scale bar, 1000µm. Dot plots show quantifications of total tubule length (µm) and branch point index (branches divided by total length) (a.u.). N=9 organotypic co-cultures from three independent experiments (indicated by different grey dots on the dot plot). Statistical test for pair-wise comparison is Student t-test.

5.4 DOCK4 influences tubule establishment under FGF and VEGF conditions

I set out to investigate how tubules and lumenisation are affected by DOCK4 knockdown 14 days after co-culture. Following growth factor treatment on days two, four and six after seeding of HUVEC onto HDF, the medium was switched to low growth factor for tubule establishment and lumen formation and assessed lumen formation on day 14 by immunofluorescence staining. First, I calculated total length and the trend of stimulation with DOCK4 knockdown under FGF condition was not significant, potentially because growth factor treatment stops after day 6 to allow lumen formation. Consistently with the earlier time points (Figure 5.3), the decrease in branch point index persisted on day 14 under conditions of VEGF stimulation. I noticed there was a significant increase in branch points with FGF stimulation suggesting that those may have formed from the process of anastomosis due to the stimulation of elongation with DOCK4 knockdown. Therefore, on day 14 there was still stimulation of total length, and additionally there was increased branch formation with DOCK4 knockdown under FGF stimulation. This shows that DOCK4 suppresses angiogenesis under conditions of FGF stimulation. Quantification of lumen formation on day 14 showed reduced lumen formation under conditions of VEGF stimulation with DOCK4 knockdown as previously shown (Abraham et al., 2015). There was high variability in lumen formation amongst different co-cultures under conditions of no growth factor (11μm) or FGF stimulation (17μm), and no significant difference between control (17μm) with DOCK4 knockdown under conditions of FGF stimulation (13μm). Altogether the data show that differences in the growth and patterning of tubules can still be observed under FGF and VEGF conditions with DOCK4 knockdown after 14 days of co-culture. Whilst under conditions of FGF stimulation DOCK4 knockdown increases tubule formation it does not stimulate lumen formation. Altogether, I conclude that there is more tubule formation during angiogenic sprouting suggesting that DOCK4 suppresses FGF driven angiogenesis but lumen formation is not affected by DOCK4 knockdown under conditions of FGF stimulation.

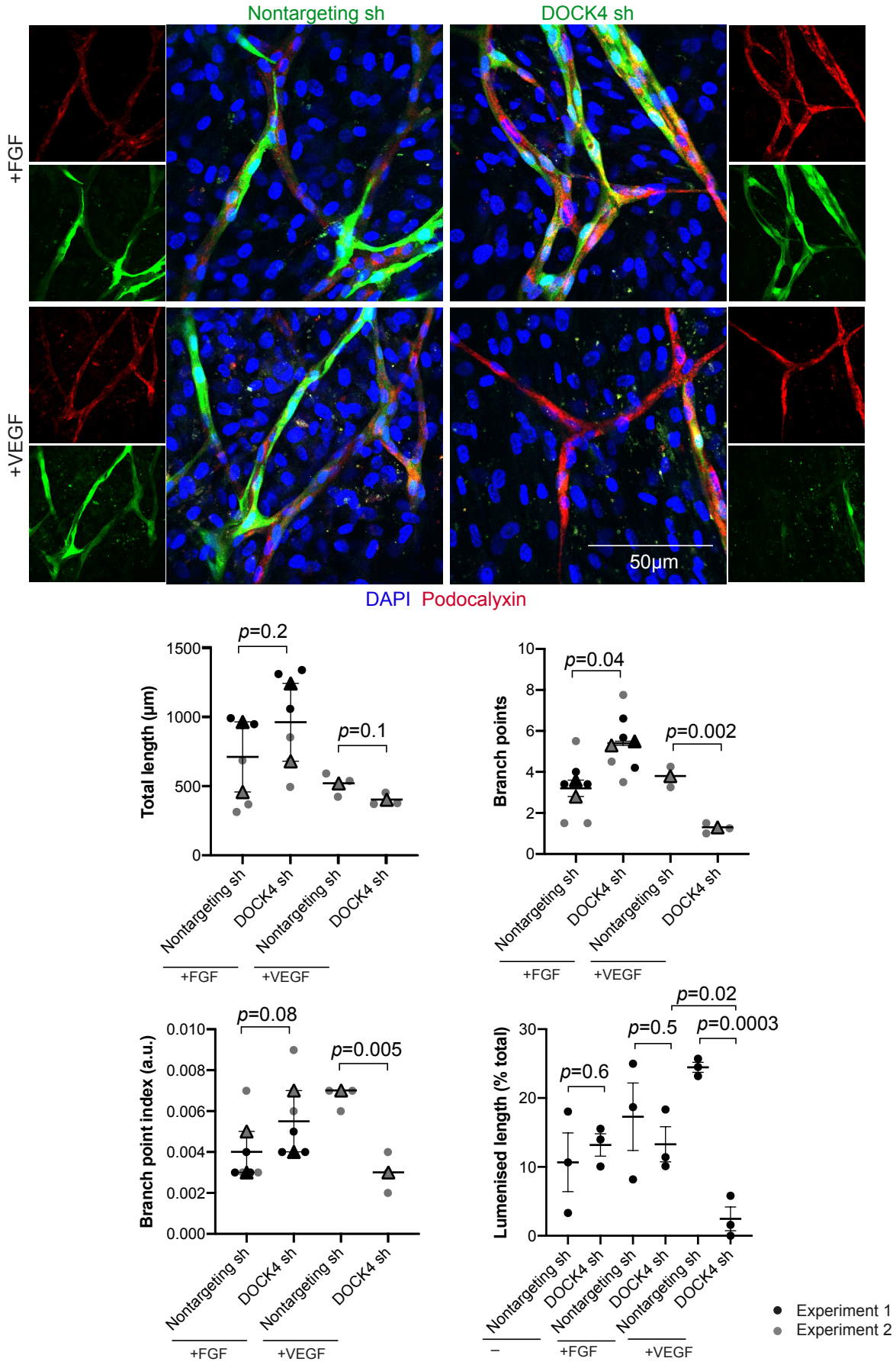
Nontargeting sh
DOCK4 sh
+FGF
+VEGF
50µm
DAPI Podocalyxin
Total length (µm)
p=0.2
p=0.1
Branch points
p=0.04
p=0.002
Branch point index (a.u.)
p=0.08
p=0.005
Lumenised length (% total)
p=0.6
p=0.5
p=0.02
p=0.0003
Nontargeting sh
DOCK4 sh
–
+FGF
+VEGF
Experiment 1
Experiment 2

Figure 5.3 Effect of DOCK4 knockdown on tube and lumen formation.
Immunofluorescence images show tube and lumen formation in organotypic co-culture of HDF with control HUVEC (Nontargeting sh), or HUVEC with DOCK4 knockdown (DOCK4 sh) with no added growth factors, or in the presence of bFGF (10ng/ml) or VEGFA (25ng/ml) 14 days after seeding onto confluent HDF. Growth factors were applied on days two, four and six after seeding. Images taken using a Nikon A1R confocal microscope, 40X magnification. Scale bar, 50μm. Green: HUVEC Nontargeting sh or DOCK4 sh, blue: DAPI and red: podocalyxin. Dot plots show quantifications of total length (μm), branch points, branch point index (branches divided by total length) (a.u.) and lumenised length (% total). The FGF stimulation data are from n=6 organotypic co-cultures of two independent experiments, the VEGF stimulation data are from n=3 organotypic co-cultures of one experiment (indicated by different grey dots on the dot plot). Statistical test for pair-wise comparison is Student t-test.

5.5 DOCK4 does not regulate lateral adhesions under conditions of FGF stimulation

Previously it was shown that the decrease in lumenised length with DOCK4 knockdown under conditions of VEGF stimulation was associated with a decrease in lateral cell-cell adhesions and the tubules under the VEGF conditions were thinner (Abraham et al., 2015). In addition to increasing tubule length FGF stimulation also appeared to promote lateral cell-cell adhesion. Therefore, to analyse this better, I quantified lateral cell-cell adhesion in the presence of FGF. As junctional staining was not easily quantifiable (previous work) I set out to quantify the number of nuclei per length, as I expected those would increase in the presence of more lateral cell-cell adhesions (Figure 5.4), although cell shape and length may also contribute to this read-out. Interestingly, FGF stimulation increased the number of nuclei per length (from 0.03u/μm to 0.04u/μm), however this was not affected by DOCK4 knockdown (0.04u/μm). On the other hand, there was a trend for decrease of nuclei per length (0.04u/μm to 0.03u/μm) suggesting

lower cell-cell adhesions with DOCK4 knockdown under conditions of VEGF stimulation.

The data suggest that stimulation with FGF increases lateral adhesion but does not stimulate lumen formation, whilst VEGF stimulation increases both lateral adhesion and lumen formation. Under conditions of VEGF stimulation DOCK4 knockdown appears to suppress formation of lateral adhesions, also suppresses lumen formation. Altogether the data show a trend for increase in nuclei per length and hence lateral adhesion with both growth factors, and decrease with DOCK4 knockdown under conditions of VEGF but not FGF stimulation. However, with the exception of stimulation with FGF the differences in nuclei per length are not statistically significant and therefore more experiments are necessary to conclude on the effects of growth factor stimulation and DOCK4 knockdown on lateral adhesions.

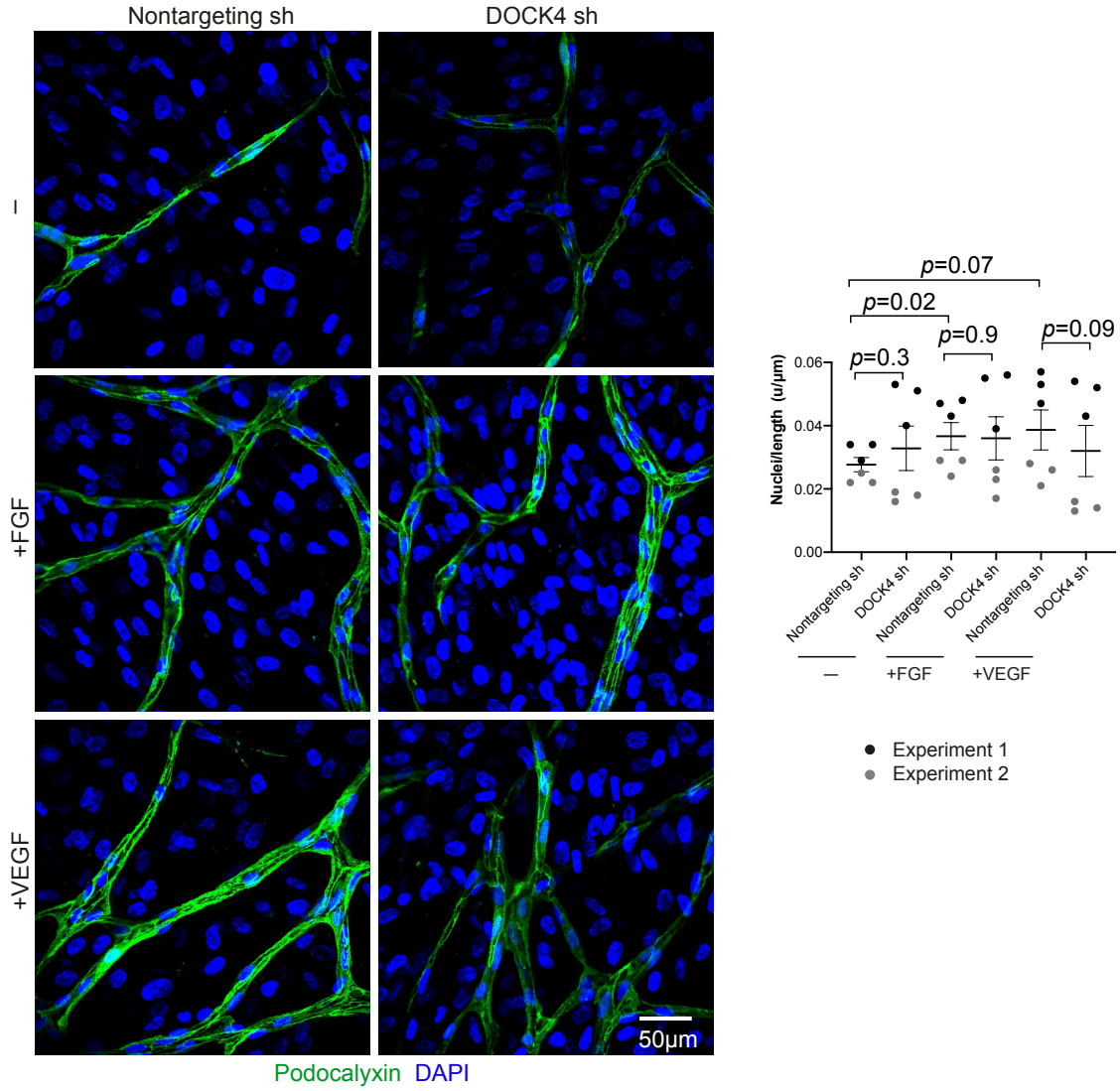

Figure 5.4 The effect of DOCK4 knockdown on lateral adhesion.

Immunofluorescence images show lateral adhesion in organotypic co-culture of HDF with control HUVEC (Nontargeting sh), or HUVEC with DOCK4 knockdown (DOCK4 sh) with no added growth factors, or in the presence of bFGF (10ng/ml) or VEGFA (25ng/ml) 14 days after seeding onto confluent HDF. Growth factors were applied on days two, four and six after seeding. Images taken using a Nikon A1R confocal microscope, 40X magnification. Scale bar, 50µm. Green: podocalyxin, blue: DAPI. Dot plots show quantifications of nuclei divided by length (u/µm). N=6 organotypic co-cultures from two independent experiments (indicated by different grey dots on the dot plot). Statistical test for pair-wise comparison is Student t-test.

5.6 Influence of HUVEC with DOCK4 knockdown on control HUVEC

In chapter 3, I observed that in the microfluidic device, additional cells that were integrated into the microchannels after initial tube formation, were influenced by the established tubes and followed their pattern. This suggested that endothelial cells and tubules influence each other via paracrine factors and/or by modifying the matrix. To investigate whether DOCK4 plays a role in this interaction, and to understand better how DOCK4 suppresses angiogenesis under FGF conditions but stimulates angiogenesis under VEGF conditions, I co-cultured control HUVEC expressing TurboRFP, with HUVEC stably expressing EGFP and control Nontargeting shRNA, or EGFP and DOCK*4* shRNA. The co-culture was assessed six days after adding the HUVEC onto confluent HDFs. As expected, DOCK4 knockdown stimulated tubule length and growth of EGFP cells under FGF conditions (from 456µm to 825µm). However, HUVEC-RFP control tubules were not influenced by DOCK4 knockdown. The data show that paracrine activity of HUVEC towards other HUVEC in the co-culture is independent of DOCK4 (Figure 5.5).

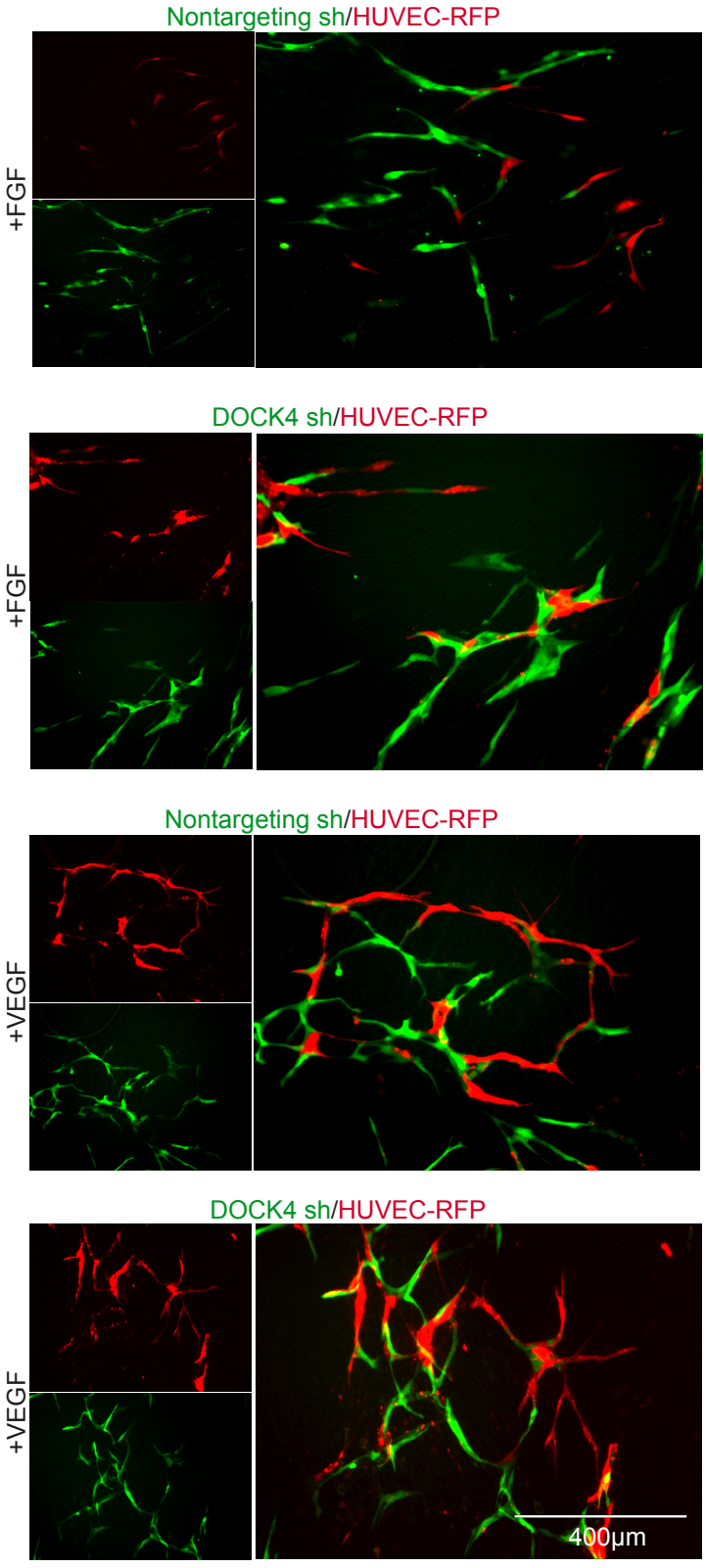
Nontargeting sh/HUVEC-RFP
+FGF
DOCK4 sh/HUVEC-RFP
+FGF
Nontargeting sh/HUVEC-RFP
+VEGF
DOCK4 sh/HUVEC-RFP
+VEGF
400μm

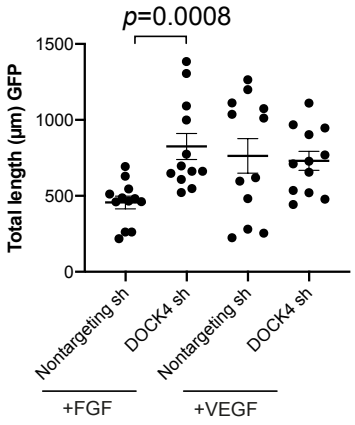
p=0.0008
Total length (μm) GFP
1500
1000
500
0
Nontargeting sh
DOCK4 sh
Nontargeting sh
DOCK4 sh
+FGF
+VEGF

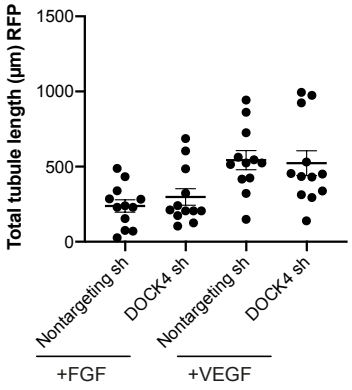
Total tubule length (μm) RFP
1500
1000
500
0
Nontargeting sh
DOCK4 sh
Nontargeting sh
DOCK4 sh
+FGF
+VEGF

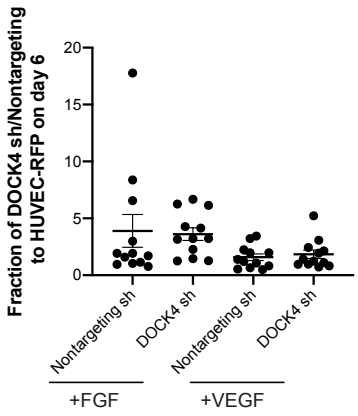
Fraction of DOCK4 sh/Nontargeting to HUVEC-RFP on day 6
20
15
10
5
0
Nontargeting sh
DOCK4 sh
Nontargeting sh
DOCK4 sh
+FGF
+VEGF

Figure 5.5 Tubules with DOCK4 knockdown do not influence newly forming HUVEC-RFP (control) tubules.

Images show tubule formation in organotypic co-cultures of HDF with a mixture of HUVEC-RFP and HUVEC EGFP either with Nontargeting shRNA, or DOCK4 shRNA in the presence of bFGF (10ng/ml), or VEGFA (25ng/ml) six days after seeding onto confluent HDF. Growth factors were applied days 2 and 4 after seeding. Images taken using an EVOS microscope, 10X magnification. Scale bar, 400μm. Green: HUVEC Nontargeting sh or DOCK4 sh, red: HUVEC-RFP. Dot plots show quantifications of total tubule length of HUVEC-RFP (μm), total tubule length of HUVEC-EGFP (μm), and fraction of HUVEC Nontargeting sh, or HUVEC DOCK4 sh to HUVEC-RFP. N=3 organotypic co-culture from one experiment (the data are from twelve images indicated by black dots on the dot plot). Statistical test for unpair-wise comparison is Student t-test.

5.7 DOCK4 suppresses EC proliferation under FGF stimulation conditions

As it was concluded that DOCK4 suppresses angiogenesis specifically in the presence of FGF, I hypothesized that it may act as suppressor of endothelial cell proliferation under conditions of FGF but not VEGF stimulation. Endothelial cell proliferation was assessed in order to begin to understand how DOCK4 suppresses angiogenesis in FGF conditions but stimulates angiogenesis in the presence of VEGF. Ki67 was used as a proliferation marker on day 6 after seeding HUVEC onto confluent HDF in order to quantify the fraction of proliferating with DOCK4 shRNA and Nontargeting shRNA. As the available Ki67 antibody was conjugated to RFP, it was possible to determine proliferation in the EGFP expressing tubules. Following staining with Ki67, quantification of Ki67 expressing cells showed significant stimulation of proliferation with DOCK4 knockdown in FGF but not in VEGF conditions, consistent with the suppression in the presence of FGF (Figure 5.6).

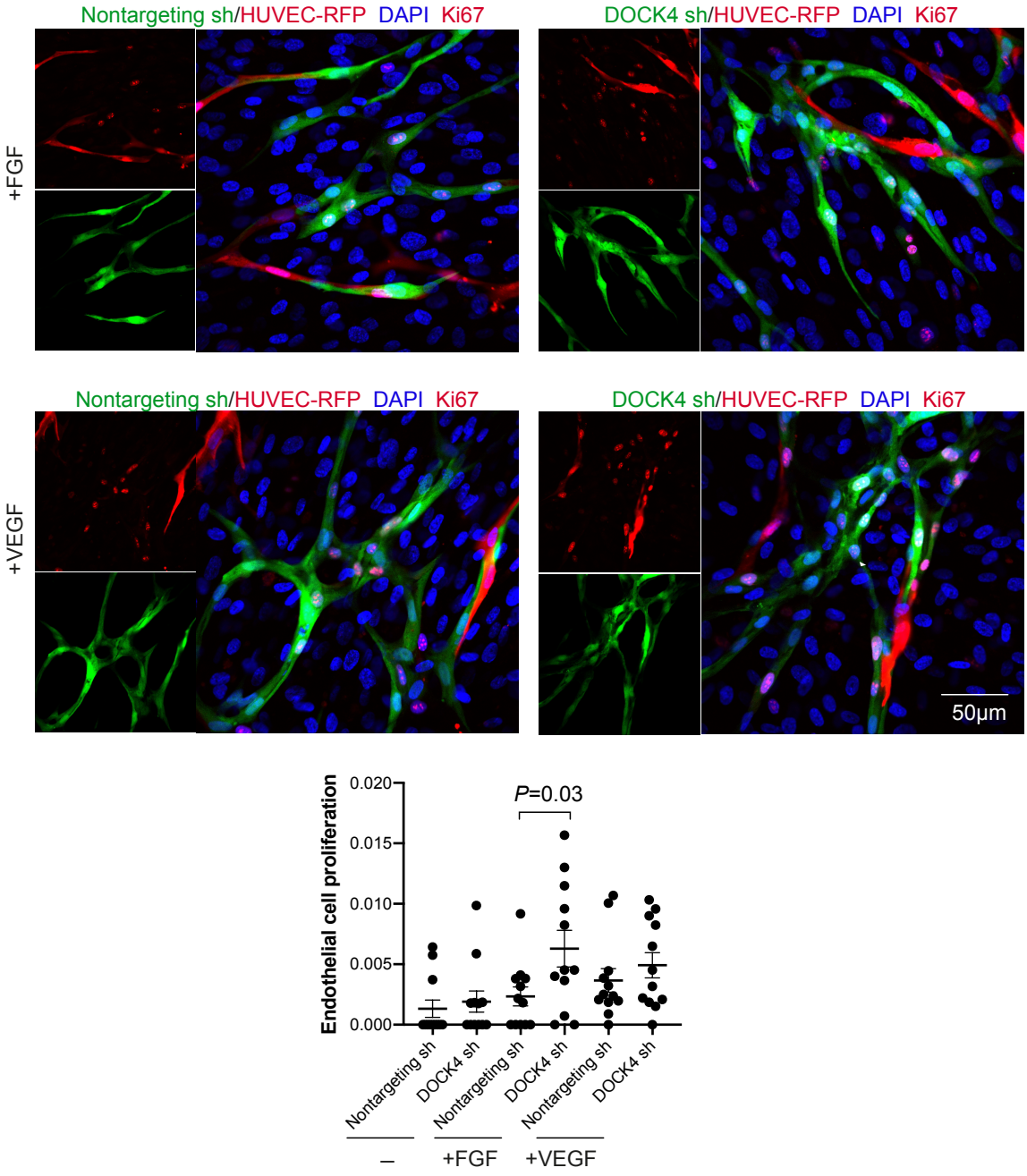

Figure 5.6 DOCK4 knockdown stimulates endothelial cells proliferation in tubules under FGF conditions.

Immunofluorescence images show proliferation in organotypic co-cultures of HDF and HUVEC-RFP with control HUVEC (Nontargeting sh), or HUVEC with DOCK4 knockdown (DOCK4 sh) in the presence of bFGF (10ng/ml), or VEGFA (25ng/ml) 6 days after seeding onto confluent HDF. Growth factors were applied on days 2 and 4 after seeding. Images taken using a Nikon A1R confocal microscope, 40X magnification. Scale bar, 50μm. Green: HUVEC Nontargeting sh or DOCK4 sh, red: Ki67 and HUVEC-RFP, blue: DAPI. Dot plot shows

quantifications of proliferation of HUVEC Nontargeting sh, and HUVEC DOCK4 sh. N=3 organotypic co-cultures from one experiment (the data are from twelve images indicated by black dots on the dot plot). Statistical test for unpair-wise comparison is Student t-test.

5.8 DOCK4 stimulates cilia incidence and suppresses tubule formation under FGF conditions

As primary cilia are post-mitotic cellular organelles and most of cells assemble their cilia in response to cellular quiescence, it was hypothesized that cilia incidence would decrease with DOCK4 knockdown and subsequent increase in proliferation. To find out how ciliary length and incidence change with DOCK4 knockdown in HUVEC and under FGF conditions, cilia were assessed in control conditions without added growth factors, under FGF conditions with and without DOCK4 knockdown. For this purpose, HUVEC were added to the confluent layer of HDF, FGF (10ng/ml) added on day two, four and six, and the organotypic co-cultures were fixed and stained with cilia markers on day 7. The results show in the absence of added FGF there are more cilia and longer ciliary length, compared to the no GF conditions with more quiescent cells, that confirm stimulation of proliferation with added FGF (Figure 5.7). Under FGF conditions DOCK4 knockdown decreased cilia incidence, consistent with the increase in endothelial cell proliferation and stimulation of angiogenesis that shown in Figure 5.6, Figure 5.3 and Figure 5.2.

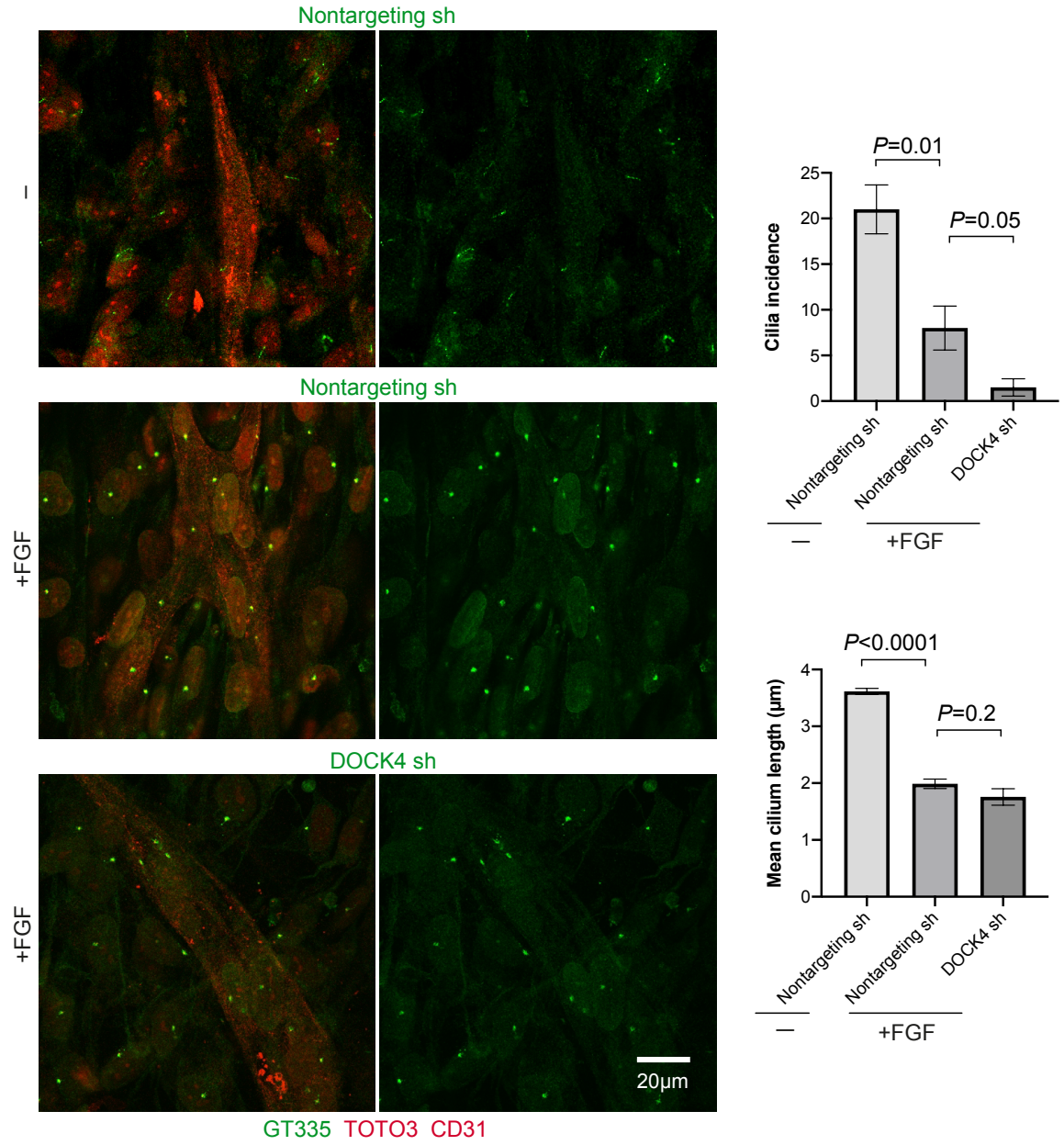

Figure 5.7 Effect of DOCK4 knockdown on cilia.

Immunofluorescence images show cilia in organotypic co-cultures of HDF and control HUVEC (Nontargeting sh), or HUVEC with DOCK4 knockdown (DOCK4 sh) in the presence of bFGF (10ng/ml) 7 days after seeding onto confluent HDF. FGF was applied on days two, four and six after seeding. Images taken using a Nikon A1R confocal microscope, 40X magnification. Scale bar, 20μm. Green: HUVEC Nontargeting sh or DOCK4 sh and GT335, red: TOTO3 and CD31. Bar graphs show quantifications of cilia incidence as the proportion of cells with a primary cilium >2μm in length and mean cilium length (μm). N=3 organotypic co-

cultures from one experiment (indicated by different grey bars on the bar plot). Statistical test for unpair-wise comparison is Student t-test.

5.9 Effect of DOCK4 knockdown on tubule and lumen formation under conditions of flow

In order to assess how angiogenesis is affected by DOCK4 knockdown in the presence of fluid flow, HDF with control HUVEC or HUVEC with DOCK4 knockdown in fibrin were added to single chamber microfluidic devices and media were changed every 24 hours. Tubule formation was assessed nine days after seeding the cells. Result shows presence of DOCK4 stimulate tubule formation, lumen formation and angiogenesis when there is fluid flow inside and around the tubules. Total length and lumen formation were significantly decreased by DOCK4 knockdown under conditions of flow (Figure 5.8).

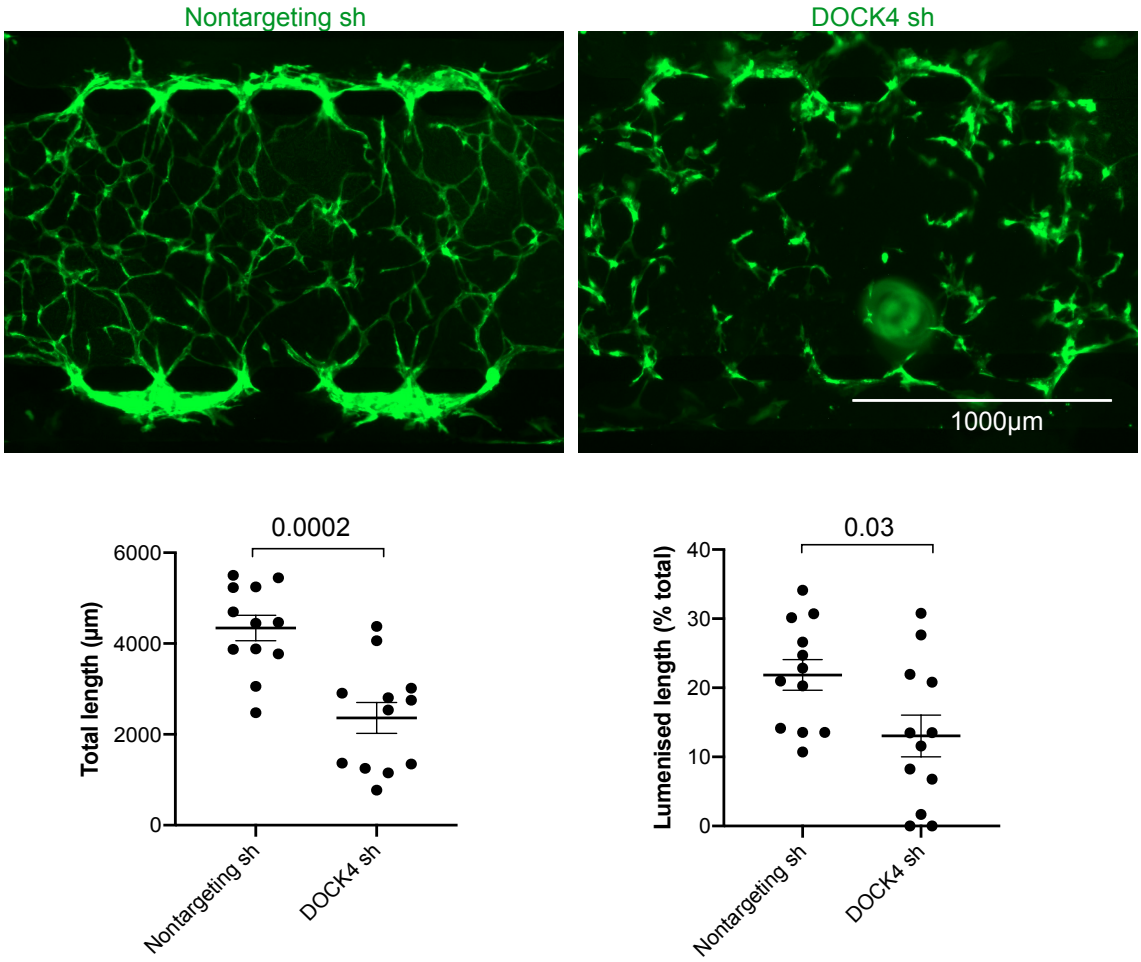

Figure 5.8 Effect of DOCK4 knockdown on tubule formation and lumenised length under condition of flow.

Fluorescence images show tubule formation in organotypic co-culture of HDF with control HUVEC (Nontargeting sh), or HUVEC with DOCK4 knockdown (DOCK4 sh) nine days after seeding in a single-chamber device. Images taken by an EVOS microscope, 4X. Scale bar, 1000µm. Green: HUVEC-EGFP. Dot plot shows total length (µm) and lumenised length (% total). The data are from 12 channel squares of n=1 experiment (indicated by black dots on the dot plot). Statistical test for unpair-wise comparison is Student t-test.

5.10 Discussion

Blood vessel formation is vital for organs function during development and in adulthood. A better understanding of the vascular vessel formation and the mechanisms that underpin this process is crucial in order to be able to intervene in pathophysiological conditions of abnormal blood vessel development. Blood vessel tube formation demands intricate dynamic changes of the endothelial cell actin cytoskeleton controlled by the Rho family of small GTPases (Barlow & Cleaver, 2019). Rho GTPases are known to be involved in various cellular functions consist of controlling the actin cytoskeleton and cell shape changes which are crucial steps in the vascular tube formation. Guanine nucleotide exchange factors (GEFs) activate GTPases, and understanding the role of individual GEFs during angiogenesis is imperative.

DOCK4, a Rac1 GEF, is a regulator of lumen formation (Abraham et al., 2015). Whilst the studies show that DOCK4 operates downstream of VEGF signalling to control filopodia formation and sprouting, it's potential role downstream of FGF signalling has not been investigated. Therefore, to expand upon the understanding of DOCK4 function within angiogenesis, in this chapter DOCK4 signalling was investigated and I have shown that under conditions of FGF stimulation: (i) DOCK4 suppresses angiogenesis but lumen formation is not affected by DOCK4 knockdown; (ii) DOCK4 is not a regulator of lateral adhesions; (iii) DOCK4 suppress proliferation and therefore stimulates cilia incidence. Moreover, iv) the paracrine activity of HUVEC towards other ECs is independent of DOCK4.

The organotypic co-culture of HUVEC with HDF in the co-culture assay is an ideal method to observe the effect of DOCK4 on tubule morphogenesis as it provides the opportunity to investigate different stages of tubule growth. This method of organotypic co-culture (Abraham et al., 2015) was used as an *in vitro* model for this study on a culture plate (2D) and in the microfluidic device (3D) with fluid flow around and inside tubes as described in chapter 3. For vascular tubules to develop in the co-culture system, growth factors are added to stimulate growth up to day seven after seeding HUVEC onto confluent fibroblasts, after which time

formation of tubes with lumen requires a period of lack of stimulation with growth factors. Therefore, FGF only was added to the co-culture for seven days and then effect of DOCK4 knockdown was observed on either day 7 or day 14 after seeding. Tubules go through multiple stages of angiogenic growth and tubule morphogenesis as described in (Figure 3.1 B) with sprouting observed by IHC using CD31 staining on day 7 (Hetheridge et al., 2011) (Figure 5.2), and lumen formation detected by IF using podocalyxin staining on day 14 (lumenised length, Figure 5.3).

The two pro-angiogenic growth factors FGF and VEGF establish various phenotypical blood vessel growth responses throughout angiogenesis (Stewart, L., PhD Thesis). DOCK4 was previously described to be necessary for stimulation of angiogenesis under VEGF conditions (Abraham et al., 2015). Surprisingly, I found that DOCK4 is suppressor of FGF driven angiogenesis. Furthermore, whilst there was a decrease in lumenised length with DOCK4 knockdown under VEGF conditions, there was no significant difference in lumenised length with DOCK4 knockdown under FGF conditions (Figure 5.3).

Studies show that lateral adhesions between endothelial cells precedes the opening of a lumen as shown by the apical localization of podocalyxin (Abraham et al., 2015). FGF and VEGF may stimulate lateral adhesion in different ways. However, the increase in FGF driven lateral adhesions does not appear associated with increase in lumen formation under FGF conditions (Figure 5.3). On the other hand, there was trend for increase of both lateral adhesion and lumenised length with VEGF stimulation. It appears that DOCK4 may be necessary only for lateral adhesion under condition of VEGF but not FGF stimulation. These results show that DOCK4 does not regulate lateral adhesion and is not required for lumen formation under conditions of FGF stimulation. This needs to be further confirmed in repeat experiments to conclude and obtain statistical significance.

Altogether, the results presented in this chapter show a different role of DOCK4 in FGF compared to VEGF driven angiogenesis. Although DOCK4 stimulates angiogenesis under VEGF conditions, it suppresses FGF driven angiogenesis.

Chapter 6

Discussion

6.1 Introduction

Angiogenesis requires rearrangement of intercellular junctions, acquisition of tip cell morphology, extension of filopodial protrusions and migration of endothelial cells to form new blood vessels. Dynamic alterations of the endothelial cell actin cytoskeleton are required for all of these processes (Abraham et al., 2015). Complex regulation of the actin machinery via actin nucleation, extension and branching orchestrated by the Rho family of small GTPases activated by numerous angiogenic stimuli is required for the alterations in endothelial cell shape during sprouting and migration. However, how endothelial cells sense and transmit biomechanical stimuli is still only partially understood.

In this study, I established a 3D cell culture perfused system of endothelial cells in the microfluidic device that can be used as a new vascular model and can be applied in angiogenesis, vascular disease, cancer research, and drug development screening.

At the start of this project it was not understood whether the Rac1 GEF DOCK4 operated downstream of FGF signalling and whether DOCK4, and if ROCK or cilia have an effect on blood vessel lumen formation and expansion under conditions of flow. In this thesis I show that although DOCK4 operates downstream of VEGF to stimulate proliferation and sprouting, it acts as an angiogenic suppressor in the presence of FGF. Furthermore, ROCK which has been shown to be a key regulator of ciliogenesis, is necessary for lumen formation under conditions of fluid flow. I have shown that cilia which are mechanosensors of fluid flow are necessary for lumen formation and lumen expansion.

6.2 Forming a closed circulatory system of perfused endothelial tubes in the microfluidic device

The primary function of the circulatory system is respiratory gas exchange and delivery of nutrients and hormones to cells. Respiratory gas exchange needs transit time which is low enough to allow equilibration of oxygen and carbon dioxide concentrations, and high enough to inhibit clot formation by maintaining shear rates. Natural blood shear rates and velocities in human capillaries range from 100 to 500 s^{-1} and 500 to 1500μm/s, respectively depending on different elements such as the specific tissue physiology, metabolic demand and haematocrit (Hathcock, 2006) 424). The flow system developed in the microfluidic device not only establishes interstitial flow during tubule formation, but also provides force for fluid flow necessary for tube development and lumen expansion. By changing the height of medium in the media reservoirs in the single chamber device a wide range of shear stress can be provided and velocities that represent the normal physiologic range.

Hence, the single chamber device has the ability to establish different flow rates with changing the amount of media in reservoirs and as a result changes in hydrostatic pressure that makes this system a useful tool to test vasculature development in physiological and pathological conditions characterized by changed interstitial flow, including wound healing, tumour development, and exercise. Previous studies have shown that cells in a 3D matrix respond to interstitial shear stress via membrane-bound receptors (Z. D. Shi et al., 2011). Despite the interstitial flow rate of fluid flow passing throughout spaces between pillars into tubes in the microchamber being variable, an interconnected vasculature developed under different conditions. After 14 days different vessel densities and diameter was observed within the single chamber. This microfluidic device due to having 10 pillars that provide 12 pores for entrance of fluid flow and perfusion within the tubules, establishes multiple tubes with larger diameter at the sides compare to the middle part of the chamber. This hierarchy resembles physiological blood vessel development, and it allows different calibre tube to be analysed in the same time. The hierarchy of the endothelial tubes inside the microfluidic device resembles the arteries and venules in the human body, as

tubes forming at the sides of the chamber where fluid enters with higher shear stress are up to 100μm in diameter, whilst tubes in middle of the chamber where there is lower shear stress are 8-15μm in diameter.

Interestingly, although formation of a network of tubes was observed everywhere within the single chamber, those on the side of the chamber exposed to a supraphysiological flow, showed higher perfusion network and anastomosis with endothelial cells in the microfluidic channel. This shows parallels with the observations by le Noble et al. (2008) that fluid flow drives vessels to fuse to produce large arteries and veins. Furthermore, interstitial flow is necessary for filtration, and pathophysiological alterations of this flow can cause a vasculature remodelling response. Previous studies have demonstrated increase in interstitial flow of 4-10μm/s in a matrix can stimulate TGF-β_1 production and drive the differentiation of fibroblasts to myofibroblasts and rise in production of collagen (Ng & Swartz, 2003) (Ng et al., 2005). In my model, elevated interstitial flow may stimulate migration of endothelial cells towards the pores between the pillars thus forming tubes with higher diameter and stimulating anastomosis. Alternatively, faster vasculature development and expansion could be due to exposure of the cells to a higher interstitial flow, and as a result increased mass transport through convection of nutrients (Hsu et al., 2013).

My experimental protocol focused on manipulating the endothelial cells and observing the effects of cilia and cytoskeletal regulators on tubule formation and lumen expansion in perfused tubes. However, the same approach can be utilised to regulate and determine additional variables related to the tissue microenvironment, such as: nutrient and growth factor concentration, pH, oxygen tension, and waste products. Moreover, the system can be used to establish optimal conditions for vasculature growth or cell proliferation in the tissue microenvironment, or screening of different drugs and at varying concentrations.

Drugs can be potentially absorbed by the microcirculation and can either influence the microvascular system directly, or can be transferred to a distant site. In the same way, tumour cells as it was shown can either stay inside the

vasculature or adhere to the vasculature wall and extravasate to a targeted organ. Hence, the ability to monitor drugs or toxins, to determine vascular permeability, or to understand the direct effects of chemicals on the microcirculation is massively important in understanding the integrated effect of an individual compound. Moreover, for all established micro-physiological systems that recapitulate complicated and metabolically demanding organ functions, such organoids and tumours on-chip a functional vasculature is needed in to supply with nutrients and to remove waste products. Furthermore, filtration requires a semi-permeable vessel wall that can retain large proteins. Capillaries normally retain proteins bigger than 70kDa (Enis et al., 2005) which is consistent with the forming tubules filtration in my microfluidic device. In my model I used 70kDa fluorescent dextran to test if they are retained inside the tubes. First, the dextran was stuck inside the forming tubules and after few minutes extravasated from the vessel wall.

In addition to all of these applications, my work demonstrates that many different traits of angiogenic blood vessels can be observed in this device; for example, observing intussusceptive angiogenesis and formation of pillars. Intussusceptive pillars form initially by changes in blood flow (Burri et al., 2004) and their extension depends on intravascular fluid flow (Mentzer & Konerding, 2014). Interestingly, I observed pillar-like structures forming in the tubes in a process akin to intussusceptive angiogenesis (Figure 3.15). That could be as a result of alteration in fluid flow within the perfusable tubes, because in my model shear stress is reduced with time after filling the reservoirs due to the decrease in hydrostatic pressure, which is then re-established when the reservoirs are re-filled. Despite the many different model systems of angiogenesis available, there are currently no reliable histologic markers or convincing *in vitro* models of intussusceptive pillars (Mentzer & Konerding, 2014). Further characterisation of my system for example by RNA sequencing analysis of micro-dissected tubes with pillars could provide potential markers of intussusceptive angiogenesis that may be tested *in vivo,* thus validating intussusceptive angiogenesis in the microfluidic model.

The exact cellular mechanisms of contribution of incoming ECs to vascularisation are unknown. In this study, ECs added to an established network in the microfluidic system were marked with a fluorescent marker which made it possible to observe how incoming endothelial cells communicate and interact with established tubes under conditions of flow. In the same way as adult vasculogenesis during capillary formation post ischemia (Asahara et al., 1997), or in tumours (Bussolati et al., 2011) when EC progenitors are mobilised from the bone marrow and contribute to vascular formation, in this system endothelial cells were injected into a device containing pre-formed endothelial tubes. I showed that incoming ECs can contribute in tubule development by interacting with ECs in pre-established tubes, and cooperate in the process of angiogenesis, lateral adhesion and lumen formation.

In the process of EC interaction inside the microfluidic device, there is retraction that resembles pruning in pre-established vessels (Korn & Augustin, 2015), and incoming cells appear to follow the tracks of empty sleeves (Brown, 2010) and generate the tubules along those pre-existing passes. Strikingly, ECs added to the microfluidic channels can also be found inside the pre-established tubes from where they integrate within the vessel wall (Figure 3.18) and (Figure 3.20). All these processes can be investigated further and analysed in detail in future studies employing the microfluidic device.

6.3 Role of cilia and ROCK in lumen formation and expansion

The establishment of a functional vasculature features complex cellular mechanisms including rearrangement of cellular junctions to pattern ECs into vessels and to form venous and arterial hierarchies. The first step in the formation of perfusable blood vessels is tubulogenesis that can take place in the absence of flow (Y. Wang et al., 2010). The next step is the process of blood vessel morphogenesis, including lumen formation, which is essential for the transformation of cords into a tube that is perfusable. Lumen expansion and maturation that allows formation of perfusable system of blood vessels takes

place after conditions of fluid flow (Herwig et al., 2011) (Lenard et al., 2013). Alteration in blood flow or velocity has various effects on ECs, causing changes in vasculature phenotypes and functions, a process known as hemodynamic stimulation (Chistiakov et al., 2017). It is believed that primary cilia, which extend into the vascular EC lumen, act as fluid flow sensors that transmit extracellular signals into the cell (R. Pala et al., 2017) and make changes in the orientation and positions of ECs. Therefore, cilia have been proposed to be regulators of lumen formation and lumen expansion by mechanosensing of blood flow (Ernandez et al., 2017).

It is thought that endothelial membrane biosensors sense chemical and mechanical signals in the blood and transduce them into intracellular signalling cascades. These then regulate cellular processes that include ion transport, cell proliferation, gene expression and cell death. Moreover, the primary cilium is known to be a biosensor of shear stress (Atkinson et al., 2019). To substantiate this observation, I used microfluidic device to form a closed circulatory system of endothelial cells that are perfusable and to ascertain the possible role of primary cilia in mechanotransduction of flow and its effect on lumen formation. The hypothesis of mechanosensing of blood flow by cilia arises from the fact that primary cilia have been already implicated in sensing of the chemical cues and the mechanical forces (Masyuk et al., 2006) (Kwon et al., 2010) (Jin et al., 2014) (K. L. Lee et al., 2015). For example, primary cilia sense the microenvironment in the *Caenorhabditis elegans* nervous system and are required for chemosensation (Bae & Barr, 2008). Epithelial cells that line the renal collecting duct display primary cilia (Ernandez et al., 2017) and loss of primary cilia in the choroid plexus results in autocrine signalling defects and mis-regulation in production of CSF (Narita et al., 2010).

In this current study, it has been shown that cilia affect angiogenesis both in the absence and the presence of blood flow. The purpose of this study has been to investigate the role of cilia on tubule formation in the absence of fluid flow, and the effect of conditional ablation of cilia on lumen formation and lumen expansion under conditions of flow in the closed circulatory system of perfusable tubes. Interestingly, primary cilia on ECs appear in early stages of angiogenesis when

there is no fluid flow and many crucial changes throughout vascular morphogenesis happen independently of fluid flow (Eisa-Beygi et al., 2018). This suggests that the role of primary cilia in early stages can be different from their roles in regulating vasculature by flow sensing. However, the enrichment of primary cilia situated on the sides of the budding intravascular spaces that form the boundaries of angiogenic capillaries suggests that primary cilia have a fundamental role during endothelial lumen formation (Eisa-Beygi et al., 2018). In this current study, cilia were knocked down in ECs using an inducible shRNA system, and tubules were formed by co-culture of ECs with fibroblasts in the absence of fluid flow to mimic the early stages of angiogenesis. I showed that cilia control tubule formation in early stages without fluid flow in the *in vitro* 2D system, and total tubule formation was decreased in the absence of cilia.

Gebala et al. (2016) showed that flow forces expand a provisional vessel lumen through deformations of the endothelial apical membrane, resulting in actomyosin recruitment and contraction. An *in vivo* study by J. G. Goetz et al. (2014) using zebrafish has shown that primary cilia of ECs sense haemodynamic forces and affect EC remodelling. An additional study showed that primary cilia can also control the directional migration and barrier integrity of ECs through actin cytoskeletal organization (T. J. Jones et al., 2012) (Ma & Zhou, 2020). To test the effect of cilia on lumen formation and lumen expansion due to sensing blood flow, I tested tube formation following conditional ablation of primary cilia in ECs under conditions of flow, and then observed the process of lumen formation and lumen expansion. I showed that cilia regulate tubule and lumen formation and, more importantly, lumen expansion under conditions of fluid flow in the microfluidic device.

The involvement of cilia in regulating lumen formation and lumen expansion under conditions of flow is poorly understood. In order to investigate it further and visualise cilia in endothelial cells and to have the ability to track movement and alteration in the shape of cilia, I made a construct of HTR6-CFP2 that enables live-cell imaging of EC cilia. However, due to the limited size of stages on all available inverted microscopes, I was unable to do live-cell imaging of the

microfluidic device with attached reservoirs, in order to visualise cilia during flow sensing. An appropriate microscope is needed for this purpose in future studies.

Cellular and molecular mechanisms underlying the cilia mechanosensing of blood flow remain elusive. IFT proteins are crucial for formation and maintenance of cilia (Huangfu et al., 2003) (Huangfu & Anderson, 2005) and mutations in IFT88 results in either absent or very shortened cilia (Bay & Caspary, 2012). This study showed that IFT88 knockdown and as a result cilia loss supressed lumen formation and lumen expansion. It has been shown that cilia regulate sonic hedgehog (Shh) and Wnt/beta-Catenin signalling (Haycraft et al., 2005) (Corbit et al., 2008) and IFT88 transports proteins such as Hedgehog (HH) and Wnt signalling components during cilium-related signalling (S. C. Goetz & Anderson, 2010). The regulatory mechanism of lumen formation and lumen expansion by cilia could be related to Shh signalling pathway and transportation of mediators by IFT88. Shh is known to be controlled by cilia and loss of cilia is associated with decreased Shh signalling (Bangs & Anderson, 2017) which is consistent with the known effect of Shh signalling on promotion of blood vessel development, maturity and integrity (Kusano et al., 2004) (Chapouly et al., 2019). Shh signalling promotes SMC proliferation (H. Li et al., 2012) (Morrow et al., 2007) and survival (Sicklick et al., 2005) (Morrow et al., 2007) (G. Wang et al., 2010), whereas decreased expression of Shh caused pericyte loss and increased capillary permeability (H. Huang et al., 2015). Therefore, cilium defects may cause defective mural cell recruitment, including pericytes and smooth muscle cells, leading to the impairment of angiogenesis. Furthermore, Shh signalling has been shown to play a role in pathological angiogenesis in cancer and ischemia (Pola et al., 2003) and to control vascular maturation (Lawson et al., 2002). It also promotes vascular integrity via maintenance of intracellular junctions of ECs at the BBB (Alvarez et al., 2011) and in peripheral tissues (Caradu et al., 2018). Furthermore, a study in zebrafish showed that when there are cilia defects due to perturbed Shh signalling, this is associated with intracranial haemorrhage. Conversely, the risk of cerebral haemorrhage decreased following activation of Shh signalling (Kallakuri et al., 2015). In summary, these observations show that primary cilia in ECs may regulate blood vessel integrity via the Shh signalling pathway.

Since cilia affect angiogenesis in the absence of flow, Shh signalling can also be a regulator of tube formation in the absence of fluid flow. Studies have shown that during the early stages of vasculature tubulogenesis Shh signalling is required for angioblast assembly and tube formation during development of the aorta (Vokes et al., 2004) and in the yolk sac (Byrd et al., 2002). Shh signalling also has a role in embryonic angiogenesis (Pola et al., 2003). Therefore, mechanosensation by primary cilia during early stages of angiogenesis could also be regulated by Shh signalling.

Cilia deflection *in vivo* increases with increasing fluid flow, and this has been suggested to correlate with increased intracellular calcium levels in the ECs (J. G. Goetz et al., 2014). Furthermore, dynamic regulation of cilium length is interlinked with cellular calcium flux (Besschetnova et al., 2010). Endothelial cilia control vascular function via calcium and NO signalling (Nauli et al., 2008). Therefore, these studies suggest that decreased lumen formation and lumen expansion as a result of cilia loss may be due to altered calcium flux in endothelial cells. A number of studies have demonstrated that shear stress of fluid flow triggers ciliary calcium signalling (Jin et al., 2014), and therefore one of the mechanisms that mediates the transduction of flow by cilia could be calcium level which can be affected in response to flow.

Several cellular processes associated with EC migration such as stress fibre rearrangement, actomyosin contraction and focal adhesion formation (Lamalice et al., 2007) are regulated by ROCK (Liu et al., 2018). ROCK is a downstream effector of the small GTPase RhoA and can affect both cilia and the endothelial cytoskeleton (Ridley & Hall, 1992). Defects of the actin cytoskeleton seem to cause many of the cellular phenotypes observed in ciliopathies (Valente et al., 2010) (M. Adams et al., 2012) (Hernandez-Hernandez et al., 2013). Therefore, the effect of cilia ablation on lumen formation could be mediated through cytoskeletal changes mediated by ROCK.

Previous work in our lab by Dr Gary Grant showed that using a ROCK inhibitor (Y-27632) increased cilium length in hTERT-RPE1 and endothelial cells (Grant,

G., PhD Thesis) (Kakiuchi et al., 2019). Furthermore, in a whole genome siRNA-based reverse genetics screens in the Johnson lab, ROCK2 was identified as the strongest positive regulator of cilia formation (Wheway et al., 2015). Therefore, effects of ROCK inhibition on tubule and lumen formation could be due to deregulation of cilia. To test this further, I used ROCK inhibition at different stages of lumen formation and observed results on days 8,12 and 16. The results showed defects in lumen formation with ROCK inhibition similar to the results observed with inducible cilia ablation. Consistent with this notion delocalised cilia and haemorrhages were observed in cerebral blood vessels in ROCK2 knockout embryos (Grant, G., PhD Thesis).

6.4 DOCK4 suppresses angiogenesis downstream of FGF signalling

VEGF stimulates key events of the angiogenic process including endothelial cell survival, proliferation and migration. VEGF signalling to Rho GTPases results in actin polymerization and formation of stress fibers and filopodial protrusions, and recruitment of vinculin to ventral plaques (Rousseau et al., 1997) (Rousseau et al., 2000). Previous work in our laboratory in a heterozygous DOCK4 depleted murine model of hindlimb ischemia has shown that DOCK4 knockdown stimulates angiogenesis in the lower limb but inhibits reperfusion (Stewart, L., PhD Thesis). Both VEGF and FGF have been shown to drive angiogenesis in limb ischemia (Stewart, L., PhD Thesis). FGF stimulates the angiogenic phenotype including enhancement of endothelial cell proliferation, migration and expression of specific integrins (Moscatelli et al., 1986) (Klein et al., 1993) (Klein et al., 1996). As DOCK4 was previously shown by this group to be necessary for VEGF driven filopodial protrusions and sprouting angiogenesis I investigated how DOCK4 influences angiogenesis driven by FGF.

Angiogenesis can occur through elongation or sprouting of developing endothelial tubules both of which necessitate migration of a leading cell called the tip cell (Gerhardt et al., 2003). Migration of ECs is driven by actin polymerization with broad lamellipodia and filopodia at the leading edge

extending and being stabilized by extracellular matrix adhesions. Fundamental regulators of the actin cytoskeleton are members of the Rho family of small GTPases that cycle between active GTP- and inactive GDP-bound states controlled by GEFs and GAPs. Particularly, RAC1 activation is essential for EC lamellipodia and filopodial extensions (Abraham et al., 2015). Expression of DOCK4 stimulates RAC1 activation in cells (Lu et al., 2005) (Yan et al., 2006). In addition to lamellipodia and filopodia RAC activity is essential for the formation of endothelial cell-cell contacts (Fukata & Kaibuchi, 2001) (Sakisaka & Takai, 2004). During angiogenesis, signalling to the actin cytoskeleton is crucial for growth factor activity (Rousseau et al., 2000) (Fan et al., 2012). A study by Abraham et al. (2015) demonstrates that DOCK4 is required for filopodia formation and sprouting downstream of VEGF. The result suggests that DOCK4 is essential for the regulation of RAC1-dependent sprouting under conditions of VEGF stimulation. Since it has been illustrated that DOCK4 is important for angiogenesis downstream of VEGF signalling, I investigate further if it also operates downstream of FGF signalling. Changes in cell shape and the actin cytoskeleton occur in response to FGF stimulation in a RAC1 and CDC42 dependent manner (J. G. Lee & Kay, 2006), hence I investigated whether DOCK4 operates downstream of FGF signalling. I showed that DOCK4 downstream of FGF is not required for stimulation of angiogenesis and dynamic behaviour of endothelial cells in developing tubules. As there was increased angiogenesis with DOCK4 knockdown under conditions of FGF stimulation, this implies that DOCK4 plays a role as a suppressor of angiogenesis under FGF stimulation.

Both angiogenic factors VEGF and FGF impact angiogenesis through activation of RhoG in ECs (Abraham et al., 2015). Abraham et al. (2015) has shown that in VEGF driven angiogenesis SGEF (SH3-containing Guanine Nucleotide Exchange Factor) and RhoG act upstream of RAC1 and DOCK4 to regulate sprouting and branching, and the signalling module SGEF→RhoG→DOCK4→Rac1→DOCK9→Cdc42 downstream of VEGF was discovered (Abraham et al., 2015). Another study in the lab showed that FGF activates RhoG via the GEF TRIO (Scarcia, M., PhD Thesis). Therefore, in ECs VEGF activation of RhoG is via the GEF SGEF and FGF activation of RhoG is via the GEF TRIO. However, the downstream signalling from RhoG may affect

VEGF and FGF driven angiogenesis in opposing ways. It would be interesting to elucidate whether like DOCK4, RhoG also suppresses FGF driven angiogenesis.

Interestingly, bFGF activates RAC1 and CDC42 in ECs (Tkachenko et al., 2004). FGF activates RAC1 downstream of syndecan 4 (S4) (Tkachenko et al., 2004) and FGF activates RhoG to mediate RAC1 activation (Elfenbein et al., 2009). bFGF signalling influences EC migration and angiogenesis through two receptors; FGFR1 which is a receptor tyrosine kinase, and S4 which is a heparan sulfate proteoglycan (Elfenbein et al., 2012) that signals via RhoG and RAC1 (Elfenbein et al., 2009). In the same study Elfenbein et al. (2009) showed that RhoG interacts with DOCK180 and ELMO1 downstream of FGF to generate a functional GEF complex that can activate RAC1 in fibroblasts. Therefore, although DOCK4 also interacts with ELMO (Kanai et al. (2008) (Abraham et al., 2015) this can be only downstream of VEGF, and not FGF signalling. It is possible that in the absence of VEGF DOCK4 is available to participate in pathways that suppress angiogenesis. Interestingly, DOCK180 has been implicated in angiogenesis (Sanematsu et al., 2010) (Huttenlocher & Horwitz, 2011) (Zhao & Guan, 2011) (Wary et al., 2012) and therefore it is plausible that like in fibroblasts DOCK180 controls RAC1 activation in endothelial cells. It is also possible that TRIO is involved, because it has been known that TRIO can act as a GEF for both RhoG and RAC1 (Bellanger et al., 1998) (Blangy et al., 2000). It was shown before in the lab that knockdown of TRIO results in tubules of shorter length in the HUVEC-fibroblast co-culture assay (Scarcia, M., PhD Thesis) and TRIO has been shown to be important in angiogenesis (Eelen et al., 2020) (Klems et al., 2020). In future studies stimulation of ECs with FGF in presence and absence of different GEFs using siRNAs followed by RAC pull-down activation assays can determine which GEFs are required for RAC1 activation in conditions of FGF stimulation. Because I have now established a more physiological model incorporating fluid flow in the microfluidic device, knockdown of GEFs under fluid flow and with FGF stimulation would provide a more accurate picture of what processes are regulated by those GEFs.

I have found that DOCK4 suppresses angiogenesis via suppression of EC proliferation. Interestingly, DOCK4 was initially described as a tumour suppressor

in mouse osteosarcoma cells (Yajnik et al., 2003) and in glioblastoma promotes loss of proliferation (Debruyne et al., 2018). Moreover, it has been shown that DOCK4 regulates adherens junctions via RAC1 (Yajnik et al., 2003). It would be interesting to find out whether RAC1 also suppresses proliferation under FGF conditions, or whether the effect of suppression of proliferation by DOCK4 is RAC1-independent, and whether DOCK4 suppresses proliferation via a different mechanism that does not involve GTPase activation. It has been known that DOCK4 is involved in Wnt signalling where it acts as scaffold protein to bring together components of the APC- GSK3β degradation complex of beta-catenin (Upadhyay et al., 2008). Hence, as DOCK4 is a large protein (Sundaravel et al., 2019) it can have RAC independent functions for example, such as the regulation of levels of beta-catenin (Upadhyay et al., 2008). How DOCK4 suppress proliferation and angiogenesis in ECs is unknown, but the mechanism can be investigated by proteomics approaches and analysing DOCK4 interaction partners such as cyclin dependent kinase (CDK) 1 (unpublished data in the Mavria's lab). In future studies it would be interesting to investigate whether DOCK4 regulates beta-catenin in endothelial cells and whether it interacts with CDK1 to control EC proliferation.

6.5 Concluding remarks

Taking everything together, in the microfluidic device, I have illustrated perfusion of a living network of dynamic human vasculature in a microphysical system which has potentially extensive therapeutic and diagnostic applications. Although microfluidic technology is useful for studying many biological processes, challenges remain in general and regarding the study of angiogenesis. First, the design and operation of microfluidic devices rely on trial and error methods with inadequate systematic optimization and secondly the effect of microenvironmental factors on angiogenesis and EC migration are empirical with restricted theoretical information (Kuzmic et al., 2019). Systematic optimisation and incorporation of blood vessel supporting cell types in the microfluidic device will provide improved organotypic models of angiogenesis in the future.

Some of my experiments have n=1 or n=2 and they will need to be repeated in future for the purpose of producing robust data for publication. Specifically, the experiments relating to the role of ROCK on lumen formation (Figures 4.13, Figure 4.14, and Figure 4.15) and the role of DOCK4 on lumen formation and lateral adhesion (Figure 5.3 and Figure 5.4) will be repeated. However, the effect of ciliary loss tested by two important ciliary proteins IFT88 and RPGRIP1L shown in Figure 4.4 with two experiments and Figure 4.5 with one experiment, also under conditions of flow shown in Figure 4.6 with three experiments and Figure 4.7 with two experiments are complete, given cilia ablation was by knockdown of two different ciliary proteins.

Knowledge of the association between cilium defects and human diseases is expanding, and blood vessel dysfunction has an important role in some ciliary diseases. A better understanding of this association will be undoubtedly beneficial to the treatment of vascular-related diseases. This study shows that tubule formation and lumen expansion in the organotypic co-culture system is influenced by the presence of cilia. Further research needed to supply new strategies for the treatment of vascular diseases caused by endothelial ciliary defects.

Many endothelial cellular processes are controlled by Rho family GTPases and regulatory GEFs and GAPs. Understanding the role of individual GEFs and GAPs will be critical in identifying new ways to improve vascularisation in ischemic disease, or target angiogenesis in disease dependent on neoangiogenesis such as cancer. In this study I investigate effect of ROCK and DOCK4 on angiogenesis, but further investigation is necessary.

List of References

Abraham, S., Scarcia, M., Bagshaw, R. D., McMahon, K., Grant, G., Harvey, T., . . . Mavria, G. (2015). A Rac/Cdc42 exchange factor complex promotes formation of lateral filopodia and blood vessel lumen morphogenesis. *Nat Commun, 6*, 7286. doi:10.1038/ncomms8286

Abraham, S., Yeo, M., Montero-Balaguer, M., Paterson, H., Dejana, E., Marshall, C. J., & Mavria, G. (2009). VE-Cadherin-mediated cell-cell interaction suppresses sprouting via signaling to MLC2 phosphorylation. *Curr Biol, 19*(8), 668-674. doi:10.1016/j.cub.2009.02.057

Adams, M., Simms, R. J., Abdelhamed, Z., Dawe, H. R., Szymanska, K., Logan, C. V., . . . Johnson, C. A. (2012). A meckelin-filamin A interaction mediates ciliogenesis. *Hum Mol Genet, 21*(6), 1272-1286. doi:10.1093/hmg/ddr557

Adams, R. H., & Alitalo, K. (2007). Molecular regulation of angiogenesis and lymphangiogenesis. *Nat Rev Mol Cell Biol, 8*(6), 464-478. doi:10.1038/nrm2183

Aguilar-Cazares, D., Chavez-Dominguez, R., Carlos-Reyes, A., Lopez-Camarillo, C., Hernadez de la Cruz, O. N., & Lopez-Gonzalez, J. S. (2019). Contribution of Angiogenesis to Inflammation and Cancer. *Front Oncol, 9*, 1399. doi:10.3389/fonc.2019.01399

Ahrberg, C. D., Manz, A., & Chung, B. G. (2016). Polymerase chain reaction in microfluidic devices. *Lab Chip, 16*(20), 3866-3884. doi:10.1039/c6lc00984k

Akbari, E., Spychalski, G. B., & Song, J. W. (2017). Microfluidic approaches to the study of angiogenesis and the microcirculation. *Microcirculation, 24*(5). doi:10.1111/micc.12363

Alazami, A. M., Alshammari, M. J., Salih, M. A., Alzahrani, F., Hijazi, H., Seidahmed, M. Z., . . . Alkuraya, F. S. (2012). Molecular characterization of Joubert syndrome in Saudi Arabia. *Hum Mutat, 33*(10), 1423-1428. doi:10.1002/humu.22134

Alitalo, K., Tammela, T., & Petrova, T. V. (2005). Lymphangiogenesis in development and human disease. *Nature, 438*(7070), 946-953. doi:10.1038/nature04480

Allen, J. W., Khetani, S. R., & Bhatia, S. N. (2005). In vitro zonation and toxicity in a hepatocyte bioreactor. *Toxicol Sci, 84*(1), 110-119. doi:10.1093/toxsci/kfi052

Alonso, M. J. (2004). Nanomedicines for overcoming biological barriers. *Biomed Pharmacother, 58*(3), 168-172. doi:10.1016/j.biopha.2004.01.007

Alvarez, J. I., Dodelet-Devillers, A., Kebir, H., Ifergan, I., Fabre, P. J., Terouz, S., . . . Prat, A. (2011). The Hedgehog pathway promotes blood-brain barrier integrity and CNS immune quiescence. *Science, 334*(6063), 1727-1731. doi:10.1126/science.1206936

Anderson, C. T., & Stearns, T. (2009). Centriole age underlies asynchronous primary cilium growth in mammalian cells. *Curr Biol, 19*(17), 1498-1502. doi:10.1016/j.cub.2009.07.034

Antoniades, I., Stylianou, P., & Skourides, P. A. (2014). Making the connection: ciliary adhesion complexes anchor basal bodies to the actin cytoskeleton. *Dev Cell, 28*(1), 70-80. doi:10.1016/j.devcel.2013.12.003

Archer, F. L., & Wheatley, D. N. (1971). Cilia in cell-cultured fibroblasts. II. Incidence in mitotic and post-mitotic BHK 21-C13 fibroblasts. *J Anat, 109*(Pt 2), 277-292.

Arts, H. H., Doherty, D., van Beersum, S. E., Parisi, M. A., Letteboer, S. J., Gorden, N. T., . . . Roepman, R. (2007). Mutations in the gene encoding the basal body protein RPGRIP1L, a nephrocystin-4 interactor, cause Joubert syndrome. *Nat Genet, 39*(7), 882-888. doi:10.1038/ng2069

Asahara, T., Murohara, T., Sullivan, A., Silver, M., van der Zee, R., Li, T., . . . Isner, J. M. (1997). Isolation of putative progenitor endothelial cells for angiogenesis. *Science, 275*(5302), 964-967. doi:10.1126/science.275.5302.964

Atkinson, K. F., Kathem, S. H., Jin, X., Muntean, B. S., Abou-Alaiwi, W. A., Nauli, A. M., & Nauli, S. M. (2015). Dopaminergic signaling within the primary cilia in the renovascular system. *Front Physiol, 6*, 103. doi:10.3389/fphys.2015.00103

Atkinson, K. F., Sherpa, R. T., & Nauli, S. M. (2019). The Role of the Primary Cilium in Sensing Extracellular pH. *Cells, 8*(7). doi:10.3390/cells8070704

Attwell, D., Mishra, A., Hall, C. N., O'Farrell, F. M., & Dalkara, T. (2016). What is a pericyte? *J Cereb Blood Flow Metab, 36*(2), 451-455. doi:10.1177/0271678X15610340

Augustin, H. G., & Koh, G. Y. (2017). Organotypic vasculature: From descriptive heterogeneity to functional pathophysiology. *Science, 357*(6353). doi:10.1126/science.aal2379

Avasthi, P., & Marshall, W. F. (2012). Stages of ciliogenesis and regulation of ciliary length. *Differentiation, 83*(2), S30-42. doi:10.1016/j.diff.2011.11.015

Bae, Y. K., & Barr, M. M. (2008). Sensory roles of neuronal cilia: cilia development, morphogenesis, and function in C. elegans. *Front Biosci, 13*, 5959-5974. doi:10.2741/3129

Bailly, M., & Condeelis, J. (2002). Cell motility: insights from the backstage. *Nat Cell Biol, 4*(12), E292-294. doi:10.1038/ncb1202-e292

Bangs, F., & Anderson, K. V. (2017). Primary Cilia and Mammalian Hedgehog Signaling. *Cold Spring Harb Perspect Biol, 9*(5). doi:10.1101/cshperspect.a028175

Barlow, H. R., & Cleaver, O. (2019). Building Blood Vessels-One Rho GTPase at a Time. *Cells, 8*(6). doi:10.3390/cells8060545

Barry, D. M., Koo, Y., Norden, P. R., Wylie, L. A., Xu, K., Wichaidit, C., . . . Cleaver, O. (2016). Rasip1-Mediated Rho GTPase Signaling Regulates Blood Vessel Tubulogenesis via Nonmuscle Myosin II. *Circ Res, 119*(7), 810-826. doi:10.1161/CIRCRESAHA.116.309094

Barry, D. M., Xu, K., Meadows, S. M., Zheng, Y., Norden, P. R., Davis, G. E., & Cleaver, O. (2015). Cdc42 is required for cytoskeletal support of endothelial cell adhesion during blood vessel formation in mice. *Development, 142*(17), 3058-3070. doi:10.1242/dev.125260

Bay, S. N., & Caspary, T. (2012). What are those cilia doing in the neural tube? *Cilia, 1*(1), 19. doi:10.1186/2046-2530-1-19

Beckers, C. M., van Hinsbergh, V. W., & van Nieuw Amerongen, G. P. (2010). Driving Rho GTPase activity in endothelial cells regulates barrier integrity. *Thromb Haemost, 103*(1), 40-55. doi:10.1160/TH09-06-0403

Bellanger, J. M., Lazaro, J. B., Diriong, S., Fernandez, A., Lamb, N., & Debant, A. (1998). The two guanine nucleotide exchange factor domains of Trio

link the Rac1 and the RhoA pathways in vivo. *Oncogene, 16*(2), 147-152. doi:10.1038/sj.onc.1201532

Benson, C. E., & Southgate, L. (2021). The DOCK protein family in vascular development and disease. *Angiogenesis, 24*(3), 417-433. doi:10.1007/s10456-021-09768-8

Berbari, N. F., Bishop, G. A., Askwith, C. C., Lewis, J. S., & Mykytyn, K. (2007). Hippocampal neurons possess primary cilia in culture. *J Neurosci Res, 85*(5), 1095-1100. doi:10.1002/jnr.21209

Berbari, N. F., Johnson, A. D., Lewis, J. S., Askwith, C. C., & Mykytyn, K. (2008). Identification of ciliary localization sequences within the third intracellular loop of G protein-coupled receptors. *Mol Biol Cell, 19*(4), 1540-1547. doi:10.1091/mbc.E07-09-0942

Bershteyn, M., Atwood, S. X., Woo, W. M., Li, M., & Oro, A. E. (2010). MIM and cortactin antagonism regulates ciliogenesis and hedgehog signaling. *Dev Cell, 19*(2), 270-283. doi:10.1016/j.devcel.2010.07.009

Besschetnova, T. Y., Kolpakova-Hart, E., Guan, Y., Zhou, J., Olsen, B. R., & Shah, J. V. (2010). Identification of signaling pathways regulating primary cilium length and flow-mediated adaptation. *Curr Biol, 20*(2), 182-187. doi:10.1016/j.cub.2009.11.072

Bhatia, S. N., & Ingber, D. E. (2014). Microfluidic organs-on-chips. *Nat Biotechnol, 32*(8), 760-772. doi:10.1038/nbt.2989

Bischel, L. L., Young, E. W., Mader, B. R., & Beebe, D. J. (2013). Tubeless microfluidic angiogenesis assay with three-dimensional endothelial-lined microvessels. *Biomaterials, 34*(5), 1471-1477. doi:10.1016/j.biomaterials.2012.11.005

Blanco, R., & Gerhardt, H. (2013). VEGF and Notch in tip and stalk cell selection. *Cold Spring Harb Perspect Med, 3*(1), a006569. doi:10.1101/cshperspect.a006569

Blangy, A., Vignal, E., Schmidt, S., Debant, A., Gauthier-Rouviere, C., & Fort, P. (2000). TrioGEF1 controls Rac- and Cdc42-dependent cell structures through the direct activation of rhoG. *J Cell Sci, 113 (Pt 4)*, 729-739. doi:10.1242/jcs.113.4.729

Blum, Y., Belting, H. G., Ellertsdottir, E., Herwig, L., Luders, F., & Affolter, M. (2008). Complex cell rearrangements during intersegmental vessel

sprouting and vessel fusion in the zebrafish embryo. *Dev Biol, 316*(2), 312-322. doi:10.1016/j.ydbio.2008.01.038

Bonura, C., Paterlini-Brechot, P., & Brechot, C. (1999). Structure and expression of Tg737, a putative tumor suppressor gene, in human hepatocellular carcinomas. *Hepatology, 30*(3), 677-681. doi:10.1002/hep.510300325

Boo, Y. C., & Jo, H. (2003). Flow-dependent regulation of endothelial nitric oxide synthase: role of protein kinases. *Am J Physiol Cell Physiol, 285*(3), C499-508. doi:10.1152/ajpcell.00122.2003

Booth, R., Noh, S., & Kim, H. (2014). A multiple-channel, multiple-assay platform for characterization of full-range shear stress effects on vascular endothelial cells. *Lab Chip, 14*(11), 1880-1890. doi:10.1039/c3lc51304a

Borasch, K., Richardson, K., & Plendl, J. (2020). Cardiogenesis with a focus on vasculogenesis and angiogenesis. *Anat Histol Embryol, 49*(5), 643-655. doi:10.1111/ahe.12549

Brailov, I., Bancila, M., Brisorgueil, M. J., Miquel, M. C., Hamon, M., & Verge, D. (2000). Localization of 5-HT(6) receptors at the plasma membrane of neuronal cilia in the rat brain. *Brain Res, 872*(1-2), 271-275. doi:10.1016/s0006-8993(00)02519-1

Brancati, F., Travaglini, L., Zablocka, D., Boltshauser, E., Accorsi, P., Montagna, G., . . . Valente, E. M. (2008). RPGRIP1L mutations are mainly associated with the cerebello-renal phenotype of Joubert syndrome-related disorders. *Clin Genet, 74*(2), 164-170. doi:10.1111/j.1399-0004.2008.01047.x

Brodsky, M., Lesiak, A. J., Croicu, A., Cohenca, N., Sullivan, J. M., & Neumaier, J. F. (2017). 5-HT6 receptor blockade regulates primary cilia morphology in striatal neurons. *Brain Res, 1660*, 10-19. doi:10.1016/j.brainres.2017.01.010

Brown, W. R. (2010). A review of string vessels or collapsed, empty basement membrane tubes. *J Alzheimers Dis, 21*(3), 725-739. doi:10.3233/JAD-2010-100219

Bryan, B. A., & D'Amore, P. A. (2007). What tangled webs they weave: Rho-GTPase control of angiogenesis. *Cell Mol Life Sci, 64*(16), 2053-2065. doi:10.1007/s00018-007-7008-z

Burri, P. H., Hlushchuk, R., & Djonov, V. (2004). Intussusceptive angiogenesis: its emergence, its characteristics, and its significance. *Dev Dyn, 231*(3), 474-488. doi:10.1002/dvdy.20184

Bussolati, B., Grange, C., & Camussi, G. (2011). Tumor exploits alternative strategies to achieve vascularization. *FASEB J, 25*(9), 2874-2882. doi:10.1096/fj.10-180323

Byrd, N., Becker, S., Maye, P., Narasimhaiah, R., St-Jacques, B., Zhang, X., . . . Grabel, L. (2002). Hedgehog is required for murine yolk sac angiogenesis. *Development, 129*(2), 361-372. doi:10.1242/dev.129.2.361

Caduff, J. H., Fischer, L. C., & Burri, P. H. (1986). Scanning electron microscope study of the developing microvasculature in the postnatal rat lung. *Anat Rec, 216*(2), 154-164. doi:10.1002/ar.1092160207

Campochiaro, P. A. (2015). Molecular pathogenesis of retinal and choroidal vascular diseases. *Prog Retin Eye Res, 49*, 67-81. doi:10.1016/j.preteyeres.2015.06.002

Cao, J., Shen, Y., Zhu, L., Xu, Y., Zhou, Y., Wu, Z., . . . Zhu, X. (2012). miR-129-3p controls cilia assembly by regulating CP110 and actin dynamics. *Nat Cell Biol, 14*(7), 697-706. doi:10.1038/ncb2512

Caplan, A. I. (1985). The vasculature and limb development. *Cell Differ, 16*(1), 1-11. doi:10.1016/0045-6039(85)90602-5

Caradu, C., Couffinhal, T., Chapouly, C., Guimbal, S., Hollier, P. L., Ducasse, E., . . . Renault, M. A. (2018). Restoring Endothelial Function by Targeting Desert Hedgehog Downstream of Klf2 Improves Critical Limb Ischemia in Adults. *Circ Res, 123*(9), 1053-1065. doi:10.1161/CIRCRESAHA.118.313177

Carmeliet, P. (2000). Mechanisms of angiogenesis and arteriogenesis. *Nat Med, 6*(4), 389-395. doi:10.1038/74651

Carmeliet, P. (2003). Angiogenesis in health and disease. *Nat Med, 9*(6), 653-660. doi:10.1038/nm0603-653

Carmeliet, P. (2005). Angiogenesis in life, disease and medicine. *Nature, 438*(7070), 932-936. doi:10.1038/nature04478

Carmeliet, P., Ferreira, V., Breier, G., Pollefeyt, S., Kieckens, L., Gertsenstein, M., . . . Nagy, A. (1996). Abnormal blood vessel development and lethality

in embryos lacking a single VEGF allele. *Nature, 380*(6573), 435-439. doi:10.1038/380435a0

Carmeliet, P., & Jain, R. K. (2011). Molecular mechanisms and clinical applications of angiogenesis. *Nature, 473*(7347), 298-307. doi:10.1038/nature10144

Carmeliet, P., Lampugnani, M. G., Moons, L., Breviario, F., Compernolle, V., Bono, F., . . . Dejana, E. (1999). Targeted deficiency or cytosolic truncation of the VE-cadherin gene in mice impairs VEGF-mediated endothelial survival and angiogenesis. *Cell, 98*(2), 147-157. doi:10.1016/s0092-8674(00)81010-7

Caron, C., DeGeer, J., Fournier, P., Duquette, P. M., Luangrath, V., Ishii, H., . . . Royal, I. (2016). CdGAP/ARHGAP31, a Cdc42/Rac1 GTPase regulator, is critical for vascular development and VEGF-mediated angiogenesis. *Sci Rep, 6*, 27485. doi:10.1038/srep27485

Chaitin, M. H., & Burnside, B. (1989). Actin filament polarity at the site of rod outer segment disk morphogenesis. *Invest Ophthalmol Vis Sci, 30*(12), 2461-2469.

Chaki, M., Hoefele, J., Allen, S. J., Ramaswami, G., Janssen, S., Bergmann, C., . . . Hildebrandt, F. (2011). Genotype-phenotype correlation in 440 patients with NPHP-related ciliopathies. *Kidney Int, 80*(11), 1239-1245. doi:10.1038/ki.2011.284

Chang, L., Yang, J., Jo, C. H., Boland, A., Zhang, Z., McLaughlin, S. H., . . . Barford, D. (2020). Structure of the DOCK2-ELMO1 complex provides insights into regulation of the auto-inhibited state. *Nat Commun, 11*(1), 3464. doi:10.1038/s41467-020-17271-9

Chapouly, C., Guimbal, S., Hollier, P. L., & Renault, M. A. (2019). Role of Hedgehog Signaling in Vasculature Development, Differentiation, and Maintenance. *Int J Mol Sci, 20*(12). doi:10.3390/ijms20123076

Charpentier, M. S., & Conlon, F. L. (2014). Cellular and molecular mechanisms underlying blood vessel lumen formation. *Bioessays, 36*(3), 251-259. doi:10.1002/bies.201300133

Chen, L. J., & Kaji, H. (2017). Modeling angiogenesis with micro- and nanotechnology. *Lab Chip, 17*(24), 4186-4219. doi:10.1039/c7lc00774d

Chen, Q., Jiang, L., Li, C., Hu, D., Bu, J. W., Cai, D., & Du, J. L. (2012). Haemodynamics-driven developmental pruning of brain vasculature in zebrafish. *PLoS Biol, 10*(8), e1001374. doi:10.1371/journal.pbio.1001374

Cherfils, J., & Zeghouf, M. (2013). Regulation of small GTPases by GEFs, GAPs, and GDIs. *Physiol Rev, 93*(1), 269-309. doi:10.1152/physrev.00003.2012

Chistiakov, D. A., Orekhov, A. N., & Bobryshev, Y. V. (2017). Effects of shear stress on endothelial cells: go with the flow. *Acta Physiol (Oxf), 219*(2), 382-408. doi:10.1111/apha.12725

Chopra, H., Hung, M. K., Kwong, D. L., Zhang, C. F., & Pow, E. H. N. (2018). Insights into Endothelial Progenitor Cells: Origin, Classification, Potentials, and Prospects. *Stem Cells Int, 2018*, 9847015. doi:10.1155/2018/9847015

Cines, D. B., Pollak, E. S., Buck, C. A., Loscalzo, J., Zimmerman, G. A., McEver, R. P., . . . Stern, D. M. (1998). Endothelial cells in physiology and in the pathophysiology of vascular disorders. *Blood, 91*(10), 3527-3561.

Collin, J., Murie, J., & Morris, P. J. (1989). Two year prospective analysis of the Oxford experience with surgical treatment of abdominal aortic aneurysm. *Surg Gynecol Obstet, 169*(6), 527-531.

Cook, D. R., Rossman, K. L., & Der, C. J. (2014). Rho guanine nucleotide exchange factors: regulators of Rho GTPase activity in development and disease. *Oncogene, 33*(31), 4021-4035. doi:10.1038/onc.2013.362

Corbit, K. C., Shyer, A. E., Dowdle, W. E., Gaulden, J., Singla, V., Chen, M. H., . . . Reiter, J. F. (2008). Kif3a constrains beta-catenin-dependent Wnt signalling through dual ciliary and non-ciliary mechanisms. *Nat Cell Biol, 10*(1), 70-76. doi:10.1038/ncb1670

Costa, C., Incio, J., & Soares, R. (2007). Angiogenesis and chronic inflammation: cause or consequence? *Angiogenesis, 10*(3), 149-166. doi:10.1007/s10456-007-9074-0

Cote, J. F., Motoyama, A. B., Bush, J. A., & Vuori, K. (2005). A novel and evolutionarily conserved PtdIns(3,4,5)P3-binding domain is necessary for DOCK180 signalling. *Nat Cell Biol, 7*(8), 797-807. doi:10.1038/ncb1280

Coultas, L., Chawengsaksophak, K., & Rossant, J. (2005). Endothelial cells and VEGF in vascular development. *Nature, 438*(7070), 937-945. doi:10.1038/nature04479

Dai, C., Webster, K. A., Bhatt, A., Tian, H., Su, G., & Li, W. (2021). Concurrent Physiological and Pathological Angiogenesis in Retinopathy of Prematurity and Emerging Therapies. *Int J Mol Sci, 22*(9). doi:10.3390/ijms22094809

Das, A., Lauffenburger, D., Asada, H., & Kamm, R. D. (2010). A hybrid continuum-discrete modelling approach to predict and control angiogenesis: analysis of combinatorial growth factor and matrix effects on vessel-sprouting morphology. *Philos Trans A Math Phys Eng Sci, 368*(1921), 2937-2960. doi:10.1098/rsta.2010.0085

Davis, G. E., & Bayless, K. J. (2003). An integrin and Rho GTPase-dependent pinocytic vacuole mechanism controls capillary lumen formation in collagen and fibrin matrices. *Microcirculation, 10*(1), 27-44. doi:10.1038/sj.mn.7800175

Dawe, H. R., Smith, U. M., Cullinane, A. R., Gerrelli, D., Cox, P., Badano, J. L., . . . Johnson, C. A. (2007). The Meckel-Gruber Syndrome proteins MKS1 and meckelin interact and are required for primary cilium formation. *Hum Mol Genet, 16*(2), 173-186. doi:10.1093/hmg/ddl459

de Groot, D., Pasterkamp, G., & Hoefer, I. E. (2009). Cardiovascular risk factors and collateral artery formation. *Eur J Clin Invest, 39*(12), 1036-1047. doi:10.1111/j.1365-2362.2009.02205.x

Debruyne, D. N., Turchi, L., Burel-Vandenbos, F., Fareh, M., Almairac, F., Virolle, V., . . . Virolle, T. (2018). DOCK4 promotes loss of proliferation in glioblastoma progenitor cells through nuclear beta-catenin accumulation and subsequent miR-302-367 cluster expression. *Oncogene, 37*(2), 241-254. doi:10.1038/onc.2017.323

Degnim, A. C., Nassar, A., Stallings-Mann, M., Keith Anderson, S., Oberg, A. L., Vierkant, R. A., . . . Radisky, D. C. (2015). Gene signature model for breast cancer risk prediction for women with sclerosing adenosis. *Breast Cancer Res Treat, 152*(3), 687-694. doi:10.1007/s10549-015-3513-1

Delong, C., & Sharma, S. (2022). Physiology, Peripheral Vascular Resistance. In *StatPearls*. Treasure Island (FL).

Delous, M., Baala, L., Salomon, R., Laclef, C., Vierkotten, J., Tory, K., . . . Saunier, S. (2007). The ciliary gene RPGRIP1L is mutated in cerebello-

oculo-renal syndrome (Joubert syndrome type B) and Meckel syndrome. *Nat Genet, 39*(7), 875-881. doi:10.1038/ng2039

Deng, Z., Jia, Y., Liu, H., He, M., Yang, Y., Xiao, W., & Li, Y. (2019). RhoA/ROCK pathway: implication in osteoarthritis and therapeutic targets. *Am J Transl Res, 11*(9), 5324-5331.

DePina, A. S., & Langford, G. M. (1999). Vesicle transport: the role of actin filaments and myosin motors. *Microsc Res Tech, 47*(2), 93-106. doi:10.1002/(SICI)1097-0029(19991015)47:2<93::AID-JEMT2>3.0.CO;2-P

Derda, R., Laromaine, A., Mammoto, A., Tang, S. K., Mammoto, T., Ingber, D. E., & Whitesides, G. M. (2009). Paper-supported 3D cell culture for tissue-based bioassays. *Proc Natl Acad Sci U S A, 106*(44), 18457-18462. doi:10.1073/pnas.0910666106

Di Costanzo, E., Ingangi, V., Angelini, C., Carfora, M. F., Carriero, M. V., & Natalini, R. (2016). A Macroscopic Mathematical Model for Cell Migration Assays Using a Real-Time Cell Analysis. *PLoS One, 11*(9), e0162553. doi:10.1371/journal.pone.0162553

Dinsmore, C., & Reiter, J. F. (2016). Endothelial primary cilia inhibit atherosclerosis. *EMBO reports, 17*(2), 156-166. doi:10.15252/embr.201541019

Djonov, V., Baum, O., & Burri, P. H. (2003). Vascular remodeling by intussusceptive angiogenesis. *Cell Tissue Res, 314*(1), 107-117. doi:10.1007/s00441-003-0784-3

Djonov, V., Schmid, M., Tschanz, S. A., & Burri, P. H. (2000). Intussusceptive angiogenesis: its role in embryonic vascular network formation. *Circ Res, 86*(3), 286-292. doi:10.1161/01.res.86.3.286

Djonov, V. G., Kurz, H., & Burri, P. H. (2002). Optimality in the developing vascular system: branching remodeling by means of intussusception as an efficient adaptation mechanism. *Dev Dyn, 224*(4), 391-402. doi:10.1002/dvdy.10119

Doherty, D., Parisi, M. A., Finn, L. S., Gunay-Aygun, M., Al-Mateen, M., Bates, D., . . . Glass, I. A. (2010). Mutations in 3 genes (MKS3, CC2D2A and RPGRIP1L) cause COACH syndrome (Joubert syndrome with congenital hepatic fibrosis). *J Med Genet, 47*(1), 8-21. doi:10.1136/jmg.2009.067249

Domansky, K., Inman, W., Serdy, J., Dash, A., Lim, M. H., & Griffith, L. G. (2010). Perfused multiwell plate for 3D liver tissue engineering. *Lab Chip, 10*(1), 51-58. doi:10.1039/b913221j

Dominguez, R. (2009). Actin filament nucleation and elongation factors--structure-function relationships. *Crit Rev Biochem Mol Biol, 44*(6), 351-366. doi:10.3109/10409230903277340

Douville, N. J., Zamankhan, P., Tung, Y. C., Li, R., Vaughan, B. L., Tai, C. F., . . . Takayama, S. (2011). Combination of fluid and solid mechanical stresses contribute to cell death and detachment in a microfluidic alveolar model. *Lab Chip, 11*(4), 609-619. doi:10.1039/c0lc00251h

Duhr, F., Deleris, P., Raynaud, F., Seveno, M., Morisset-Lopez, S., Mannoury la Cour, C., . . . Chaumont-Dubel, S. (2014). Cdk5 induces constitutive activation of 5-HT6 receptors to promote neurite growth. *Nat Chem Biol, 10*(7), 590-597. doi:10.1038/nchembio.1547

Eelen, G., Treps, L., Li, X., & Carmeliet, P. (2020). Basic and Therapeutic Aspects of Angiogenesis Updated. *Circ Res, 127*(2), 310-329. doi:10.1161/CIRCRESAHA.120.316851

Egginton, S., Zhou, A. L., Brown, M. D., & Hudlicka, O. (2001). Unorthodox angiogenesis in skeletal muscle. *Cardiovasc Res, 49*(3), 634-646. doi:10.1016/s0008-6363(00)00282-0

Eilken, H. M., & Adams, R. H. (2010). Dynamics of endothelial cell behavior in sprouting angiogenesis. *Curr Opin Cell Biol, 22*(5), 617-625. doi:10.1016/j.ceb.2010.08.010

Eisa-Beygi, S., Benslimane, F. M., El-Rass, S., Prabhudesai, S., Abdelrasoul, M. K. A., Simpson, P. M., . . . Ramchandran, R. (2018). Characterization of Endothelial Cilia Distribution During Cerebral-Vascular Development in Zebrafish (Danio rerio). *Arterioscler Thromb Vasc Biol, 38*(12), 2806-2818. doi:10.1161/ATVBAHA.118.311231

El-Ali, J., Sorger, P. K., & Jensen, K. F. (2006). Cells on chips. *Nature, 442*(7101), 403-411. doi:10.1038/nature05063

Elfenbein, A., Lanahan, A., Zhou, T. X., Yamasaki, A., Tkachenko, E., Matsuda, M., & Simons, M. (2012). Syndecan 4 regulates FGFR1 signaling in endothelial cells by directing macropinocytosis. *Sci Signal, 5*(223), ra36. doi:10.1126/scisignal.2002495

Elfenbein, A., Rhodes, J. M., Meller, J., Schwartz, M. A., Matsuda, M., & Simons, M. (2009). Suppression of RhoG activity is mediated by a syndecan 4-synectin-RhoGDI1 complex and is reversed by PKCalpha in a Rac1 activation pathway. *J Cell Biol, 186*(1), 75-83. doi:10.1083/jcb.200810179

Engel, B. D., Ludington, W. B., & Marshall, W. F. (2009). Intraflagellar transport particle size scales inversely with flagellar length: revisiting the balance-point length control model. *J Cell Biol, 187*(1), 81-89. doi:10.1083/jcb.200812084

Enis, D. R., Shepherd, B. R., Wang, Y., Qasim, A., Shanahan, C. M., Weissberg, P. L., . . . Schechner, J. S. (2005). Induction, differentiation, and remodeling of blood vessels after transplantation of Bcl-2-transduced endothelial cells. *Proc Natl Acad Sci U S A, 102*(2), 425-430. doi:10.1073/pnas.0408357102

Ernandez, T., Komarynets, O., Chassot, A., Sougoumarin, S., Soulie, P., Wang, Y., . . . Feraille, E. (2017). Primary cilia control the maturation of tubular lumen in renal collecting duct epithelium. *Am J Physiol Cell Physiol, 313*(1), C94-C107. doi:10.1152/ajpcell.00290.2016

Esch, E. W., Bahinski, A., & Huh, D. (2015). Organs-on-chips at the frontiers of drug discovery. *Nat Rev Drug Discov, 14*(4), 248-260. doi:10.1038/nrd4539

Fahim, A. T., Bowne, S. J., Sullivan, L. S., Webb, K. D., Williams, J. T., Wheaton, D. K., . . . Daiger, S. P. (2011). Allelic heterogeneity and genetic modifier loci contribute to clinical variation in males with X-linked retinitis pigmentosa due to RPGR mutations. *PLoS One, 6*(8), e23021. doi:10.1371/journal.pone.0023021

Fan, Y., Arif, A., Gong, Y., Jia, J., Eswarappa, S. M., Willard, B., . . . Fox, P. L. (2012). Stimulus-dependent phosphorylation of profilin-1 in angiogenesis. *Nat Cell Biol, 14*(10), 1046-1056. doi:10.1038/ncb2580

Ferrara, N., & Alitalo, K. (1999). Clinical applications of angiogenic growth factors and their inhibitors. *Nat Med, 5*(12), 1359-1364. doi:10.1038/70928

Ferrara, N., & Davis-Smyth, T. (1997). The biology of vascular endothelial growth factor. *Endocr Rev, 18*(1), 4-25. doi:10.1210/edrv.18.1.0287

Fischer, R. S., Lam, P. Y., Huttenlocher, A., & Waterman, C. M. (2019). Filopodia and focal adhesions: An integrated system driving branching

morphogenesis in neuronal pathfinding and angiogenesis. *Dev Biol, 451*(1), 86-95. doi:10.1016/j.ydbio.2018.08.015

Folkman, J. (1971). Tumor angiogenesis: therapeutic implications. *N Engl J Med, 285*(21), 1182-1186. doi:10.1056/NEJM197111182852108

Folkman, J. (1995). Angiogenesis in cancer, vascular, rheumatoid and other disease. *Nat Med, 1*(1), 27-31. doi:10.1038/nm0195-27

Fonte, V. G., Searls, R. L., & Hilfer, S. R. (1971). The relationship of cilia with cell division and differentiation. *J Cell Biol, 49*(1), 226-229. doi:10.1083/jcb.49.1.226

Francis, S. S., Sfakianos, J., Lo, B., & Mellman, I. (2011). A hierarchy of signals regulates entry of membrane proteins into the ciliary membrane domain in epithelial cells. *J Cell Biol, 193*(1), 219-233. doi:10.1083/jcb.201009001

Fukata, M., & Kaibuchi, K. (2001). Rho-family GTPases in cadherin-mediated cell-cell adhesion. *Nat Rev Mol Cell Biol, 2*(12), 887-897. doi:10.1038/35103068

Fukui, Y., Hashimoto, O., Sanui, T., Oono, T., Koga, H., Abe, M., . . . Sasazuki, T. (2001). Haematopoietic cell-specific CDM family protein DOCK2 is essential for lymphocyte migration. *Nature, 412*(6849), 826-831. doi:10.1038/35090591

Gadea, G., & Blangy, A. (2014). Dock-family exchange factors in cell migration and disease. *Eur J Cell Biol, 93*(10-12), 466-477. doi:10.1016/j.ejcb.2014.06.003

Gaertig, J., & Wloga, D. (2008). Ciliary tubulin and its post-translational modifications. *Curr Top Dev Biol, 85*, 83-113. doi:10.1016/S0070-2153(08)00804-1

Gale, N. W., & Yancopoulos, G. D. (1999). Growth factors acting via endothelial cell-specific receptor tyrosine kinases: VEGFs, angiopoietins, and ephrins in vascular development. *Genes Dev, 13*(9), 1055-1066. doi:10.1101/gad.13.9.1055

Gamba, A., Ambrosi, D., Coniglio, A., de Candia, A., Di Talia, S., Giraudo, E., . . . Bussolino, F. (2003). Percolation, morphogenesis, and burgers dynamics in blood vessels formation. *Phys Rev Lett, 90*(11), 118101. doi:10.1103/PhysRevLett.90.118101

Garcia-Gonzalo, F. R., & Reiter, J. F. (2012). Scoring a backstage pass: mechanisms of ciliogenesis and ciliary access. *J Cell Biol, 197*(6), 697-709. doi:10.1083/jcb.201111146

Garcia-Martinez, V., & Schoenwolf, G. C. (1993). Primitive-streak origin of the cardiovascular system in avian embryos. *Dev Biol, 159*(2), 706-719. doi:10.1006/dbio.1993.1276

Gebala, V., Collins, R., Geudens, I., Phng, L. K., & Gerhardt, H. (2016). Blood flow drives lumen formation by inverse membrane blebbing during angiogenesis in vivo. *Nat Cell Biol, 18*(4), 443-450. doi:10.1038/ncb3320

Gerhardt, H., Golding, M., Fruttiger, M., Ruhrberg, C., Lundkvist, A., Abramsson, A., . . . Betsholtz, C. (2003). VEGF guides angiogenic sprouting utilizing endothelial tip cell filopodia. *J Cell Biol, 161*(6), 1163-1177. doi:10.1083/jcb.200302047

Gilula, N. B., & Satir, P. (1972). The ciliary necklace. A ciliary membrane specialization. *J Cell Biol, 53*(2), 494-509. doi:10.1083/jcb.53.2.494

Glass, C. K., & Witztum, J. L. (2001). Atherosclerosis. the road ahead. *Cell, 104*(4), 503-516. doi:10.1016/s0092-8674(01)00238-0

Goetz, J. G., Steed, E., Ferreira, R. R., Roth, S., Ramspacher, C., Boselli, F., . . . Vermot, J. (2014). Endothelial cilia mediate low flow sensing during zebrafish vascular development. *Cell Rep, 6*(5), 799-808. doi:10.1016/j.celrep.2014.01.032

Goetz, S. C., & Anderson, K. V. (2010). The primary cilium: a signalling centre during vertebrate development. *Nat Rev Genet, 11*(5), 331-344. doi:10.1038/nrg2774

Goley, E. D., & Welch, M. D. (2006). The ARP2/3 complex: an actin nucleator comes of age. *Nat Rev Mol Cell Biol, 7*(10), 713-726. doi:10.1038/nrm2026

Goncalves, J., & Pelletier, L. (2017). The Ciliary Transition Zone: Finding the Pieces and Assembling the Gate. *Mol Cells, 40*(4), 243-253. doi:10.14348/molcells.2017.0054

Goral, V. N., Hsieh, Y. C., Petzold, O. N., Clark, J. S., Yuen, P. K., & Faris, R. A. (2010). Perfusion-based microfluidic device for three-dimensional dynamic primary human hepatocyte cell culture in the absence of

biological or synthetic matrices or coagulants. *Lab Chip, 10*(24), 3380-3386. doi:10.1039/c0lc00135j

Gory-Faure, S., Prandini, M. H., Pointu, H., Roullot, V., Pignot-Paintrand, I., Vernet, M., & Huber, P. (1999). Role of vascular endothelial-cadherin in vascular morphogenesis. *Development, 126*(10), 2093-2102. doi:10.1242/dev.126.10.2093

Goto, H., Inaba, H., & Inagaki, M. (2017). Mechanisms of ciliogenesis suppression in dividing cells. *Cell Mol Life Sci, 74*(5), 881-890. doi:10.1007/s00018-016-2369-9

Greenberg, J. I., Shields, D. J., Barillas, S. G., Acevedo, L. M., Murphy, E., Huang, J., . . . Cheresh, D. A. (2008). A role for VEGF as a negative regulator of pericyte function and vessel maturation. *Nature, 456*(7223), 809-813. doi:10.1038/nature07424

Grosberg, A., Alford, P. W., McCain, M. L., & Parker, K. K. (2011). Ensembles of engineered cardiac tissues for physiological and pharmacological study: heart on a chip. *Lab Chip, 11*(24), 4165-4173. doi:10.1039/c1lc20557a

Guadiana, S. M., Semple-Rowland, S., Daroszewski, D., Madorsky, I., Breunig, J. J., Mykytyn, K., & Sarkisian, M. R. (2013). Arborization of dendrites by developing neocortical neurons is dependent on primary cilia and type 3 adenylyl cyclase. *J Neurosci, 33*(6), 2626-2638. doi:10.1523/JNEUROSCI.2906-12.2013

Gupta, M. K., & Qin, R. Y. (2003). Mechanism and its regulation of tumor-induced angiogenesis. *World J Gastroenterol, 9*(6), 1144-1155. doi:10.3748/wjg.v9.i6.1144

Haase, K., & Kamm, R. D. (2017). Advances in on-chip vascularization. *Regen Med, 12*(3), 285-302. doi:10.2217/rme-2016-0152

Hackam, D. G. (2007). Translating animal research into clinical benefit. *BMJ, 334*(7586), 163-164. doi:10.1136/bmj.39104.362951.80

Halbritter, J., Diaz, K., Chaki, M., Porath, J. D., Tarrier, B., Fu, C., . . . Otto, E. A. (2012). High-throughput mutation analysis in patients with a nephronophthisis-associated ciliopathy applying multiplexed barcoded array-based PCR amplification and next-generation sequencing. *J Med Genet, 49*(12), 756-767. doi:10.1136/jmedgenet-2012-100973

Hall, A. (1998). Rho GTPases and the actin cytoskeleton. *Science, 279*(5350), 509-514. doi:10.1126/science.279.5350.509

Hall, A., & Nobes, C. D. (2000). Rho GTPases: molecular switches that control the organization and dynamics of the actin cytoskeleton. *Philos Trans R Soc Lond B Biol Sci, 355*(1399), 965-970. doi:10.1098/rstb.2000.0632

Hamel, B. L. (2010). Atypical Guanine Nucleotide Exchange Factors for Rho Family GTPases: DOCK9 Activation of Cdc42 and SmgGDS activation of RhoA. doi:https://doi.org/10.17615/kmq6-qg97

Hanahan, D., & Folkman, J. (1996). Patterns and emerging mechanisms of the angiogenic switch during tumorigenesis. *Cell, 86*(3), 353-364. doi:10.1016/s0092-8674(00)80108-7

Harvey F. Lodish , A. B., .; Chris Kaiser , .; Monty Krieger ,.; Anthony Bretscher,.; Hidde L. Ploegh ,.; Angelika Amon ,.; Kelsey C. Martin (2016). Molecular cell biology.

Hasan, A., Paul, A., Vrana, N. E., Zhao, X., Memic, A., Hwang, Y.-S., . . . Khademhosseini, A. (2014). Microfluidic techniques for development of 3D vascularized tissue. *Biomaterials, 35*(26), 7308-7325. doi:10.1016/j.biomaterials.2014.04.091

Hathcock, J. J. (2006). Flow effects on coagulation and thrombosis. *Arterioscler Thromb Vasc Biol, 26*(8), 1729-1737. doi:10.1161/01.ATV.0000229658.76797.30

Haycraft, C. J., Banizs, B., Aydin-Son, Y., Zhang, Q., Michaud, E. J., & Yoder, B. K. (2005). Gli2 and Gli3 localize to cilia and require the intraflagellar transport protein polaris for processing and function. *PLoS Genet, 1*(4), e53. doi:10.1371/journal.pgen.0010053

Haycraft, C. J., Swoboda, P., Taulman, P. D., Thomas, J. H., & Yoder, B. K. (2001). The C. elegans homolog of the murine cystic kidney disease gene Tg737 functions in a ciliogenic pathway and is disrupted in osm-5 mutant worms. *Development, 128*(9), 1493-1505. doi:10.1242/dev.128.9.1493

Hellstrom, M., Phng, L. K., Hofmann, J. J., Wallgard, E., Coultas, L., Lindblom, P., . . . Betsholtz, C. (2007). Dll4 signalling through Notch1 regulates formation of tip cells during angiogenesis. *Nature, 445*(7129), 776-780. doi:10.1038/nature05571

Herbert, S. P., & Stainier, D. Y. (2011). Molecular control of endothelial cell behaviour during blood vessel morphogenesis. *Nat Rev Mol Cell Biol, 12*(9), 551-564. doi:10.1038/nrm3176

Hernandez-Garcia, R., Iruela-Arispe, M. L., Reyes-Cruz, G., & Vazquez-Prado, J. (2015). Endothelial RhoGEFs: A systematic analysis of their expression profiles in VEGF-stimulated and tumor endothelial cells. *Vascul Pharmacol, 74*, 60-72. doi:10.1016/j.vph.2015.10.003

Hernandez-Hernandez, V., Pravincumar, P., Diaz-Font, A., May-Simera, H., Jenkins, D., Knight, M., & Beales, P. L. (2013). Bardet-Biedl syndrome proteins control the cilia length through regulation of actin polymerization. *Hum Mol Genet, 22*(19), 3858-3868. doi:10.1093/hmg/ddt241

Herwig, L., Blum, Y., Krudewig, A., Ellertsdottir, E., Lenard, A., Belting, H. G., & Affolter, M. (2011). Distinct cellular mechanisms of blood vessel fusion in the zebrafish embryo. *Curr Biol, 21*(22), 1942-1948. doi:10.1016/j.cub.2011.10.016

Hetheridge, C., Mavria, G., & Mellor, H. (2011). Uses of the in vitro endothelial-fibroblast organotypic co-culture assay in angiogenesis research. *Biochem Soc Trans, 39*(6), 1597-1600. doi:10.1042/BST20110738

Hinshaw, D. C., & Shevde, L. A. (2019). The Tumor Microenvironment Innately Modulates Cancer Progression. *Cancer Res, 79*(18), 4557-4566. doi:10.1158/0008-5472.CAN-18-3962

Hiramoto, K., Negishi, M., & Katoh, H. (2006). Dock4 is regulated by RhoG and promotes Rac-dependent cell migration. *Exp Cell Res, 312*(20), 4205-4216. doi:10.1016/j.yexcr.2006.09.006

Hsu, Y. H., Moya, M. L., Abiri, P., Hughes, C. C., George, S. C., & Lee, A. P. (2013). Full range physiological mass transport control in 3D tissue cultures. *Lab Chip, 13*(1), 81-89. doi:10.1039/c2lc40787f

Hu, L., Wang, B., & Zhang, Y. (2017). Serotonin 5-HT6 receptors affect cognition in a mouse model of Alzheimer's disease by regulating cilia function. *Alzheimers Res Ther, 9*(1), 76. doi:10.1186/s13195-017-0304-4

Huang, H., He, J., Johnson, D., Wei, Y., Liu, Y., Wang, S., . . . Semba, R. D. (2015). Deletion of placental growth factor prevents diabetic retinopathy and is associated with Akt activation and HIF1alpha-VEGF pathway inhibition. *Diabetes, 64*(1), 200-212. doi:10.2337/db14-0016

Huang, L., Chambliss, K. L., Gao, X., Yuhanna, I. S., Behling-Kelly, E., Bergaya, S., . . . Shaul, P. W. (2019). SR-B1 drives endothelial cell LDL transcytosis via DOCK4 to promote atherosclerosis. *Nature, 569*(7757), 565-569. doi:10.1038/s41586-019-1140-4

Huangfu, D., & Anderson, K. V. (2005). Cilia and Hedgehog responsiveness in the mouse. *Proc Natl Acad Sci U S A, 102*(32), 11325-11330. doi:10.1073/pnas.0505328102

Huangfu, D., Liu, A., Rakeman, A. S., Murcia, N. S., Niswander, L., & Anderson, K. V. (2003). Hedgehog signalling in the mouse requires intraflagellar transport proteins. *Nature, 426*(6962), 83-87. doi:10.1038/nature02061

Huh, D., Hamilton, G. A., & Ingber, D. E. (2011). From 3D cell culture to organs-on-chips. *Trends Cell Biol, 21*(12), 745-754. doi:10.1016/j.tcb.2011.09.005

Huh, D., Matthews, B. D., Mammoto, A., Montoya-Zavala, M., Hsin, H. Y., & Ingber, D. E. (2010). Reconstituting organ-level lung functions on a chip. *Science, 328*(5986), 1662-1668. doi:10.1126/science.1188302

Huh, D., Torisawa, Y. S., Hamilton, G. A., Kim, H. J., & Ingber, D. E. (2012). Microengineered physiological biomimicry: organs-on-chips. *Lab Chip, 12*(12), 2156-2164. doi:10.1039/c2lc40089h

Hussey, P. J., Ketelaar, T., & Deeks, M. J. (2006). Control of the actin cytoskeleton in plant cell growth. *Annu Rev Plant Biol, 57*, 109-125. doi:10.1146/annurev.arplant.57.032905.105206

Huttenlocher, A., & Horwitz, A. R. (2011). Integrins in cell migration. *Cold Spring Harb Perspect Biol, 3*(9), a005074. doi:10.1101/cshperspect.a005074

Hynes, R. O. (2007). Cell-matrix adhesion in vascular development. *J Thromb Haemost, 5 Suppl 1*, 32-40. doi:10.1111/j.1538-7836.2007.02569.x

Iomini, C., Tejada, K., Mo, W., Vaananen, H., & Piperno, G. (2004). Primary cilia of human endothelial cells disassemble under laminar shear stress. *J Cell Biol, 164*(6), 811-817. doi:10.1083/jcb.200312133

Ishikawa, H., & Marshall, W. F. (2011). Ciliogenesis: building the cell's antenna. *Nat Rev Mol Cell Biol, 12*(4), 222-234. doi:10.1038/nrm3085

Jackson, J. R., Seed, M. P., Kircher, C. H., Willoughby, D. A., & Winkler, J. D. (1997). The codependence of angiogenesis and chronic inflammation. *FASEB J, 11*(6), 457-465.

Jain, R. K. (2003). Molecular regulation of vessel maturation. *Nat Med, 9*(6), 685-693. doi:10.1038/nm0603-685

Jaipersad, A. S., Lip, G. Y., Silverman, S., & Shantsila, E. (2014). The role of monocytes in angiogenesis and atherosclerosis. *J Am Coll Cardiol, 63*(1), 1-11. doi:10.1016/j.jacc.2013.09.019

Jakobsson, L., Bentley, K., & Gerhardt, H. (2009). VEGFRs and Notch: a dynamic collaboration in vascular patterning. *Biochem Soc Trans, 37*(Pt 6), 1233-1236. doi:10.1042/BST0371233

Jakobsson, L., Franco, C. A., Bentley, K., Collins, R. T., Ponsioen, B., Aspalter, I. M., . . . Gerhardt, H. (2010). Endothelial cells dynamically compete for the tip cell position during angiogenic sprouting. *Nat Cell Biol, 12*(10), 943-953. doi:10.1038/ncb2103

Jang, K. J., Cho, H. S., Kang, D. H., Bae, W. G., Kwon, T. H., & Suh, K. Y. (2011). Fluid-shear-stress-induced translocation of aquaporin-2 and reorganization of actin cytoskeleton in renal tubular epithelial cells. *Integr Biol (Camb), 3*(2), 134-141. doi:10.1039/c0ib00018c

Jang, K. J., & Suh, K. Y. (2010). A multi-layer microfluidic device for efficient culture and analysis of renal tubular cells. *Lab Chip, 10*(1), 36-42. doi:10.1039/b907515a

Jensen, V. L., Li, C., Bowie, R. V., Clarke, L., Mohan, S., Blacque, O. E., & Leroux, M. R. (2015). Formation of the transition zone by Mks5/Rpgrip1L establishes a ciliary zone of exclusion (CIZE) that compartmentalises ciliary signalling proteins and controls PIP2 ciliary abundance. *EMBO J, 34*(20), 2537-2556. doi:10.15252/embj.201488044

Jin, X., Mohieldin, A. M., Muntean, B. S., Green, J. A., Shah, J. V., Mykytyn, K., & Nauli, S. M. (2014). Cilioplasm is a cellular compartment for calcium signaling in response to mechanical and chemical stimuli. *Cell Mol Life Sci, 71*(11), 2165-2178. doi:10.1007/s00018-013-1483-1

Joberty, G., Petersen, C., Gao, L., & Macara, I. G. (2000). The cell-polarity protein Par6 links Par3 and atypical protein kinase C to Cdc42. *Nat Cell Biol, 2*(8), 531-539. doi:10.1038/35019573

Jones, E. A., le Noble, F., & Eichmann, A. (2006). What determines blood vessel structure? Genetic prespecification vs. hemodynamics. *Physiology (Bethesda), 21*, 388-395. doi:10.1152/physiol.00020.2006

Jones, T. J., Adapala, R. K., Geldenhuys, W. J., Bursley, C., AbouAlaiwi, W. A., Nauli, S. M., & Thodeti, C. K. (2012). Primary cilia regulates the directional migration and barrier integrity of endothelial cells through the modulation of hsp27 dependent actin cytoskeletal organization. *J Cell Physiol, 227*(1), 70-76. doi:10.1002/jcp.22704

Kakiuchi, A., Kohno, T., Kakuki, T., Kaneko, Y., Konno, T., Hosaka, Y., . . . Kojima, T. (2019). Rho-kinase and PKCalpha Inhibition Induces Primary Cilia Elongation and Alters the Behavior of Undifferentiated and Differentiated Temperature-sensitive Mouse Cochlear Cells. *J Histochem Cytochem, 67*(7), 523-535. doi:10.1369/0022155419841013

Kallakuri, S., Yu, J. A., Li, J., Li, Y., Weinstein, B. M., Nicoli, S., & Sun, Z. (2015). Endothelial cilia are essential for developmental vascular integrity in zebrafish. *J Am Soc Nephrol, 26*(4), 864-875. doi:10.1681/ASN.2013121314

Kanai, A., Ihara, S., Ohdaira, T., Shinohara-Kanda, A., Iwamatsu, A., & Fukui, Y. (2008). Identification of DOCK4 and its splicing variant as PIP3 binding proteins. *IUBMB Life, 60*(7), 467-472. doi:10.1002/iub.67

Kang, E., & Shin, J. W. (2016). Pericyte-targeting drug delivery and tissue engineering. *Int J Nanomedicine, 11*, 2397-2406. doi:10.2147/IJN.S105274

Kang, H., Davis-Dusenbery, B. N., Nguyen, P. H., Lal, A., Lieberman, J., Van Aelst, L., . . . Hata, A. (2012). Bone morphogenetic protein 4 promotes vascular smooth muscle contractility by activating microRNA-21 (miR-21), which down-regulates expression of family of dedicator of cytokinesis (DOCK) proteins. *J Biol Chem, 287*(6), 3976-3986. doi:10.1074/jbc.M111.303156

Kawada, K., Upadhyay, G., Ferandon, S., Janarthanan, S., Hall, M., Vilardaga, J. P., & Yajnik, V. (2009). Cell migration is regulated by platelet-derived growth factor receptor endocytosis. *Mol Cell Biol, 29*(16), 4508-4518. doi:10.1128/MCB.00015-09

Kesavan, G., Sand, F. W., Greiner, T. U., Johansson, J. K., Kobberup, S., Wu, X., . . . Semb, H. (2009). Cdc42-mediated tubulogenesis controls cell specification. *Cell, 139*(4), 791-801. doi:10.1016/j.cell.2009.08.049

Khaitlina, S. Y. (2014). Intracellular transport based on actin polymerization. *Biochemistry (Mosc), 79*(9), 917-927. doi:10.1134/S0006297914090089

Khanna, H., Davis, E. E., Murga-Zamalloa, C. A., Estrada-Cuzcano, A., Lopez, I., den Hollander, A. I., . . . Katsanis, N. (2009). A common allele in RPGRIP1L is a modifier of retinal degeneration in ciliopathies. *Nat Genet, 41*(6), 739-745. doi:10.1038/ng.366

Kiesel, P., Alvarez Viar, G., Tsoy, N., Maraspini, R., Gorilak, P., Varga, V., . . . Pigino, G. (2020). The molecular structure of mammalian primary cilia revealed by cryo-electron tomography. *Nat Struct Mol Biol, 27*(12), 1115-1124. doi:10.1038/s41594-020-0507-4

Kilkenny, C., Browne, W., Cuthill, I. C., Emerson, M., Altman, D. G., & Group, N. C. R. R. G. W. (2010). Animal research: reporting in vivo experiments: the ARRIVE guidelines. *Br J Pharmacol, 160*(7), 1577-1579. doi:10.1111/j.1476-5381.2010.00872.x

Kim, H. J., Huh, D., Hamilton, G., & Ingber, D. E. (2012). Human gut-on-a-chip inhabited by microbial flora that experiences intestinal peristalsis-like motions and flow. *Lab Chip, 12*(12), 2165-2174. doi:10.1039/c2lc40074j

Kim, J., Jo, H., Hong, H., Kim, M. H., Kim, J. M., Lee, J. K., . . . Kim, J. (2015). Actin remodelling factors control ciliogenesis by regulating YAP/TAZ activity and vesicle trafficking. *Nat Commun, 6*, 6781. doi:10.1038/ncomms7781

Kim, J., Lee, J. E., Heynen-Genel, S., Suyama, E., Ono, K., Lee, K., . . . Gleeson, J. G. (2010). Functional genomic screen for modulators of ciliogenesis and cilium length. *Nature, 464*(7291), 1048-1051. doi:10.1038/nature08895

Kim, M., A, M. S., Ewald, A. J., Werb, Z., & Mostov, K. E. (2015). p114RhoGEF governs cell motility and lumen formation during tubulogenesis through a ROCK-myosin-II pathway. *J Cell Sci, 128*(23), 4317-4327. doi:10.1242/jcs.172361

Kim, S., Lee, H., Chung, M., & Jeon, N. L. (2013). Engineering of functional, perfusable 3D microvascular networks on a chip. *Lab Chip, 13*(8), 1489-1500. doi:10.1039/c3lc41320a

Kinzel, D., Boldt, K., Davis, E. E., Burtscher, I., Trumbach, D., Diplas, B., . . . Lickert, H. (2010). Pitchfork regulates primary cilia disassembly and left-right asymmetry. *Dev Cell, 19*(1), 66-77. doi:10.1016/j.devcel.2010.06.005

Klein, S., Bikfalvi, A., Birkenmeier, T. M., Giancotti, F. G., & Rifkin, D. B. (1996). Integrin regulation by endogenous expression of 18-kDa fibroblast growth factor-2. *J Biol Chem, 271*(37), 22583-22590. doi:10.1074/jbc.271.37.22583

Klein, S., Giancotti, F. G., Presta, M., Albelda, S. M., Buck, C. A., & Rifkin, D. B. (1993). Basic fibroblast growth factor modulates integrin expression in microvascular endothelial cells. *Mol Biol Cell, 4*(10), 973-982. doi:10.1091/mbc.4.10.973

Klems, A., van Rijssel, J., Ramms, A. S., Wild, R., Hammer, J., Merkel, M., . . . le Noble, F. (2020). The GEF Trio controls endothelial cell size and arterial remodeling downstream of Vegf signaling in both zebrafish and cell models. *Nat Commun, 11*(1), 5319. doi:10.1038/s41467-020-19008-0

Kobialka, P., & Graupera, M. (2019). Revisiting PI3-kinase signalling in angiogenesis. *Vasc Biol, 1*(1), H125-H134. doi:10.1530/VB-19-0025

Kochhan, E., Lenard, A., Ellertsdottir, E., Herwig, L., Affolter, M., Belting, H. G., & Siekmann, A. F. (2013). Blood flow changes coincide with cellular rearrangements during blood vessel pruning in zebrafish embryos. *PLoS One, 8*(10), e75060. doi:10.1371/journal.pone.0075060

Koh, W., Mahan, R. D., & Davis, G. E. (2008). Cdc42- and Rac1-mediated endothelial lumen formation requires Pak2, Pak4 and Par3, and PKC-dependent signaling. *J Cell Sci, 121*(Pt 7), 989-1001. doi:10.1242/jcs.020693

Konerding, M. A., Turhan, A., Ravnic, D. J., Lin, M., Fuchs, C., Secomb, T. W., . . . Mentzer, S. J. (2010). Inflammation-induced intussusceptive angiogenesis in murine colitis. *Anat Rec (Hoboken), 293*(5), 849-857. doi:10.1002/ar.21110

Korn, C., & Augustin, H. G. (2015). Mechanisms of Vessel Pruning and Regression. *Dev Cell, 34*(1), 5-17. doi:10.1016/j.devcel.2015.06.004

Korpelainen, E. I., & Alitalo, K. (1998). Signaling angiogenesis and lymphangiogenesis. *Curr Opin Cell Biol, 10*(2), 159-164. doi:10.1016/s0955-0674(98)80137-3

Krock, B. L., Skuli, N., & Simon, M. C. (2011). Hypoxia-induced angiogenesis: good and evil. *Genes Cancer, 2*(12), 1117-1133. doi:10.1177/1947601911423654

Krugmann, S., Jordens, I., Gevaert, K., Driessens, M., Vandekerckhove, J., & Hall, A. (2001). Cdc42 induces filopodia by promoting the formation of an IRSp53:Mena complex. *Curr Biol, 11*(21), 1645-1655. doi:10.1016/s0960-9822(01)00506-1

Kubis, N., & Levy, B. I. (2003). Vasculogenesis and angiogenesis: molecular and cellular controls. Part 1: growth factors. *Interv Neuroradiol, 9*(3), 227-237. doi:10.1177/159101990300900301

Kubo, T., Yanagisawa, H. A., Yagi, T., Hirono, M., & Kamiya, R. (2010). Tubulin polyglutamylation regulates axonemal motility by modulating activities of inner-arm dyneins. *Curr Biol, 20*(5), 441-445. doi:10.1016/j.cub.2009.12.058

Kucera, T., Strilic, B., Regener, K., Schubert, M., Laudet, V., & Lammert, E. (2009). Ancestral vascular lumen formation via basal cell surfaces. *PLoS One, 4*(1), e4132. doi:10.1371/journal.pone.0004132

Kuczynski, E. A., Vermeulen, P. B., Pezzella, F., Kerbel, R. S., & Reynolds, A. R. (2019). Vessel co-option in cancer. *Nat Rev Clin Oncol, 16*(8), 469-493. doi:10.1038/s41571-019-0181-9

Kurz, H., Burri, P. H., & Djonov, V. G. (2003). Angiogenesis and vascular remodeling by intussusception: from form to function. *News Physiol Sci, 18*, 65-70. doi:10.1152/nips.01417.2002

Kusano, K. F., Allendoerfer, K. L., Munger, W., Pola, R., Bosch-Marce, M., Kirchmair, R., . . . Losordo, D. W. (2004). Sonic hedgehog induces arteriogenesis in diabetic vasa nervorum and restores function in diabetic neuropathy. *Arterioscler Thromb Vasc Biol, 24*(11), 2102-2107. doi:10.1161/01.ATV.0000144813.44650.75

Kuzmic, N., Moore, T., Devadas, D., & Young, E. W. K. (2019). Modelling of endothelial cell migration and angiogenesis in microfluidic cell culture systems. *Biomech Model Mechanobiol, 18*(3), 717-731. doi:10.1007/s10237-018-01111-3

Kwei, S., Stavrakis, G., Takahas, M., Taylor, G., Folkman, M. J., Gimbrone, M. A., Jr., & Garcia-Cardena, G. (2004). Early adaptive responses of the vascular wall during venous arterialization in mice. *Am J Pathol, 164*(1), 81-89. doi:10.1016/S0002-9440(10)63099-4

Kwon, R. Y., Temiyasathit, S., Tummala, P., Quah, C. C., & Jacobs, C. R. (2010). Primary cilium-dependent mechanosensing is mediated by adenylyl cyclase 6 and cyclic AMP in bone cells. *FASEB J, 24*(8), 2859-2868. doi:10.1096/fj.09-148007

Laham, R. J., Rezaee, M., Post, M., Sellke, F. W., Braeckman, R. A., Hung, D., & Simons, M. (1999). Intracoronary and intravenous administration of basic fibroblast growth factor: myocardial and tissue distribution. *Drug Metab Dispos, 27*(7), 821-826.

Lake, A. V. R., , C. E. L. S., Subaashini Natarajan, , B. B., , S. K. B., , T. S., , R. T., . . . , R. F., Colin A. Johnson. (2020). Drug and siRNA screens identify ROCK2 as a therapeutic target for ciliopathies. *bioRXiv*. doi: https://doi.org/10.1101/2020.11.26.393801

Lamalice, L., Le Boeuf, F., & Huot, J. (2007). Endothelial cell migration during angiogenesis. *Circ Res, 100*(6), 782-794. doi:10.1161/01.RES.0000259593.07661.1e

Lammert, E., & Axnick, J. (2012). Vascular lumen formation. *Cold Spring Harb Perspect Med, 2*(4), a006619. doi:10.1101/cshperspect.a006619

Lampugnani, M. G. (2012). Endothelial cell-to-cell junctions: adhesion and signaling in physiology and pathology. *Cold Spring Harb Perspect Med, 2*(10). doi:10.1101/cshperspect.a006528

Lampugnani, M. G., Orsenigo, F., Rudini, N., Maddaluno, L., Boulday, G., Chapon, F., & Dejana, E. (2010). CCM1 regulates vascular-lumen organization by inducing endothelial polarity. *J Cell Sci, 123*(Pt 7), 1073-1080. doi:10.1242/jcs.059329

Lavina, B., Castro, M., Niaudet, C., Cruys, B., Alvarez-Aznar, A., Carmeliet, P., . . . Gaengel, K. (2018). Defective endothelial cell migration in the absence of Cdc42 leads to capillary-venous malformations. *Development, 145*(13). doi:10.1242/dev.161182

Lawson, N. D., Vogel, A. M., & Weinstein, B. M. (2002). sonic hedgehog and vascular endothelial growth factor act upstream of the Notch pathway during arterial endothelial differentiation. *Dev Cell, 3*(1), 127-136. doi:10.1016/s1534-5807(02)00198-3

le Noble, F., Klein, C., Tintu, A., Pries, A., & Buschmann, I. (2008). Neural guidance molecules, tip cells, and mechanical factors in vascular development. *Cardiovasc Res, 78*(2), 232-241. doi:10.1093/cvr/cvn058

Lechtreck, K. F., Brown, J. M., Sampaio, J. L., Craft, J. M., Shevchenko, A., Evans, J. E., & Witman, G. B. (2013). Cycling of the signaling protein phospholipase D through cilia requires the BBSome only for the export phase. *J Cell Biol, 201*(2), 249-261. doi:10.1083/jcb.201207139

Lee, J. G., & Kay, E. P. (2006). FGF-2-mediated signal transduction during endothelial mesenchymal transformation in corneal endothelial cells. *Exp Eye Res, 83*(6), 1309-1316. doi:10.1016/j.exer.2006.04.007

Lee, K. L., Guevarra, M. D., Nguyen, A. M., Chua, M. C., Wang, Y., & Jacobs, C. R. (2015). The primary cilium functions as a mechanical and calcium signaling nexus. *Cilia, 4*, 7. doi:10.1186/s13630-015-0016-y

Lee, S., Tan, H. Y., Geneva, II, Kruglov, A., & Calvert, P. D. (2018). Actin filaments partition primary cilia membranes into distinct fluid corrals. *J Cell Biol, 217*(8), 2831-2849. doi:10.1083/jcb.201711104

Lenard, A., Ellertsdottir, E., Herwig, L., Krudewig, A., Sauteur, L., Belting, H. G., & Affolter, M. (2013). In vivo analysis reveals a highly stereotypic morphogenetic pathway of vascular anastomosis. *Dev Cell, 25*(5), 492-506. doi:10.1016/j.devcel.2013.05.010

Leung, D. W., Cachianes, G., Kuang, W. J., Goeddel, D. V., & Ferrara, N. (1989). Vascular endothelial growth factor is a secreted angiogenic mitogen. *Science, 246*(4935), 1306-1309. doi:10.1126/science.2479986

Li, A., Saito, M., Chuang, J. Z., Tseng, Y. Y., Dedesma, C., Tomizawa, K., . . . Sung, C. H. (2011). Ciliary transition zone activation of phosphorylated Tctex-1 controls ciliary resorption, S-phase entry and fate of neural progenitors. *Nat Cell Biol, 13*(4), 402-411. doi:10.1038/ncb2218

Li, H., Li, J., Li, Y., Singh, P., Cao, L., Xu, L. J., . . . Zheng, X. L. (2012). Sonic hedgehog promotes autophagy of vascular smooth muscle cells. *Am J Physiol Heart Circ Physiol, 303*(11), H1319-1331. doi:10.1152/ajpheart.00160.2012

Li, J., Liu, Y., Jin, Y., Wang, R., Wang, J., Lu, S., . . . Peng, X. (2017). Essential role of Cdc42 in cardiomyocyte proliferation and cell-cell adhesion during

heart development. *Dev Biol, 421*(2), 271-283. doi:10.1016/j.ydbio.2016.12.012

Lin, A., Peiris, N. J., Dhaliwal, H., Hakim, M., Li, W., Ganesh, S., . . . Misra, A. (2021). Mural Cells: Potential Therapeutic Targets to Bridge Cardiovascular Disease and Neurodegeneration. *Cells, 10*(3). doi:10.3390/cells10030593

Liu, J., Wada, Y., Katsura, M., Tozawa, H., Erwin, N., Kapron, C. M., . . . Liu, J. (2018). Rho-Associated Coiled-Coil Kinase (ROCK) in Molecular Regulation of Angiogenesis. *Theranostics, 8*(21), 6053-6069. doi:10.7150/thno.30305

Lizama, C. O., & Zovein, A. C. (2013). Polarizing pathways: balancing endothelial polarity, permeability, and lumen formation. *Exp Cell Res, 319*(9), 1247-1254. doi:10.1016/j.yexcr.2013.03.028

Louvi, A., & Grove, E. A. (2011). Cilia in the CNS: the quiet organelle claims center stage. *Neuron, 69*(6), 1046-1060. doi:10.1016/j.neuron.2011.03.002

Lu, M., Kinchen, J. M., Rossman, K. L., Grimsley, C., Hall, M., Sondek, J., . . . Ravichandran, K. S. (2005). A Steric-inhibition model for regulation of nucleotide exchange via the Dock180 family of GEFs. *Curr Biol, 15*(4), 371-377. doi:10.1016/j.cub.2005.01.050

Lugano, R., Ramachandran, M., & Dimberg, A. (2020). Tumor angiogenesis: causes, consequences, challenges and opportunities. *Cell Mol Life Sci, 77*(9), 1745-1770. doi:10.1007/s00018-019-03351-7

Luu, V. Z., Chowdhury, B., Al-Omran, M., Hess, D. A., & Verma, S. (2018). Role of endothelial primary cilia as fluid mechanosensors on vascular health. *Atherosclerosis, 275*, 196-204. doi:10.1016/j.atherosclerosis.2018.06.818

Ma, N., & Zhou, J. (2020). Functions of Endothelial Cilia in the Regulation of Vascular Barriers. *Front Cell Dev Biol, 8*, 626. doi:10.3389/fcell.2020.00626

Machacek, M., Hodgson, L., Welch, C., Elliott, H., Pertz, O., Nalbant, P., . . . Danuser, G. (2009). Coordination of Rho GTPase activities during cell protrusion. *Nature, 461*(7260), 99-103. doi:10.1038/nature08242

Madou, M. J. (2011). Manufacturing Techniques for Microfabrication and Nanotechnology. *2*, 670.

Makanya, A. N., Hlushchuk, R., & Djonov, V. G. (2009). Intussusceptive angiogenesis and its role in vascular morphogenesis, patterning, and remodeling. *Angiogenesis, 12*(2), 113-123. doi:10.1007/s10456-009-9129-5

Malicki, J. J., & Johnson, C. A. (2017). The Cilium: Cellular Antenna and Central Processing Unit. *Trends Cell Biol, 27*(2), 126-140. doi:10.1016/j.tcb.2016.08.002

Mammoto, T., Mammoto, A., Torisawa, Y. S., Tat, T., Gibbs, A., Derda, R., . . . Ingber, D. E. (2011). Mechanochemical control of mesenchymal condensation and embryonic tooth organ formation. *Dev Cell, 21*(4), 758-769. doi:10.1016/j.devcel.2011.07.006

Masyuk, A. I., Masyuk, T. V., Splinter, P. L., Huang, B. Q., Stroope, A. J., & LaRusso, N. F. (2006). Cholangiocyte cilia detect changes in luminal fluid flow and transmit them into intracellular Ca2+ and cAMP signaling. *Gastroenterology, 131*(3), 911-920. doi:10.1053/j.gastro.2006.07.003

Mavria, G., Vercoulen, Y., Yeo, M., Paterson, H., Karasarides, M., Marais, R., . . . Marshall, C. J. (2006). ERK-MAPK signaling opposes Rho-kinase to promote endothelial cell survival and sprouting during angiogenesis. *Cancer Cell, 9*(1), 33-44. doi:10.1016/j.ccr.2005.12.021

Mazurek, R., Dave, J. M., Chandran, R. R., Misra, A., Sheikh, A. Q., & Greif, D. M. (2017). Vascular Cells in Blood Vessel Wall Development and Disease. *Adv Pharmacol, 78*, 323-350. doi:10.1016/bs.apha.2016.08.001

McMahon, H. T., & Gallop, J. L. (2005). Membrane curvature and mechanisms of dynamic cell membrane remodelling. *Nature, 438*(7068), 590-596. doi:10.1038/nature04396

Mehidi, A., Rossier, O., Schaks, M., Chazeau, A., Biname, F., Remorino, A., . . . Giannone, G. (2019). Transient Activations of Rac1 at the Lamellipodium Tip Trigger Membrane Protrusion. *Curr Biol, 29*(17), 2852-2866 e2855. doi:10.1016/j.cub.2019.07.035

Melincovici, C. S., Bosca, A. B., Susman, S., Marginean, M., Mihu, C., Istrate, M., . . . Mihu, C. M. (2018). Vascular endothelial growth factor (VEGF) - key factor in normal and pathological angiogenesis. *Rom J Morphol Embryol, 59*(2), 455-467.

Mentzer, S. J., & Konerding, M. A. (2014). Intussusceptive angiogenesis: expansion and remodeling of microvascular networks. *Angiogenesis, 17*(3), 499-509. doi:10.1007/s10456-014-9428-3

Mielczarek, W. S., Obaje, E. A., Bachmann, T. T., & Kersaudy-Kerhoas, M. (2016). Microfluidic blood plasma separation for medical diagnostics: is it worth it? *Lab Chip, 16*(18), 3441-3448. doi:10.1039/c6lc00833j

Mirvis, M., Stearns, T., & James Nelson, W. (2018). Cilium structure, assembly, and disassembly regulated by the cytoskeleton. *Biochem J, 475*(14), 2329-2353. doi:10.1042/BCJ20170453

Miyamoto, Y., Yamauchi, J., Sanbe, A., & Tanoue, A. (2007). Dock6, a Dock-C subfamily guanine nucleotide exchanger, has the dual specificity for Rac1 and Cdc42 and regulates neurite outgrowth. *Exp Cell Res, 313*(4), 791-804. doi:10.1016/j.yexcr.2006.11.017

Mohieldin, A. M., Zubayer, H. S., Al Omran, A. J., Saternos, H. C., Zarban, A. A., Nauli, S. M., & AbouAlaiwi, W. A. (2016). Vascular Endothelial Primary Cilia: Mechanosensation and Hypertension. *Curr Hypertens Rev, 12*(1), 57-67. doi:10.2174/1573402111666150630140615

Molla-Herman, A., Ghossoub, R., Blisnick, T., Meunier, A., Serres, C., Silbermann, F., . . . Benmerah, A. (2010). The ciliary pocket: an endocytic membrane domain at the base of primary and motile cilia. *J Cell Sci, 123*(Pt 10), 1785-1795. doi:10.1242/jcs.059519

Montero-Balaguer, M., Swirsding, K., Orsenigo, F., Cotelli, F., Mione, M., & Dejana, E. (2009). Stable vascular connections and remodeling require full expression of VE-cadherin in zebrafish embryos. *PLoS One, 4*(6), e5772. doi:10.1371/journal.pone.0005772

Morrow, D., Sweeney, C., Birney, Y. A., Guha, S., Collins, N., Cummins, P. M., . . . Cahill, P. A. (2007). Biomechanical regulation of hedgehog signaling in vascular smooth muscle cells in vitro and in vivo. *Am J Physiol Cell Physiol, 292*(1), C488-496. doi:10.1152/ajpcell.00337.2005

Morton, W. M., Ayscough, K. R., & McLaughlin, P. J. (2000). Latrunculin alters the actin-monomer subunit interface to prevent polymerization. *Nat Cell Biol, 2*(6), 376-378. doi:10.1038/35014075

Moscatelli, D., Presta, M., & Rifkin, D. B. (1986). Purification of a factor from human placenta that stimulates capillary endothelial cell protease

production, DNA synthesis, and migration. *Proc Natl Acad Sci U S A, 83*(7), 2091-2095. doi:10.1073/pnas.83.7.2091

Moya, M. L., Hsu, Y. H., Lee, A. P., Hughes, C. C., & George, S. C. (2013). In vitro perfused human capillary networks. *Tissue Eng Part C Methods, 19*(9), 730-737. doi:10.1089/ten.TEC.2012.0430

Moyer, J. H., Lee-Tischler, M. J., Kwon, H. Y., Schrick, J. J., Avner, E. D., Sweeney, W. E., . . . Woychik, R. P. (1994). Candidate gene associated with a mutation causing recessive polycystic kidney disease in mice. *Science, 264*(5163), 1329-1333. doi:10.1126/science.8191288

Murrant, C. L., Lamb, I. R., & Novielli, N. M. (2017). Capillary endothelial cells as coordinators of skeletal muscle blood flow during active hyperemia. *Microcirculation, 24*(3). doi:10.1111/micc.12348

Nachury, M. V., Seeley, E. S., & Jin, H. (2010). Trafficking to the ciliary membrane: how to get across the periciliary diffusion barrier? *Annu Rev Cell Dev Biol, 26*, 59-87. doi:10.1146/annurev.cellbio.042308.113337

Nagai, T., & Mizuno, K. (2017). Jasplakinolide induces primary cilium formation through cell rounding and YAP inactivation. *PLoS One, 12*(8), e0183030. doi:10.1371/journal.pone.0183030

Nagata, A., Hamamoto, A., Horikawa, M., Yoshimura, K., Takeda, S., & Saito, Y. (2013). Characterization of ciliary targeting sequence of rat melanin-concentrating hormone receptor 1. *Gen Comp Endocrinol, 188*, 159-165. doi:10.1016/j.ygcen.2013.02.020

Nager, A. R., Goldstein, J. S., Herranz-Perez, V., Portran, D., Ye, F., Garcia-Verdugo, J. M., & Nachury, M. V. (2017). An Actin Network Dispatches Ciliary GPCRs into Extracellular Vesicles to Modulate Signaling. *Cell, 168*(1-2), 252-263 e214. doi:10.1016/j.cell.2016.11.036

Narita, K., Kawate, T., Kakinuma, N., & Takeda, S. (2010). Multiple primary cilia modulate the fluid transcytosis in choroid plexus epithelium. *Traffic, 11*(2), 287-301. doi:10.1111/j.1600-0854.2009.01016.x

Nauli, S. M., Alenghat, F. J., Luo, Y., Williams, E., Vassilev, P., Li, X., . . . Zhou, J. (2003). Polycystins 1 and 2 mediate mechanosensation in the primary cilium of kidney cells. *Nat Genet, 33*(2), 129-137. doi:10.1038/ng1076

Nauli, S. M., Kawanabe, Y., Kaminski, J. J., Pearce, W. J., Ingber, D. E., & Zhou, J. (2008). Endothelial cilia are fluid shear sensors that regulate calcium

signaling and nitric oxide production through polycystin-1. *Circulation, 117*(9), 1161-1171. doi:10.1161/CIRCULATIONAHA.107.710111

Nauli, S. M., & Zhou, J. (2004). Polycystins and mechanosensation in renal and nodal cilia. *Bioessays, 26*(8), 844-856. doi:10.1002/bies.20069

Ng, C. P., Hinz, B., & Swartz, M. A. (2005). Interstitial fluid flow induces myofibroblast differentiation and collagen alignment in vitro. *J Cell Sci, 118*(Pt 20), 4731-4739. doi:10.1242/jcs.02605

Ng, C. P., & Swartz, M. A. (2003). Fibroblast alignment under interstitial fluid flow using a novel 3-D tissue culture model. *Am J Physiol Heart Circ Physiol, 284*(5), H1771-1777. doi:10.1152/ajpheart.01008.2002

Nielsen, J. S., & McNagny, K. M. (2008). Novel functions of the CD34 family. *J Cell Sci, 121*(Pt 22), 3683-3692. doi:10.1242/jcs.037507

Nowak-Sliwinska, P., Alitalo, K., Allen, E., Anisimov, A., Aplin, A. C., Auerbach, R., . . . Griffioen, A. W. (2018). Consensus guidelines for the use and interpretation of angiogenesis assays. *Angiogenesis, 21*(3), 425-532. doi:10.1007/s10456-018-9613-x

Olsson, A. K., Dimberg, A., Kreuger, J., & Claesson-Welsh, L. (2006). VEGF receptor signalling - in control of vascular function. *Nat Rev Mol Cell Biol, 7*(5), 359-371. doi:10.1038/nrm1911

Otto, E. A., Ramaswami, G., Janssen, S., Chaki, M., Allen, S. J., Zhou, W., . . . Group, G. P. N. S. (2011). Mutation analysis of 18 nephronophthisis associated ciliopathy disease genes using a DNA pooling and next generation sequencing strategy. *J Med Genet, 48*(2), 105-116. doi:10.1136/jmg.2010.082552

P.Reynolds, O. O. Y. G. (2010). Functional Pharmacogenetics of Serotonin Receptors in Psychiatric Drug Action. *21*, 791-806. doi:https://doi.org/10.1016/S1569-7339(10)70110-7

Pala, R., Alomari, N., & Nauli, S. M. (2017). Primary Cilium-Dependent Signaling Mechanisms. *Int J Mol Sci, 18*(11). doi:10.3390/ijms18112272

Pala, R., Jamal, M., Alshammari, Q., & Nauli, S. M. (2018). The Roles of Primary Cilia in Cardiovascular Diseases. *Cells, 7*(12), 233. doi:10.3390/cells7120233

Palis, J., & Yoder, M. C. (2001). Yolk-sac hematopoiesis: the first blood cells of mouse and man. *Exp Hematol, 29*(8), 927-936. doi:10.1016/s0301-472x(01)00669-5

Pan, J., & Snell, W. J. (2005). Chlamydomonas shortens its flagella by activating axonemal disassembly, stimulating IFT particle trafficking, and blocking anterograde cargo loading. *Dev Cell, 9*(3), 431-438. doi:10.1016/j.devcel.2005.07.010

Pan, J., You, Y., Huang, T., & Brody, S. L. (2007). RhoA-mediated apical actin enrichment is required for ciliogenesis and promoted by Foxj1. *J Cell Sci, 120*(Pt 11), 1868-1876. doi:10.1242/jcs.005306

Park, T. H., & Shuler, M. L. (2003). Integration of cell culture and microfabrication technology. *Biotechnol Prog, 19*(2), 243-253. doi:10.1021/bp020143k

Parker, J. D., Hilton, L. K., Diener, D. R., Rasi, M. Q., Mahjoub, M. R., Rosenbaum, J. L., & Quarmby, L. M. (2010). Centrioles are freed from cilia by severing prior to mitosis. *Cytoskeleton (Hoboken), 67*(7), 425-430. doi:10.1002/cm.20454

Parsons, J. T., Horwitz, A. R., & Schwartz, M. A. (2010). Cell adhesion: integrating cytoskeletal dynamics and cellular tension. *Nat Rev Mol Cell Biol, 11*(9), 633-643. doi:10.1038/nrm2957

Patel-Hett, S., & D'Amore, P. A. (2011). Signal transduction in vasculogenesis and developmental angiogenesis. *Int J Dev Biol, 55*(4-5), 353-363. doi:10.1387/ijdb.103213sp

Pathak, N., Obara, T., Mangos, S., Liu, Y., & Drummond, I. A. (2007). The zebrafish fleer gene encodes an essential regulator of cilia tubulin polyglutamylation. *Mol Biol Cell, 18*(11), 4353-4364. doi:10.1091/mbc.e07-06-0537

Pazour, G. J., Baker, S. A., Deane, J. A., Cole, D. G., Dickert, B. L., Rosenbaum, J. L., . . . Besharse, J. C. (2002). The intraflagellar transport protein, IFT88, is essential for vertebrate photoreceptor assembly and maintenance. *J Cell Biol, 157*(1), 103-113. doi:10.1083/jcb.200107108

Pazour, G. J., Dickert, B. L., Vucica, Y., Seeley, E. S., Rosenbaum, J. L., Witman, G. B., & Cole, D. G. (2000). Chlamydomonas IFT88 and its mouse homologue, polycystic kidney disease gene tg737, are required for

assembly of cilia and flagella. *J Cell Biol, 151*(3), 709-718. doi:10.1083/jcb.151.3.709

Pedersen, L. B., & Rosenbaum, J. L. (2008). Intraflagellar transport (IFT) role in ciliary assembly, resorption and signalling. *Curr Top Dev Biol, 85*, 23-61. doi:10.1016/S0070-2153(08)00802-8

Pennisi, D. J., & Mikawa, T. (2005). Normal patterning of the coronary capillary plexus is dependent on the correct transmural gradient of FGF expression in the myocardium. *Dev Biol, 279*(2), 378-390. doi:10.1016/j.ydbio.2004.12.028

Pepper, M. S., & Skobe, M. (2003). Lymphatic endothelium: morphological, molecular and functional properties. *J Cell Biol, 163*(2), 209-213. doi:10.1083/jcb.200308082

Peralta, M., Ortiz Lopez, L., Jerabkova, K., Lucchesi, T., Vitre, B., Han, D., . . . Vermot, J. (2020). Intraflagellar Transport Complex B Proteins Regulate the Hippo Effector Yap1 during Cardiogenesis. *Cell Rep, 32*(3), 107932. doi:10.1016/j.celrep.2020.107932

Perrin, S. (2014). Preclinical research: Make mouse studies work. *Nature, 507*(7493), 423-425. doi:10.1038/507423a

Phng, L. K., & Gerhardt, H. (2009). Angiogenesis: a team effort coordinated by notch. *Dev Cell, 16*(2), 196-208. doi:10.1016/j.devcel.2009.01.015

Phua, S. C., Chiba, S., Suzuki, M., Su, E., Roberson, E. C., Pusapati, G. V., . . . Inoue, T. (2017). Dynamic Remodeling of Membrane Composition Drives Cell Cycle through Primary Cilia Excision. *Cell, 168*(1-2), 264-279 e215. doi:10.1016/j.cell.2016.12.032

Piao, T., Luo, M., Wang, L., Guo, Y., Li, D., Li, P., . . . Pan, J. (2009). A microtubule depolymerizing kinesin functions during both flagellar disassembly and flagellar assembly in Chlamydomonas. *Proc Natl Acad Sci U S A, 106*(12), 4713-4718. doi:10.1073/pnas.0808671106

Piperno, G., Mead, K., & Henderson, S. (1996). Inner dynein arms but not outer dynein arms require the activity of kinesin homologue protein KHP1(FLA10) to reach the distal part of flagella in Chlamydomonas. *J Cell Biol, 133*(2), 371-379. doi:10.1083/jcb.133.2.371

Pola, R., Ling, L. E., Aprahamian, T. R., Barban, E., Bosch-Marce, M., Curry, C., . . . Losordo, D. W. (2003). Postnatal recapitulation of embryonic

hedgehog pathway in response to skeletal muscle ischemia. *Circulation, 108*(4), 479-485. doi:10.1161/01.CIR.0000080338.60981.FA

Pollard, T. D. (2016). Actin and Actin-Binding Proteins. *Cold Spring Harb Perspect Biol, 8*(8). doi:10.1101/cshperspect.a018226

Pollard, T. D., & Borisy, G. G. (2003). Cellular motility driven by assembly and disassembly of actin filaments. *Cell, 112*(4), 453-465. doi:10.1016/s0092-8674(03)00120-x

Polycystic kidney disease: the complete structure of the PKD1 gene and its protein. The International Polycystic Kidney Disease Consortium. (1995). *Cell, 81*(2), 289-298. doi:10.1016/0092-8674(95)90339-9

Potente, M., Gerhardt, H., & Carmeliet, P. (2011). Basic and therapeutic aspects of angiogenesis. *Cell, 146*(6), 873-887. doi:10.1016/j.cell.2011.08.039

Praetorius, H. A. (2015). The primary cilium as sensor of fluid flow: new building blocks to the model. A review in the theme: cell signaling: proteins, pathways and mechanisms. *Am J Physiol Cell Physiol, 308*(3), C198-208. doi:10.1152/ajpcell.00336.2014

Pugacheva, E. N., Jablonski, S. A., Hartman, T. R., Henske, E. P., & Golemis, E. A. (2007). HEF1-dependent Aurora A activation induces disassembly of the primary cilium. *Cell, 129*(7), 1351-1363. doi:10.1016/j.cell.2007.04.035

Rajendran, P., Rengarajan, T., Thangavel, J., Nishigaki, Y., Sakthisekaran, D., Sethi, G., & Nishigaki, I. (2013). The vascular endothelium and human diseases. *Int J Biol Sci, 9*(10), 1057-1069. doi:10.7150/ijbs.7502

Ramo, K., Sugamura, K., Craige, S., Keaney, J. F., & Davis, R. J. (2016). Suppression of ischemia in arterial occlusive disease by JNK-promoted native collateral artery development. *Elife, 5*. doi:10.7554/eLife.18414

Ran, J., Liu, M., Feng, J., Li, H., Ma, H., Song, T., . . . Zhou, J. (2020). ASK1-Mediated Phosphorylation Blocks HDAC6 Ubiquitination and Degradation to Drive the Disassembly of Photoreceptor Connecting Cilia. *Dev Cell, 53*(3), 287-299 e285. doi:10.1016/j.devcel.2020.03.010

Rangel, L., Bernabe-Rubio, M., Fernandez-Barrera, J., Casares-Arias, J., Millan, J., Alonso, M. A., & Correas, I. (2019). Caveolin-1alpha regulates primary cilium length by controlling RhoA GTPase activity. *Sci Rep, 9*(1), 1116. doi:10.1038/s41598-018-38020-5

Reale, A., Melaccio, A., Lamanuzzi, A., Saltarella, I., Dammacco, F., Vacca, A., & Ria, R. (2016). Functional and Biological Role of Endothelial Precursor Cells in Tumour Progression: A New Potential Therapeutic Target in Haematological Malignancies. *Stem Cells Int, 2016*, 7954580. doi:10.1155/2016/7954580

Reichman-Fried, M., & Raz, E. (2016). Blood, blebs and lumen expansion. *Nat Cell Biol, 18*(4), 366-367. doi:10.1038/ncb3334

Reiter, J. F., & Leroux, M. R. (2017). Genes and molecular pathways underpinning ciliopathies. *Nat Rev Mol Cell Biol, 18*(9), 533-547. doi:10.1038/nrm.2017.60

Reynolds, D. S., Tevis, K. M., Blessing, W. A., Colson, Y. L., Zaman, M. H., & Grinstaff, M. W. (2017). Breast Cancer Spheroids Reveal a Differential Cancer Stem Cell Response to Chemotherapeutic Treatment. *Sci Rep, 7*(1), 10382. doi:10.1038/s41598-017-10863-4

Ribatti, D., & Djonov, V. (2012). Intussusceptive microvascular growth in tumors. *Cancer Lett, 316*(2), 126-131. doi:10.1016/j.canlet.2011.10.040

Ridley, A. J. (2006). Rho GTPases and actin dynamics in membrane protrusions and vesicle trafficking. *Trends Cell Biol, 16*(10), 522-529. doi:10.1016/j.tcb.2006.08.006

Ridley, A. J., & Hall, A. (1992). The small GTP-binding protein rho regulates the assembly of focal adhesions and actin stress fibers in response to growth factors. *Cell, 70*(3), 389-399. doi:10.1016/0092-8674(92)90163-7

Risau, W. (1997). Mechanisms of angiogenesis. *Nature, 386*(6626), 671-674. doi:10.1038/386671a0

Risau, W., & Flamme, I. (1995). Vasculogenesis. *Annu Rev Cell Dev Biol, 11*, 73-91. doi:10.1146/annurev.cb.11.110195.000445

Risau, W., Sariola, H., Zerwes, H. G., Sasse, J., Ekblom, P., Kemler, R., & Doetschman, T. (1988). Vasculogenesis and angiogenesis in embryonic-stem-cell-derived embryoid bodies. *Development, 102*(3), 471-478. doi:10.1242/dev.102.3.471

Robert, A., Margall-Ducos, G., Guidotti, J. E., Bregerie, O., Celati, C., Brechot, C., & Desdouets, C. (2007). The intraflagellar transport component IFT88/polaris is a centrosomal protein regulating G1-S transition in non-ciliated cells. *J Cell Sci, 120*(Pt 4), 628-637. doi:10.1242/jcs.03366

Rodriguez-Fraticelli, A. E., Galvez-Santisteban, M., & Martin-Belmonte, F. (2011). Divide and polarize: recent advances in the molecular mechanism regulating epithelial tubulogenesis. *Curr Opin Cell Biol, 23*(5), 638-646. doi:10.1016/j.ceb.2011.07.002

Rosenbaum, J. L., & Witman, G. B. (2002). Intraflagellar transport. *Nat Rev Mol Cell Biol, 3*(11), 813-825. doi:10.1038/nrm952

Ross, A. J., May-Simera, H., Eichers, E. R., Kai, M., Hill, J., Jagger, D. J., . . . Beales, P. L. (2005). Disruption of Bardet-Biedl syndrome ciliary proteins perturbs planar cell polarity in vertebrates. *Nat Genet, 37*(10), 1135-1140. doi:10.1038/ng1644

Rousseau, S., Houle, F., & Huot, J. (2000). Integrating the VEGF signals leading to actin-based motility in vascular endothelial cells. *Trends Cardiovasc Med, 10*(8), 321-327. doi:10.1016/s1050-1738(01)00072-x

Rousseau, S., Houle, F., Landry, J., & Huot, J. (1997). p38 MAP kinase activation by vascular endothelial growth factor mediates actin reorganization and cell migration in human endothelial cells. *Oncogene, 15*(18), 2169-2177. doi:10.1038/sj.onc.1201380

Ruhrberg, C., Gerhardt, H., Golding, M., Watson, R., Ioannidou, S., Fujisawa, H., . . . Shima, D. T. (2002). Spatially restricted patterning cues provided by heparin-binding VEGF-A control blood vessel branching morphogenesis. *Genes Dev, 16*(20), 2684-2698. doi:10.1101/gad.242002

Ruoslahti, E. (2002). Specialization of tumour vasculature. *Nat Rev Cancer, 2*(2), 83-90. doi:10.1038/nrc724

Sakisaka, T., & Takai, Y. (2004). Biology and pathology of nectins and nectin-like molecules. *Curr Opin Cell Biol, 16*(5), 513-521. doi:10.1016/j.ceb.2004.07.007

Salinas, R. Y., Pearring, J. N., Ding, J. D., Spencer, W. J., Hao, Y., & Arshavsky, V. Y. (2017). Photoreceptor discs form through peripherin-dependent suppression of ciliary ectosome release. *J Cell Biol, 216*(5), 1489-1499. doi:10.1083/jcb.201608081

Sanchez, I., & Dynlacht, B. D. (2016). Cilium assembly and disassembly. *Nat Cell Biol, 18*(7), 711-717. doi:10.1038/ncb3370

Sanematsu, F., Hirashima, M., Laurin, M., Takii, R., Nishikimi, A., Kitajima, K., . . . Fukui, Y. (2010). DOCK180 is a Rac activator that regulates

cardiovascular development by acting downstream of CXCR4. *Circ Res, 107*(9), 1102-1105. doi:10.1161/CIRCRESAHA.110.223388

Sankar, K. S., Green, B. J., Crocker, A. R., Verity, J. E., Altamentova, S. M., & Rocheleau, J. V. (2011). Culturing pancreatic islets in microfluidic flow enhances morphology of the associated endothelial cells. *PLoS One, 6*(9), e24904. doi:10.1371/journal.pone.0024904

Satir, P., & Christensen, S. T. (2007). Overview of structure and function of mammalian cilia. *Annu Rev Physiol, 69*, 377-400. doi:10.1146/annurev.physiol.69.040705.141236

Satir, P., & Christensen, S. T. (2008). Structure and function of mammalian cilia. *Histochem Cell Biol, 129*(6), 687-693. doi:10.1007/s00418-008-0416-9

Satir, P., Pedersen, L. B., & Christensen, S. T. (2010). The primary cilium at a glance. *J Cell Sci, 123*(Pt 4), 499-503. doi:10.1242/jcs.050377

Schwartz, E. A., Leonard, M. L., Bizios, R., & Bowser, S. S. (1997). Analysis and modeling of the primary cilium bending response to fluid shear. *Am J Physiol, 272*(1 Pt 2), F132-138. doi:10.1152/ajprenal.1997.272.1.F132

Serini, G., Ambrosi, D., Giraudo, E., Gamba, A., Preziosi, L., & Bussolino, F. (2003). Modeling the early stages of vascular network assembly. *EMBO J, 22*(8), 1771-1779. doi:10.1093/emboj/cdg176

Sevajol, M., Reiser, J. B., Chouquet, A., Perard, J., Ayala, I., Gans, P., . . . Housset, D. (2012). The C-terminal polyproline-containing region of ELMO contributes to an increase in the life-time of the ELMO-DOCK complex. *Biochimie, 94*(3), 823-828. doi:10.1016/j.biochi.2011.11.014

Shalaby, F., Rossant, J., Yamaguchi, T. P., Gertsenstein, M., Wu, X. F., Breitman, M. L., & Schuh, A. C. (1995). Failure of blood-island formation and vasculogenesis in Flk-1-deficient mice. *Nature, 376*(6535), 62-66. doi:10.1038/376062a0

Sharma, N., Kosan, Z. A., Stallworth, J. E., Berbari, N. F., & Yoder, B. K. (2011). Soluble levels of cytosolic tubulin regulate ciliary length control. *Mol Biol Cell, 22*(6), 806-816. doi:10.1091/mbc.E10-03-0269

Shi, L. (2013). Dock protein family in brain development and neurological disease. *Commun Integr Biol, 6*(6), e26839. doi:10.4161/cib.26839

Shi, Z. D., Wang, H., & Tarbell, J. M. (2011). Heparan sulfate proteoglycans mediate interstitial flow mechanotransduction regulating MMP-13

expression and cell motility via FAK-ERK in 3D collagen. *PLoS One, 6*(1), e15956. doi:10.1371/journal.pone.0015956

Sicklick, J. K., Li, Y. X., Choi, S. S., Qi, Y., Chen, W., Bustamante, M., . . . Diehl, A. M. (2005). Role for hedgehog signaling in hepatic stellate cell activation and viability. *Lab Invest, 85*(11), 1368-1380. doi:10.1038/labinvest.3700349

Sidawy, A. N. (2019). Ischemia. *ScienceDirect*, https://www.sciencedirect.com/topics/medicine-and-dentistry/ischemia.

Silvestre, J. S., Mallat, Z., Tedgui, A., & Levy, B. I. (2008). Post-ischaemic neovascularization and inflammation. *Cardiovasc Res, 78*(2), 242-249. doi:10.1093/cvr/cvn027

Singh, S., Adam, M., Matkar, P. N., Bugyei-Twum, A., Desjardins, J. F., Chen, H. H., . . . Singh, K. K. (2020). Endothelial-specific Loss of IFT88 Promotes Endothelial-to-Mesenchymal Transition and Exacerbates Bleomycin-induced Pulmonary Fibrosis. *Sci Rep, 10*(1), 4466. doi:10.1038/s41598-020-61292-9

Singla, V., & Reiter, J. F. (2006). The primary cilium as the cell's antenna: signaling at a sensory organelle. *Science, 313*(5787), 629-633. doi:10.1126/science.1124534

Sinha, S., & Yang, W. (2008). Cellular signaling for activation of Rho GTPase Cdc42. *Cell Signal, 20*(11), 1927-1934. doi:10.1016/j.cellsig.2008.05.002

Smith, C. E. L., Lake, A. V. R., & Johnson, C. A. (2020). Primary Cilia, Ciliogenesis and the Actin Cytoskeleton: A Little Less Resorption, A Little More Actin Please. *Front Cell Dev Biol, 8*, 622822. doi:10.3389/fcell.2020.622822

Song, J. W., Bazou, D., & Munn, L. L. (2012). Anastomosis of endothelial sprouts forms new vessels in a tissue analogue of angiogenesis. *Integr Biol (Camb), 4*(8), 857-862. doi:10.1039/c2ib20061a

Song, J. W., & Munn, L. L. (2011). Fluid forces control endothelial sprouting. *Proc Natl Acad Sci U S A, 108*(37), 15342-15347. doi:10.1073/pnas.1105316108

Spasic, M., & Jacobs, C. R. (2017). Primary cilia: Cell and molecular mechanosensors directing whole tissue function. *Seminars in cell & developmental biology, 71*, 42-52. doi:10.1016/j.semcdb.2017.08.036

Stepanek, L., & Pigino, G. (2016). Microtubule doublets are double-track railways for intraflagellar transport trains. *Science, 352*(6286), 721-724. doi:10.1126/science.aaf4594

Stewart, L., Egnuni, T., Esteves, F., Yuldasheva, N., Wheatcroft, S., & Mavria, G. (2018). DOCK4 genetic deletion impairs vascular recovery following an ischemic event. *120*, 48-49. doi:https://doi.org/10.1016/j.yjmcc.2018.05.143

Streets, A. J., Prosseda, P. P., & Ong, A. C. (2020). Polycystin-1 regulates ARHGAP35-dependent centrosomal RhoA activation and ROCK signaling. *JCI Insight, 5*(16). doi:10.1172/jci.insight.135385

Strilic, B., Eglinger, J., Krieg, M., Zeeb, M., Axnick, J., Babal, P., . . . Lammert, E. (2010). Electrostatic cell-surface repulsion initiates lumen formation in developing blood vessels. *Curr Biol, 20*(22), 2003-2009. doi:10.1016/j.cub.2010.09.061

Strilic, B., Kucera, T., Eglinger, J., Hughes, M. R., McNagny, K. M., Tsukita, S., . . . Lammert, E. (2009). The molecular basis of vascular lumen formation in the developing mouse aorta. *Dev Cell, 17*(4), 505-515. doi:10.1016/j.devcel.2009.08.011

Strilic, B., Kucera, T., & Lammert, E. (2010). Formation of cardiovascular tubes in invertebrates and vertebrates. *Cell Mol Life Sci, 67*(19), 3209-3218. doi:10.1007/s00018-010-0400-0

Summers, A. C., Snow, J., Wiggs, E., Liu, A. G., Toro, C., Poretti, A., . . . Gunay-Aygun, M. (2017). Neuropsychological phenotypes of 76 individuals with Joubert syndrome evaluated at a single center. *Am J Med Genet A, 173*(7), 1796-1812. doi:10.1002/ajmg.a.38272

Sundaravel, S., Kuo, W. L., Jeong, J. J., Choudhary, G. S., Gordon-Mitchell, S., Liu, H., . . . Wickrema, A. (2019). Loss of Function of DOCK4 in Myelodysplastic Syndromes Stem Cells is Restored by Inhibitors of DOCK4 Signaling Networks. *Clin Cancer Res, 25*(18), 5638-5649. doi:10.1158/1078-0432.CCR-19-0924

Svitkina, T. (2018). The Actin Cytoskeleton and Actin-Based Motility. *Cold Spring Harb Perspect Biol, 10*(1). doi:10.1101/cshperspect.a018267

Sweeney, M. D., Kisler, K., Montagne, A., Toga, A. W., & Zlokovic, B. V. (2018). The role of brain vasculature in neurodegenerative disorders. *Nat Neurosci, 21*(10), 1318-1331. doi:10.1038/s41593-018-0234-x

Swift, M. R., & Weinstein, B. M. (2009). Arterial-venous specification during development. *Circ Res, 104*(5), 576-588. doi:10.1161/CIRCRESAHA.108.188805

Szczepanowska, J. (2009). Involvement of Rac/Cdc42/PAK pathway in cytoskeletal rearrangements. *Acta Biochim Pol, 56*(2), 225-234.

Szymanska, K., Berry, I., Logan, C. V., Cousins, S. R., Lindsay, H., Jafri, H., . . . Johnson, C. A. (2012). Founder mutations and genotype-phenotype correlations in Meckel-Gruber syndrome and associated ciliopathies. *Cilia, 1*(1), 18. doi:10.1186/2046-2530-1-18

Tabas, I., Garcia-Cardena, G., & Owens, G. K. (2015). Recent insights into the cellular biology of atherosclerosis. *J Cell Biol, 209*(1), 13-22. doi:10.1083/jcb.201412052

Tan, W., Palmby, T. R., Gavard, J., Amornphimoltham, P., Zheng, Y., & Gutkind, J. S. (2008). An essential role for Rac1 in endothelial cell function and vascular development. *FASEB J, 22*(6), 1829-1838. doi:10.1096/fj.07-096438

Taniguchi, K., & Karin, M. (2018). NF-kappaB, inflammation, immunity and cancer: coming of age. *Nat Rev Immunol, 18*(5), 309-324. doi:10.1038/nri.2017.142

Thazhath, R., Jerka-Dziadosz, M., Duan, J., Wloga, D., Gorovsky, M. A., Frankel, J., & Gaertig, J. (2004). Cell context-specific effects of the beta-tubulin glycylation domain on assembly and size of microtubular organelles. *Mol Biol Cell, 15*(9), 4136-4147. doi:10.1091/mbc.e04-03-0247

Theberge, A. B., Yu, J., Young, E. W., Ricke, W. A., Bushman, W., & Beebe, D. J. (2015). Microfluidic multiculture assay to analyze biomolecular signaling in angiogenesis. *Anal Chem, 87*(6), 3239-3246. doi:10.1021/ac503700f

Thuillez, C., & Richard, V. (2005). Targeting endothelial dysfunction in hypertensive subjects. *J Hum Hypertens, 19 Suppl 1*, S21-25. doi:10.1038/sj.jhh.1001889

Tian, H., Feng, J., Li, J., Ho, T. V., Yuan, Y., Liu, Y., . . . Chai, Y. (2017). Intraflagellar transport 88 (IFT88) is crucial for craniofacial development in

mice and is a candidate gene for human cleft lip and palate. *Hum Mol Genet, 26*(5), 860-872. doi:10.1093/hmg/ddx002

Tkachenko, E., Lutgens, E., Stan, R. V., & Simons, M. (2004). Fibroblast growth factor 2 endocytosis in endothelial cells proceed via syndecan-4-dependent activation of Rac1 and a Cdc42-dependent macropinocytic pathway. *J Cell Sci, 117*(Pt 15), 3189-3199. doi:10.1242/jcs.01190

Tobin, J. L., & Beales, P. L. (2009). The nonmotile ciliopathies. *Genet Med, 11*(6), 386-402. doi:10.1097/GIM.0b013e3181a02882

Tojkander, S., Gateva, G., & Lappalainen, P. (2012). Actin stress fibers--assembly, dynamics and biological roles. *J Cell Sci, 125*(Pt 8), 1855-1864. doi:10.1242/jcs.098087

Tomanek, R. J., Christensen, L. P., Simons, M., Murakami, M., Zheng, W., & Schatteman, G. C. (2010). Embryonic coronary vasculogenesis and angiogenesis are regulated by interactions between multiple FGFs and VEGF and are influenced by mesenchymal stem cells. *Dev Dyn, 239*(12), 3182-3191. doi:10.1002/dvdy.22460

Tomanek, R. J., Hansen, H. K., & Christensen, L. P. (2008). Temporally expressed PDGF and FGF-2 regulate embryonic coronary artery formation and growth. *Arterioscler Thromb Vasc Biol, 28*(7), 1237-1243. doi:10.1161/ATVBAHA.108.166454

Tomanek, R. J., Sandra, A., Zheng, W., Brock, T., Bjercke, R. J., & Holifield, J. S. (2001). Vascular endothelial growth factor and basic fibroblast growth factor differentially modulate early postnatal coronary angiogenesis. *Circ Res, 88*(11), 1135-1141. doi:10.1161/hh1101.091191

Tonini, T., Rossi, F., & Claudio, P. P. (2003). Molecular basis of angiogenesis and cancer. *Oncogene, 22*(42), 6549-6556. doi:10.1038/sj.onc.1206816

Toret, C. P., Collins, C., & Nelson, W. J. (2014). An Elmo-Dock complex locally controls Rho GTPases and actin remodeling during cadherin-mediated adhesion. *J Cell Biol, 207*(5), 577-587. doi:10.1083/jcb.201406135

Torisawa, Y. S., Mosadegh, B., Bersano-Begey, T., Steele, J. M., Luker, K. E., Luker, G. D., & Takayama, S. (2010). Microfluidic platform for chemotaxis in gradients formed by CXCL12 source-sink cells. *Integr Biol (Camb), 2*(11-12), 680-686. doi:10.1039/c0ib00041h

Torres-Vazquez, J., Kamei, M., & Weinstein, B. M. (2003). Molecular distinction between arteries and veins. *Cell Tissue Res, 314*(1), 43-59. doi:10.1007/s00441-003-0771-8

Tsang, W. Y., Bossard, C., Khanna, H., Peranen, J., Swaroop, A., Malhotra, V., & Dynlacht, B. D. (2008). CP110 suppresses primary cilia formation through its interaction with CEP290, a protein deficient in human ciliary disease. *Dev Cell, 15*(2), 187-197. doi:10.1016/j.devcel.2008.07.004

Tucker, W. D., Arora, Y., & Mahajan, K. (2022). Anatomy, Blood Vessels. In *StatPearls*. Treasure Island (FL).

Tung, Y. C., Hsiao, A. Y., Allen, S. G., Torisawa, Y. S., Ho, M., & Takayama, S. (2011). High-throughput 3D spheroid culture and drug testing using a 384 hanging drop array. *Analyst, 136*(3), 473-478. doi:10.1039/c0an00609b

Ueda, S., Fujimoto, S., Hiramoto, K., Negishi, M., & Katoh, H. (2008). Dock4 regulates dendritic development in hippocampal neurons. *J Neurosci Res, 86*(14), 3052-3061. doi:10.1002/jnr.21763

Unger, E. F., Goncalves, L., Epstein, S. E., Chew, E. Y., Trapnell, C. B., Cannon, R. O., 3rd, & Quyyumi, A. A. (2000). Effects of a single intracoronary injection of basic fibroblast growth factor in stable angina pectoris. *Am J Cardiol, 85*(12), 1414-1419. doi:10.1016/s0002-9149(00)00787-6

Upadhyay, G., Goessling, W., North, T. E., Xavier, R., Zon, L. I., & Yajnik, V. (2008). Molecular association between beta-catenin degradation complex and Rac guanine exchange factor DOCK4 is essential for Wnt/beta-catenin signaling. *Oncogene, 27*(44), 5845-5855. doi:10.1038/onc.2008.202

Vaggi, F., Disanza, A., Milanesi, F., Di Fiore, P. P., Menna, E., Matteoli, M., . . . Ciliberto, A. (2011). The Eps8/IRSp53/VASP network differentially controls actin capping and bundling in filopodia formation. *PLoS Comput Biol, 7*(7), e1002088. doi:10.1371/journal.pcbi.1002088

Valente, E. M., Logan, C. V., Mougou-Zerelli, S., Lee, J. H., Silhavy, J. L., Brancati, F., . . . Gleeson, J. G. (2010). Mutations in TMEM216 perturb ciliogenesis and cause Joubert, Meckel and related syndromes. *Nat Genet, 42*(7), 619-625. doi:10.1038/ng.594

van Buul, J. D., Geerts, D., & Huveneers, S. (2014). Rho GAPs and GEFs: controling switches in endothelial cell adhesion. *Cell Adh Migr, 8*(2), 108-124. doi:10.4161/cam.27599

Van der Heiden, K., Groenendijk, B. C., Hierck, B. P., Hogers, B., Koerten, H. K., Mommaas, A. M., . . . Poelmann, R. E. (2006). Monocilia on chicken embryonic endocardium in low shear stress areas. *Dev Dyn, 235*(1), 19-28. doi:10.1002/dvdy.20557

Van der Heiden, K., Hierck, B. P., Krams, R., de Crom, R., Cheng, C., Baiker, M., . . . Poelmann, R. E. (2008). Endothelial primary cilia in areas of disturbed flow are at the base of atherosclerosis. *Atherosclerosis, 196*(2), 542-550. doi:10.1016/j.atherosclerosis.2007.05.030

van der Helm, M. W., van der Meer, A. D., Eijkel, J. C., van den Berg, A., & Segerink, L. I. (2016). Microfluidic organ-on-chip technology for blood-brain barrier research. *Tissue Barriers, 4*(1), e1142493. doi:10.1080/21688370.2016.1142493

van der Meer, A. D., & van den Berg, A. (2012). Organs-on-chips: breaking the in vitro impasse. *Integr Biol (Camb), 4*(5), 461-470. doi:10.1039/c2ib00176d

van der Worp, H. B., Howells, D. W., Sena, E. S., Porritt, M. J., Rewell, S., O'Collins, V., & Macleod, M. R. (2010). Can animal models of disease reliably inform human studies? *PLoS Med, 7*(3), e1000245. doi:10.1371/journal.pmed.1000245

Vanlandewijck, M., He, L., Mae, M. A., Andrae, J., Ando, K., Del Gaudio, F., . . . Betsholtz, C. (2018). A molecular atlas of cell types and zonation in the brain vasculature. *Nature, 554*(7693), 475-480. doi:10.1038/nature25739

Verhamme, P., & Hoylaerts, M. F. (2006). The pivotal role of the endothelium in haemostasis and thrombosis. *Acta Clin Belg, 61*(5), 213-219. doi:10.1179/acb.2006.036

Vickerman, V., Blundo, J., Chung, S., & Kamm, R. (2008). Design, fabrication and implementation of a novel multi-parameter control microfluidic platform for three-dimensional cell culture and real-time imaging. *Lab Chip, 8*(9), 1468-1477. doi:10.1039/b802395f

Vickerman, V., & Kamm, R. D. (2012). Mechanism of a flow-gated angiogenesis switch: early signaling events at cell-matrix and cell-cell junctions. *Integr Biol (Camb), 4*(8), 863-874. doi:10.1039/c2ib00184e

Vinci, M., Gowan, S., Boxall, F., Patterson, L., Zimmermann, M., Court, W., . . . Eccles, S. A. (2012). Advances in establishment and analysis of three-dimensional tumor spheroid-based functional assays for target validation and drug evaluation. *BMC Biol, 10*, 29. doi:10.1186/1741-7007-10-29

Vokes, S. A., Yatskievych, T. A., Heimark, R. L., McMahon, J., McMahon, A. P., Antin, P. B., & Krieg, P. A. (2004). Hedgehog signaling is essential for endothelial tube formation during vasculogenesis. *Development, 131*(17), 4371-4380. doi:10.1242/dev.01304

Wallmeier, J., Nielsen, K. G., Kuehni, C. E., Lucas, J. S., Leigh, M. W., Zariwala, M. A., & Omran, H. (2020). Motile ciliopathies. *Nat Rev Dis Primers, 6*(1), 77. doi:10.1038/s41572-020-0209-6

Wang, G., Zhang, Z., Xu, Z., Yin, H., Bai, L., Ma, Z., . . . Wu, G. (2010). Activation of the sonic hedgehog signaling controls human pulmonary arterial smooth muscle cell proliferation in response to hypoxia. *Biochim Biophys Acta, 1803*(12), 1359-1367. doi:10.1016/j.bbamcr.2010.09.002

Wang, S., Zhuang, S., & Dong, Z. (2021). IFT88 deficiency in proximal tubular cells exaggerates cisplatin-induced injury by suppressing autophagy. *Am J Physiol Renal Physiol, 321*(3), F269-F277. doi:10.1152/ajprenal.00672.2020

Wang, X., Phan, D. T., Sobrino, A., George, S. C., Hughes, C. C., & Lee, A. P. (2016). Engineering anastomosis between living capillary networks and endothelial cell-lined microfluidic channels. *Lab Chip, 16*(2), 282-290. doi:10.1039/c5lc01050k

Wang, Y., Kaiser, M. S., Larson, J. D., Nasevicius, A., Clark, K. J., Wadman, S. A., . . . Essner, J. J. (2010). Moesin1 and Ve-cadherin are required in endothelial cells during in vivo tubulogenesis. *Development, 137*(18), 3119-3128. doi:10.1242/dev.048785

Wann, A. K., Zuo, N., Haycraft, C. J., Jensen, C. G., Poole, C. A., McGlashan, S. R., & Knight, M. M. (2012). Primary cilia mediate mechanotransduction through control of ATP-induced Ca2+ signaling in compressed chondrocytes. *FASEB J, 26*(4), 1663-1671. doi:10.1096/fj.11-193649

Wary, K. K., Kohler, E. E., & Chatterjee, I. (2012). Focal adhesion kinase regulation of neovascularization. *Microvasc Res, 83*(1), 64-70. doi:10.1016/j.mvr.2011.05.002

Waters, A. M., & Beales, P. L. (2011). Ciliopathies: an expanding disease spectrum. *Pediatr Nephrol, 26*(7), 1039-1056. doi:10.1007/s00467-010-1731-7

Wayne W. Wu, F. M. R., Paul Sternberg Jr. (2016). Pharmacotherapy of Choroidal Neovascularization.

Wheatley, D. N. (1969). Cilia in cell-cultured fibroblasts. I. On their occurrence and relative frequencies in primary cultures and established cell lines. *J Anat, 105*(Pt 2), 351-362.

Wheatley, D. N. (1982). *The centriole, a central enigma of cell biology*. Amsterdam ; New York

New York, N.Y.: Elsevier Biomedical Press ;

Sole distributors for the U.S.A. and Canada, Elsevier/North-Holland.

Wheway, G., Schmidts, M., Mans, D. A., Szymanska, K., Nguyen, T. T., Racher, H., . . . Johnson, C. A. (2015). An siRNA-based functional genomics screen for the identification of regulators of ciliogenesis and ciliopathy genes. *Nat Cell Biol, 17*(8), 1074-1087. doi:10.1038/ncb3201

Whitesides, G. M. (2006). The origins and the future of microfluidics. *Nature, 442*(7101), 368-373. doi:10.1038/nature05058

Wiegering, A., Ruther, U., & Gerhardt, C. (2018). The ciliary protein Rpgrip1l in development and disease. *Dev Biol, 442*(1), 60-68. doi:10.1016/j.ydbio.2018.07.024

Williams, C. K., Li, J. L., Murga, M., Harris, A. L., & Tosato, G. (2006). Up-regulation of the Notch ligand Delta-like 4 inhibits VEGF-induced endothelial cell function. *Blood, 107*(3), 931-939. doi:10.1182/blood-2005-03-1000

Wilmer, M. J., Ng, C. P., Lanz, H. L., Vulto, P., Suter-Dick, L., & Masereeuw, R. (2016). Kidney-on-a-Chip Technology for Drug-Induced Nephrotoxicity Screening. *Trends Biotechnol, 34*(2), 156-170. doi:10.1016/j.tibtech.2015.11.001

Wojciak-Stothard, B., & Ridley, A. J. (2002). Rho GTPases and the regulation of endothelial permeability. *Vascul Pharmacol, 39*(4-5), 187-199. doi:10.1016/s1537-1891(03)00008-9

Wolf, M. T., Saunier, S., O'Toole, J. F., Wanner, N., Groshong, T., Attanasio, M., . . . Hildebrandt, F. (2007). Mutational analysis of the RPGRIP1L gene in patients with Joubert syndrome and nephronophthisis. *Kidney Int, 72*(12), 1520-1526. doi:10.1038/sj.ki.5002630

Wong, S. Y., Seol, A. D., So, P. L., Ermilov, A. N., Bichakjian, C. K., Epstein, E. H., Jr., . . . Reiter, J. F. (2009). Primary cilia can both mediate and suppress Hedgehog pathway-dependent tumorigenesis. *Nat Med, 15*(9), 1055-1061. doi:10.1038/nm.2011

Xu, C., Rossetti, S., Jiang, L., Harris, P. C., Brown-Glaberman, U., Wandinger-Ness, A., . . . Alper, S. L. (2007). Human ADPKD primary cyst epithelial cells with a novel, single codon deletion in the PKD1 gene exhibit defective ciliary polycystin localization and loss of flow-induced Ca2+ signaling. *Am J Physiol Renal Physiol, 292*(3), F930-945. doi:10.1152/ajprenal.00285.2006

Yajnik, V., Paulding, C., Sordella, R., McClatchey, A. I., Saito, M., Wahrer, D. C., . . . Haber, D. A. (2003). DOCK4, a GTPase activator, is disrupted during tumorigenesis. *Cell, 112*(5), 673-684. doi:10.1016/s0092-8674(03)00155-7

Yamamoto, Y., & Mizushima, N. (2021). Autophagy and Ciliogenesis. *JMA J, 4*(3), 207-215. doi:10.31662/jmaj.2021-0090

Yan, D., Li, F., Hall, M. L., Sage, C., Hu, W. H., Giallourakis, C., . . . Liu, X. Z. (2006). An isoform of GTPase regulator DOCK4 localizes to the stereocilia in the inner ear and binds to harmonin (USH1C). *J Mol Biol, 357*(3), 755-764. doi:10.1016/j.jmb.2006.01.017

Yancopoulos, G. D., Davis, S., Gale, N. W., Rudge, J. S., Wiegand, S. J., & Holash, J. (2000). Vascular-specific growth factors and blood vessel formation. *Nature, 407*(6801), 242-248. doi:10.1038/35025215

Yang, J., Zhang, Z., Roe, S. M., Marshall, C. J., & Barford, D. (2009). Activation of Rho GTPases by DOCK exchange factors is mediated by a nucleotide sensor. *Science, 325*(5946), 1398-1402. doi:10.1126/science.1174468

Yang, Y., Hao, H., Wu, X., Guo, S., Liu, Y., Ran, J., . . . Zhou, J. (2019). Mixed-lineage leukemia protein 2 suppresses ciliary assembly by the modulation of actin dynamics and vesicle transport. *Cell Discov, 5*, 33. doi:10.1038/s41421-019-0100-3

Yoder, B. K., Hou, X., & Guay-Woodford, L. M. (2002). The polycystic kidney disease proteins, polycystin-1, polycystin-2, polaris, and cystin, are co-localized in renal cilia. *J Am Soc Nephrol, 13*(10), 2508-2516. doi:10.1097/01.asn.0000029587.47950.25

Yoder, M. C. (2012). Human endothelial progenitor cells. *Cold Spring Harb Perspect Med, 2*(7), a006692. doi:10.1101/cshperspect.a006692

Yu, F., Ran, J., & Zhou, J. (2016). Ciliopathies: Does HDAC6 Represent a New Therapeutic Target? *Trends Pharmacol Sci, 37*(2), 114-119. doi:10.1016/j.tips.2015.11.002

Yu, F., Selva Kumar, N. D., Choudhury, D., Foo, L. C., & Ng, S. H. (2018). Microfluidic platforms for modeling biological barriers in the circulatory system. *Drug Discov Today, 23*(4), 815-829. doi:10.1016/j.drudis.2018.01.036

Zaragoza, C., Marquez, S., & Saura, M. (2012). Endothelial mechanosensors of shear stress as regulators of atherogenesis. *Curr Opin Lipidol, 23*(5), 446-452. doi:10.1097/MOL.0b013e328357e837

Zeng, A., Wang, S. R., He, Y. X., Yan, Y., & Zhang, Y. (2021). Progress in understanding of the stalk and tip cells formation involvement in angiogenesis mechanisms. *Tissue Cell, 73*, 101626. doi:10.1016/j.tice.2021.101626

Zervantonakis, I. K., Hughes-Alford, S. K., Charest, J. L., Condeelis, J. S., Gertler, F. B., & Kamm, R. D. (2012). Three-dimensional microfluidic model for tumor cell intravasation and endothelial barrier function. *Proc Natl Acad Sci U S A, 109*(34), 13515-13520. doi:10.1073/pnas.1210182109

Zhao, X., & Guan, J. L. (2011). Focal adhesion kinase and its signaling pathways in cell migration and angiogenesis. *Adv Drug Deliv Rev, 63*(8), 610-615. doi:10.1016/j.addr.2010.11.001

Zhuge, Y., Zhang, J., Qian, F., Wen, Z., Niu, C., Xu, K., . . . Jia, C. (2020). Role of smooth muscle cells in Cardiovascular Disease. *Int J Biol Sci, 16*(14), 2741-2751. doi:10.7150/ijbs.49871

Zovein, A. C., Luque, A., Turlo, K. A., Hofmann, J. J., Yee, K. M., Becker, M. S., . . . Iruela-Arispe, M. L. (2010). Beta1 integrin establishes endothelial cell polarity and arteriolar lumen formation via a Par3-dependent mechanism. *Dev Cell, 18*(1), 39-51. doi:10.1016/j.devcel.2009.12.006